UNIVERSITY OF LONDON,

IMPERIAL COLLEGE OF SCIENCE AND TECHNOLOGY,

PHYSICS DEPARTMENT,

BIOPHYSICS SECTION.

COLOUR AND SPATIAL PATTERN DISCRIMINATION IN HUMAN VISION.

BY

VICKI ANN WATERFIELD

Thesis submitted for the Degree of
Ph.d of the University of London.

1980

TABLE OF CONTENTS

ABSTRACT

This thesis describes a psychophysical study of the visual mechanisms responsible for spatial, form and colour perception in subjects with normal and abnormal visual pathways.

The main investigation is concerned with the post-receptoral organization of colour vision in the human visual system. An adaptation method derived from the contrast threshold elevation effect (Blakemore and Campbell, 1969a,b) and the associated binocular inhibitory effect (Ruddock and Wigley, 1976) is described, and it is shown that with a suitable choice of grating parameters the inhibitory interaction is colour selective. Three independent spectral response mechanisms have been found, and their spectral responses have been derived. One mechanism exhibits red-green opponent responses similar to that observed in electrophysiological studies (Gouras, 1974). The spectral responses of all three mechanisms have been analysed in terms of the absorption spectra of the cone photopigments (Marks, Dobelle and MacNichol, 1964) and the non-linear transmission of signals along the visual pathways. Some data are also presented for a deuteranopic dichromat, who lacks the green-sensitive cone mechanism (Rushton, 1965)

The remainder of the thesis describes visual responses to spatially structured stimuli found in subjects with abnormal vision including an albino, a hemiope, and a subject(M.W.) with a rare central colour vision defect (Bender and Ruddock, 1974). It is shown that the spatial resolving power in the albino is not set at the photoreceptor level and that M.W.'s central visual defect involves a gross loss of spatial resolution for long-wavelength stimuli. Results for this last subject have been examined in relation to current theories about both the representation of different stimulus parameters at central levels in the visual pathways and the origins of visual illusions.

CHAPTER I

General Introduction

Eyes are sensory organs, whose function is to detect light and initiate the sequence of events which leads to the perception of stimulus brightness, colour, form and movement. As a result it must contain a photochemical pigment capable of photon absorption to indicate the presence of a light stimulus. The pigment molecules mediate the absorption process over a wide spectral range, and are contained in the receptor cells which transform the spatial and temporal properties of the retinal image into equivalent electrical signals as required for transmission to higher stages of visual processing. The majority of retinal fibres carrying visual information project to the visual cortex which contains a point by point mapping of the retinal surface, although not on a one:one basis, and appears to constitute the input stage to further processing units (Zeki, 1978e).

Functional aspects of the visual system can be investigated by an objective or subjective approach. Objective techniques involve neurophysiological measurements of single cell responses as a result of visual stimulation, whilst subjective methods utilize the responses of the visual system as a whole in psychophysical measurements involving threshold or matching criteria, in which the system itself is treated as a variable input - constant output device. An improved understanding of the visual system is obtained by combining studies of both kinds, and in view of the close similarities which exist between man and the higher primate species, especially with respect to their visual systems, it is therefore possible to make comparisons between results obtained by the two methods.

In this introduction, a review is given of previous investigations, both psychophysical and electrophysiological, which are relevant to the research to be described in later chapters.

A. Anatomical Structure of the Visual Sensory System

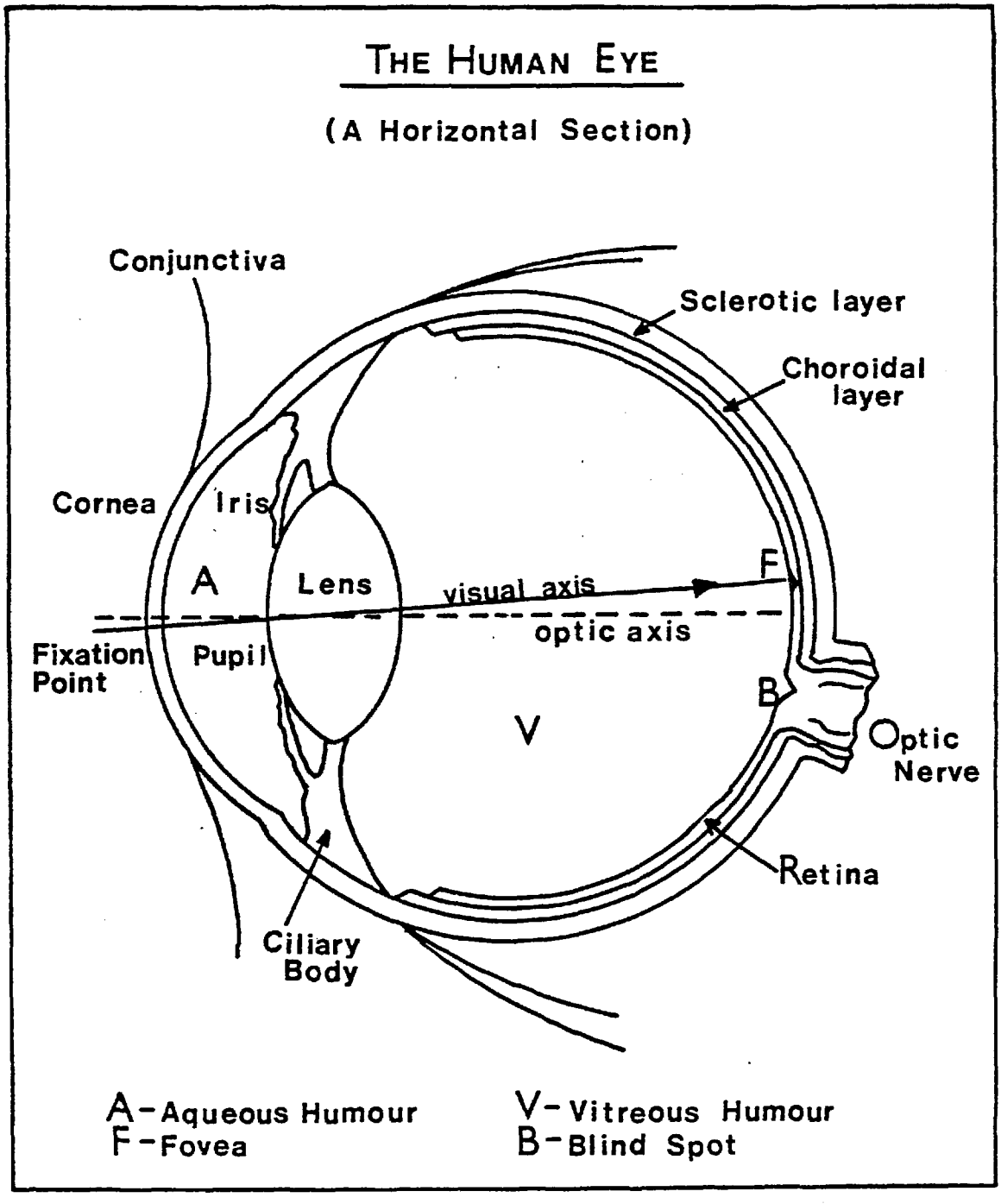

Fig. 1.1 A Horizontal Cross Section through the Human Eye (after Polyak, 1957).

The eye, fig. 1.1, constitutes the peripheral sense organ of the visual system. Light from objects in the external surroundings enters the eye and is focused to form an image on the retina, by refraction at the transparent corneal membrane and crystalline lens. The retina lines the posterior chamber containing the vitreous humour, and consists not only of the receptoral layer of rods and cones, but also of several other classes of functionally and morphologically distinct cells organized into layers lying perpendicular to the light rays. The photoreceptor layer of rods and cones comprises the innermost layer, adjacent to the choroid, thus incident light passes through the other retinal cells before being absorbed by the visual pigments contained in the rod and cone receptors.

Not all of the light entering the eye is absorbed in the visual pigments. The lens absorbs any ultra-violet radiation entering, and the useful range of wavelengths for the receptors extends between wavelengths of around 380 nm to 700 nm - the visible portion of the spectrum. Further reductions in overall sensitivity are caused by absorption prior to receptors in the optical media and by scattering losses.

Several anatomical features which distinguish between rods and cones are revealed by optical-and electron-microscopy (see fig. 1.2). Essentially the two classes derive their names from their morphology. The outer limb of cones is typically conical in shape, its inner limb is bulbous, and their pedicles which establish synapses with other cells, are spatially diffuse. However, at the fovea, a specialized region of the retinal surface, the cone outer segments become more cylindrical (diameter 2 μm, Polyak, 1941), and their high density in the fovea accounts for its high spatial acuity.

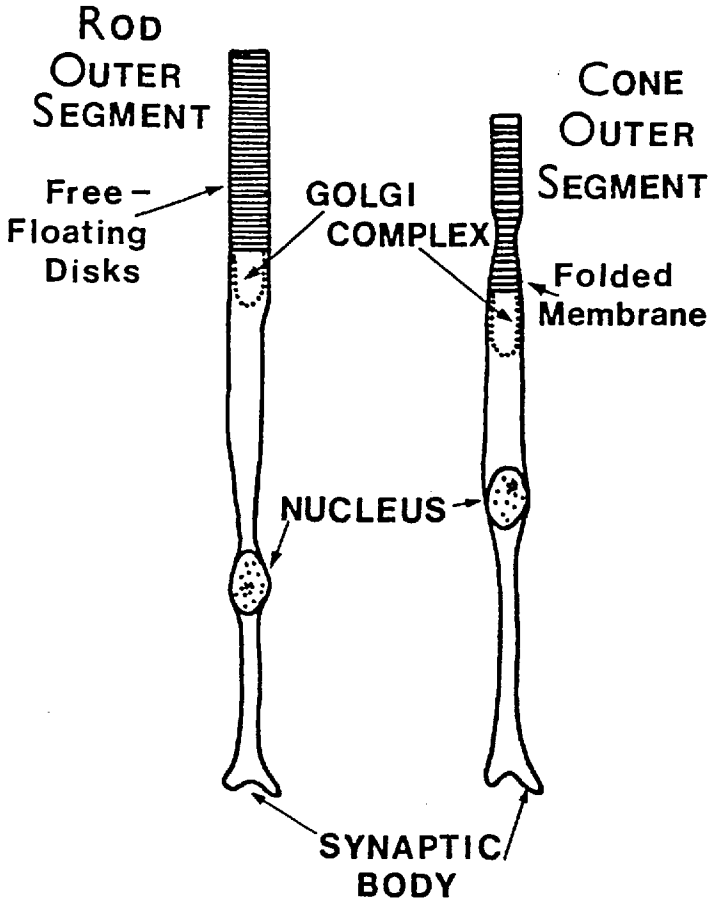

FIG.1.2 Typical ROD and CONE CELLS in MAN

(after Young, 1960)

The rods, in contrast to the cones are cylindrical in shape of diameter 2 μm and length 60 μm, and have two distinct segments with a spherule at which synapses are made with other cells. It can be seen that both receptors possess a lamellar internal membrane structure, which is continuous in the envelope structure of cones, but forms separate disc structures in rod outer segments. It is in this membrane that the photolabile pigment is distributed. In rods, the pigment has been extracted and investigated (Dartnell, 1957) and subsequently given the name rhodopsin. On exposure to light it undergoes a series of chemical changes, regenerating as light is removed (Wald and Brown, 1956; Brindley, 1970), the time course of recovery being reflected in dark adaptation curves of sensitivity. Cone pigments, however, have proved more difficult to identify, as they have not been extracted successfully. Microspectrophotometric studies on primate cones

(Marks, Dobelle and MacNichol, 1964; Brown and Wald, 1964) show that there are three spectral classes of cone pigments, and thus establish trivariancy at the receptoral level (see fig. 1.3).

FIG.1.3

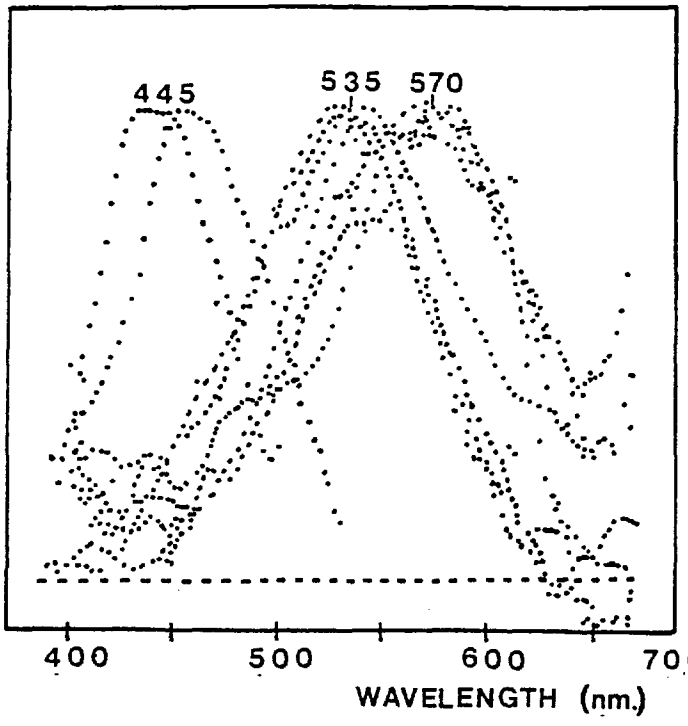

Difference Spectra recorded from Primate Parafoveal Cones

(after Marks, Dobelle and MacNichol, 1964)

It should be noted, however, that there is significant spread between individual cone spectra, and that the data refer to parafoveal, not foveal, cones.

The distribution of rods and cones in the human retina is approximately symmetric about a small depression (1.5 mm) in the retinal surface lying close to the optical axis of the eye, fig. 1.4. This region is called the fovea. The optic disc, however, being the region where the nerve fibres leave the eye on their way to the brain, is completely void of any photoreceptors, and for this reason is termed the 'blind spot'. The fovea, on the other hand, contains a dense distribution of cones, approximately 10^5 in number out of a total of 10^6, and is virtually rod-free. Since these cones are closely packed and maintain local

neural connections, the structure corresponds very well to the high acuity in the central 2^{o} of the visual field. There are in all some 10^{8} rods with peak density at 10^{o} -15^{o} from the fovea, fig. 1.4.

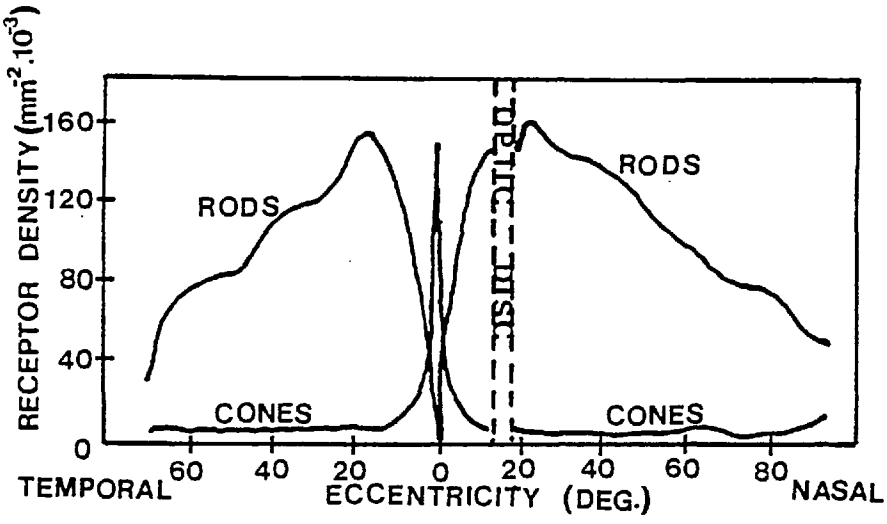

FIG.1.4 Density of Rods and Cones in the Human Retina.

(after Pirenne, 1967; original Østerberg, 1935)

As stated in a previous section, the retina consists of a number of classes of neurones, which receive signals from receptor cells. The connections between these various types of cell and their projections to the higher visual centres have been studied in part by neural atrophy with subsequent degeneration (Hubel and Wiesel, 1969; Cowey, 1974), by the transmission of electrical signals generated in the rods and cones to the bipolar cells and hence to higher visual centres (Dowling and Boycott, 1966; Dowling, 1968; Witkovsky and Dowling, 1969; Boycott and Dowling, 1969) and by staining techniques (Ramon y Cajal, 1911; Polyak, 1941).

A.i. The Retinal Structure

Golgi staining shows that the retina contains six classes of neurone, plus supporting Glial tissue and Müller fibres. The six types of cells are photoreceptors, horizontal cells, bipolar cells, amacrine cells, inter-plexiform cells and ganglion cells. The retinal structure possesses two principal synaptic layers, at which the different neuronal classes establish contact. The outer plexiform layer consists of the processes from the receptor, horizontal and bipolar cells, and the inner plexiform layer consists of the processes of the bipolar, amacrine and ganglion cells (see fig. 1.5). The inter-plexiform cells appear to make post-synaptic contacts at the inner plexiform layer and pre-synaptic contact at the outer plexiform layer.

The information flows through the retina in a preferred direction, i.e., from photoreceptors via bipolars to ganglion cells, the axons of which constitute the optic nerve fibres as they pass out of the eye. At this stage in the inner plexiform layer, the two classes of receptor of the primate retina have separate bipolar pathways. The terminal spherule of each rod is invaginated by the dendrites of rod bipolars, whereas the terminal pedicule of the cones, synapses with clusters of three dendrites, at least twenty-five clusters per cone. Dowling and Boycott (1966) postulate that the middle one originates in a midget bipolar cell, whereas the others are from the diffuse cone or flat bipolar cells.

There are two classes of nerve cells termed inter-neurones which synapse laterally across the retina. One of these, the horizontal cells, is situated at the level of the photoreceptor-bipolar synapse

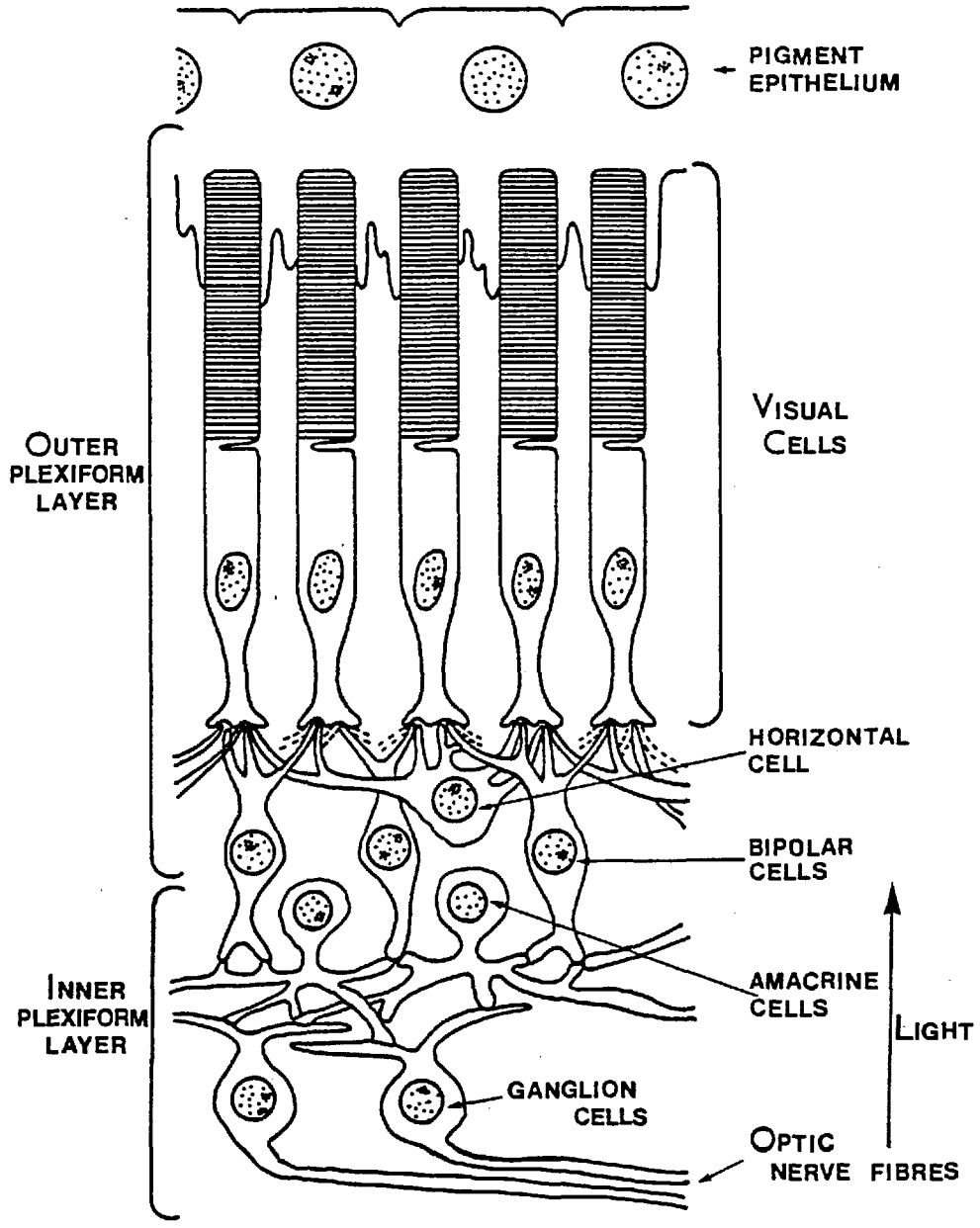

FIG.1.5 SCHEMATIC REPRESENTATION OF CELL RELATIONS IN THE RETINA

(after Boycott and Dowling, 1969)

(fig. 1.5), and the other, the amacrine cells situated at the level of the bipolar-ganglion cell synapse (Dowling and Werblin, 1969). Amacrine cell was the term applied by Cajal (1933) to a group of

retinal nerve cells which had no axon, and these cells can synapse both pre- and post- synaptically to bipolar cell axon terminals to provide a reciprocal probability of feedback between amacrine and bipolar cells (Werblin, 1973). In addition, two types of horizontal cells have been found in fish (Stell, 1967; Parthe, 1972) and monkey (Boycott and Dowling, 1969) retinae. These have specific connections; type A, external to cones, whilst type B, intermediate are connected to rods.

Boycott and Dowling (1966) showed that most ganglion cells in the primate retina receive their input directly from bipolar neurones, and the six classes of ganglion cell described by Polyak (1941) are now grouped into two classes - midget and diffuse ganglion cells. The midget ganglion cell is characterized in being unique to primates and has a single dendrite, unbranched in the inner plexiform layer except where it branches at its tip to synapse with the terminal of midget bipolar cells. In contrast, the diffuse ganglion cell dendrites branch at all levels in the inner plexiform layer.

A.ii. The Optic Nerve and the Lateral Geniculate Nucleus

The axons of the ganglion cells leave the eye and merge to form the optic nerve, which is therefore composed of about 10^6 fibres (Ogden and Miller, 1966; Potts et al., 1972a,b), fig. 1.6. About 20% of the optic nerve fibres project directly to the mid-brain region of the superior colliculus, and as yet the precise function of these non-geniculate fibres is undefined, but they are thought to be responsible for control of eye movements and may mediate the pupillary response in cortically blind patients (Brindley, Gautier-Smith and

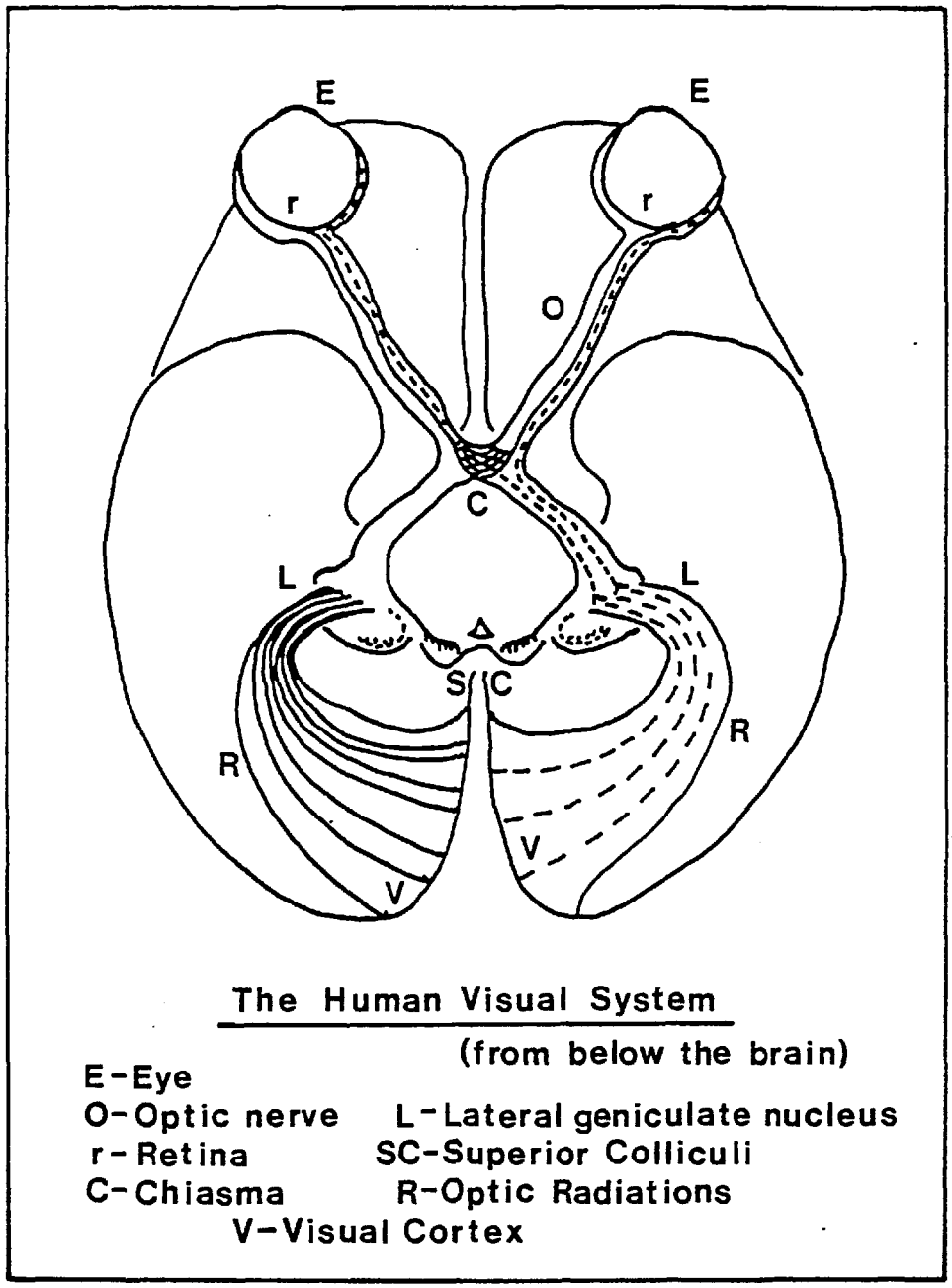

Fig. 1.6 The visual pathways (seen from below the brain). (after Polyak, 1957)

Levin, 1969). The rest of the optic nerves intersect at the 'optic chiasma', fig. 1.6, where partial decussation occurs, that is, there is a crossing over of nerve fibres towards opposite hemispheres in the brain, with the remainder continuing to innervate on the same side as the eye from which they came. It is found that fibres from the nasal hemi-retina cross to the brain on the opposite (contralateral) side, whereas the temporal fibres continue to the same (ipsilateral) side.

The visual field is therefore divided at the central point and represented in different halves of the brain. However, it is thought that the area corresponding to the central 2^{o} of the visual field may be bilaterally represented (Teuber, Battersby and Bender, 1960). In albinos, this decussation is complete and thus there is no longer the half-field representation in the cerebral hemispheres; each hemisphere receives a complete mapping of the visual field (Guillery and Kaas, 1971; Guillery, 1974; Creel, Witkop and King, 1974).

These nerve fibres connect the retina to the lateral geniculate nucleus (L.G.N.), fig. 1.6, which functions primarily as a relay station, but the information from the two eyes still remains separate at this stage. In primates, the L.G.N. consists of six sheets of neurones, and a point by point projection produces an ordered two dimensional map of the retina (Minkowski, 1920; Le Gros Clark and Penman, 1934; Glees, 1961). Three sheets of L.G.N. neurones receive input from the ipsilateral eye (numbers 2, 3 and 5, fig. 1.7), and

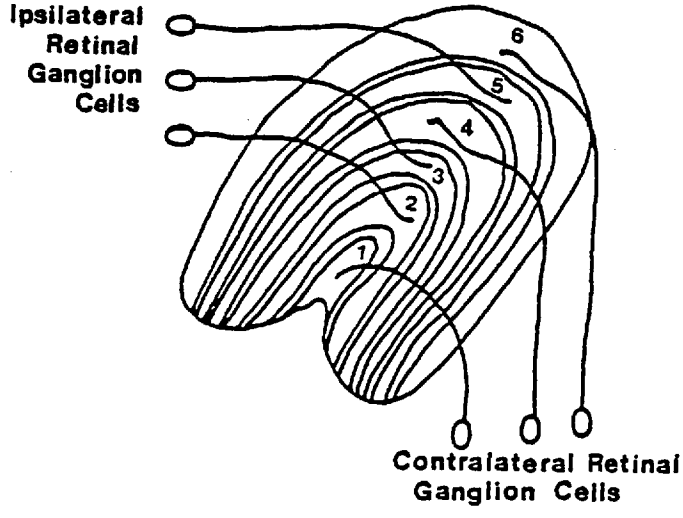

FIG.1.7 Innervation by Optic Tract Fibres into the Laminae of the L.G.N.

the contralateral eye projects to the three sheets, numbers 1, 4 and 6 (fig. 1.7). These projections are in register and as a result a single line through the six sheets can be drawn representing a single retinal projection point. The visual cortex receives this mapping of the retinal surface by input from the geniculo-calcarine tracts or optic radiations, fig. 1.6, and it is there that an interaction between the two visual half-fields occurs.

A.iii. The Visual Cortex

This is essentially a two-dimensional layer of cells, which spread out over the surface of the cortical hemispheres to which the visual pathways make their primary connections. It is also known as area 17, and projects itself to two adjacent cortical areas, the para- and pre-striate areas, referenced areas 18 and 19 (Hubel and Wiesel, 1965 and 1968).

The cortical mapping has been established in many different ways; degeneration of nerve fibres and neurones following surgical lesions, recording of electrical signals from single neurones (Talbot and Marshall, 1941; Daniel and Whitteridge, 1961) and more directly (Holmes, 1918, 1919; Teuber, Battersby and Bender, 1960) from subjects with brain damage localized in restricted regions of the cortex. Brindley and Lewin (1968) mapped out the area by direct electrical stimulation and generation of phosphenes. From these results it is found that area 17 contains a two-dimensional map of the visual half-field, with a separate map in area 18. It appears that the two maps are mirror symmetric around the point of connection between the two areas (Cowey and Rolls, 1974; Zeki, 1978b,c) and the boundary

represents the vertical meridian in the visual field. In all cases, there is a large cortical representation of the fovea - the area centralis, fig. 1.8.

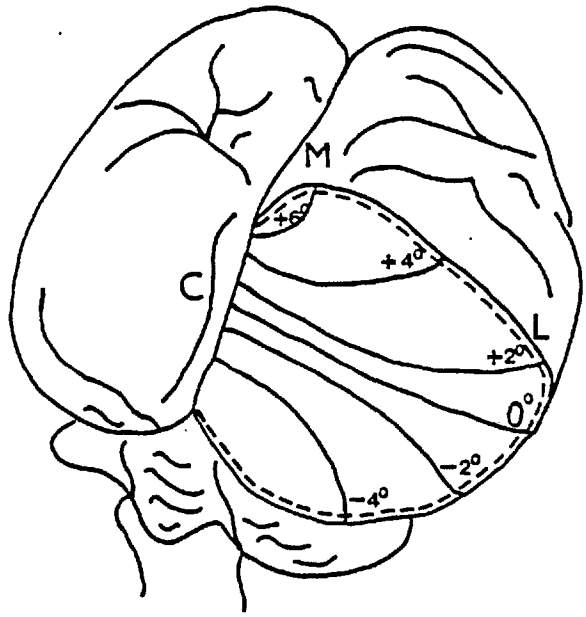

Mapping of the Visual Field onto the Visual Cortex (Area 17)

Fig. 1.8 Schematic view of lower rear right handside of primate brain. Continuous lines show the mapping of lines parallel to the horizontal meridian at different eccentricities (positive values refer to above horizontal meridian, negative values refer to lines lying below the horizontal meridian). C - Calcarine fissure, L - Lunate sulcus (after Levay et al., 1975)

Initially, damage to the striate visual cortex in man was thought to produce permanent blindness, but after studies on monkey, the striate cortices of which have been removed, light discrimination ability is re-acquired if a sufficient time interval elapses (Pasik and Pasik, 1966, 1971; Weiskrantz, 1963, 1972), and therefore permanent blindness may be caused by damage of non-striate areas.

The visual cortex is composed of six layers of neurones parallel

to and arranged in columns perpendicular to its surface (Hubel and Wiesel, 1962). Connections from the L.G.N. are made into Layer IV of area 17 (Wiesel, Hubel and Lam, 1974; Levay, Hubel and Wiesel, 1975) and in a similar manner to the L.G.N., all the layers are in register, but the banded structure established by the autoradiographic technique concludes that at this point the signals from the two eyes are still separate.

The transcallosal fibres connect the visual cortices in the two halves of the brain and cross from area 18 of the visual cortex on one side of the brain to terminate in area 18 of the other side. This connects the boundary layers between area 17 and 18, and therefore the two half-field representations of the visual field along the vertical meridian (Choudhury, Whitteridge and Wilson, 1965). Beyond this point there is still speculation as to the functions and the pathways of the visual system. Jones and Powell (1970) and Zeki (1973, 1978b,c&d) have investigated some. The projections which mediate colour reponses are thought to be found in area V4 (Zeki, 1978d), and also numerous fibres from the visual cortex extend to the superior colliculus responsible for direct eye movements and pupillary response (Schiller, Stryker, Cyander and Berman, 1974; Finlay, Schiller, and Volman, 1976; Mohler and Wurtz, 1976, 1977, 1978; Goldberg and Wurtz, 1972a,b, 1977; Wurtz and Goldberg, 1972a,b; Ward and Morgan, 1978).

B. Functional Organization of the Visual Sensory System

The functional organization of the retinal network signals at the level of the ganglion cells has been obtained mainly from investigations on fish, amphibia and reptiles. The responses of the

cells in this region are all amplitude modulated with respect to illumination level, and Werblin (1973) has proposed a functional model of the vertebrate retina based on the recordings of such classes of response in the mudpuppy retina (Werblin and Dowling, 1969; Werblin, 1970). From these recordings, the spatial organization of the visual system can be found and the extent of the receptive fields, which are defined as the retinal area within which any illumination will alter the cell's response. Consequently, cells were found to have centre-surround receptive fields, exhibiting on-off reponses between central and peripheral regions. Intracellular recordings in photoreceptors are limited due to their size, and are only possible in large outer segments (e.g., Borţoff, 1964; Tomita, 1965; Toyoda, Nosaki and Tomita, 1969; Baylor and Fuortes, 1970). The spectral functions of the electrical responses correlate well with microspectrophotometric data obtained with the carp (Oikawa, Ogawa and Motokawa, 1959; Marks, 1965; Tomita, Kaneko, Murakami and Pautler, 1967).

B.i. Horizontal Cells

Svaetichin (1953) recorded responses known as 'S' potentials from the horizontal cells in fish. At first they were thought to be the receptor responses, but this was later shown not to be the case. There are two classes of 'S' potentials. In both, the amplitudes of the electrical responses are graded with the illumination level and are more or less maintained during the period of stimulation (Svaetichin and MacNichol, 1958; Kaneko, 1970). The luminance or L-type response is always negative, i.e., in a hyperpolarizing direction, fig. 1.9a, whereas the other, the chromatic or C-type

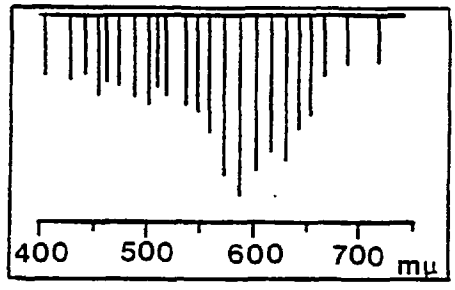

FIG.1.9.a L-Type of Response of unit in Fish Retina

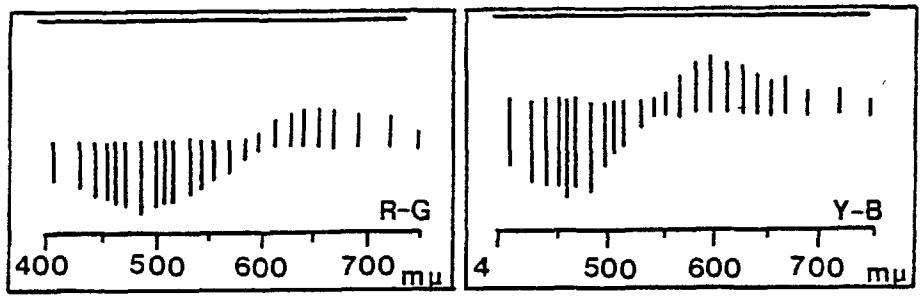

a. b.

FIG.1.9.b a.C-Type of unit - Red-Green variety.
b.C-Type - Yellow-Blue variety.

(after Svaetichin and MacNichol, 1958)

response, is positive or negative, in depolarizing or hyperpolarizing directions, depending upon the wavelengths of the light stimulus, fig. 1.9b. In general, the horizontal cells are classified according to the receptor from which they receive their input; rod horizontal cells are hyperpolarizing for all wavelengths and have the spectral sensitivity of rhodopsin, whereas cone horizontal cells are divided into L- or C-type. L-type again hyperpolarize to all wavelengths of stimuli, but the C-type are of two kinds, fig. 1.9, those which hyperpolarize for short wavelengths and depolarize for long

wavelengths and the reverse.

In fish, there is no interaction between the rods and cones at horizontal cell response level (Kaneko and Yamada, 1972; Ruddock and Svaetichin, 1973), although the horizontal cells do sum over their respective inputs. Some have restricted receptive fields, others extend over the whole retina, however, there is no antagonism between the different regions within the receptive field. This is also found true in the turtle retina (Lamb, 1976). Although horizontal cells may not be involved specifically in the transfer of visual information, electrophysiological evidence indicates they may control receptive fields of bipolar and ganglion cells by a lateral propagation of visual signals within the retina (Naka and Nye, 1970).

B.ii. Bipolar Cells

Horizontal cells and photoreceptors send signals to the bipolar cells, which from microelectrode recordings of fish cells (Kaneko 1970, 1971; Naka, 1977) and mudpuppy (Werblin and Dowling, 1969) are shown to have a centre-surround antagonistic receptive field organization. The central region shows either a hyperpolarizing or depolarizing response, whilst the surround is the reverse. Bipolar cells can also be subdivided into groups of colour and non-colour coded neurones.

B.iii. Amacrine Cells

Werblin (1970) showed that the concentric type of receptive field organization probably extends to the amacrine cells, which are driven by the bipolar cells and have similar receptive field properties. Werblin and Dowling (1969) found all responses in the mudpuppy

amacrine cells to be depolarizing in nature until a critical level at which spikes were produced. This spike response was elicited at onset or offset of the response, or at both onset and offset, dependent on the position of the stimulus (see fig. 1.10). Recently two types of

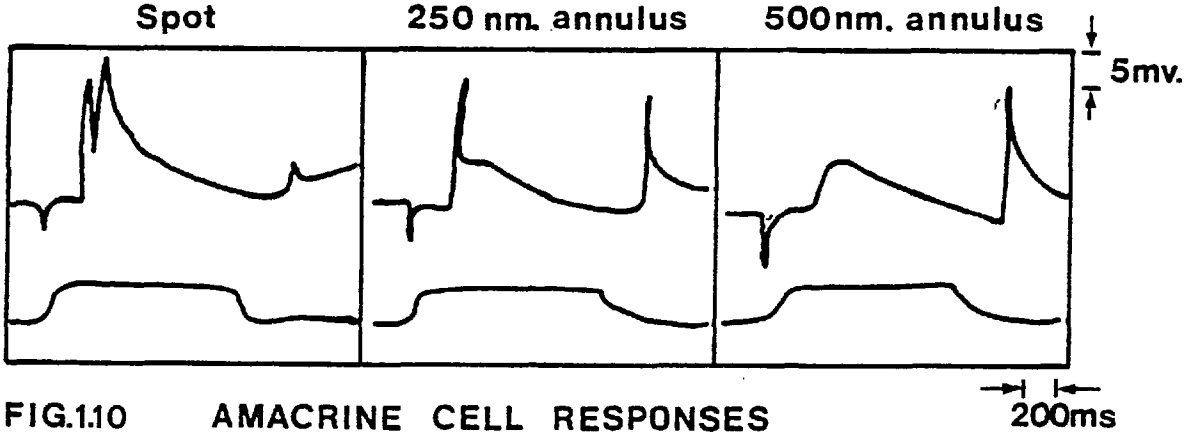

FIG.1.10 AMACRINE CELL RESPONSES
(Redrawn from Werblin & Dowling, 1969)

amacrine cells have been identified by Chan and Naka (1976) in the catfish, and Ruddock and Djamgoz (1978) provide evidence for mixed rod-cone input in cyprinid fish.

B.iv. Ganglion Cells

Responses from ganglion cells are far easier to isolate. Hartline (1938) first accomplished this by recording from the frog's optic nerve to show the fibres belong to three groups: 'on-off' fibres of two kinds, those which give a burst of spike discharge at illumination onset and a sustained discharge for the duration of the illumination, and those which respond only whilst the light is on, giving a spike discharge when it is extinguished. The third group are 'off' fibres, which respond only when the light is terminated. Granit and Svaetichin (1939) improved the method by recording from the cell

bodies themselves, and Kuffler (1952, 1953) made intracellular recordings from the cat retina to show that it is arranged into two circular and concentric zones, again antagonistic. This means that illumination of the centre of the field may excite the ganglion cell and elicit an 'on' response, whereas illumination of the periphery 'inhibits' the cell and elicits an 'off' response or vice versa (see fig. 1.11). Illumination of both regions together produces little or

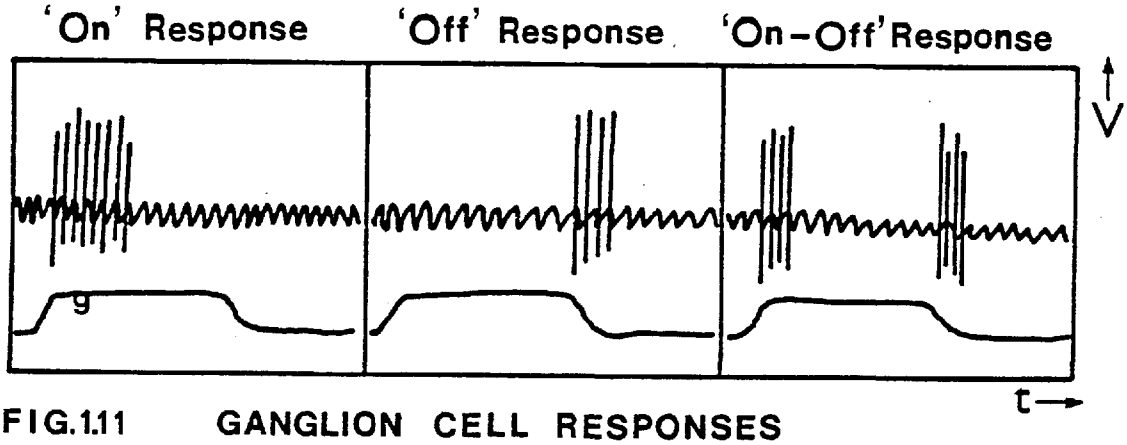

FIG.1.11 GANGLION CELL RESPONSES
(Redrawn from KUFFLER, 1953)

no response. Such ganglion cells are found in a number of species, e.g., rabbit (Barlow and Hill, 1963; Barlow, Hill and Levick, 1964; Barlow and Levick, 1965), rat (Brown and Rojas, 1965), cat (Brown and Wiesel, 1959; Wiesel, 1960), spider monkey (Hubel and Wiesel, 1960) and ground squirrel (Michael, 1966).

In animals with well developed colour vision, the antagonistic zones may be colour coded, that is, the centre of the field responds maximally to light of one wavelength, whereas the antagonistic periphery responds greatest to another wavelength (Wagner, MacNichol and Wolbarsht,1960), fig. 1.12. Ganglion cells with this complex activity have been identified in the gold-fish retina (Daw, 1967,

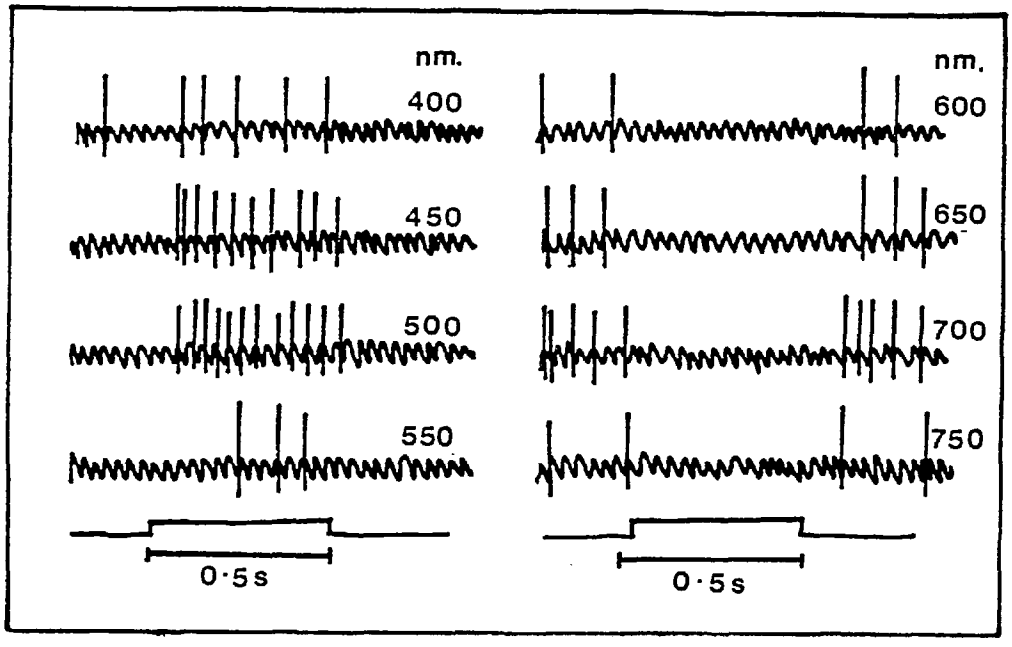

Fig. 1.12 Variation of response from a single ganglion cell with change in stimulus wavelength. (after Wagner, MacNichol and Wolbarsht, 1960)

1968), ground squirrel (Michael, 1968) and also in the monkey where the majority of receptive fields of the ganglion cells are not only concentrically arranged (Hubel and Wiesel, 1960; Gouras, 1969) but also colour-opponent, i.e., centre and surround regions are driven by different types of receptor input (Gouras, 1968; Marrocco, 1972; De Monasterio and Gouras, 1975; De Monasterio, Gouras and Tolhurst, 1975a,b and De Monasterio, 1978a,b & c).

De Monasterio and Gouras (1975) introduced three functionally distinct classes of ganglion cells in the rhesus monkey. These consist of a concentrically organized receptive field with sustained colour-opponent response produced by one cone input into the centre, and one or two cone inputs into the antagonistic surround, or broad-band cells which show transient responses and have concentric,

a. OPPONENT COLOUR CELLS with CENTRE-SURROUND arrangement

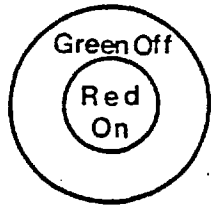

Wiesel & Hubel, 1966 (Type 1)
Michael, 1968 (Class 3)

b. OPPONENT COLOUR CELLS with NO CENTRE-SURROUND arrangement

Wiesel & Hubel, 1966 (Type 1)
Michael, 1963 (Class 1)
Norton, Spekreijse
Wolbarsht, Wagner, 1968

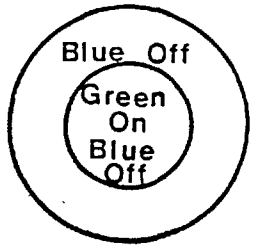

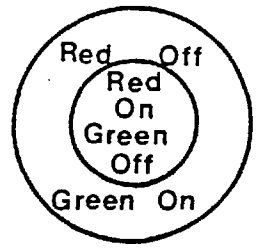

c.

Wagner, MacNichol & Wolbarsht, 1963
Michael, 1968 (Class 2)
Kaneko, 1972

d. DOUBLE OPPONENT CELLS

Daw, 1968
Hubel & Wiesel, 1968
Michael, 1970
Pearlman & Dow 1970

Fig. 1.13

antagonistic receptive fields, whose centre response is mediated by two cone inputs, and whose surround has a spectral sensitivity identical to that of the centre. Some cells which had different spectral sensitivities in the two regions were classified as colour-opponent broad-band cells. The third class of cells, however, did not have a concentric receptive field organization, and only gave a spontaneous response to moving stimuli. Figure 1.14 shows the

FIG.1.14

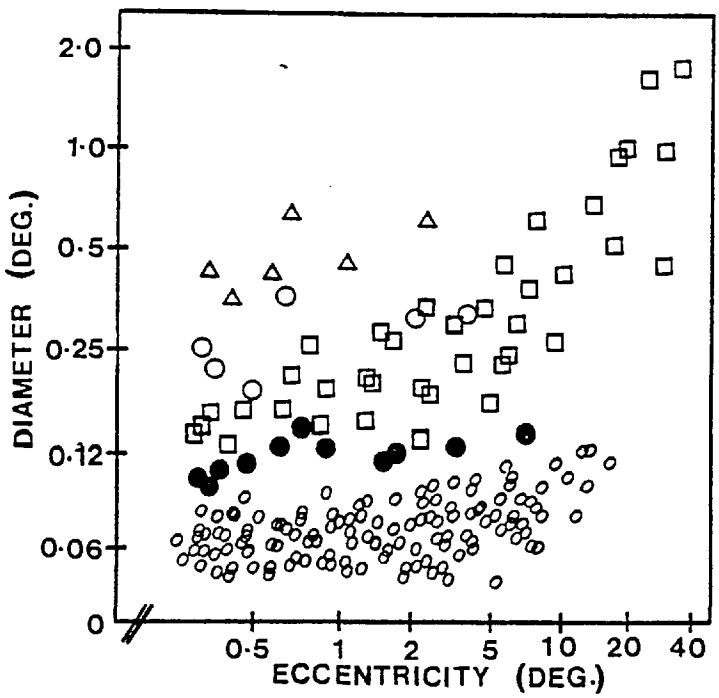

Distribution of Receptive-Field centres in relation to Retinal Eccentricity

Concentric Colour-opponent cells
°° - one cone input
● - two cone input
○ - Non-Concentric Colour-opponent cells
□ - Broad-Band cells
△ - Non-Concentric cells-phasic response

(after De Monasterio and Gouras, 1975)

relative distributions of these classes of cells from De Monasterio and Gouras (1975). A further study of the rhesus monkey by De Monasterio et al. (1975a,b) revealed a class of cells driven by all three cone types. In the majority of cases, the blue-sensitive cones opposed the red and green ones, but there were others found to have responses of the same sign at each end of the visible spectrum mediated by the red-sensitive cones, and a mid-spectral response of opposite sign from the green-sensitive cones (De Monasterio and

Gouras, 1977), furthermore, all those cells receiving a blue cone input were trichromatic (De Monasterio et al., 1975c). In macaque monkeys, however, all ganglion cells are driven by both rods and cones (Gouras and Link, 1966; Gouras, 1967) and the blue-sensitive cones show a tri-cone opponent arrangement (De Monasterio, 1979).

Enroth-Cugell and Robson (1966) classified cat ganglion cells into those exhibiting linear spatial summation of excitation over their receptive fields, and those which did not (X-and Y-cells responses, respectively). Subdivisions also exist for brisk, sluggish, transient and sustained response types (Cleland and Levick, 1974a,b). W-cells have been found (Stone and Fabian, 1966; Rodieck, 1973) which possess a non-concentric receptive field organization, and most probably project to the mid-brain region rather than to the L.G.N. Recently, similar cells with atypical receptive fields have been identified in the rhesus monkey (De Monasterio, 1979) from responses to moving coloured stimuli.

Morphological data can be compared with conduction time and receptive field size measurements (Boycott and Wässle, 1974; Cleland and Levick, 1974) to correlate with the functional classes (Wässle, Levick and Cleland, 1975).

Ganglion cells show a selective response for movement (Barlow and Hill, 1963; Barlow and Levick, 1965) and for linear stimuli of specific orientation (Levick, 1967) in the rabbit retina, which as yet has not been observed in cat or primate ganglion cells. Barlow, Fitzhugh and Kuffler (1957) and Barlow and Levick (1965) showed that antagonistic surround effects disappear for a fully dark adapted eye or when the stimulus is presented in brief flashes. This is

explained by the two different lateral conduction pathways (Werblin and Dowling, 1969; Naka and Nye, 1970), and is independent of the Purkinje Shift or the rod-cone excitation of ganglion cells.

B.v. The Lateral Geniculate Nucleus (L.G.N.)

Recordings from units in the L.G.N. of the cat (Hubel and Wiesel, 1962; Kozak, Rodieck and Bishop, 1965) and the monkey (De Valois, 1965; De Valois, Abramov and Jacobs, 1966; Wiesel and Hubel, 1966) suggest a similar functional organization to retinal ganglion cells, except for the ones which project to the superior colliculus. However, the response types found in the L.G.N. of the monkey (Wiesel and Hubel, 1966; De Valois, 1965) were not as numerous as those found in the ganglion cells (Hubel and Wiesel, 1960; Gouras, 1968). Only the first two classes of ganglion cell found by De Monasterio and Gouras (1965) are reflected in responses in the L.G.N. (Wiesel and Hubel, 1966).

The precise function of the L.G.N. in the primate visual system has never been fully established. It appears to be a relay station for visual signals transmitted along the visual pathways, as at present there is no evidence to suggest any re-organization of the information takes place at the L.G.N. level. However, there is some segregation of the inputs to the different laminae; colour-opponent ganglion cells appear to terminate in the parvo-cellular (inner) layers, whereas the broad-band cells terminate in the magno-cellular (outer) layers (Dreher, Fukada and Rodieck, 1976). Cells of the L.G.N. are classified in terms of response latency to visual stimuli (Marrocco, 1976); cells of the parvo-cellular layers are driven by the

tonic (slow-conducting) ganglion cells, i.e., off-centre colour-opponent responses as well as the sustained colour-opponent cells, whereas the phasic (fast-conducting) ganglion cells innervate the magno-cellular layers. The responses of the third class of ganglion cell (γ) -W cells have not been identified in the L.G.N. of the primate. Their properties appear to correspond with the recordings from the superior colliculus of the macaque monkey (Schiller and Koener, 1971; Goldberg and Wurtz, 1972), and therefore link the retina to the mid-brain region (Schiller, Stryker, Cyander and Berman, 1974). Binocular interaction is completely absent from the L.G.N. in primates, as is also the directional selectivity found at the L.G.N. cell level in rabbits (Levick, Oyster and Takakashi, 1969).

B.vi. The Visual Cortex

There is considerable difference in the organization of the receptive fields of the cells in the striate cortex as compared to those of the L.G.N.. Hubel and Wiesel (1959, 1962, 1965, 1968) classified the cells of area 17 of the cat and monkey visual cortex into circular concentric fibres, simple, complex and hypercomplex cells. A more recent classification by Schiller, Finlay and Volman (1976a,b,c,d & e) and Henry (1977) is of a more specific nature. Except for the class of circular concentric fibres, the others all have a different receptive field organization to peripheral neurones of the visual system. They are orientation specific, and do not have concentrically organized receptive fields. For the maximum response from a cell, the stimulus has to be correctly positioned within the receptive field. Most cortical cells appear to be binocularly driven

as they respond to stimulation of either eye, whereas retinal and L.G.N. cells respond only to stimulation of the eye with which they are associated. An ocular dominance is however found; some cells respond more favourably to stimulation of one eye than to that of the other. Some respond equally well to either eye and at the same time others appear to be monocularly driven. Another feature of cortical cells is that there are some which only respond if a disparity exists between the retinal images in the two eyes (Barlow, Blakemore and Pettigrew, 1967; Nikara, Bishop and Pettigrew, 1968). Optimal disparity varies from cell to cell, and therefore, different units encode objects at different distances (Blakemore, 1969, 1970) and different tilts (Blakemore et al., 1972).

a. Simple Cells

Simple cell responses reflect those of L.G.N. cells. They not only have an antagonistic centre-surround receptive field organization, but also parallel line boundaries. The most effective stimulus for this cell is one which corresponds in shape and orientation to this long, narrow central region with flanking surrounds, and an increased response occurs if this stimulus were to move across the borders of the antagonistic regions. The optimal rate of movement varies from cell to cell, but a summation occurs, since if the stimulus exceeds the width of the central region, invading the antagonistic flanks, then a reduction in overall response is obtained. An edge is the most appropriate stimulus for those cells in which only two receptive field regions are distinguishable. Figure 1.15 shows a possible scheme for explaining the organization of simple receptive

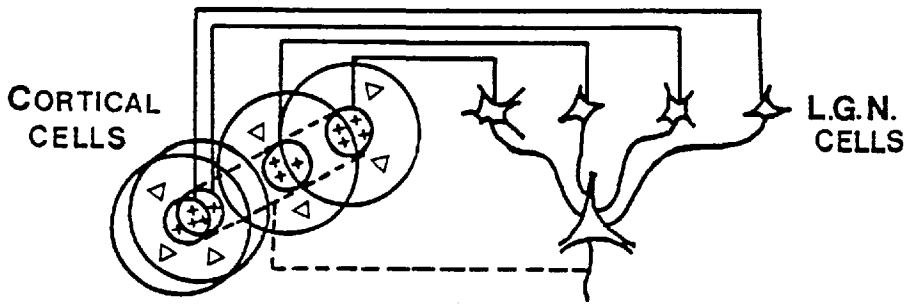

Fig. 1.15 Organization of Simple Receptive fields. A large number of L.G.N. cells have receptive fields with 'on' centres arranged along a straight line on the retina. All of these project upon a single cortical cell, and the synapses are supposed to be excitatory. The receptive field of a cortical cell will then have an elongated 'on' centre, indicated by broken lines in the diagram. (after Hubel and Wiesel, 1962)

fields (Hubel and Wiesel, 1962).

b. Complex Cells

These are unresponsive or give mixed 'on-off' responses to spots of light, but respond well to properly oriented slit stimuli, edges and dark bars. An improved response can be obtained by moving the stimulus, but unlike simple cells, it is the orientation and not the position of the stimulus with respect to the receptive field which is important to gain maximum response. A scheme was proposed by

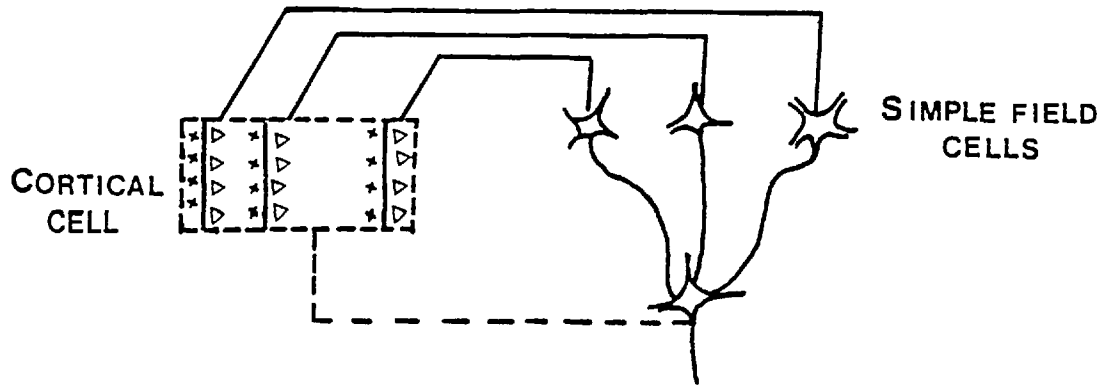

Fig. 1.16 Organization of Complex Receptive fields. A number of cells with simple fields project to a single cortical cell of higher order. Each projecting neurone has a receptive field arranged as shown; an excitatory region (+) and an inhibitory region (Δ) divided by a straight-line boundary. The boundaries of the fields are staggered within an area outlined by broken lines. Any vertical edge stimulus falling across this rectangle, regardless of its position, will excite some simple field cells, leading to excitation of the higher order cell. (after Hubel and Wiesel, 1962)

Hubel and Wiesel (1962), fig. 1.16, for explaining the organization of complex receptive fields.

c. Hypercomplex Cells

These form an even more specialized group. The lower order cells respond to slits, edges or dark bars providing the stimulus terminates within the region of the receptive field. The higher order ones respond to either of two preferred directions which are at right angles to each other, and termination of the stimulus is no longer

important. However, they are particularly sensitive to corners. Three alternative schemes, shown in fig. 1.17, have been proposed to explain the organization of the hypercomplex receptive fields (Hubel and Wiesel, 1965).

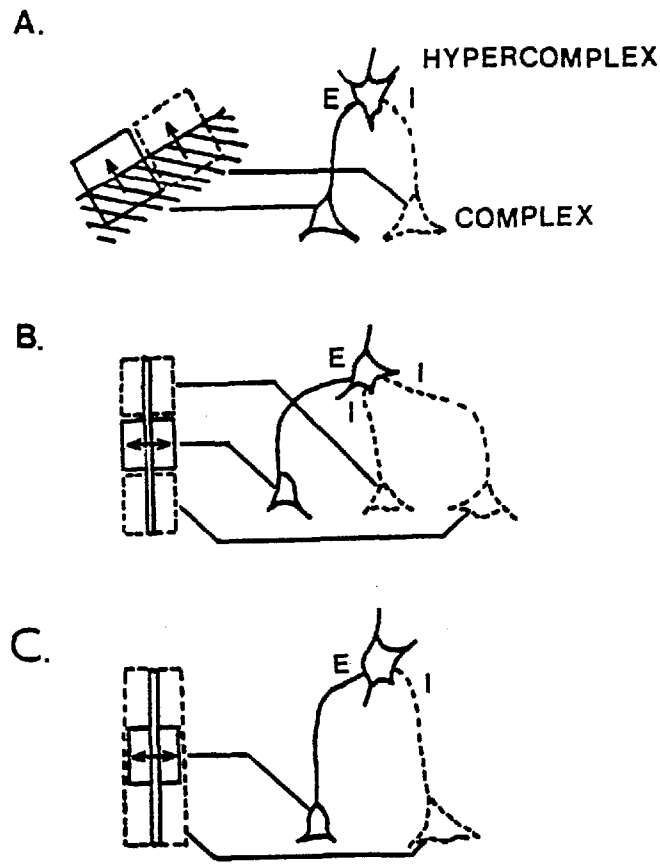

Fig. 1.17 Explanation for Hypercomplex cells which respond to bars of specific length.

i. The cell receives excitatory input from a complex cell whose vertically orientated field is indicated to the left by a continuous rectangle; two additional complex cells, inhibitory to the hypercomplex cell have vertically oriented fields flanking the first one above and below, shown by the rectangles outlined with a broken line.

ii. Alternatively, the inhibitory input is supplied by a single cell with a large field indicated by the entire interrupted rectangle.

In either case, a slit covering the entire field would be ineffective, and in the second alternative, a slit covering, but restricted to the centre region, would be too short to affect the inhibitory cell.
(after Hubel and Wiesel, 1965).

Electrophysiological recordings and intra-cellular staining by Van Essen and Kelly (1973a,b) and Kelly and Van Essen (1974) correlate the simple cell type responses with the stellate cells, which have spherical dendritic fields, whereas the complex and hypercomplex cells have properties which correlate well with pyramidal cells and have elongated receptive fields. Campbell, Cooper and Enroth-Cugell (1969), and Campbell, Cooper, Robson and Sachs (1969) showed that the simple cells of the cat and monkey are activated specifically by gratings of an optimum spatial frequency and orientation (Campbell, Cleland, Cooper and Enroth-Cugell, 1968). Evidence of this in man has been obtained by Campbell and Maffei (1970), and indications for lateral interactions between frequency specific neurones in the cat have been found (Blakemore and Tobin, 1972).

Investigation of the properties of neighbouring cells led Hubel and Wiesel (1963 and 1968) to propose a columnar organization of cells with the same receptive field orientation. Cells were also divided into columns of the same ocular dominance (Hubel and Wiesel, 1962 and 1965), same movement response, same preferred stimulus characteristics, and to a lesser extent same colour selectivity (Wiesel and Hubel, 1966). These specializations were found to change in continuous fashions in the recordings from adjacent columns and from directions parallel to the surface of the cortex or from scanning across the columns.

Colour selective responses without any orientation selectivity are found for approximately 28% of the cells with foveal receptive fields (Boles, 1971; Poggio et al., 1971; Gouras, 1972 and 1974; Dow

and Gouras, 1973; Gouras and Padmos, 1974; Yates, 1974). Yates also distinguished hue detecting cells, as postulated by Estévez (1979). Dow (1974) found colour cells in the middle layers of the cortex to have all three cone inputs, and give a response to chromatic content irrespective of the wavelength with active inhibition to luminous contrast. Motokawa et al. (1962) have found a number of spatially opponent (on-off) cells in the monkey striate cortex which were wavelength specific, and suggested that information regarding shape and colour are transmitted together. However, the opposite conclusions were reached by Anderson et al. (1962), who observed that most of the responses from cortical cells are of the narrow spectral band non-opponent type. Hubel and Wiesel (1968), recording mainly from cells in the para-foveal region, found 25% of simple cells and 7% of complex and hypercomplex cells in the monkey striate cortex to have colour-opponent properties. The simple cells had red-orientated centres flanked by green-sensitive surrounds. Gouras (1972) showed that Hubel and Wiesel's (1968) observation of the probability of a cell having colour-selective properties, decreasing as its spatial complexity increased, was not necessarily true. Trichromatic responses for units of the striate cortex are shown in graded potential recordings from the surface of the foveal striate cortex (Padmos and Van Norren, 1973; Gouras and Padmos, 1974). This agrees with the behavioural data of Sperling and Harwerth (1971), and graded potential recordings in man yield spectral sensitivities of rods and cones consistent with the psychophysical data (Estévez, Spekreijse, Van den Berg and Cavonius, 1975; Regan, 1975).

A hierachical arrangement of cells in the visual cortex has been put forward by Hubel and Wiesel (1962 and 1968), in which simple cells represent the first stage, and modify the incoming signals from the L.G.N. The proposed wiring diagram, shown in fig. 1.15, (Hubel and Wiesel, 1962) accounts for the fact that the widths of cortical receptive field centres have the same order of magnitude as the diameters of the geniculate receptive field centres. In a similar manner, a complex field may receive its afferents from a set of simple cells (fig. 1.16), and likewise a hypercomplex field from a set of complex cells (fig. 1.17). These studies showed that the single unit activity found in cat and monkey cortex is highly specialized compared with simple response projections of the receptors. Nevertheless, these units only represent the initial stages in the transformation of the complex visual information, and the continuation of the processing is still being investigated.

The ability to perceive depth, defined as stereovision, results from an overlapping of the visual fields in the two eyes. These fields are slightly displaced on the two retinae, due to the separation of the two eyes. A disparity is therefore introduced between the images and the actual object viewed. Barlow et al. (1967) gave evidence of depth-sensitive cells in the cat cortex when they showed that some cells responded better to a binocular disparate input than to a monocular stimulus, i.e., binocularly presented, non-corresponding images produced more excitation than one correctly positioned monocular image (fig. 1.18). The range of disparities for optimum response varied in horizontal and vertical directions.

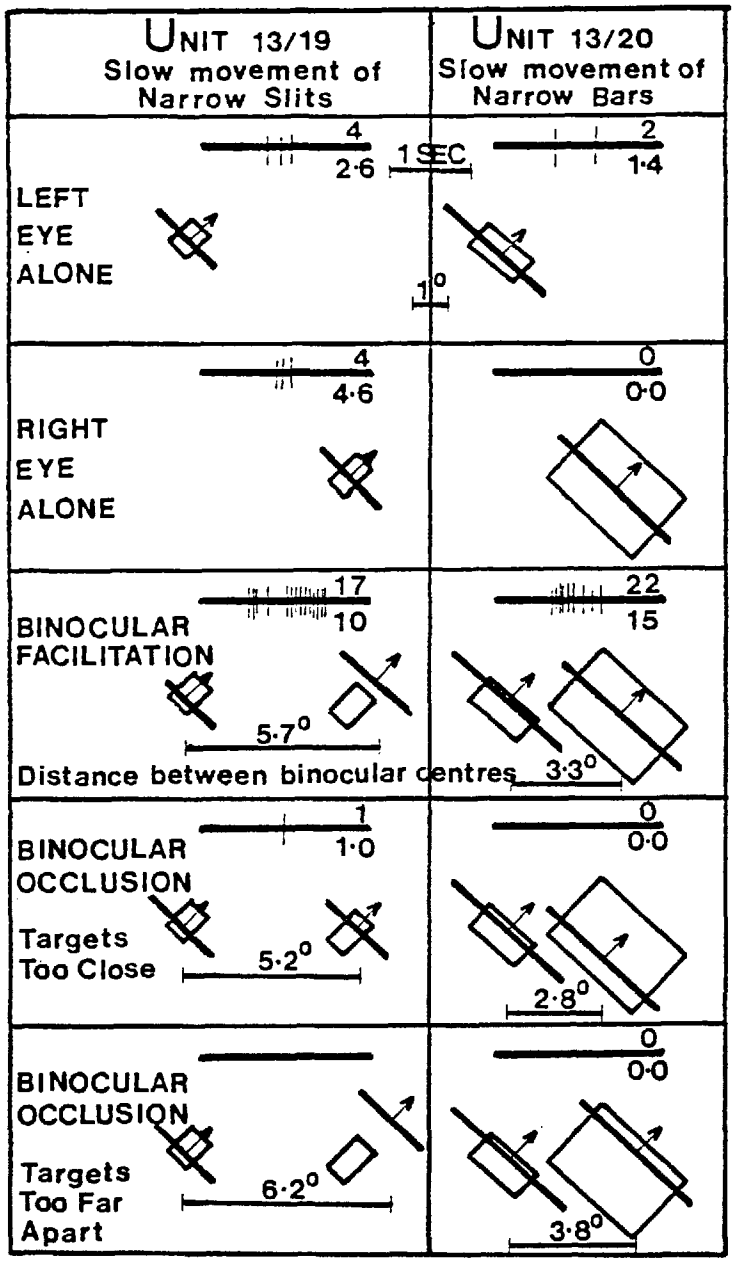

Fig. 1.18
Binocular interactions showing that facilitatory responses occur at different disparities in two cortical neurones from the same cat. Consecutively studied units had receptive fields lying close together in the visual field and the same axis orientations. Each box shows a sample spike record; number of spikes (top) and average number (over 5 repetitions) of spikes (bottom). The positions of the stimuli and the minimum response fields on the tangent screen are illustrated diagramatically. (after Barlow et al., 1967)

Cells sensitive to depth in area 18 of the monkey have been reported by Hubel and Wiesel (1970a), where half of the cells had characteristics corresponding to binocular depth perception, with the rest responsive to stimulation of either eye. The former cells give maximum response for similarly oriented shapes presented to either

eye, but each cell has a specific disparity. Blakemore (1970), fig. 1.19, revealed a two-column arrangement, a constant depth column,

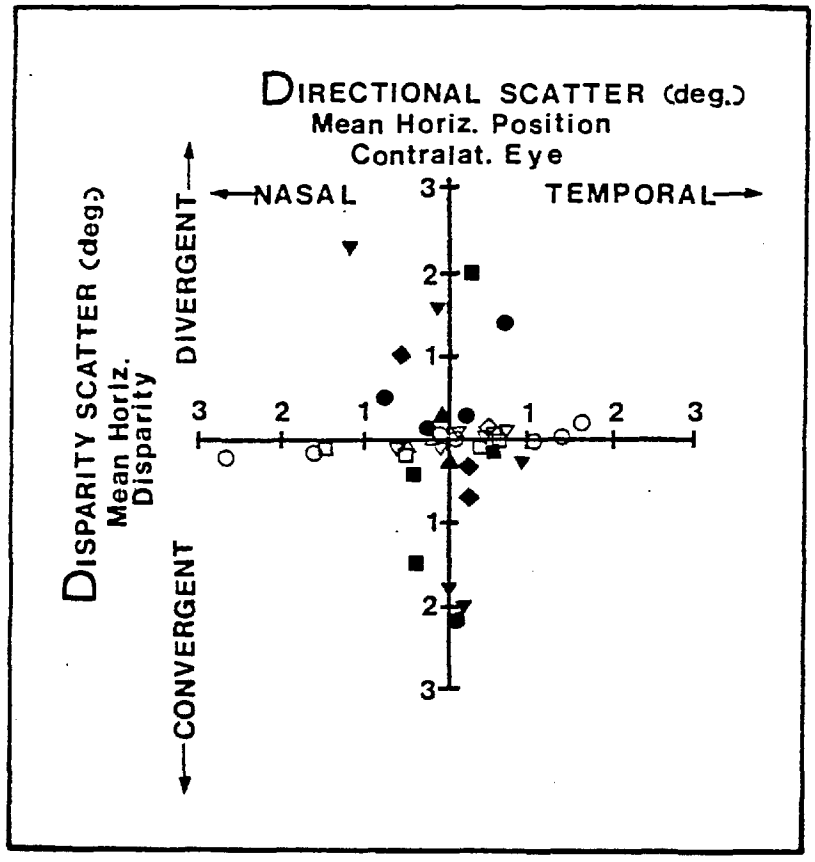

Fig. 1.19
Diagram representing the variation of depth and oculocentric direction within each column sample. Variation in disparity (ordinate) is plotted as a function of oculocentric direction variation. Filled symbols are for direction columns, open ones are for depth. Depth columns have a larger variation in eccentricity from unit to unit than variation in depth, thus they cluster around the abscissa. Direction columns show less scatter of response field position in the contralateral eye than variation of horizontal disparity, and group around the ordinate. (after Blakemore, 1970).

in which cells corresponded to a sheet in visual space subtending a few degrees of visual angle and located at a particular depth, and a constant direction column, where cells are mainly responsive to a cone of visual space directed towards the contralateral eye. Blakemore and Pettigrew (1970) give evidence of a contralateral eye dominance from an investigation of neurones in area 17 of the cat. This may be the result of a more accurate retinal cortical mapping for the contra -

as opposed to the ipsilateral eye.

C. The Psychophysical Approach

Direct electrical responses of the human visual system are difficult to record, and therefore it is necessary to adopt a psychophysical approach, where a subject is instructed to adjust a light stimulus to a chosen response criterion. In this type of measurement, the subject indicates his ability to distinguish between two stimuli by setting the threshold of a test to the level of its background or by matching colour, brightness or spatial characteristics of two separate stimuli.

C.i. Visual Acuity

Visual performance is measured in terms of the resolving power for spatially structured stimuli, which is defined as visual acuity. There are a number of tests designed to obtain a measure of acuity, e.g., the detection of bright objects against dark backgrounds or vice versa. Another series of tests include standardized alphabet letters (Snellen, 1862) or the Landholt ring (Landholt, 1889). These yield acuities of 22" of arc (Schlaer, 1937) for the observer, but are difficult to interpret. The best test is with a pair of bright or dark lines, or rows of alternate dark and light bars. The advantage of these tests is that each element is identified singly, but the presence of neighbouring lines can impair discrimination. With this method and moderate illumination levels, visual acuity is 1' of arc, and indicates that it is not limited by photoreceptor size (0.5').

Grating acuity does depend upon a number of parameters, e.g., pupil diameter, fig. 1.20, illumination level, fig. 1.21, and retinal

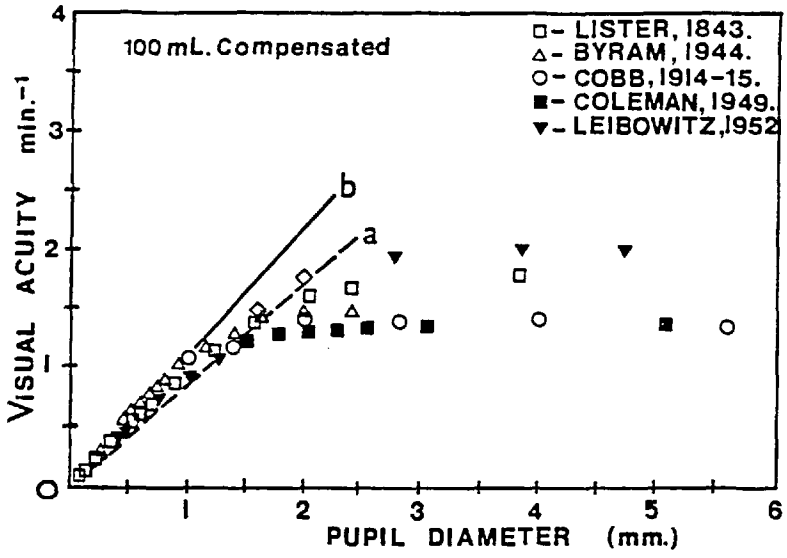

Fig. 1.20
Data to show the effect of pupil diameter on visual acuity. Straight lines represent a. the Rayleigh Limit, and b. the Dawes Limit (attributable to diffraction).

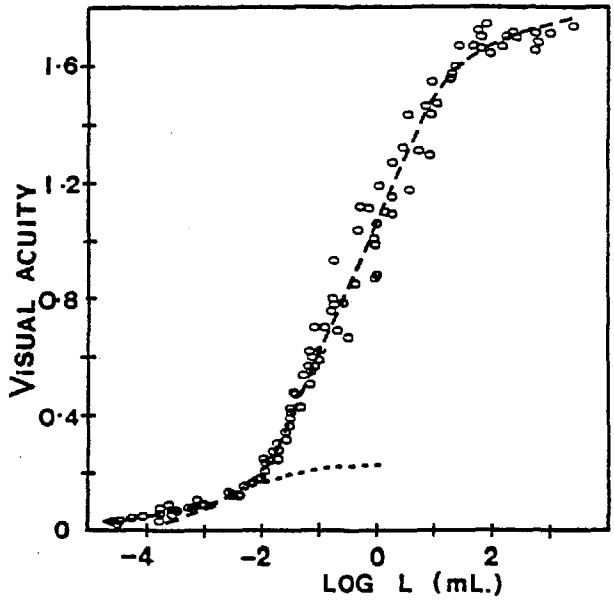

Fig. 1.21
König's data showing the relationship between visual acuity, and illumination level. Shallow curve is the component due to rods, and the upper curve is that for cones. (after Hecht, 1934)

position (Østerberg, 1935). Initially, increasing the pupil size, fig. 1.21, increases visual acuity to a maximum value, but a further increase only results in a 'fall-off' (Leibowitz, 1952). This is the result of the change in the point spread function and aberrations of the eye (Westheimer, 1963). The variation of visual acuity with

illumination, fig. 1.21, is due to two functions; at high illumination levels, cones are functioning, whereas at lower illumination levels the function is characteristic of the rods. Confinement to the central region of the field, or by use of red light, means only the cones in the fovea are functioning, and therefore the relationship between visual acuity and intensity is single and continuous (Schlaer, 1937).

C.ii. The Visual Modulation Transfer Function (M.T.F.)

The application of Fourier analysis to optical systems pioneered by Duffieux (1946) assumes that the system is linear, i.e., superposition holds, and thus the imaging properties can be defined in terms of its frequency response characteristic or point spread function. This condition is satisfied by passive optical systems, but not, however, by the neural pathways of the visual system. The visual system is assumed to be linear for near threshold signal levels, and the M.T.F. is obtained using sine-wave grating stimuli for which the subject adjusts the modulation depth, C_t, to a 'just-no-longer' detectable value for different spatial frequencies. Earlier determinations of the visual system's M.T.F. were obtained by Selwyn (1948), Schadé (1956), Oone (1959) and Westheimer (1960). More recent investigations have been conducted by Patel (1965), Daitch and Green (1969), Van Nes and Bouman (1967) and Meteren and Vos (1972), who obtained the M.T.F.'s at several different mean illumination levels (see fig. 1.22). This figure also shows that at high spatial frequencies, the visual system acts like a low-pass filter, and at higher values of mean illumination level, there is a low frequency

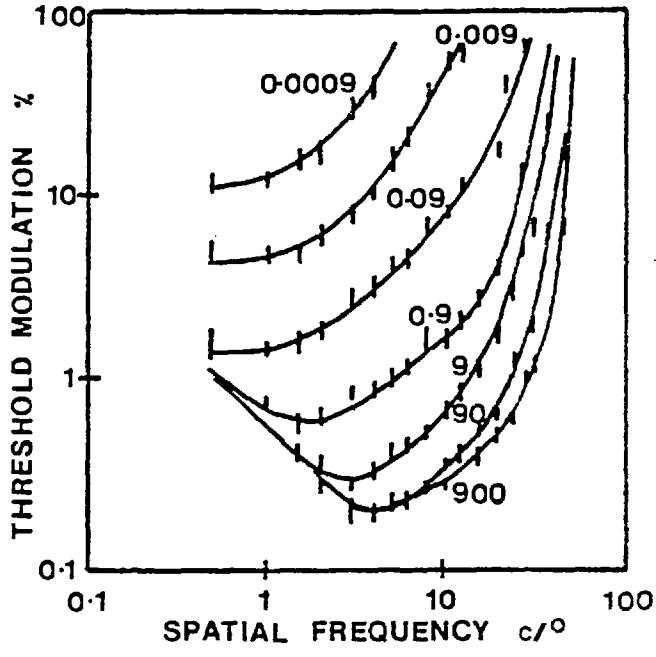

Fig. 1.22
The threshold modulation depth for visual detection of a one-dimensional sine-wave grating stimulus of spatial frequency, fc/o. Each set of data points connected by a continuous line refers to a single space average illumination level of the grating pattern, these values are shown in trolands alongside the relevant curve. (after Van Nes and Bouman, 1967)

attenuation, which is atypical of optical systems and may be the result of visual processing of the retinal image associated with some inhibitory interaction (Lowry and De Palma, 1962). The lower the illumination level, the lower the frequency where the maximum occurs, usually between 4 - 8 cycles per degree (Maffei and Fiorentini, 1973). However, by flickering (Robson, 1966) or moving the pattern across the retina (Van Nes, Koenderink, Nas and Bouman, 1967) the low frequency attenuation disappears.

This data refers to the visual system as a whole, i.e., the M.T.F. of the ocular media of the eye obtained directly from the image formed on the retina, as well as the neural units involved in the processing of the visual image. The frequency response characteristics are obtained by a Fourier transform of this distribution. However, Campbell and Gubisch (1966) showed visual performance to be limited by pupil diameter. Figure 1.23 shows the

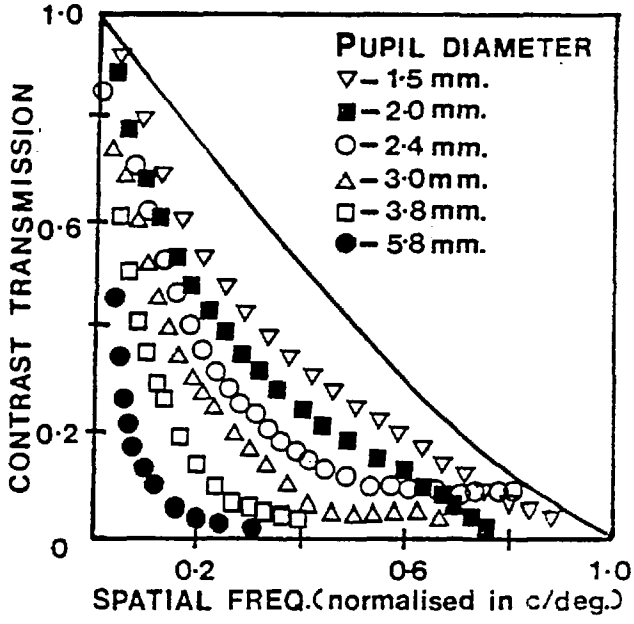

Fig. 1.23
M.T.F. of the ocular media of the human eye: each symbol refers to a particular pupil diameter as indicated. The continuous function denotes the M.T.F. of an ideal diffraction limited system (from Campbell and Gubisch, 1966).

ideal diffraction limited optical system's response compared with that of a pupil diameter, d. A large pupil diameter produces aberration effects and a smaller pupil, diffraction effects.

The M.T.F. can be divided into two components; one due to the ocular media, M_{OC}, and the other due to the neural pathways, M_{NEUR}, hence:-

$$M_{TOTAL} = M_{OC} \times M_{NEUR} . \qquad \text{Eq. 1.1}$$

M_{NEUR} can be obtained directly when interference fringes are formed on the retina, and thus by-pass the optics of the eye. Campbell and Green (1965) show that the overall characteristics of the neural system are similar to those of the whole visual system, and exhibit a low frequency reduction. Arnulf and Dupuy (1960) measured the transfer function of the ocular media by matching the contrast of interference fringes on the retina against an external grating pattern, which was imaged by the eye. The difference in the physical modulation depth of the two patterns required to give the same

appearance produced the transfer function of the ocular media. The results are consistent with those of Campbell and Green (1965); except for light scattering effects which were excluded from the latter estimate of M_{NEUR}.

C.iii. Detection of Threshold Targets

The M.T.F. of the visual system is only of value if it predicts performance in response to targets of known spatial frequency content, and it appears that it may be limited to threshold performance. Campbell and Robson (1968) determined threshold contrast levels for square-wave, sine-wave, rectangular and saw-tooth grating profiles. This showed that for each target category, the threshold response level was determined by the modulation depth of the fundamental component of the Fourier expansion of the test pattern distribution. This prompted Campbell and Robson to postulate the existence of linear and independent mechanisms in the visual system, each responding to a limited range of spatial frequency.

Sachs, Nachmias and Robson (1971) tested the hypothesis by determining the threshold sensitivity for the detection of a sine-wave test grating of fixed spatial frequency, f_1, in the presence of a second grating of spatial frequency, f_2, and of sub-threshold illumination level. The probability of detection of the test grating was measured as a function of its mean illumination level and for different values of f_2. The results showed that sine-wave gratings of different spatial frequencies are detected independently unless the frequencies differ by only a relatively small amount. This is consistent with the model of parallel independent spatial frequency

selective channels. Similar experiments were performed by Kulikowski and King-Smith (1973), who investigated the interaction between subliminal and test target patterns, and Stromeyer and Klein (1975), who investigated interactions with frequency, rather than amplitude, modulated grating patterns and concluded that interactions can occur between frequency components which differ by a factor of three. Henning, Hertz and Broadbent (1975) used complex gratings and although their data was consistent with the logarithmic relation between stimulus illumination level and the resulting visual signals, they could not predict an interaction between different frequency terms due to non-linear visual response characteristics, and therefore discounted the model for narrow-band spatial frequency selective channels.

C.iv. Spatially Structured Stimuli and Adaptation Effects

Ricco (1877) provided the first indication of spatial summation in human vision. He found that for circular fields up to 42'40" in diameter, the threshold luminance is determined by the total light within the stimulus rather than the intensity at any one point. More recent studies of areal summation (Graham et al., 1939; Blackwell, 1946) have revealed only positive summation at scotopic and photopic levels. This leads to the single detector hypothesis (Kincaid et al., 1960; Blackwell, 1963), where the contributions of each retinal element in detection is a decreasing function of the distance of the element from the centre of the stimulus image. However, increment threshold studies have now revealed that the detection of a test stimulus in the presence of an inducing strip can produce either

summation or inhibition, which is consistent with the physiological findings of Kuffler (1953) and Hubel and Wiesel (1962 and 1965). A receptive field organization with positive and negative regions was postulated by Westheimer (1965 and 1967), after he had found that contrast threshold detection for a small test spot on a circular background of variable size increased to a maximum and then decreased. Other antagonistic responses have also been obtained, e.g., the disinhibition between two thin lines (Fiorentini and Mazzantini, 1966), between rectangles of various sizes (Thomas, Padilla and Rourke, 1969) and also squares (Bagrash, Kerr and Thomas, 1971).

The existence of mechanisms in the visual cortex, which respond preferentially to bar or edge shaped stimuli of specific orientation in electrophysiological studies, correlates with psychophysical investigations. The first reported experiments for these effects were by Gibson (1933), who showed that after prolonged viewing of a series of parallel and equally spaced curved lines, the subsequent viewing of straight lines produced an appearance of curved lines in the opposite direction. This is a transient adaptation effect, but McCollough (1965) showed that a colour-specific adaptation effect can persist for a period of days.

These adaptation effects to straight lines are interpreted as evidence for detection mechanisms tuned to respond selectively to bar elements of specific width and orientation (Gilinsky, 1968). Thomas and Kerr (1971), Kerr and Thomas (1972) and Bagrash (1973) showed the adaptation effect was also true for rectangular and circular stimuli, as the visibility was subsequently decreased for stimuli of similar shape and size after adaptation. Selective adaptation can also show

other distinct optical features, i.e., tuning for line lengths (Nakayama and Roberts, 1972) or edges (Tolhurst, 1972). However, the most widely investigated adaptation effect is that of the contrast threshold elevation effect.

C.v. The Contrast Threshold Elevation Effect (C.T.E.)

Aspects of this effect were first reported by Gilinsky (1968), Pantle and Sekuler (1968 and 1969) and Blakemore and Campbell (1969 a,b). Figure 1.24 illustrates this effect.

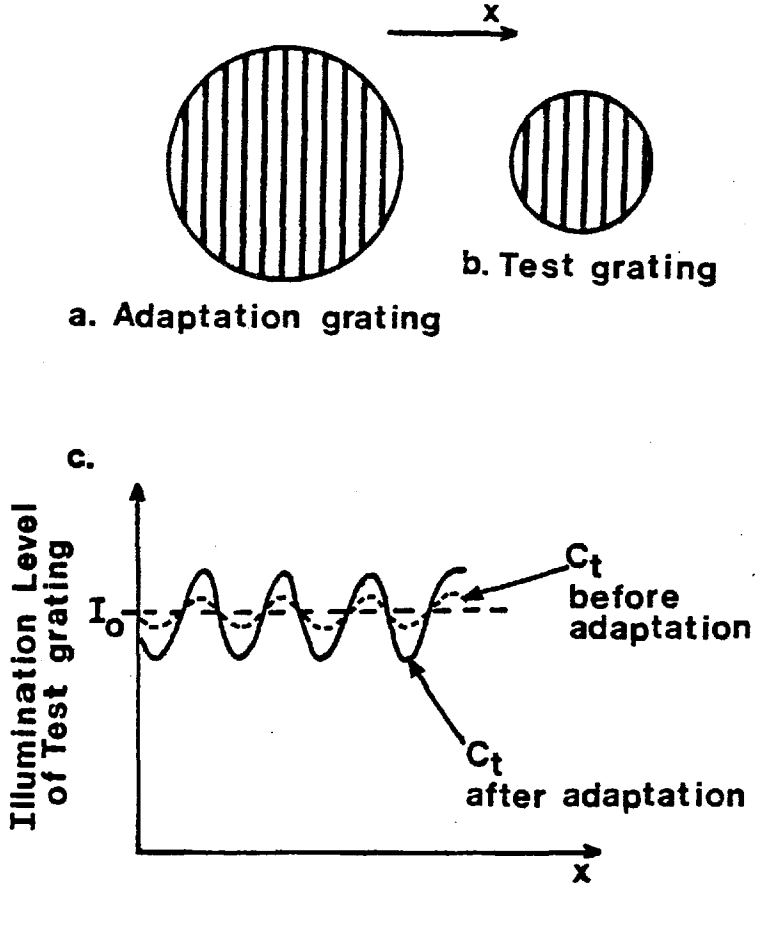

Fig. 1.24 To show the increase in contrast threshold level of a sine-wave test grating following adaptation to a similar grating of high contrast.

The subject adapts for a period of two minutes to the high contrast adaptation grating of fixed orientation and spatial frequency, $fc/^{o}$, fig. 1.24a, during which time he is instructed to allow his gaze to wander freely over the grating, thus avoiding any after-images. This grating is subsequently replaced by a low contrast test grating of similar orientation and spatial frequency, $fc/^{o}$, fig. 1.24b, but of slightly reduced dimensions to ensure that the area which is tested is that which has been adapted. The subject adjusts this grating to its contrast threshold. It is found that this contrast level is higher than that which is required for the contrast threshold of the test grating, after a similar adaptation period to a uniform field of the same mean illumination as the high contrast adaptation grating, fig. 1.24c. The amplitude of the difference of these two contrast threshold levels is taken as a measure of the effect of the adaptation grating on the detection of the test grating, and denoted, Δ.

This effect has several characteristics:-

1. The effect is transient. The increase in the contrast threshold level required, following adaptation to the grating, decays back to its pre-adaptation value over a period of a minute.

2. The effect is frequency (Blakemore and Campbell, 1969a,b) and orientation (Gilinsky and Doherty, 1969; Maudarbocus and Ruddock, 1973b) specific. The results imply that the mechanism responsible for detection of a given test grating can be influenced by only a limited range of adaptation gratings, and the maximum effect is obtained when both test and adaptation have the same fixed orientation and spatial frequency, $fc/^{o}$.

The selectivity of the response mechanism correlates with the

observed response of single neurones in the visual cortex. Maffei, Fiorentini and Bisti (1973) showed that simple cells subject to stimulation by high contrast stimuli of the correct orientation and bar width adapt in a similar manner to the psychophysical effect.

3. The effect can be binocularly transferred (Blakemore and Campbell, 1969b; Maudarbocus and Ruddock, 1973b), and thus the adaptation effect is a centrally arising property as only cortical neurones are binocularly driven. The contrast threshold elevation effect is also a function of the adaptation contrast, fig. 1.25, and adaptation time, fig. 1.26. It can be obtained irrespective of the

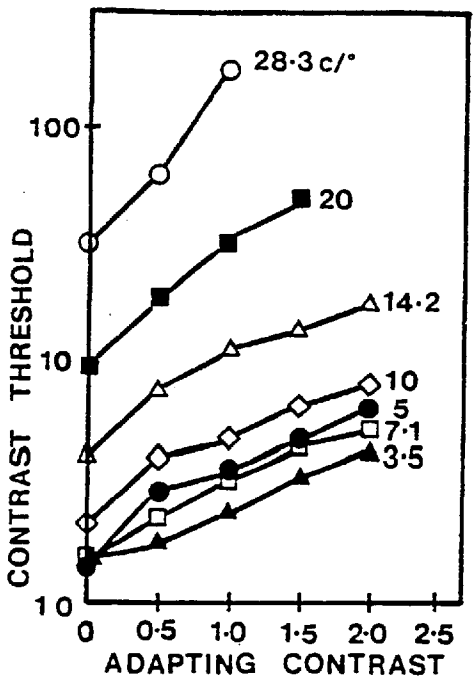

Fig. 1.25
The effect of adapting contrast for a number of spatial frequencies (adapting and test gratings equivalent).

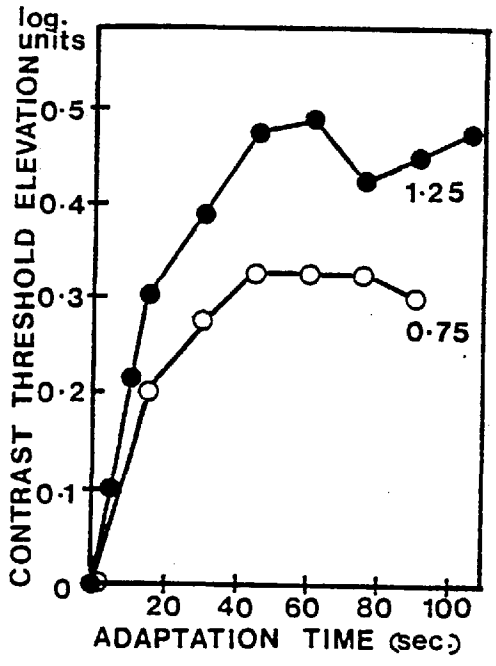

Fig. 1.26
The effect of adapting time for a 15c/o adaptation grating at two contrast levels above threshold.

(after Blakemore and Campbell, 1969b)

retinal location, providing the gratings are resolvable (Maudarbocus, 1973; Maudarbocus and Ruddock, 1973b), and is non-wavelength selective (Maudarbocus and Ruddock, 1973a). This corresponds with the uniformity of the change in the visual field observed in the organization of the primate visual cortex (Hubel and Wiesel, 1968 and 1974).

By measuring the contrast threshold elevation effect for a sinusoidal test grating for a series of spatial frequency sine-wave adaptation gratings presented to the non-test eye, a tuning curve is obtained, fig. 1.27. From this Maudarbocus and Ruddock (1973b)

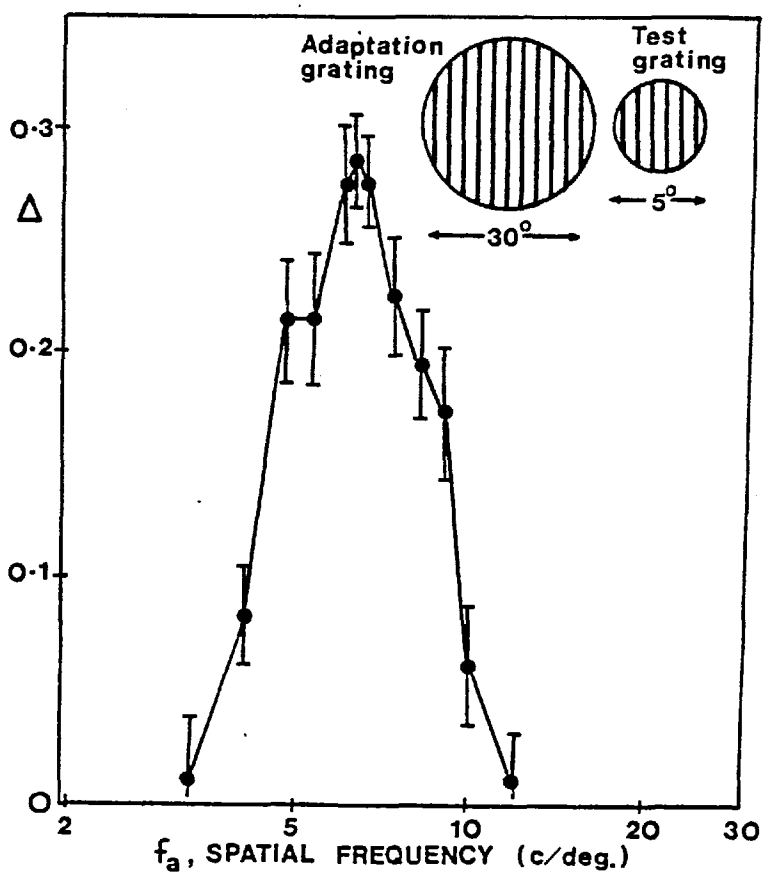

Fig. 1.27
Contrast elevation values, Δ, for a sine-wave test grating, 6.1c/o, plotted against the spatial frequency, fa, of the 100% modulated sine-wave adaptation grating. (after Maudarbocus and Ruddock, 1973b)

computed the corresponding line spread function. The line spread functions were always similar and had a principal maximum lying

between two minima, fig. 1.28. The separation of the minima was

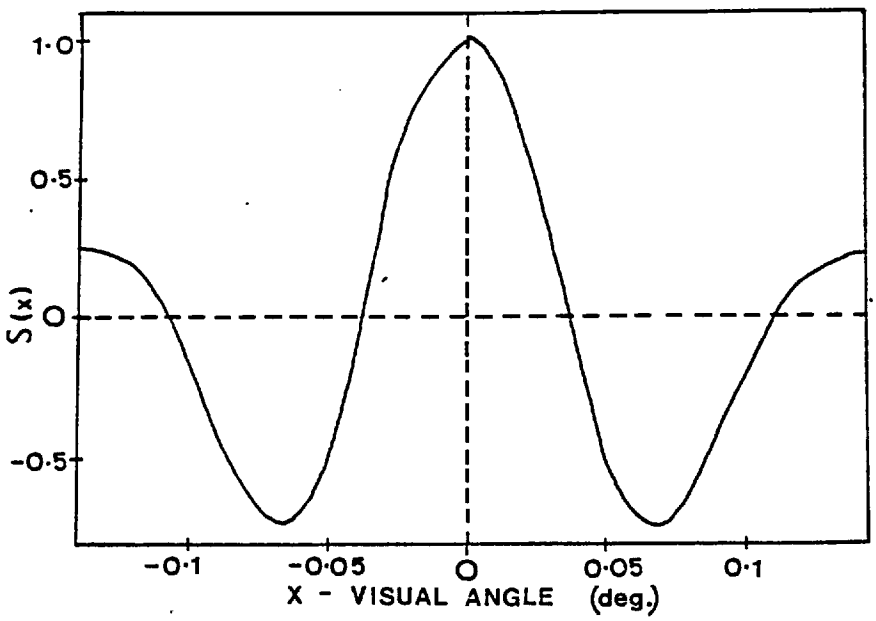

Fig. 1.28 The line spread function computed from data of fig. 1.27 representing the receptive field distribution. (after Maudarbocus and Ruddock, 1973b).

equivalent to one cycle of the test grating represented by the function. The amplitudes of the second and higher harmonics of the filtered sinusoidal test grating were almost as large as that of the fundamental for large input modulation depths, but no elevation in threshold was recorded after adaptation to these higher harmonics. The line spread function represents the excitatory and inhibitory regions of the receptive field organization compared to that of a simple cell, but conflicts with the theory of Fourier analysis in the visual system.

However, simultaneously adapting the two eyes results in an inhibition in the contrast threshold elevation effect rather than a summation. This is even more pronounced when the two adaptation gratings are of different spatial periodicity (Ruddock and Wigley, 1976). Evidence for binocular inhibition in cells of the cat visual cortex caused by non-matching stimulation of the two eyes has been

shown (Henry, Bishop and Coombs, 1969).

C.vi. The Perceived Spatial Frequency Shift Effect

A second adaptation effect was reported by Blakemore and Sutton (1969) and by Blakemore, Nachmias and Sutton (1970). In this, adaptation to a high contrast grating produces a subsequent shift in the apparent spatial frequency of a test grating. The apparent shift is in a direction to increase this displacement between the two frequencies in the two patterns, fig. 1.29. No shift occurred if the

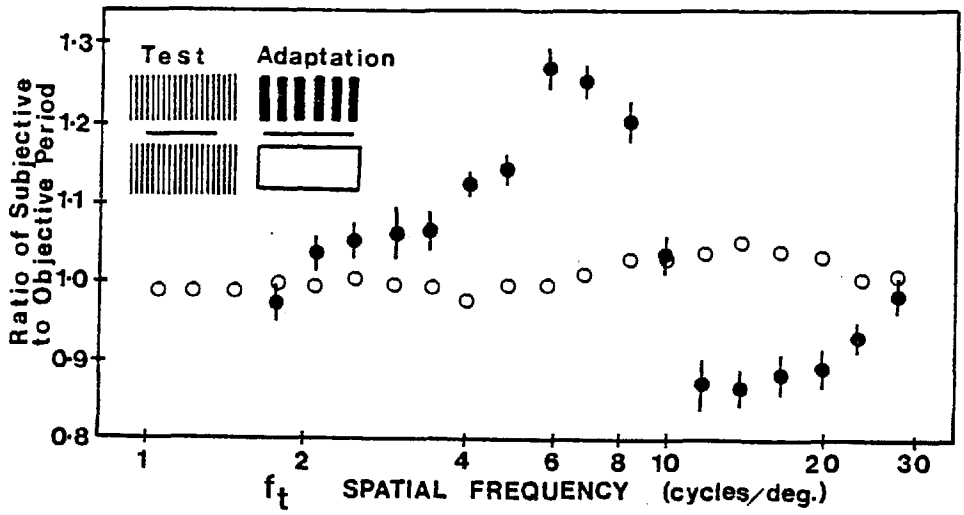

Fig. 1.29 Ratio of the apparent period following adaptation to that before adaptation to a sinusoidal test grating of spatial frequency, f_t, and a sinusoidal adaptation grating of spatial frequency, 10c/o, with f_t plotted as ordinate (full circles). Open circles represent the match between the two halves of the test field obtained without adaptation. Measurements were obtained by changing the spatial frequency of the lower half of the test field (insert) until it matched the appearance of the upper half field. The observer is instructed to scan the horizontal midline shown, so that the retinal area receiving the upper half field is adapted to a grating, whilst the lower half adaptation field is uniform but of the same mean retinal illumination level as the upper half field. (after Blakemore et al., 1970)

adaptation gratings were the same, nor if they were more than two octaves apart in spatial frequency. It has very similar characteristics to the contrast threshold elevation effect (Blakemore, Nachmias, and Sutton, 1970; Blakemore and Nachmias, 1971). There is an interocular transfer of some 80% of the monocular frequency shift, and its orientation specificity is identical with that of the contrast threshold elevation effect. This was interpreted as evidence that spatial frequency selective channels, tuned to the adaptation frequency, are suppressed more than others which creates a bias away from the adapting spatial frequency when the test grating is viewed.

In a further study of this effect Burton, Naghshineh and Ruddock (1977) and Naghshineh (1977) showed that the effect occurs with grating patterns which have different light/dark ratios but the same periodicity. A variety of test and adaptation gratings were used, and the results imply that there is an interdependence between the apparent light and dark bar width changes; the apparent width shifts in the light bar elements are found to be independent from the associated apparent change in the width of the dark bar elements and vice versa, and not therefore, as implied by previous investigators, a result of spatial frequency specific mechanisms. These data established the existence of independent mechanisms tuned specifically to the dark/light content, and implies non-linear and independent processing of the dark/light elements in the visual system. This is consistent with electrophysiological results, which show that at all levels of the visual system there are neurones which respond to bright central bars with dark surrounds, whilst others prefer the reverse configuration.

C.vii. The Tilt Aftereffect

Gibson (1933), Gibson and Radner (1937) first reported evidence of this effect, but it has been investigated more recently by Campbell and Maffei (1971) and Lovegrove and Over (1973). A vertical test grating appears to tilt in the direction opposite to that of a previously adapted tilted grating, and the effect can be almost completely interocularly transferred. The magnitude of the effect has a maximum at 8^{o} from the vertical, which suggests there are mechanisms in the visual system for detecting limiting bands of angles (Coltheart, 1971).

C.vii The McCollough Effect

McCollough (1965) showed that when a horizontal grating is viewed in blue light and a vertical grating in orange light, subsequent viewing of a grating in white light produces orientation specific colour after-effects, i.e., horizontally the grating appears orange, and vertically blue. This after-effect cannot be attributed to ordinary negative after-images (Harris and Gibson, 1968) and it does not readily transfer interocularly (Mikaelian (1975) did report a small transfer). McCollough proposed channels sensitive to both colour and orientation of the gratings, such that when they are in the adapted condition, the complementary colour can be elicited by viewing the grating in white light. The decay of this effect is prolonged (MacKay and MacKay, 1974).

Frequency specific colour aftereffects, similar to the McCollough effect, have been induced by an analogous technique, Stromeyer (1972), Lovegrove and Over (1972) and White and Wilson (1978). These

observations corroborate extensively with electrophysiological findings that some orientation specific detectors in the visual system are colour specific. Other evidence for the effect has been given by colour-selective adaptation responses to spatially periodic stimuli (May, 1972; Maudarbocus and Ruddock, 1974) and a colour-selective property in the tilt aftereffect (Lovegrove and Over, 1973).

C.ix. Stereovision and Binocular Rivalry

Two eyes, functioning together, result in the formation of two images of an object, one on each retina. However, only a single image is usually seen, because the signals are combined as they pass to the visual cortex. Nevertheless, due to the relative positions of the two eyes, these two images may differ slightly, and it is for this reason that a 3D-image is formed from an essentially 2D-situation. The images formed on the retinae contain all the information which is required for cues such as depth in space, relative sizes compared to familiar objects within the same scene or from occlusion. The term 'retinal disparity' is used to denote the relative difference in the position of the same point imaged in both eyes, and it increases for nearer points with the eyes focused at infinity.

The distinct perception of near depth is achieved by stereovision. This can be divided into two particular forms: one which is defined as 'fine' stereoscopy, and the other, 'global' stereoscopy. Fine stereoscopy is associated with the relative disposition of two points in space, whereas global stereoscopy is the correlation between two disparate images (Cowey and Porter, 1978; Hamsher, 1978; Cowey, 1979), however, individuals possess the two types to different degrees

and they are not necessarily coincidental.

Several investigators have studied the illusion of depth, e.g., Richards (1970, 1977), Richards and Regan (1973) and Tyler (1973), together with new methods of testing stereovision. The most common test is that developed by Julesz (1971) which utilizes a series of random dot patterns, having different degrees of disparity. The more usual form of this test is that using a series of coloured illustrations termed 'Analglyphs'. These are still a series of random dot patterns, but printed in red and green ink on a single plate with an incorporated disparity between the stereo images they produce, when seen in depth viewed through a stereo viewer. The stereo viewer consists of red and green filters, which are placed one before each of the eyes. Observers who have no stereovision fail to resolve the stereo images which are hidden in these dot patterns. This is because of their inability to fuse the two uncorrelated dot patterns, and they are therefore termed 'stereo blind'. This is the type of stereovision defined as 'global' stereopsis by Cowey and Porter (1978). In this investigation of primate vision, some monkeys were unable to perform on tasks which involved global stereoscopy, and yet were able to resolve the nearer disparities associated with 'fine' stereoscopy. Blake et al. (1979) give evidence from a series of utrocular experiments to suggest that stereo blind humans, like the primates who lack stereovision, most probably possess a monocularly excited cortex.

The inputs to the two eyes in stereovision are only slightly different, but another situation exists when the two visual inputs differ markedly, not only with respect to disparity, but also in colour and spatial content. This type of situation produces a

condition known as 'retinal rivalry', in which the observer sees an alternating image of the two inputs at an undetermined rate. This occurs because it is impossible to fuse and 'lock' the two images in these circumstances. Several investigations of the effects of rivalry have been reported; Abadi (1976) considered a configuration in which the two inputs were both grating stimuli. From his results, he concluded that high spatial frequencies are more easily suppressed than the lower ones, if both are presented in a vertical orientation. He also studied the effect as a function of angle, by rotating one grating with respect to the other.

Blake and Fox (1973 and 1974) investigated the effects of binocular rivalry in the contrast threshold elevation effect. They measured the monoptic elevation in threshold contrast when the adaptation grating was continuously visible in the eye to which the test would subsequently be shown. This measurement was repeated, but with the adaptation grating seen in continuous rivalry with one presented to the other eye. Thus the adaptation grating was only perceived for short intervals. They found, nevertheless, that there was no significant difference between the two contrast thresholds, and therefore the suppressed adaptation grating was still capable of exerting the same effect.

Blakemore (1970) proposed that stereopsis is dependent upon a comparison of the spatial frequencies, rather than an analysis of the retinal disparities in the images. This suggests the existence of binocularly driven neurones which have different optimal spatial frequency disparities. Blakemore and Hague (1972) tested this suggestion. They presented observers with adaptation gratings which

had specific disparities, in a stereoscopic fashion, and found that the maximum contrast threshold elevation occurred when both the adaptation and test gratings had the same disparity, and also that an apparent shift was perceived in the test if it had a disparity very close to that of the adaptation. The results are therefore analogous with the contrast threshold elevation effect, and the spatial frequency shift effect. Mitchell and Baker (1973) showed that this shift increased as a function of increasing disparity, fig. 1.30.

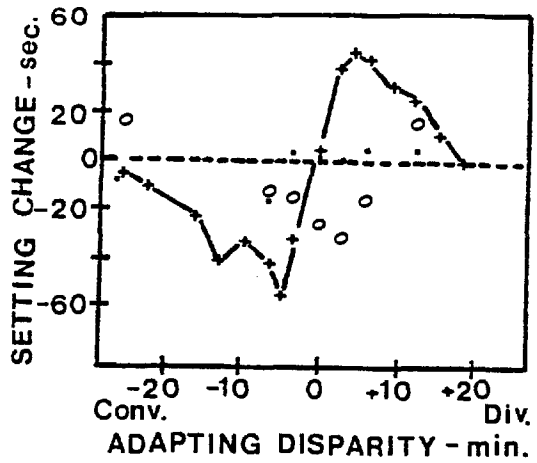

Fig. 1.30
Stereoscopic after-effects measured with lines. Ordinate shows the difference between settings of the test target made prior to, and immediately after adaptation to, the disparate target - data connected by continuous line. Other data points show changes after monoptic adaptation of either right or left eye. (after Mitchell and Baker, 1973)

Disparity specific neurones are therefore present in humans as well as in the primates, where electrophysiological techniques identified their existence. If these cells are responsible for depth perception, there is a problem for central vision, where an object will lie in front or behind an observers fixation. The retinal images will splay the nasal-temporal division of the retinae, and project images to both hemispheres in the brain. This information must be brought together for disparity and the depth to be measured. At some stage, there must be an interhemispheric connection to allow depth

information to be processed for the central visual field.

This was investigated by Blakemore (1970) in an observer who had a split optic chiasma. He showed that the observer still retained normal stereovision, i.e., identifies depth of an object briefly exposed in front of his fixation point, even though its image fell upon the temporal retina in both eyes, and therefore projects separately to the two hemispheres of the brain. This suggested the possibility of an interhemispheric link for binocular integration occurring at a higher stage in the visual system. Epilepsy is relieved to a degree by a 'split brain' operation. Such a patient was examined by Mitchell and Blakemore (1970) to test powers of stereovision. Their results showed that 'fine' stereoscopy was normal for the peripheral visual field, but was absent from the central field. This also suggests that there must be interhemispheric connections associated with central 'fine' stereoacuity.

The site of size constancy is connected not only with stereovision (Blakemore, Garner and Sweet, 1972) but also with visual illusions, i.e., the Müller-Lyer illusion (Hotopf, 1966; Gregory, 1966) and the Ponzo illusion (Fisher, 1970). Blakemore, Garner and Sweet (1972) located the site of size constancy using the contrast threshold elevation effect. Two gratings appear the same to observers, even if they differ in angular frequency due to a displacement in depth, when their actual frequencies are the same. The site of size constancy must occur, however, after the site of adaptation, perhaps in the infero-temporal cortex, as the maximum contrast threshold elevation effect was obtained only when the angular frequency of the test and adaptation gratings was identical.

In normal observers, the amount of interocular transfer is approximately 70-80% for most of the adaptation effects (Movshon, Chambers and Blakemore, 1972), but in observers who are stereo blind, this figure is reduced to 49% or less. Strabismic stereo blind observers show an even greater reduction to 12% (Mitchell and Ware, 1974). It therefore seems that the magnitude of interocular transfer is linked to the degree of stereoacuity, i.e., greatest for highest stereoacuity. The dominant eye, in a similar manner, always seems most efficient for the transfer of effects interocularly (Movshon, Chambers and Blakemore, 1972).

Colour Vision and Colour Matching

Foveally where there are only cones, and extra-foveally where there are also rods, it is found that a major proportion of the human population can establish an exact match in brightness and colour between two adjacent fields with an appropriate mixture combining only four colours, on the assumption that no two of these can mix separately to match a third (Young, 1820 a,b; Helmholtz, 1852; König and Dieterici, 1886; Abney, 1913; Wright, 1929 and 1946; Guild, 1931; Stiles, 1955; Stiles and Burch, 1959). The trivariancy of colour vision indicates the existence of at least three independent channels which relay information about the spectral composition of a light stimulus. Microspectrophotometric evidence shows that there are three spectral classes of cone in primates (see fig. 1.3). The existence of a single photo-sensitive pigment present in each of the three cone types is further established by additional experiments demonstrating additivity in colour matches, the stability of colour matches to

moderate levels of light adaptation and the matching of after-images (Brindley, 1957 and 1970). However, Wright (1936) and Brindley (1953) found that after adaptation to very bright lights, such matches as described above do become disturbed. This was thought to be a result of the relatively small change in pigment sensitivity, caused by bleaching of the pigments (Dartnall, 1957).

The W.D.W. system of colorimetry uses three matching stimuli, monochromatic red (650 nm), green (530 nm) and blue (460 nm), which are mixed to give the same appearance as the test colour of fixed composition (Wright, 1946). If the matching stimuli are denoted by R, G and B, and the test by C, with the amounts of each in the match represented as r, g, b and c, then it is possible to represent a match by the equation:

$$C(C) = R(R) + G(G) + B(B) , \qquad \text{Eq 1.2}$$

which can be normalized to give:-

$$c(C) = r(R) + g(G) + b(B) , \qquad \text{Eq 1.3}$$

where $c = C/(R + G + B)$ and $r = R/(R + G + B)$ etc.,

but $C = R + G + B$ (photometric match), Eq 1.4

and $r + g + b = 1$. Eq 1.5

The unit trichromatic equation, Eq 1.3, can be represented on a chromaticity diagram, since it is a function of two variables, and r and g are usually taken to form the orthogonal axes. Normally, in the W.D.W. system of colour matching, the amounts of red and green required to match a yellow (582.5 nm) test are equivalent, as are the amounts of blue and green in a match of blue-green (494 nm) test. From these two matches, it is possible to normalize all other matches

produced by a particular observer.

The following chapters describe further experimental investigations, which aim to extend the understanding of the functional organization of the human visual system by the analysis of the responses from observers, with both normal and defective vision, to coloured and spatially structured stimulus patterns.

CHAPTER II

The Experimental Apparatus

A. The Maxwellian Viewing System

A.i. Maxwellian View

This employs the principles devised by James Clerk Maxwell (1860), when during his experiments on colour mixing he wished to increase the quantity of monochromatic light falling on the retina of his eye. The special feature of such a system is that the light source is imaged in the pupil of the eye, instead of being observed directly, and therefore, the viewing lens is 'uniformly illuminated with light' (Westheimer, 1959 and 1966). A schematic diagram (fig. 2.1a) illustrates the principles of Maxwellian view and, for comparison, direct image formation of an extended source, S (fig. 2.1b). The most common form of Maxwellian arrangement is illustrated by fig. 2.1c.

The advantages of using this arrangement are that there is more efficient use of the light available from the source, and that the light, reaching the retina, can be measured more easily. The optimum focus of such a system can be adjusted for each individual observer, and by the use of an artificial pupil, the variation in the illumination on the retina due to differences in the pupil diameter are avoided.

The system designed for the present investigation had three channels of the kind shown in fig. 2.1c. In this arrangement, the visual angle, θ, in radians subtended at the eye by a virtual image formed by an object of length, L, located at infinity and viewed through a lens of focal length, F (fig. 2.2), is given by the

Principles of Maxwellian Viewing

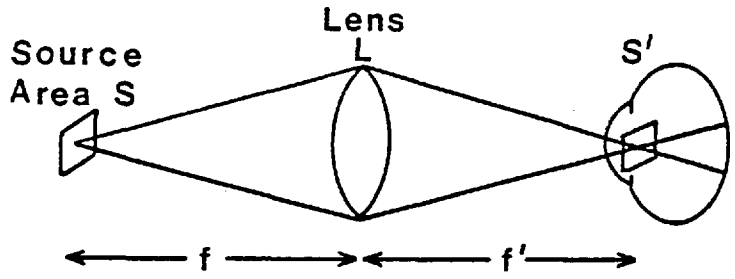

Fig. 2.1a Schematic representation of Maxwellian Viewing. A Source of area S is imaged by a lens in the pupil of the eye. The image of the source has area $S = S.f'^2/f^2$.

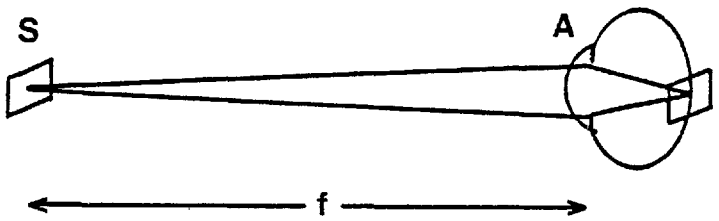

Fig. 2.1b Ordinary viewing of an extended source of area S placed a distance from an eye, with an entrance pupil of area A.

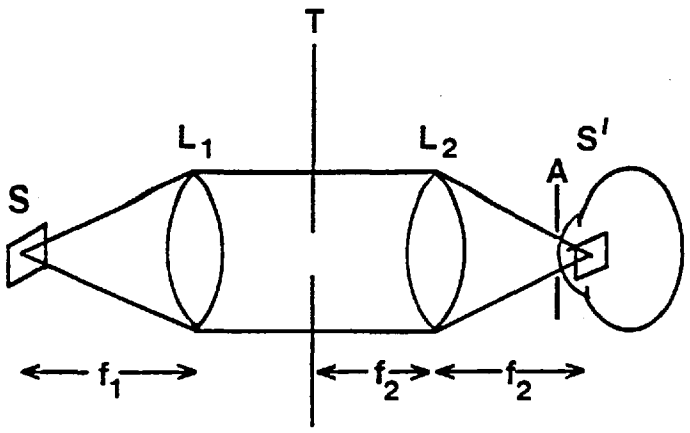

Fig. 2.1c Common Maxwellian arrangement. Source, S, is positioned at the principal focal plane of the first lens, L1, and thus target, T, is trans-illuminated by a parallel beam. (A laser may serve this purpose). The image of the source will fall in the plane of the eye's entrance pupil when it is at the principal focal plane of lens, L2. For emmetropic observers, the target, T, is placed at the first principal focal plane of lens, L1.

expression:-

$$\text{Angle, } \theta \text{ (radians)} = \text{Tan}^{-1} (L/F) . \qquad \text{Eq. 2.1}$$

Hence, if a square-wave grating with a period of length P were seen in the above arrangement, it would result in a spatial frequency, f, given by:-

$$\text{Spatial frequency, } f = [\text{Tan}^{-1} (P/F)]^{-1} \text{ cycles per degree of visual angle.} \qquad \text{Eq. 2.2}$$

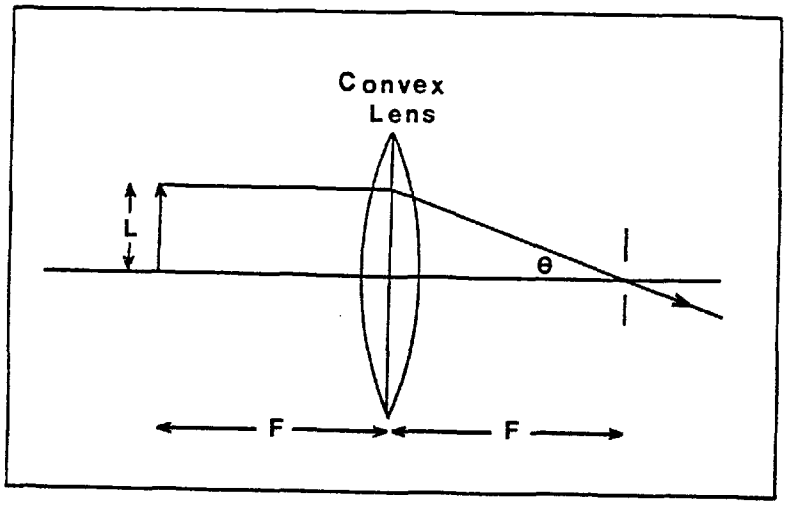

Fig. 2.2

A.ii. The Three Channel System

A schematic representation of this system is shown in fig. 2.3. The source, S, is a tungsten-halogen white light, 150W, 24V D.C. lamp, operated from a 24V stabilized D.C. power supply, equipped with fan cooling. A period of at least thirty minutes was allowed for lamp stabilization before experiments were started. Achromatic doublet lenses, L1 and L2, collect the white light emerging from the source, and collimate it to produce two parallel light beams. One of these passes into the beamsplitter, BS1, where it is split to provide two parallel light beams, which are reflected by the mirrors, M1 and M2. The other beam proceeds with division, so that three channels are

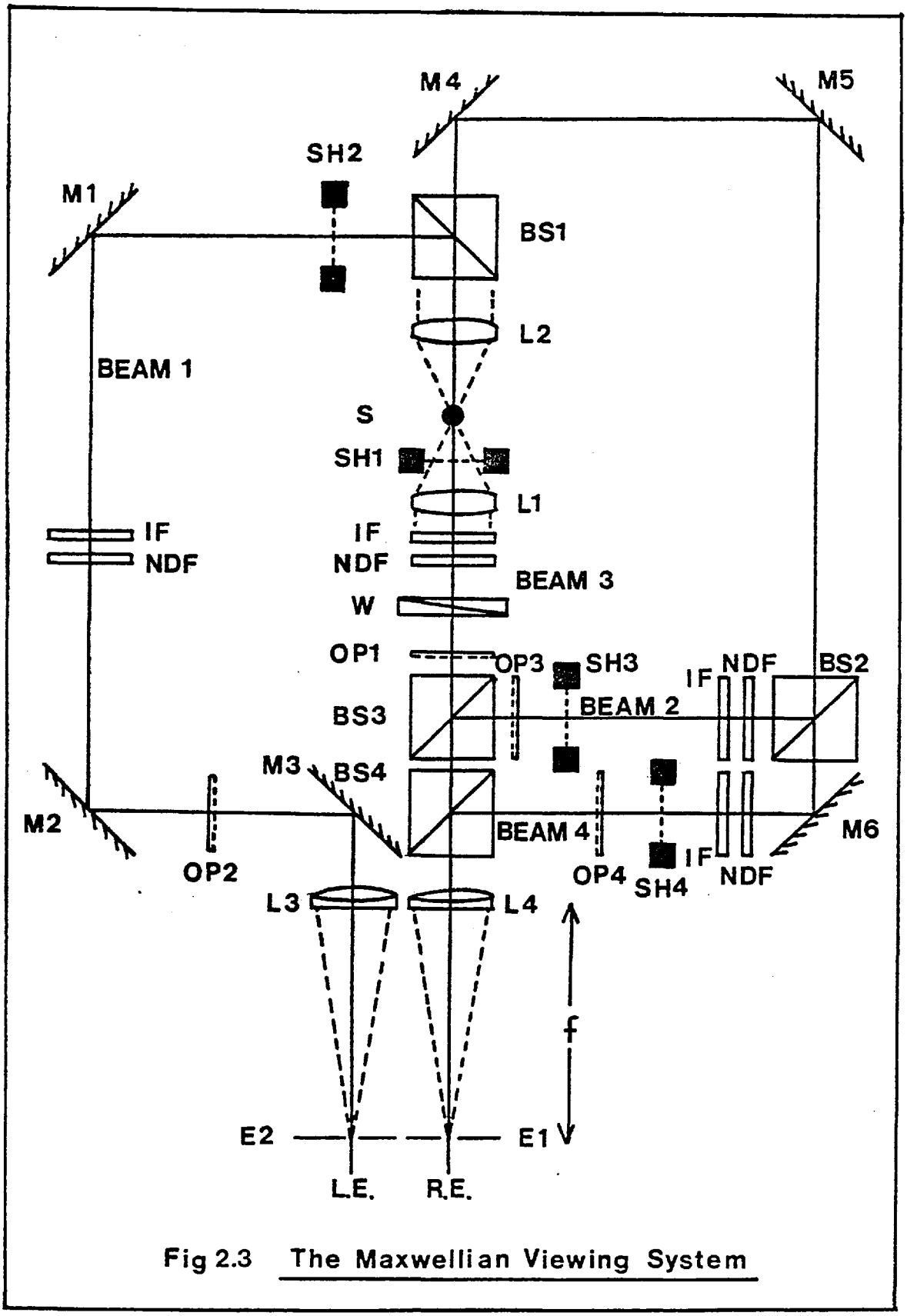

Fig 2.3 The Maxwellian Viewing System

formed, with a possible fourth provided by incorporating the beam-splitter, BS2. If these parallel beams of white light pass through Wratten broad-band gelatin filters or interference filters (Balzer, Type B40), IF in fig. 2.3, it is possible to obtain control of the spectral composition of the light in the different channels.

The illumination levels in all of the channels are controlled stepwise by Wratten (Type 1A) neutral density filters, NDF (fig. 2.3), and the test beam illumination level can be varied continuously by a Kodak (acetate) neutral density wedge, W (fig. 2.3), so that the illumination level of the test stimulus can be adjusted manually and continuously by the observer, until the threshold criterion is reached (fig. 2.3b). OP1-4 represent the object planes, in which

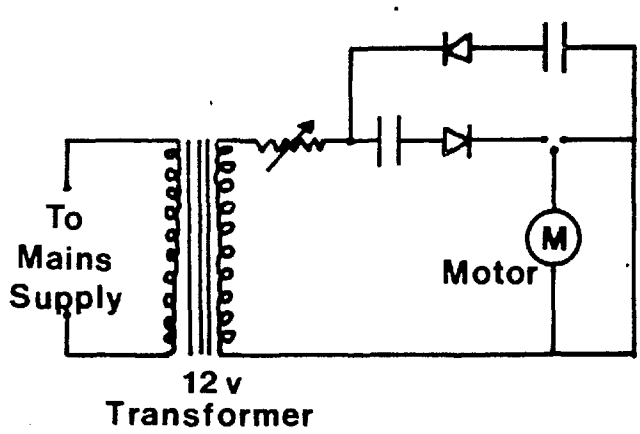

Fig. 2.3b Schematic representation of the electronic system which was used to drive the NDW (fig. 2.3) across the test stimulus beam.

photographic transparencies are placed to provide the test and adaptation stimuli. In a number of experiments, beam 2 provided a uniform background illumination, and in such cases, the test pattern was always seen superimposed upon this background field. The arrangement can be used for either monoptic or dichoptic presentation

of stimuli by translating the mirror, M2, and including the mirror, M3, to reflect the light beam to the viewing lens, L3, and the exit pupil, E2. L3 and L4 constitute the viewing lenses, and have the same focal lengths (f = 12 cm). The beamsplitters, BS3 and BS4, allow the adaptation, test and background fields to be superimposed so that they are all focused at the exit pupil, E1, by L4.

Electromagnetic shutters are positioned at SH1, SH2, SH3 and SH4. These are driven and controlled by the Timer Unit (see later and Appendix A) to give the stimulus presentation sequence required in each experiment. In the adaptation period, the adaptation grating, AG, is viewed by the right eye, RE, alone under monoptic presentation, or by the left eye, LE, in dichoptic presentation with a uniform background field presented simultaneously to the right eye, RE. However, in the test period, the adaptation grating, AG, is occluded by the shutter, and the test grating, TG, is always presented to the right eye, RE, superimposed always on the uniform background field. In later experiments, beam 1 provides the conditioning stimulus, whilst beam 2 is split by the beamsplitter, BS2, to provide a uniform background field and an adaptation stimulus. This arrangement allows a conditioning grating, CG, or conditioning matrix, CM, to be presented in beam 1 to the left eye, LE, an adaptation grating, AG, through beam 4 to the right eye, RE, a uniform mean luminance background field through beam 2 to the right eye, RE, with the test grating, TG, superimposed on this mean luminance background field through beam 3, during the relevant presentation sequence. The sequence is controlled by the switching and triggering of the Timer Unit (Appendix A) accordingly.

A.iii. The Lamp Power Supply

A means for current limiting and precise voltage stabilization were incorporated into the D.C. power supply from which the source, S, was operated (Nunn, 1978). Also included was an automatic slow turn on/fade circuit to eliminate any sudden current transients in the lamp. Therefore, the voltage applied to the lamp at turn-on increased only slowly, its rate determined by a resistor-capacitor combination, until it reached a steady value of 23.0 $\pm$ 0.003V within five minutes. The decrease in the supply at turn-off was at a similar rate.

A.iv. The Shutter Control-Timer Unit

The shutter timing unit was designed to control up to three shutters independently (Appendix A). The duration of opening, the time interval between opening, and the sequence of opening of the shutters were each controlled separately. The timer circuit was used to set constant time periods in adaptation experiments, and thereby eliminate observer differences should they operate the shutters faster than the preset rate. The timing elements in the circuit were integrated circuits, type no. ZN1034E, and the power was supplied to these via a 12V precision regulator. The output voltages of the timing elements were used to drive the shutters, via the Darlington amplifier circuits, type no. ZN6385 in fig. A.1 (Appendix A). The circuit was arranged to provide a pulse to open the shutters rapidly, followed by a sufficient potential difference to hold them open for the specified length of time (fig. 2.4). The shutters were operated by a switch mounted on a panel. This could be triggered by either the observer or the experimenter. A counter unit and buzzer device

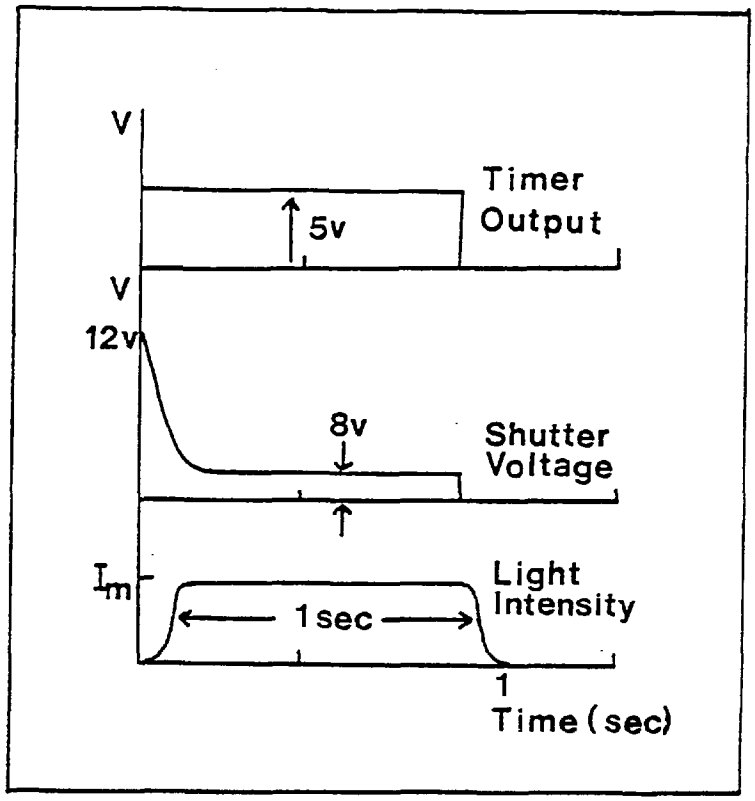

Fig. 2.4 Graphs to illustrate shutter control and operations.

(Appendix B) were also incorporated into this timer unit, to signal the end of a set of measurements.

A.v. Data Recording

Data collection was monitored by recording the setting of the continuously varying neutral density wedge, W, on a digital multimeter (DANA, model 3800B) and a digital printer (CREDSHIRE, model DP100). This was achieved by connecting a 10-turn potentiometer by gears to the wedge, with a constant voltage applied to the potentiometer. The wedge position was recorded as the change in voltage corresponding to the potentiometer setting, and the voltage displayed on the Dana. This value is printed out on the Credshire printer, (see fig. 2.5), from which data analysis could be achieved. The 'print-out' sequence was incorporated into the metal box, and by the depression of the relevant switches, the appropriate mode of operation could be selected; one switch initiated a single 'print black' sequence, another a single

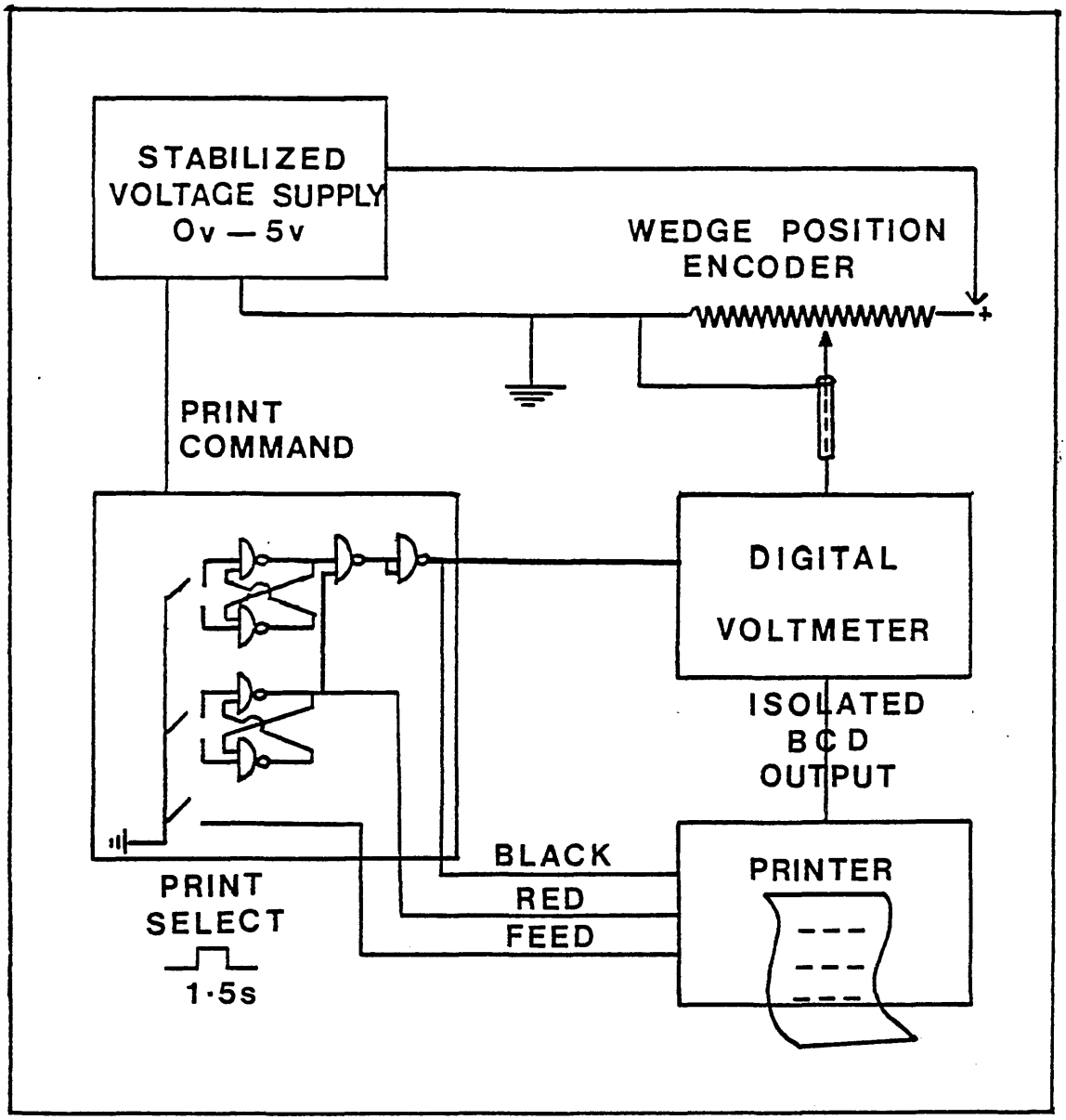

Fig. 2.5 Block diagram of the arrangement used for the automatic sampling and recording of the experimental parameters.

'print red' sequence, and the third, a 'paper feed' sequence.

A.vi. Light Level Determinations and Calibrations

Throughout all of the experiments, it was essential to maintain constant mean retinal illumination levels. This is achieved by monitoring the relative light levels with a photo-detector device. This consisted of a photodiode (a MACAM photometer head unit)

encapsulated in a brass mount. Its special feature is the current output linearity as a function of incident light level which extends over some 4 log unit change in light intensity (fig. 2.6). It

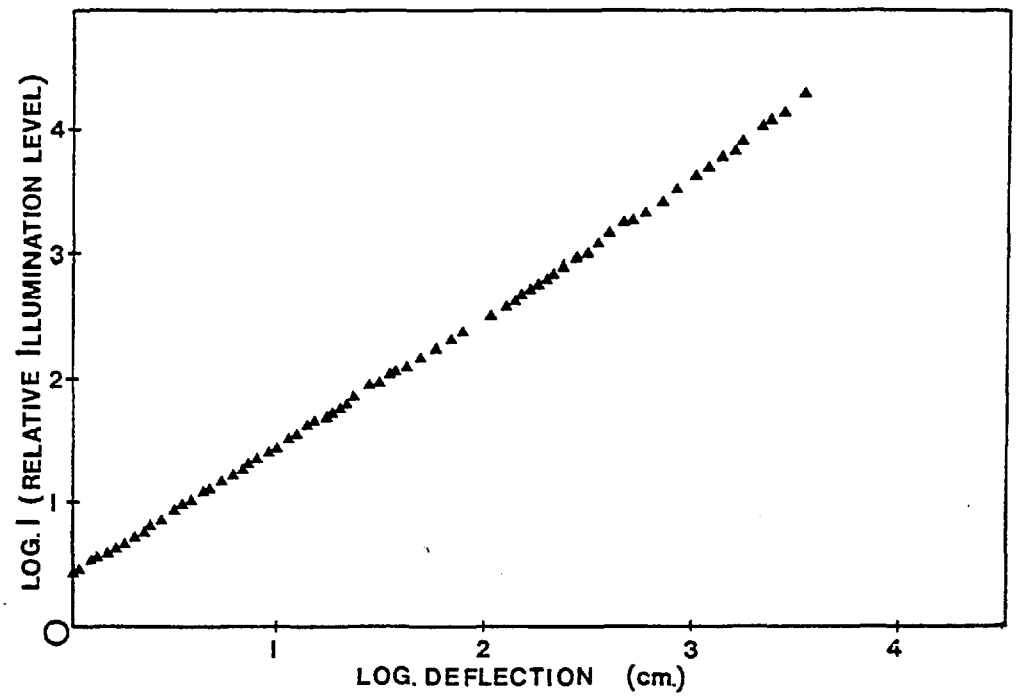

Fig. 2.6 The logarithm of the light intensity (log E), which falls onto the photodiode surface is plotted against the logarithm of the photodiode current (log i). The output linearity of the photodiode extends over some 4 log units change in light intensity.

operates by converting the light falling onto the detector surface into a current. This is measured directly with a sensitive galvanometer (PYE Scalamp, No.79041S). The calibration curve shown in fig. 2.6 was obtained in situ with the wedge, W (fig. 2.3), and the galvanometer to check the linear response characteristics over several scales. The photodiode was used to equalize the mean illumination levels in each eyepiece in the experimental investigations, by adjusting the light levels of the various stimulus beams with neutral

density filters so that each beam gave the same photocurrent. The position of the photodiode was always the same, and the light from the exit pupils, E1 and E2 (fig. 2.3), fully illuminated the photosurface.

The retinal illumination level of the light stimuli was measured using the method described by Westheimer (1966). A uniform white magnesium oxide surface was positioned at a known distance, x m, beyond the 2 mm artificial exit pupil, E1 or E2 (fig. 2.3). The surface luminance, B (in mL), produced by the light transmitted through the pupil and reflected at the white surface, was measured with a calibrated MACAM (PR3010) photometer. The required retinal illumination level provided by the source imaged at the exit pupil, E1 or E2 (fig. 2.3), is given by:-

$$\text{Retinal Illumination, } E = \frac{10B\,x^2}{A} \text{ candelas/sq.metre (cd m}^{-2}\text{)}, \qquad \text{Eq. 2.3}$$

where:-

B is the surface luminance of the source in mL,

A is the area of the pupil in square meters, and

x is the distance between the exit pupil and the perfectly diffusing surface.

The source intensity at the exit pupil is measured in lumens per steradian of visual angle, however, in most psychophysical experiments the more common unit used to describe retinal illumination level is the Troland, which is defined as the retinal illumination produced by a source of luminance one candela per square metre viewed through a pupil of area one square millimetre. Thus, the imaginary source of light imaged in the plane of the exit pupil has an intensity of $10Bx^2$ candelas and it produces a retinal illuminance given by the

following:-

$$\text{Retinal Illumination, } E = 10^{7}\ \text{Bx}\ S^{2}\ \text{Trolands,} \qquad \text{Eq. 2.4}$$

where now:-

S is the area of the exit pupil in square millimeters.

Sets of neutral density filters, NDF (fig. 2.3), were used to attenuate the various stimulus beams. These consisted of Wratten (Type 1A) gelatin filters cemented between squares of neutral (optical quality) glass, and were calibrated in situ using the photometer (MACAM, PR 3010) unit.

The wavelengths of the monochromatic light for the various experimental conditions were obtained either by Wratten broad-band gelatin filters, or by Balzer (Type B40) interference filters (bandwidth $\simeq \pm 5$ nm). The spectral transmission of all of these filters was measured on a BECKMANN recording spectrophotometer (model DK2), and by positioning the Macam photometer at the exit pupil of the apparatus, it was possible to measure the relative energy from the source transmitted through the filters in situ. The spectral response of the solid state detector head unit of this instrument was flattened by the use of a radiometric filter, so as to ensure that the current output of the light sensor was uniform to within 5% for an equal number of incident photons per second at each wavelength of light in the visible range, (400 nm to 700 nm). Figure 2.7 shows the relative energy of the spectral distribution emitted by the source and transmitted through the relevant interference filter, and figure 2.8 shows the relative energies incident at the cornea for each of the monochromatic wavelengths transmitted. Energy calibrations of the filters in situ were repeated at regular intervals to take account of

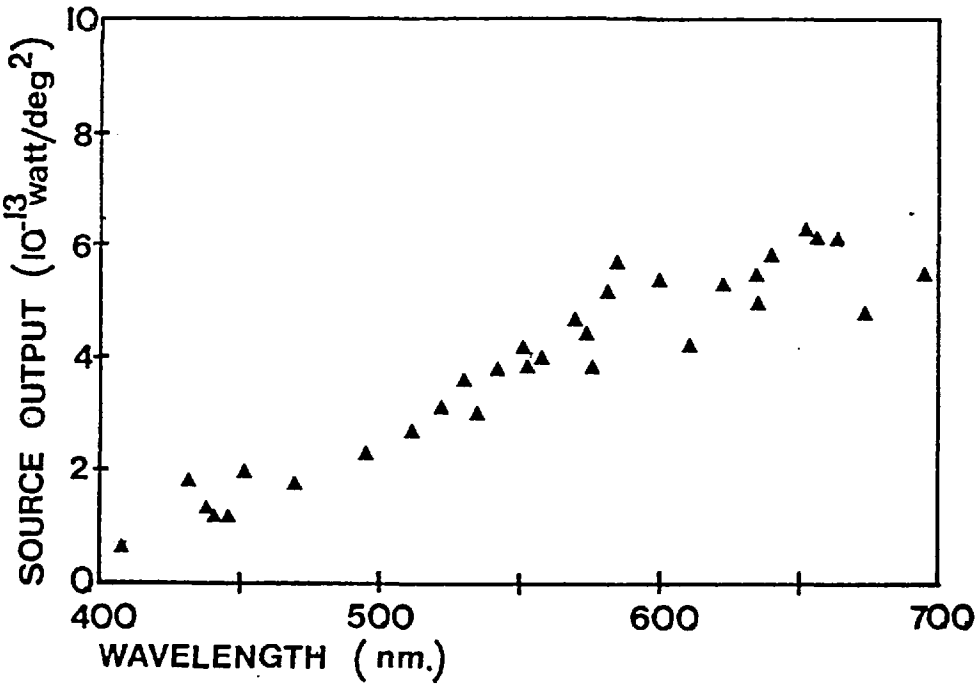

Fig. 2.7 Spectral distribution of light emitted from the source.

the slowly decreasing black body temperature of the source with age, and the effect of dust and fine particles which accumulate on the optical surfaces.

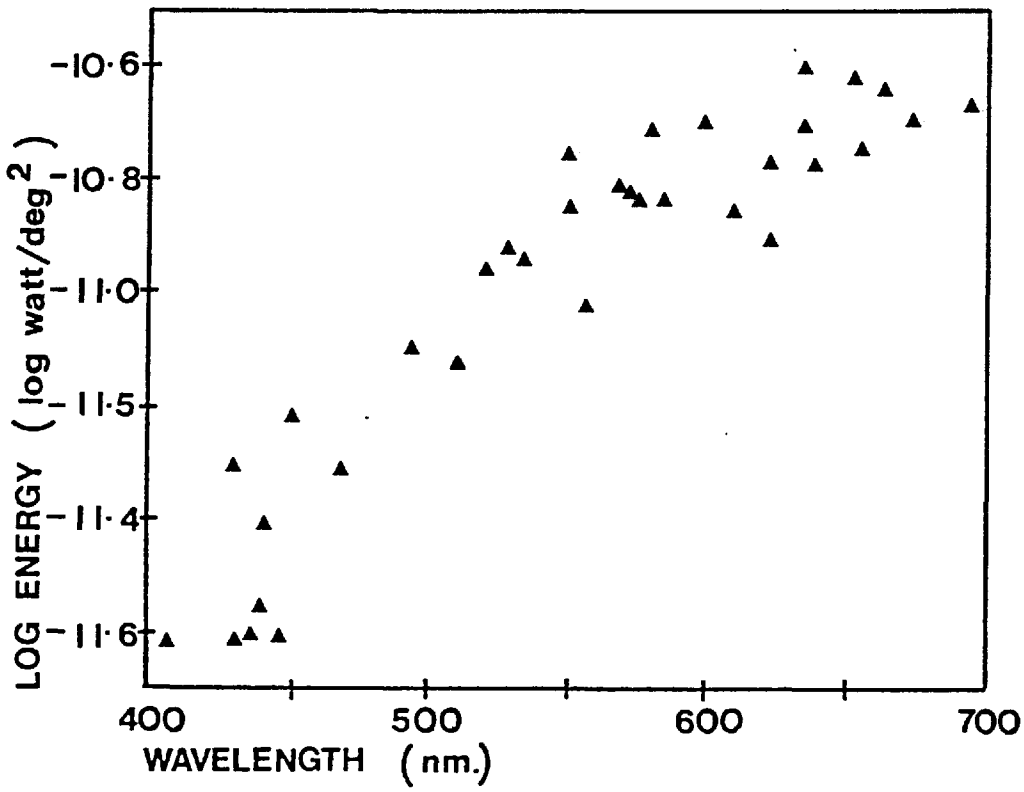

Fig. 2.8 Relative energies at the cornea of each wavelength emitted by the source.

The continuous wedge, W, was calibrated *in situ* at between twenty to thirty positions along its length, which corresponded to some 0.1 log unit change in optical density. Throughout the series of experiments, these measurements were periodically re-checked for calibration, but were found to remain stable to within 0.01 log units of absorption. It is found that the logarithm of the optical density varies linearly with position along the wedge (fig. 2.9), and it is possible to calibrate the wedge, as is illustrated by fig. 2.9, in combination with any of the interference filters, although as can be seen the wedge is effectively neutral in its absorption.

During the experimental sessions, the observer was shielded from stray light by an enclosure of matt black card, and appropriately placed curtains, whilst a cooling fan ensured that the measurements were made in comfort.

The components from which the apparatus was constructed were all optically tested. The fully-aluminized mirrors were made by vacuum deposition of aluminium on the front surface of clean, 0.06" thick, glass sheets of varying dimensions. The mounts for these mirrors were designed to allow the maximum degree of freedom in three directions by screw adjustments. The aberrations of the mounted mirrors were measured with a Twyman-Green interferometer, and were less than fifteen wavelengths of green light over the whole of the surface of the mirror. The other components were mounted in similarly designed stands allowing adjustment in all directions for alignment of the system.

A.vi. Stimulus Production

The spatial patterns required for the experiments were produced

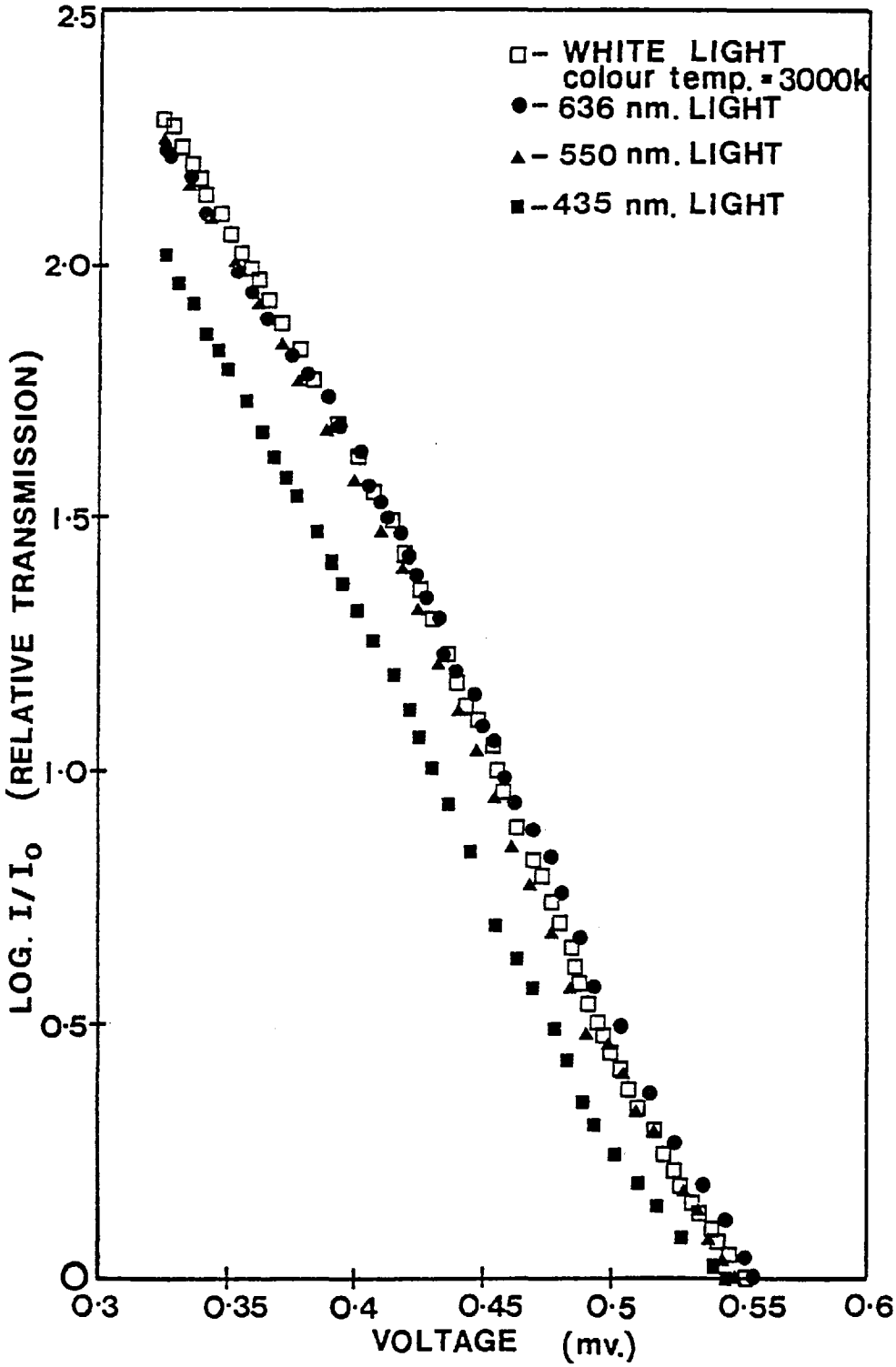

Fig. 2.9 Calibration curve for the neutral density wedge, W, in white and three monochromatic wavelengths of light. The linear relationships between the relative transmission (log I/Io) and voltage (V) can be represented by an equation. The best straight line fitted to these data points give the following set of equations.

For white light □ - Log I/Io = -10.37V + 5.68,
for 636 nm light ● - Log I/Io = - 9.55V + 5.37,
for 550 nm light ▲ - Log I/Io = -10.25V + 5.63,
and for 435 nm light ■ - Log I/Io = - 9.92V + 5.26.

photographically and were drawn either by computer programme (Appendix C) or by hand. Computer plotting was achieved by computation of the required pattern distributions with the University of London CD60 IBM computer, and the values were transferred onto microfilm in 35 mm slide format. As each stimulus occupied only one frame, it was possible to generate up to fifty frames on a roll of 35 mm film. The films produced were of positive form, i.e., the pattern generated as white, unexposed, on a black, fully exposed, background; the density of this background was approximately 2.0 to 2.5 log units. The patterns produced in this manner were then copied onto Kodalithe Graphics Art film to increase the contrast to its maximum value of at least 98%, and thereby prevent unwanted scattered light leaking through the system into the eye. Figure 2.10 shows examples of the square wave-form profiles generated in this manner, for a number of modulation depths.

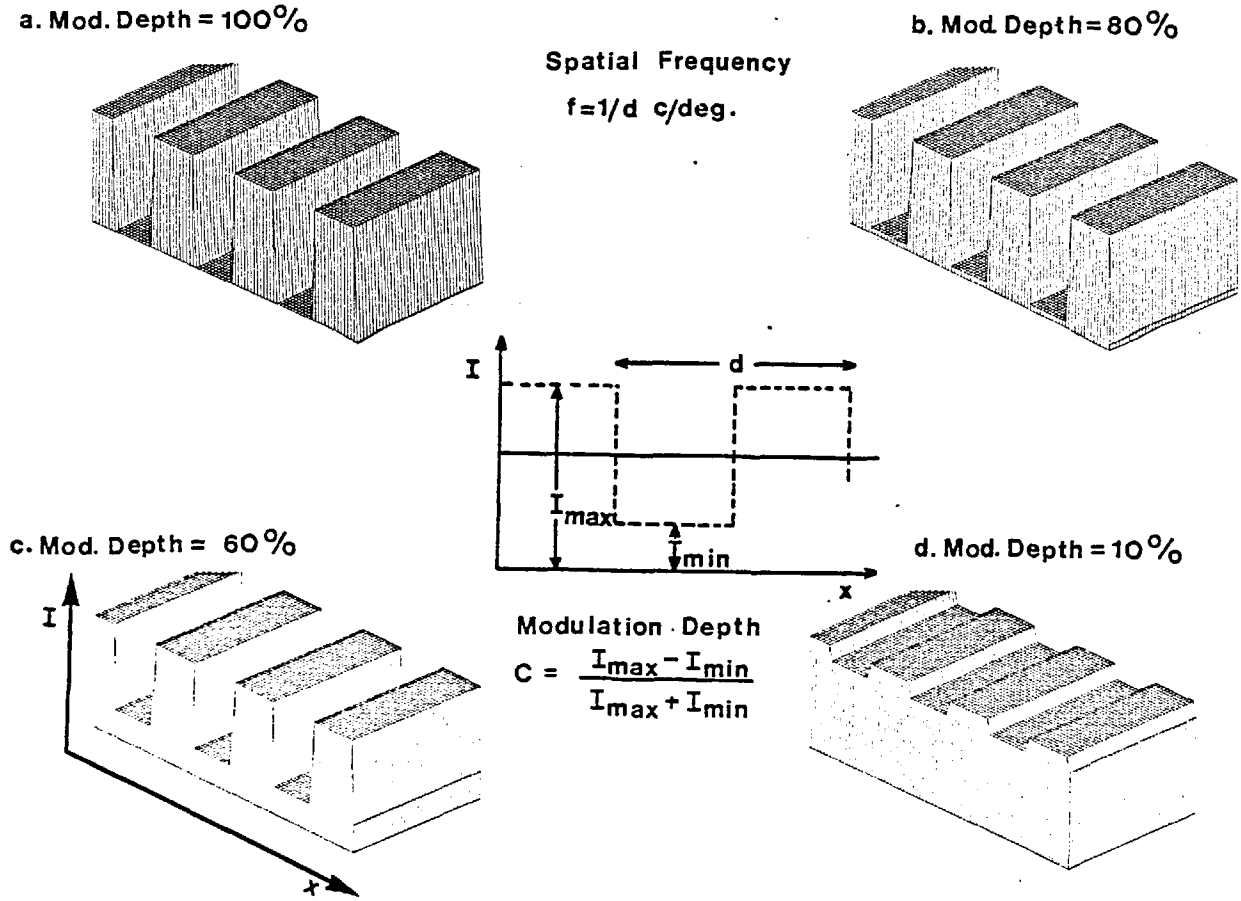

Fig2.10 To illustrate a Square-Wave Distribution of illumination level I

The wide range of facilities available in the computer programme plotting routines allowed a variety of configurations to be investigated. Possible variations included independent variation of the light/dark regions at constant period in the stimulus gratings. It was also possible to obtain spot matrix arrays which were achieved by use of one of the more special routines in the computer facilities. Figure 2.11 shows an example of such a stimulus, and again, it was possible to vary independently all the parameters of the matrix. The precision of the computer plotting routines was checked by measuring the individual dimensions of the pattern elements with a travelling microscope.

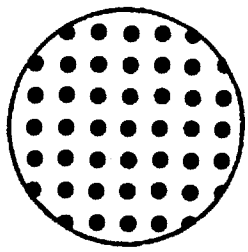

Fig. 2.11 To illustrate the stimulus composed of a spot matrix array.

More complex patterns could not be readily produced by computer plotting, so were hand drawn using a Rot-ring pen and india ink. The traced grid was photographically reproduced to the correct magnification on the 35 mm slides, which provided the stimulus patterns. The high contrast resolution was achieved by printing the stimuli on Kodalithe Graphics Art film, which again gave a modulation depth (contrast) of about 98%.

B. The Interferometer

B.i. The Interferometric System

The formation of interference fringes directly on the retina of the eye has an advantage in psychophysical measurements. It allows distortions produced by the ocular media or optics of the eye to be by-passed, and also eliminates the necessity of selecting correction

lenses for observers with focusing defects such as myopia and hypermetropia. This method, first proposed by Le Grand (1935), has been used by Byram (1944) and later by Arnulf and Dupuy (1960), and Westheimer (1960). The fringes, they produced, were of relatively low illumination level and/or high contrast due to the conventional light source used, and in an attempt to resolve this difficulty, Campbell and Green (1965) used light derived from a He-Ne laser to produce the interference fringes in an arrangement analogous to the double slit interference technique of Young (1820 a,b). Two collimated beams of coherent light derived from a single laser source were focused into the plane of the eye pupil, close to the nodal points of the eye, to produce a system of interference fringes on the retina where the two beams overlap. The frequency was changed by varying the angle, θ, at which the beams intersect.

The intensity distribution of a double slit fringe pattern is given by:-

$$I(x) = I_1 + I_2 + 2\sqrt{I_1 I_2}\ \frac{\cos 2\pi tx}{\lambda}, \qquad \text{Eq. 2.10}$$

where I_1, I_2 are the intensities of the interfering beams, respectively,

λ is the wavelength of the light employed,

x is the retinal distance measured in degrees, and

t is the separation of the interfering beams.

In the original study of Campbell and Green (1965), the single laser source is split into two collimated beams of coherent light by a reflecting plate, and then refocused to converge and intersect in a microscope objective. The fringe pattern is observed by positioning

the head so that the eye is close to the two coherent point sources, and the spatially distributed pattern of sinusoidal interference fringes form on the retina (fig. 2.12). The two coherent 'point'

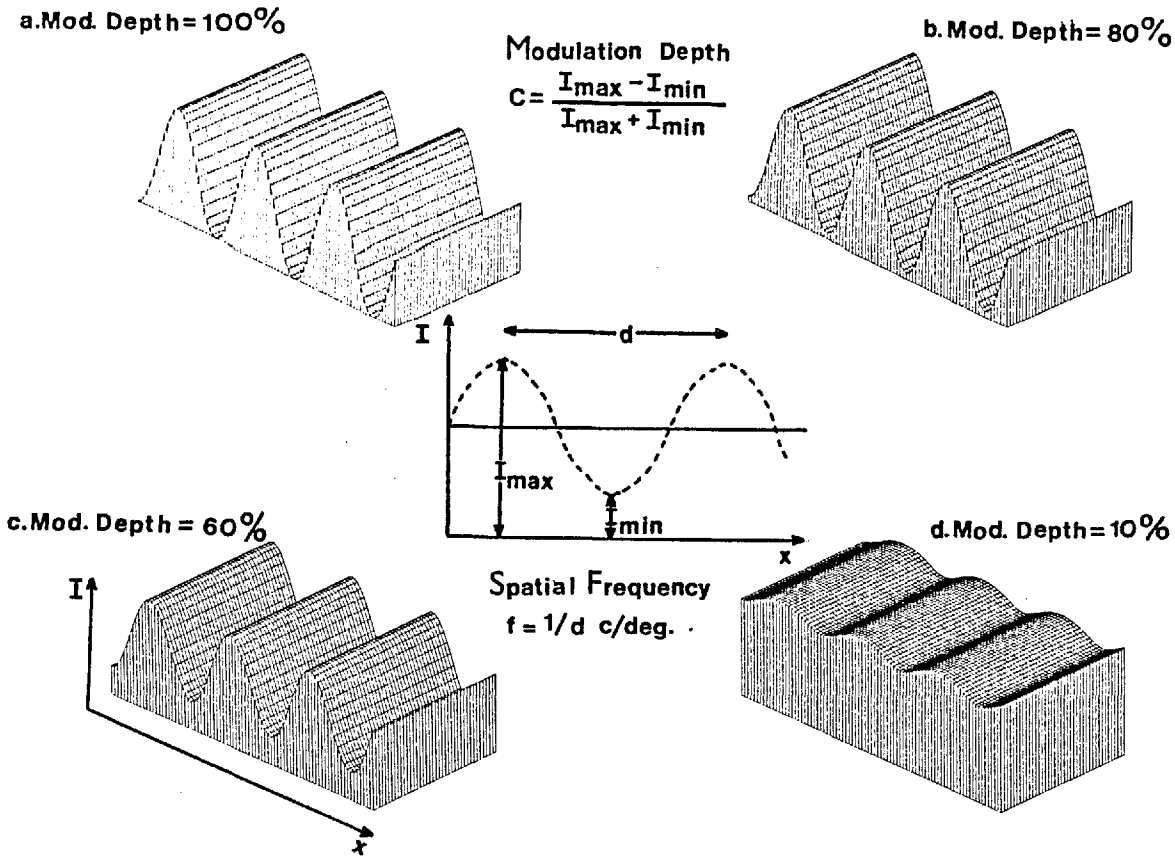

Fig. 2.12 To illustrate a Sinusoidal distribution of illumination level I

sources are close to the nodal point of the eye, but essentially the spatial frequency of the fringes is independent of the position of the cornea, and dependent only on the angle, θ, between the two interfering beams (fig. 2.13).

In the present studies, intereference fringes were produced by means of a duplicated Mach-Zehnder interferometer (Born and Wolf, 1970). This instrument is designed so that the angle of inclination of the two coherent light beams and, therefore, the spatial frequency

of the fringes can be altered whilst still maintaining their intersection at the microscope objective. This apparatus was initially designed and built by Burton (1973).

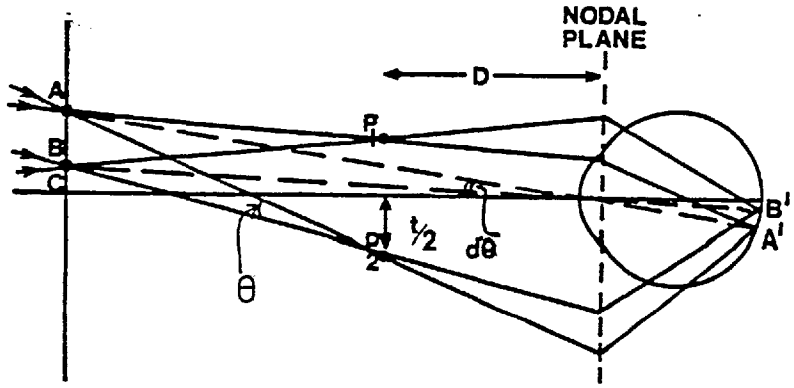

Fig. 2.13 Detailed examination of the production of fringes on the retina. The observer's eye is located with its nodal plane a distance, D, from the two focus points, P1 and P2, of the two coherent beams focused by the microscope objective.

B.ii. Production of fringes

Campbell and Green (1965) found that for interference fringes formed directly on the retina, the spatial frequency of the gratings was not critically dependent upon the position of the observer's eye, nor on the state of visual accommodation (fig. 2.13). In order to demonstrate this, the observer's eye is assumed to be located with its nodal plane a distance, D, from the two focus points, P_1 and P_2, of the two coherent beams of light focused by the microscope objective. The rays from these components are those which give rise to the adjacent interference maxima at points A' and B' on the retina. The points A and B are conjugate to A' and B' for a particular accommodation state of the eye. To obtain maxima at these points, the

path length between A' and B' must be an integral number of wavelengths, i.e.,

$$(P_1 A' - P_2 A') - (P_1 B' - P_2 B') = n\lambda , \qquad \text{Eq. 2.11}$$

where λ is the wavelength of the light and,

n is an integer,

similarly: -

$$(P_2 A - P_1 A) - (P_2 B - P_1 B) = m\lambda , \qquad \text{Eq. 2.12}$$

where m is an integer.

B.iii. The Interferometer

In the Mach-Zehnder interferometer used in the following experiments, the spatial frequency of the fringes was adjusted by changing the angle between the coherent light beams incident on the observing microscope objective, MO (fig. 2.14, simplified arrangement). Under the precise intersection of these beams at the

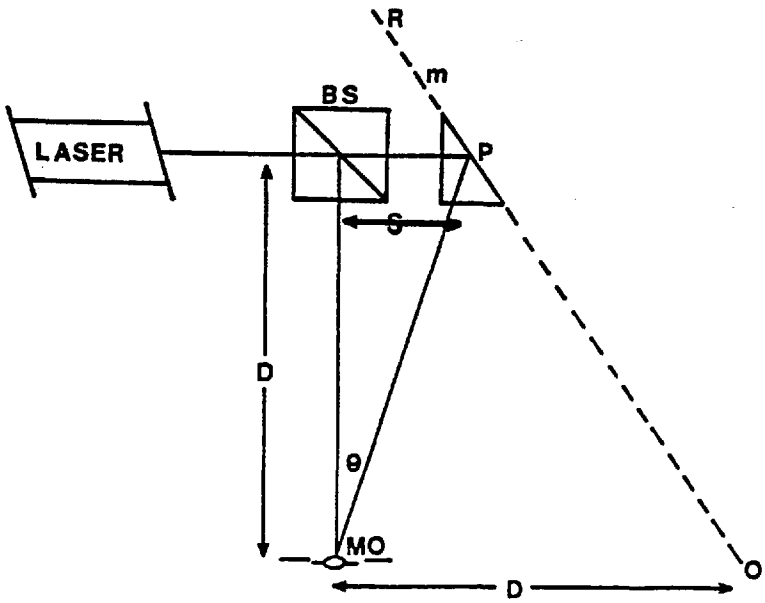

Fig. 2.14
A simplified arrangement to show the production of interference fringes in the interferometer.

objective, MO, the angle between the beams, θ, is given by:-

$$\text{Angle}, \theta = \text{Tan}^{-1} S/D , \qquad \text{Eq. 2.13}$$

where S is the distance between BS and P, and

D is the distance from BS to MO.

Such an arrangement is difficult to achieve in practice, but by rotating, as well as translating, the prism, P, it is possible to obtain an approximation to the precise intersection of the beams (Burton, 1973). The fringe system provides a range of spatial frequencies, which extend from zero to about 60 c/^{o}, by using a 10x microscope objective at the eye piece. This means that the angle, θ (fig. 2.14), is very small, and equation 2.13 can be approximated by:-

$$\text{Angle}, \theta = 2 \text{Tan}^{-1} \frac{(S/D)}{(2-S/D)} . \qquad \text{Eq. 2.14}$$

The relationship between θ and D is maintained as the prism, P, is fixed to a rotating bar, RO (fig. 2.14). This is driven by a micrometer attachment, m, so that the pivot of the bar, O, forms a right-angled issoceles triangle with the beamsplitter, BS, and eye-piece objective, MO. The values of θ achieved can be very small for low frequency fringes, but the mathematical considerations still hold.

A plan view of the interferometer is shown diagramatically in fig. 2.15. Two independent laser sources (Spectra Physics, Type no. 120) were used to provide light for the lower and upper fringe systems (inset of fig. 2.15), which ensures mutual coherence between the beams for the production of the fringes, but a mutual incoherence between the two sets of fringes to prevent them interfering. The He-Ne lasers produced plane polarized beams of light, wavelength

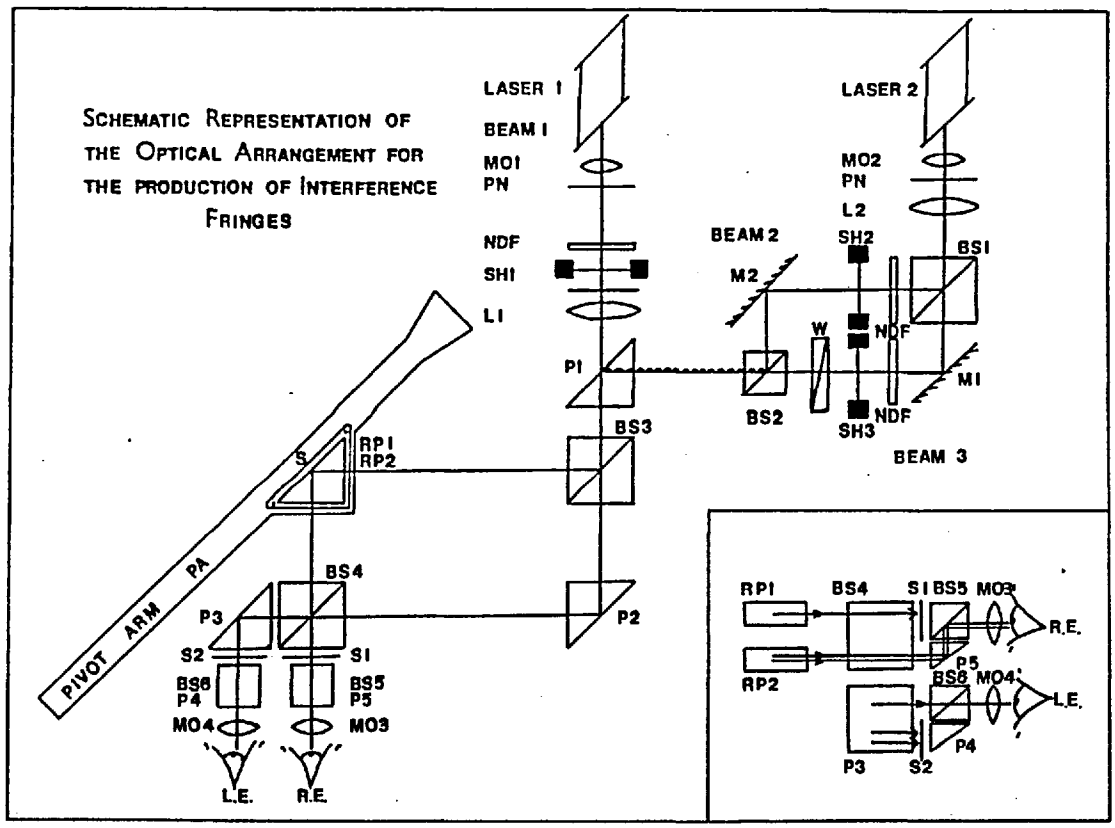

Fig. 2.15 The Interferometric Arrangement

632.8 nm, which were constant in intensity to $\pm$0.5%. Due to the split level arrangement of the apparatus, laser 2 is situated at a lower level than laser 1.

The beam from laser 1 (see fig. 2.15) is focused by a 10x microscope objective, MO1, onto a 25 nm pinhole, PN, and is then collimated by lens, L1, before entering the upper part of the interferometer through beamsplitter, BS3. In a similar manner, light from laser 2 is focused by a 10x microscope objective, MO2, onto a 25 nm pinhole, PN, before it is split into two beams by beamsplitter, BS1. One of these beams passes through a double neutral density wedge, W, to be recombined with the other beam in beamsplitter, BS2.

The light from laser 2 passes by the lower beam into the interferometer after deflection by prism, P1.

Electromagnetic shutters, SH1, SH2 and SH3, are positioned and operated in accordance with the nature of the experiment. Neutral density filters (NDF) are included in all of the beams to control the illumination levels.

After entering the interferometer, the beams are divided by the beamsplitter, BS3, and subsequently reflected by the prism, P2, or the reflecting prisms, RP1 and RP2. These beams finally enter the beam splitter, BS4. The reflecting prisms are arranged separately, one above the other, so that light from laser 1 in the upper, RP1, and that in the lower, RP2, from laser 2, can be independently translated and rotated by the two micrometer attachments on the pivot arm, PA.

These components are all rigidly attached to a thick dura-aluminium base, but one screw adjustment (S) is left on each of the RP's to allow the orientation of the fringes to be aligned with respect to the observer. Adjustment of S reflects the beams in a plane close to the vertical, and only a minimal change is produced in the spatial frequency. The microscope objectives illuminate the pinholes so that a diffraction limited point source is produced before the light rays enter the collimating lenses, and also the pinhole filters stray light, thereby, reducing the noise in the collimated beam. Stops can be placed in the beams emerging from the beamsplitter, BS4, depending upon the experimental configuration desired. The conversion to binocular viewing is achieved by reflecting the light not collected by BS4 in the prism, P3, to form sinusoidal fringes in the left eye, LE. The microscope objective,

MO4, behaves in a fashion similar to MO3, and focuses the collimated components from laser 1 to two points close to the nodal points of the observer's eye. The two beams are mutually coherent, and therefore give rise to two interfering divergent beams, which produce the sinusoidally modulated interference fringes on the observer's retina.

Judicial positioning of the stops in the emergent beams of BS4, allows a number of experimental configurations to be achieved. The inset to fig. 2.15 shows the stops inserted so that S1 prevents the upper beam from entering the right eye, RE, and allows only light from laser 2 to enter this eye by its deflection upwards in the prism, P5, and into the objective, MO3. The fringes are produced in the observer's eye, as explained previously, and only one of the collimated beams will enter the eye at any one instant. The observer sees the interference fringe pattern produced by laser 2 either in the beam which is deflected around the wedge, W, or in the beam which passes through the wedge, W, combined with the appropriate shutter operation. Stop S2 placed as shown, before prism P4, prevents the laser beams from laser 2 reaching the left eye, LE, and allows only the collimated beams from laser 1 to enter the eye to form the interference fringes. However, removal of stop, S2, and simultaneously occluding all light entering the right eye, RE, allows the light from laser 1 to reach the left eye, LE. A further stop can eliminate the beams deflected around the wedge from laser 2, and with such an arrangement, only the left eye, LE, will be stimulated.

B.iv. Calibrations

The spatial frequency of each system of fringes in both the left and the right eyepieces was obtained in terms of the readings of the

micrometer screw gauges, which drive the arms on which the reflecting prisms are mounted. The separation, t, of the two coherent spots produced (fig. 2.13), which governs the spatial frequency of the fringe pattern formed, was measured by a travelling microscope for several micrometer settings. From equation 2.10 for the intensity distribution in the interference fringe pattern, if the angle, $d\theta$ (fig. 2.13), between the successive maxima is small, then:-

$$\text{Angle}, d\theta = \lambda/t \quad , \qquad \text{Eq. 2.15}$$

and the spatial frequency, f, is related to the angular distance, $d\theta$, by:-

$$f = t\pi/\lambda 180 \text{ cycles per degree of visual angle.} \qquad \text{Eq. 2.16}$$

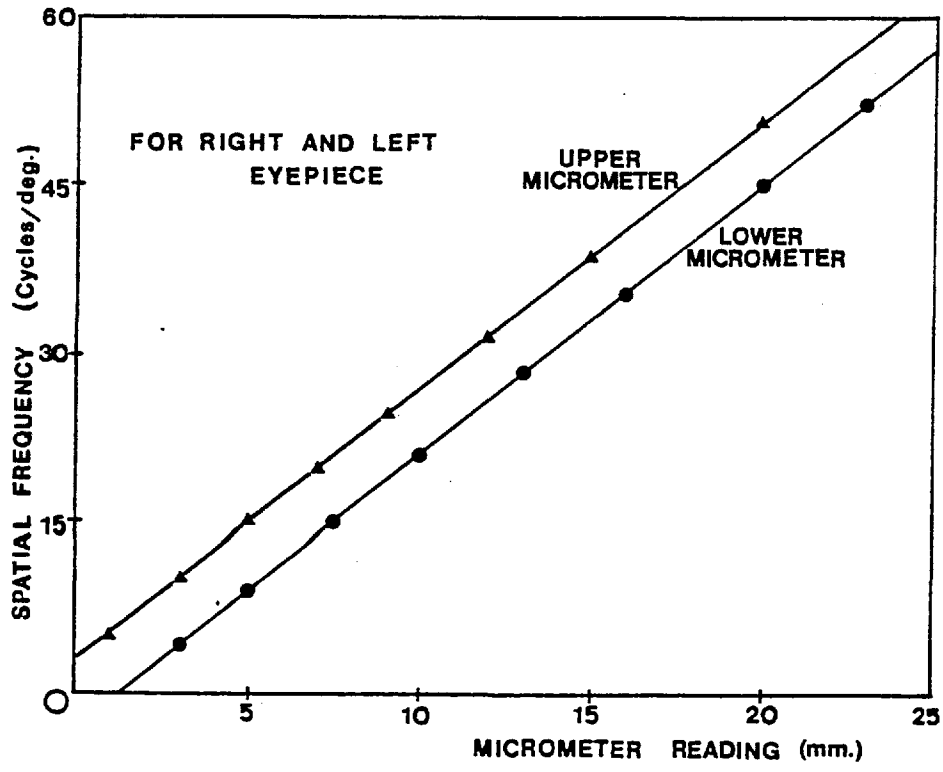

Fig. 2.16 Calibration curves for the upper and lower micrometers in the interferometer.

Figure 2.16 shows the graph plotted from this calibration procedure for the relevant eyepieces.

Fringes of different orientation, with respect to the vertical meridian relative to an observer stablilized by a mouthpiece, could be obtained by the reflecting prisms, RP1 and RP2, which were left free specifically for rotation with the screw adjustment, S. Burton (1973) checked the sinusoidal distribution of the fringes, and showed by a least squares fit approximation that a cosine curve fitted the profile, with less than 0.5% harmonic distortion.

The wedge, W, was made of blue glass. Both this wedge and the neutral density filters, NDF, were calibrated in situ by positioning a photomultiplier tube (EMI, Type 9698) at the eyepiece objective. The calibration graph (see fig. 2.17, plotting optical density against

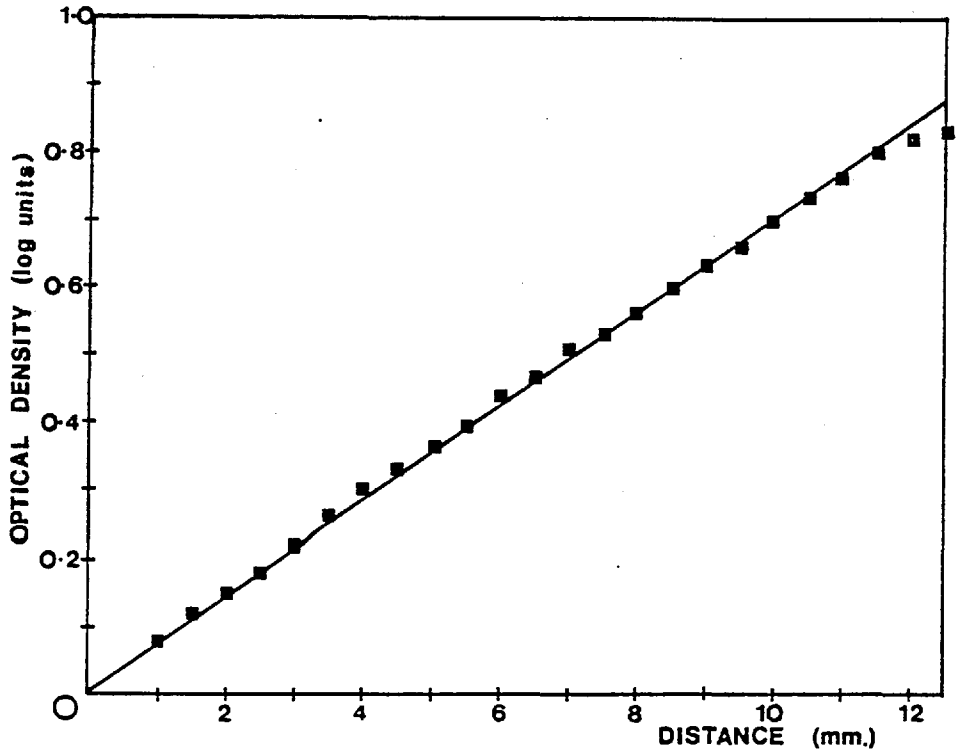

Fig. 2.17 Calibration curve for the wedge, W, in the interferometer.

the wedge setting) was obtained by taking the photomultiplier tube readings at pairs of points; T_1, without the wedge, and T_x, for the

beam transmitted at point x on the wedge. The wedge transmission at each point is given by:-

$$T = T_x / T_1 \quad , \qquad \text{Eq. 2.17}$$

and the optical density, D, by:-

$$D = \log_{10} 1/T \ \text{(log units)} \ . \qquad \text{Eq. 2.18}$$

The neutral density filters, NDF, were calibrated for transmission in a similar manner.

A photoconductor device, designed by Burton (1973), monitored the power output of the lasers, and was also used to set the retinal illumination levels for the different experimental conditions. This device is illustrated in fig. 2.18. The condensing lens, C, and photoconductor, P, are mounted in a brass tube, which fits tightly over the eyepieces. The lens forms an image of the field on the surface of the photoconductor, which produces an electrical impulse to deflect the spot on a galvanometer (PYE Scalamp, No. 79041S). The

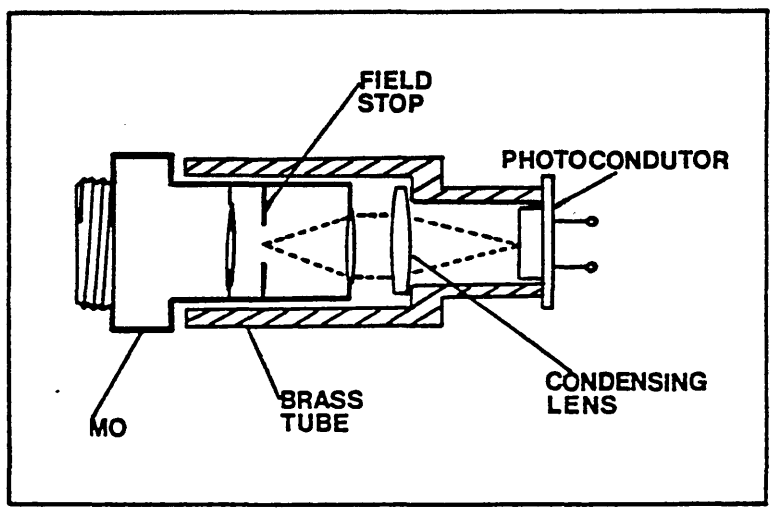

Fig. 2.18 Schematic representation of the light monitoring photo-conductor device. (after Burton, 1974)

photoconductor was also used to equalize the mean illumination levels in each eyepiece, by adjusting the neutral density filters so that each beam gave the same photocurrent.

B.v. Experimental Procedure

The adaptation phenomena studied are those associated with threshold detection of spatially periodic patterns, such as linear gratings, following a short period of adaptation to a high contrast grating with spatial characteristics similar to those of the test grating (see fig. 2.12). The threshold illumination level following such adaptation is greater than that found after adaptation to a uniform field of the same mean illumination level. If the contrast threshold setting, Tg, the illumination level of the test grating is recorded, and also the contrast threshold setting, Tu, for a uniform field of the same mean illumination level as the grating, the amount of contrast threshold elevation, Δ, is measured as:-

$$\text{Adaptation}, \Delta = \log Tg - \log Tu , \qquad \text{Eq. 2.19}$$

(see Chapter 1, Section C.v.).

At the beginning of all experiments, it was necessary to make adjustments to the interferometer, so that the observer was optimally aligned and positioned. The eye-piece separation was adjusted so that it matched the observer's interocular separation, and he saw a fused image of the two fields. Because the adaptation effects for gratings of different wavelength and spatial frequency are the same if their illumination levels are set at the same supra-threshold level, the threshold illumination levels for the detection of the different adaptation gratings were determined at the start of each experiment.

They would then be set at a fixed level above threshold for the adaptation measurements. Experimentally, neutral density filters were introduced into the adaptation field until it could 'just-no-longer' be detected; the criterion used for all threshold detection determinations. The optical density of the filters which gave the threshold setting was recorded, and by subsequent adjustment of the filters, the illumination level could be raised to a selected supra-threshold level.

During periods of adaptation the observer was instructed to keep his gaze wandering over the entire field, in order to prevent the formation of unwanted after images. The shutters, SH1 and SH3, operate so that the adaptation grating is extinguished, and the test grating becomes visible. The test grating field is of slightly smaller diameter than the adaptation grating (fig. 2.19), which

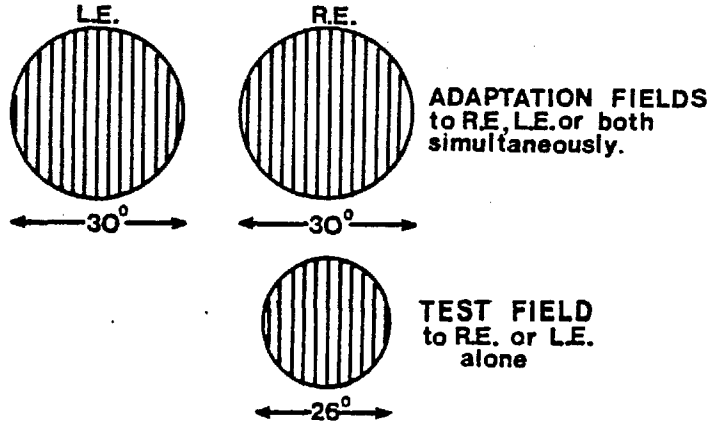

Fig. 2.19 Schematic diagram to show the type and size of fields produced by the interferometer.

ensures that the test grating is presented to a uniformly adapted retinal region. After an initial period of two minutes adaptation, the test field and adaptation fields are presented alternately for

1 second and 20 seconds respectively, and the cycle repeated until the threshold illumination setting was achieved. The test beam illumination level was set three or four times, and in the repeated measurements of the same threshold, the wedge was reset on each occasion to a random setting. For adaptation measurements with a uniform field, one of the two interfering beams was blocked and a 0.3 log filter removed from the other beam, in order to give the same mean illumination level as the grating. The experimental procedure was exactly the same as that used for the grating, thus the two settings, log Tg and log Tu, defined in equation 2.19, were obtained. The standard error associated with the measurements calculated from the standard deviation of the results is about 0.05 log units, and is acceptable compared with the magnitude of the contrast threshold elevation effect, some 0.3 to 0.4 log units. The contrast threshold elevation effect is transient, becoming insignificant within some 30 seconds of cessation of adaptation. This necessitates the brief presentation of the test pattern and subsequent re-adaptation periods during the experiment.

C.i. The Wright Colorimeter

Colour matching experiments were performed with the colorimeter, designed by Wright (1927-8, 1946), the optical system of which is illustrated schematically in fig. 2.20. The source, S1, a 100V quartz-halogen lamp, is focused by the collimating lens, L1, onto an adjustable vertical entrance slit, SL. The light, which emerges from this slit, is collimated again by lens, L2, and the beam passes over the reflecting prism, RP1, to be dispersed by the two optically dense glass prisms, DP. A split mirror arrangement, DM, which is also shown

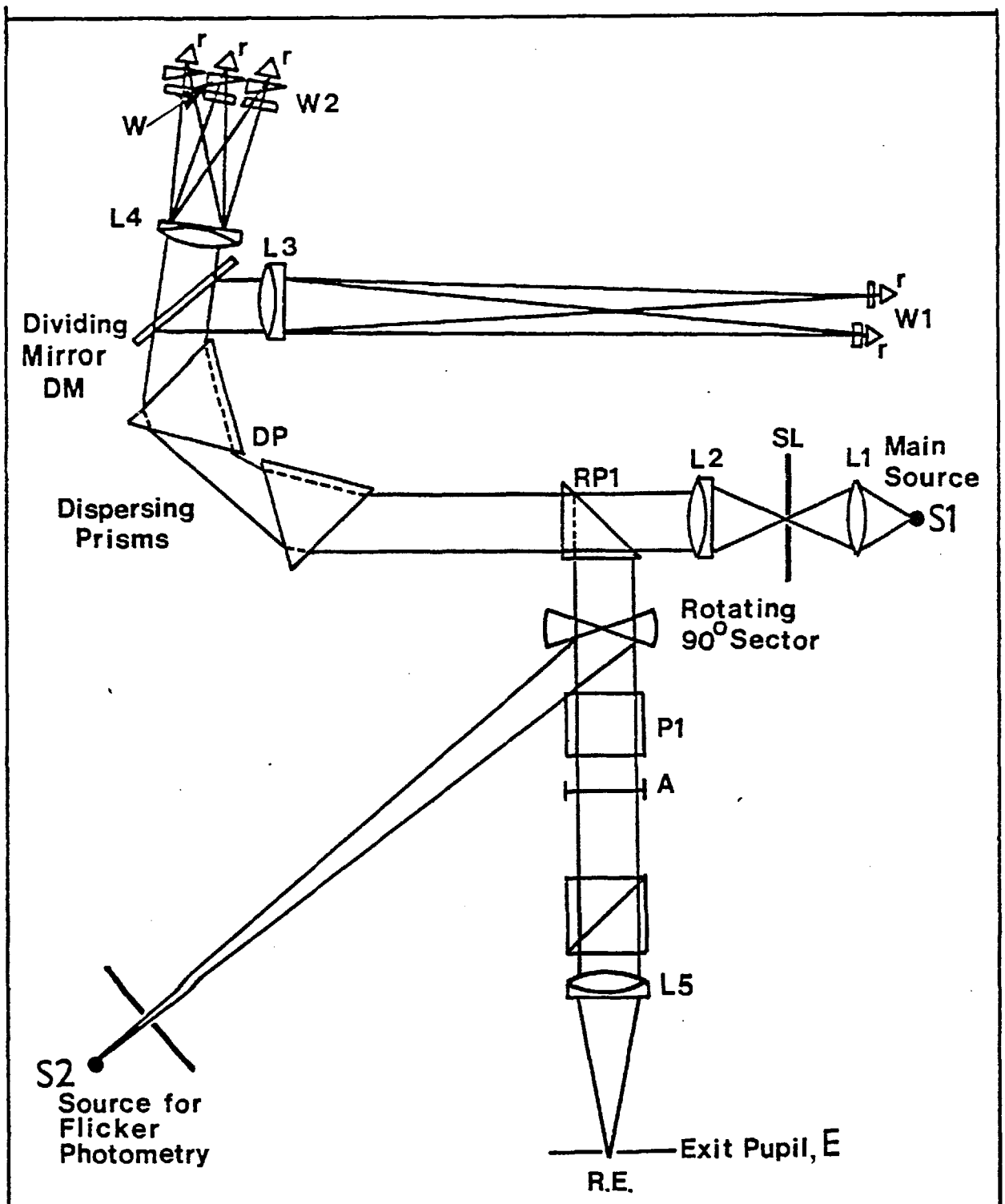

FIG2.20 A Schematic Representation of the WRIGHT Colorimeter.

in fig. 2.21, reflects the upper half of the dispersed light through the lens, L3, to form a focused spectrum, W1, whereas the lower half of the light passes through an aperture in DM, and is collected by L4 to form another spectrum, W2. Small roof-reflecting prisms, N,

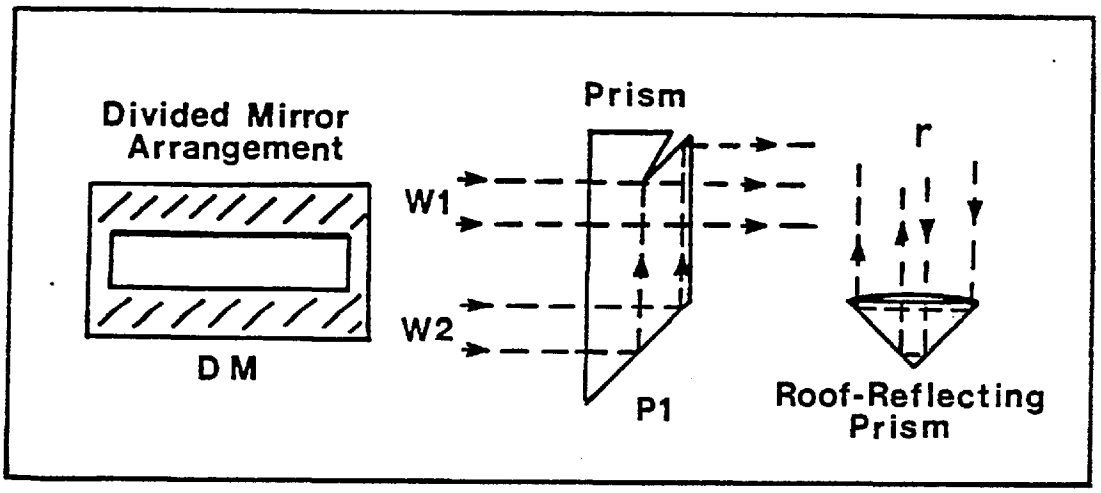

Fig. 2.21 An enlarged view of three components of the Wright Colorimeter.

(see fig. 2.21) are placed at appropriate positions in both of these spectra to reflect small bandwidth regions along paths below the incoming beam, but due to the roof prism, N, with the spectrum order reversed. Thus, the final passage through the dispersing lenses doubles the dispersion; a device which limits the effect of spectral impurity due to stray light. The W2 spectrum provides the mixture of three wavelengths required for the matching half of the bipartite field of view. A neutral density wedge, W, is suspended in front of each of the roof-reflecting prisms in the W2 spectrum for this purpose. These wedges are graduated in cm, and the observer adjusts their positions relative to the roof prisms in order to establish a colour match. The W1 spectrum carries two roof-reflecting prisms; one which provides the required wavelength for the test field, and the

other provides a desaturating field for certain critical matches. The light collected by the roof-reflecting prism providing the test field is reflected in a downward path relative to the incoming light and is collected by the lens, L3 (fig. 2.20). This light is therefore reflected back into the dispersing prisms, DP, by the lower half of the split mirror arrangement, DM (fig. 2.21). The returning light is also laterally inverted due to the roof-prism, N, (see fig. 2.21), and further dispersed by the prisms, DP. The prism, RP1, reflects this light into the prism, P1. The light reflected and similarly processed by the roof prisms in N2 passes, after collection by the lens, L4, underneath the divided mirror, DM, (see fig. 2.21) and enters the dispersing prisms, DP.

The light, which emerges from RP1, consists of two vertically displaced beams; the upper beam is a mixture of at most three monochromatic matching stimuli, and the lower beam provides the test field. Both of these beams are collected by the prism, P1 (fig. 2.21), and are focused onto the exit pupil, E, by the lens, L5, which therefore provides a Maxwellian field of view in the right eye of the observer, RE.

The light incident on the exit pupil is a dispersed 'image' of the entrance slit, SL, and the double transit through the dispersing prisms, DP, together with the slit width, produce a sufficiently large 'image' to cover an exit pupil of 2 mm diameter. The pupil contains an eye achromatising lens (Thomson and Wright, 1947), and the bipartite fields of 1^{o} 20' or 80' are obtained by positioning the appropriate field stop, A, close to the prism, P1.

C.ii. Calibration of the Colorimeter

The density gradients of the wedges which provide the adjustable colour matching field and filters are all calibrated *in situ* by means of a photomultiplier (EMI, type 9558) placed at the observing position. The brightness matching technique of Wright (1946, pp 64-66) makes it possible to check the photomultiplier calibrations of the wedges. Figure 2.22 shows the best line fits to the data for some wavelengths in these wedges. The photomultiplier was also used to obtain the relative energies of the monochromatic

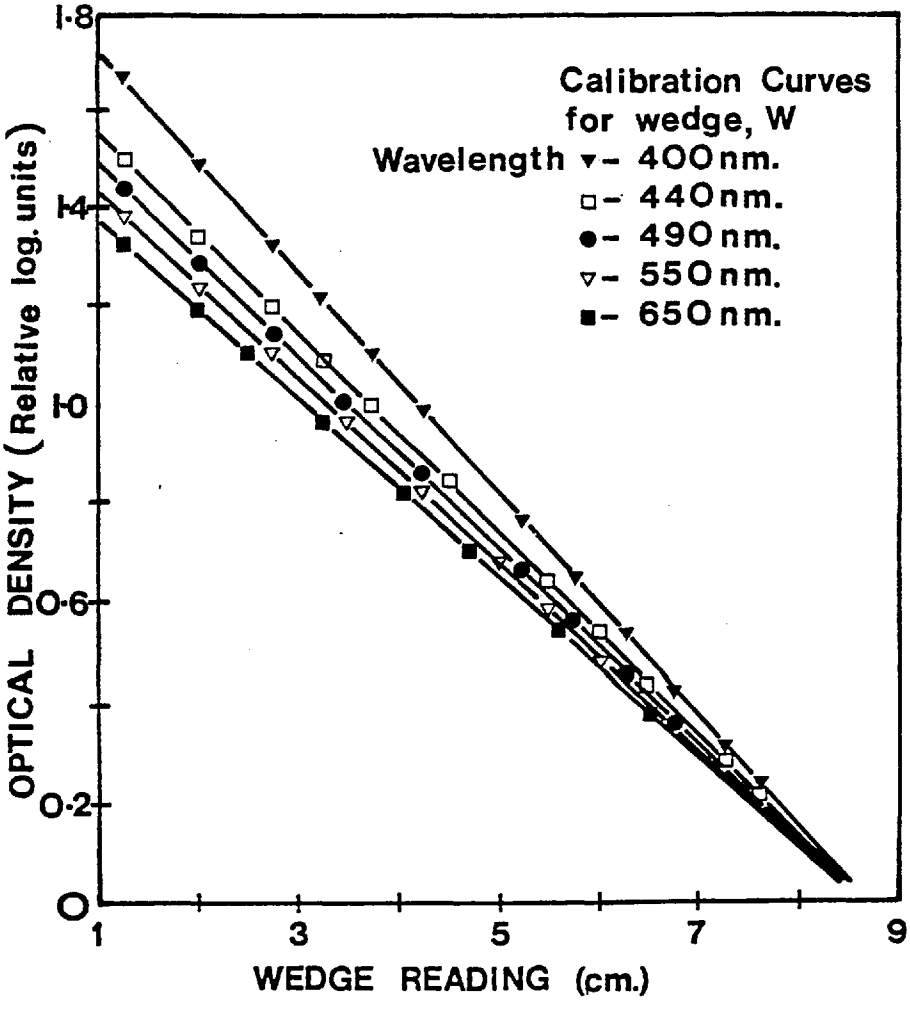

Fig. 2.22 Calibration curves for the wedge, W, showing the linear regressions for the data at five wavelengths.

lights reflected by the prisms in the W1 and W2 spectra, so that any change in the spectral output of the lamp, S1, could be accounted for, (see fig. 2.23), in the W1 spectrum.

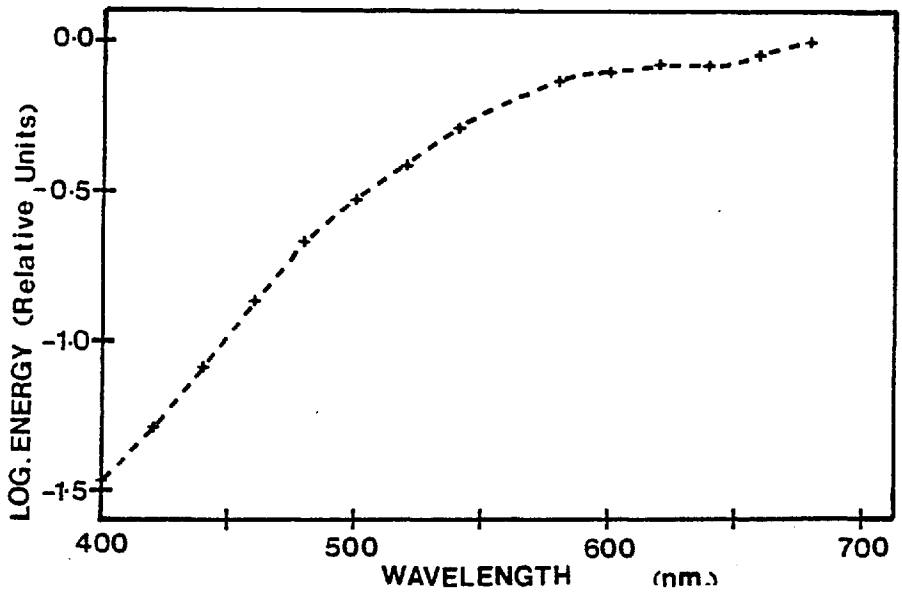

Fig. 2.23 To show the relative change in energy of the source as a function of wavelength.

A line source (Phillips, mixed gas spectral source, type Hg-Zn-Cd, 0.9A, B7) replaced the main colorimeter source, S1, to obtain the wavelength calibration of W1 and W2. Each roof prism was moved along the spectral plane until it reflected one of the spectral lines which was then seen in the exit pupil, E, focused with a lens to obtain a centrally positioned image of the line. A complete wavelength calibration was then generated by interpolation between these lines with the Cauchy Equation.

CHAPTER III

Determination of Post-Receptoral Spectral Responses in Human Vision

A.i. Introduction

Investigation of human colour discrimination mechanisms rests primarily on the psychophysical techniques of colour matching (Wright, 1929, 1936, 1946) and the increment threshold (Stiles, 1939, 1949, 1959) measurement. Both of these methods describe spectral mechanisms which occur at the first stage of vision, that is, at the receptoral stage. For observers with normal colour vision, both yield broad-band spectral responses which are closely related to the absorption spectra of the photopigments contained in the three classes of cone (Brindley, 1970). These methods are therefore not well suited to the investigation of colour vision mechanisms which involve post-receptoral responses. It is of interest to examine the spectral characteristics of post-receptoral responses because, as well as providing information on normal colour vision, they could also be used to study defective colour vision, particularly those defects which are caused by abnormal post-receptoral function. Rushton (1958) developed a technique of retinal densitometry with which he managed to isolate two cone functions in an observer with normal colour vision. To do this he compared the difference in the relative absorption of each wavelength of light projected onto neighbouring areas of the fovea before and after bleaching the photopigments with intense light of a narrow band of wavelengths. The bleached pigments then absorbed fewer photons. He repeated this measurement with several subjects with

defective colour vision, one of which was a deuteranope (Rushton, 1965). He established that in fact the deuteranope lacked the green cone photopigment (chloralabe). There may also be, however, deficiencies in congenital and, in particular, acquired colour vision defects which arise at a stage more central than the photoreceptors.

In the introduction (chapter I), it has been shown that post-receptoral mechanisms can be investigated by adaptation methods, which establish that the human visual system possesses binocularly controlled response mechanisms selectively sensitive to specific stimulus attributes, such as the orientation and width of an elongated bar (Gilinsky, 1968; Pantle and Sekuler, 1968; Blakemore and Campbell, 1969b and Maudarbocus and Ruddock, 1973b). However, the analysis of visual responses to one-dimensional stimuli leaves unresolved the problem of defining an elongated stimulus. This requires investigation of the contrast threshold elevation effect for a set of two-dimensional stimuli, in which it is possible to vary both the length and the width of the bar-shaped elements (Burton and Ruddock, 1978). Two classes of response mechanisms are evident from their results and they suggested that there is one mechanism preferentially tuned to the relative length of the bars in the test and adaptation patterns, and another which is not. The independence of these two kinds of response is demonstrated by the fact that the length-selective adaptation mechanisms are monocularly controlled, whereas the non-length-selective are under binocular control (Naghshineh and Ruddock, 1978). The receptive fields associated with the detection of elongated, bar-shaped stimuli have a length:width ratio of three, which is consistent with the orientation selectivity of the contrast

threshold elevation effect as measured with one-dimensional gratings (Burton and Ruddock, 1978).

The contrast threshold elevation effect (Gilinsky, 1968; Pantle and Sekuler, 1968 and Blakemore and Campbell, 1969b) forms the basis of the investigation to be described in this chapter. Briefly, this effect requires the adaptation of the right eye (RE) of an observer to a high contrast grating (fig. 3.1a), which consists of alternate dark and light bars, for a period of about two minutes. During this time, there is no fixation, and the observer allows his gaze to wander over the entire stimulus pattern. Subsequently, the adaptation grating, AG, is replaced by a test grating, TG, 100% contrast but of low illumination level, superimposed on a uniform background field of the same mean illuminance as that of the adaptation grating. It is found that the contrast threshold level required for the detection of the one-dimensional test grating, TG, is raised compared to the level required after adaptation to the uniform field of the same mean retinal illumination level (see fig. 3.1f, point a). This increase in the contrast threshold level is associated specifically with the spatial characteristics of the test and adaptation gratings, which must be closely matched in size and orientation to obtain any significant effect.

The effect can be interocularly transferred, as shown in fig. 3.1b, since the contrast threshold level required for the detection of the test grating, TG, presented to the right eye, following two minutes adaptation of the left eye to a high contrast grating, is also increased (see fig. 3.1f, point b); for this configuration, however, the amplitude of the effect is slightly reduced. The effect is

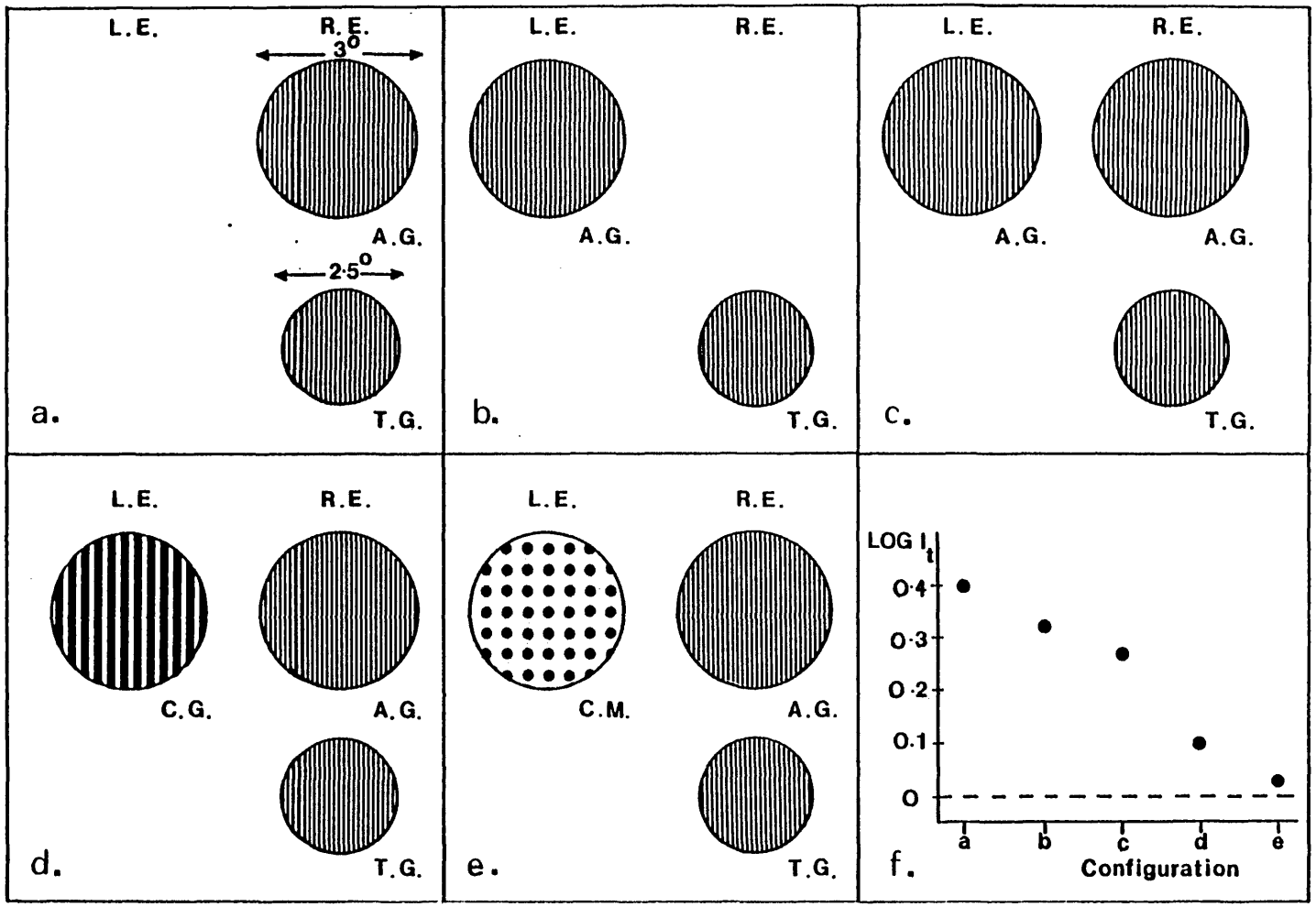

Fig. 3.1

a-e. To illustrate the various configurations of adaptation (AG) and test (TG) stimuli, presented as indicated, to the right (RE) and left (LE) eye of the observer and

f. schematic representation of the threshold illumination level required for the detection of the test grating after adaptation to each of the configurations (a-e). Log I_t equal to zero corresponds to the pre-adaptation value.

therefore attributed to adaptation in cortical units at the level where the signals from the two eyes converge. In the human visual system, the pathways from the two eyes converge anatomically after partial decussation of the optic nerve fibres at the optic chiasma. Neurophysiological studies of the visual cortex of primates show that these converging pathways carry signals from both eyes to the same cortical neurones. Interocular transfer of the contrast threshold elevation effect suggests that this kind of adaptation takes place at a central location in the cortex. Any other interpretation would involve retinal control by fibres radiating from the cortex, and there is no evidence for their presence (Brindley, 1970, pp 105). Interocular transfer is an inter-observer variable; Blakemore and Campbell (1969b) report a transfer of 70 to 80%, but Maudarbocus and Ruddock (1973b) showed that as much as a 90% transfer could be obtained in some observers. The results of Wigley (1977) show that the degree of interocular transfer is indeed dependent on the degree of an individual's stereoscopic fusion capacity. Observers, who are termed stereoblind, exhibit a complete absence of interocular transfer (Abadi, 1974).

It may be thought that by simultaneously adapting the two eyes to similar high contrast gratings, it would be possible to induce summation and thereby increase the effect. This was the aim of the investigation of Wigley (1977), but the results of adaptation of both eyes (fig. 3.1c) only leads to a further reduction in the amplitude of the effect (see fig. 3.1f, point c). Further, if the two eyes are adapted to different grating patterns, the left eye to a coarse high contrast square-wave grating, and the right eye to the test frequency

of the same mean retinal illumination level (fig. 3.1d), it was found that the effect was virtually abolished (see fig. 3.1f, point d) (Ruddock and Wigley, 1976). Thus, the interaction between the adaptation stimuli, presented to the two eyes, is inhibitory.

It has already been emphasized that there are two separate mechanisms which contribute to adaptation phenomena (Burton and Ruddock, 1978); one associated with 'long' bars and the other with 'short' bars. In addition to the contrast threshold elevation effect established as a result of adaptation to high contrast bar gratings, Naghshineh and Ruddock (1978) have shown that a contrast threshold elevation effect is also observed after adaptation to two-dimensional patterns consisting of spot stimuli. The contrast threshold elevation effect in this case is established by a class of stimuli which do not possess well-defined axes of symmetry, and therefore would not give rise to strong adaptation effects in orientation selective mechanisms, i.e., those with a length specificity (Burton and Ruddock, 1978). Naghshineh and Ruddock (1978) showed that adaptation to a high contrast spot matrix array affects the contrast threshold required for the detection of linear square-wave gratings. Therefore the two-dimensional pattern produces a selective adaptation in the visual system which affects the mechanisms that detect the contrast of one-dimensional grating stimuli.

The major conclusion which arises from such data is that adaptation to two-dimensional stimuli gives rise not only to a size specific contrast threshold elevation effect for other regular or irregular two-dimensional stimuli, but also that it selectively elevates the contrast threshold for linear grating stimuli. The

maximum elevation occurs when the diameter of the elements of the two-dimensional adaptation stimulus is equal to the width of the light bars in the test stimulus.

The investigation to be described in this chapter combines the binocular adaptation effects associated with the length- and non-length selective mechanisms, and it is shown that unlike the adaptation effects associated with elongated bars in both the contrast threshold elevation effect and in its binocular suppression (Maudarbocus and Ruddock, 1973b; Ruddock, Waterfield and Wigley, 1979), this effect is colour-selective. From this wavelength selectivity, it is possible to derive three spectral, post-receptoral response curves, which have been measured for two normal observers, and data are also presented for one dichromatic observer, a deuteranope. The remainder of this chapter is concerned with the detailed investigation of colour and spatial properties of the inhibitory binocular adaptation effect.

A.ii. Experimental Apparatus

The Maxwellian viewing system, described in section A, chapter II, adapted to provide a binocular viewing arrangement, and with four channels for stimulus presentation, was used in this investigation. In the experiments which are to be described, the circular adaptation fields were restricted to some 3^{o} in diameter, whereas the test field was of slightly smaller dimensions, 2.5^{o} in diameter. The visual fields employed in the investigation are illustrated in fig. 3.1e and in fig. 3.2. The right eye was adapted to a linear square-waveform grating with the same bar width and orientation as the test grating,

and the left eye to a two-dimensional pattern which consisted of spot stimuli in a matrix array. These stimuli were produced as described in section A.vi, chapter II. Experiments were performed with linear gratings of various bar widths, d minutes of arc, and the spot matrix arrays had diameters d' minutes of arc, which varied through the same range as the bar widths of the gratings. Thus the different stimuli could be matched in terms of equivalent spatial frequencies. The test grating, TG, was always presented to the right eye which also viewed the adaptation stimulus, AG. The left eye was adapted simultaneously with the right eye, and its adaptation stimulus is distinguished by the term conditioning matrix, and denoted by the symbol, CM.

A.iii. Experimental Procedure

The observer's head position was fixed throughout the experiments by a dental bite bar. The adjustable bite bar aided alignment of the observer's pupil relative to the artificial instrumental exit pupil of 2 mm diameter. For dichoptic stimulus presentation, it was also necessary to adjust the interocular separation of the two exit pupils, so that it matched that of the observer, who could then fuse the two visual fields (fig. 3.2).

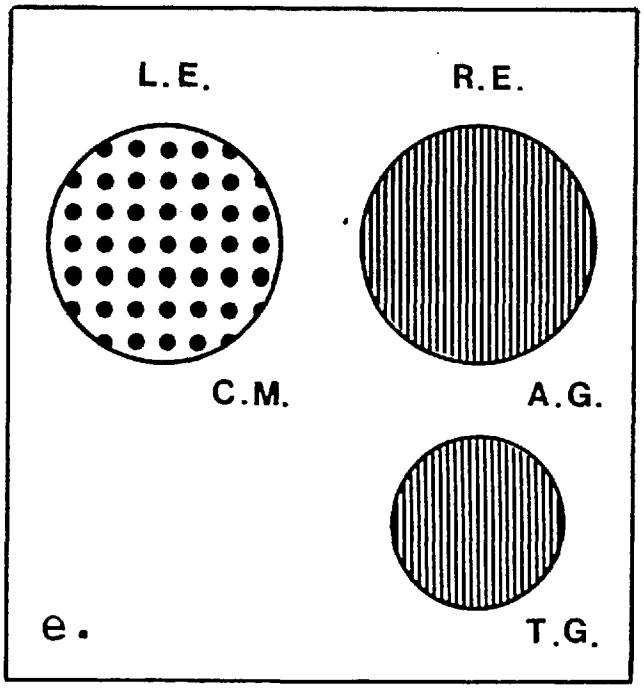

Fig. 3.2 To illustrate the visual field configuration presented to the observer.

Adaptation effects for linear gratings of different spatial frequencies and different wavelengths are equal, provided that their illuminations are set at the same supra-threshold level (Maudarbocus and Ruddock, 1973a). Thus, the threshold illumination levels for the detection of the different monochromatic gratings, AG, and conditioning matrices, CM, were determined at the beginning of each experiment. They could then be set at the same supra-threshold level for the adaptation measurements. The criterion of 'just-no-longer' seen was adopted in all threshold detection measurements, and neutral density filters were introduced into the relevant beam until this condition was satisfied. The optical density of the filters required to give the threshold setting was recorded, and the illumination level was then raised to the required supra-threshold level by adjustment of the filters.

Initially, the adaptation gratings were presented for two minutes, during which time the observer was instructed to keep his gaze wandering randomly over the entire visual field, to prevent the formation of localized after-images. After this initial period, the shutters, SH1, SH2 and SH3 (see fig. 2.3, chapter II) were triggered (see Appendix A) and operated so as to expose alternately the adaptation fields and test field for ten seconds and three seconds, respectively. The cycle was repeated until the threshold illumination setting was achieved. During the three second test period, the adaptation grating was completely occluded by shutter, SH2 (fig. 2.3), and the low illumination level test grating was seen superimposed upon the uniform background field. The illumination level of the uniform background field was equal to that of the adaptation

grating, thus the state of adaptation remained constant throughout the experiment. The brief presentation of the test pattern and the subsequent periods of re-adaptation were necessary because of the transient nature of the adaptation effect. During the periods of re-adaptation, the observer operated the wedge, W (fig. 2.3, chapter II), to reduce the illumination level. In this way, the illumination level of the test beam was adjusted to threshold level, i.e., that point at which the test grating was 'just-no-longer' detected. In the brief presentation periods of the test grating, the observer merely made the decision as to whether he did, or did not detect, the test pattern.

The procedure was repeated several times for each stimulus configuration and the settings recorded by depressing the appropriate switch on the printer (see fig. 2.5, chapter II). The threshold illumination level was determined three or four times, to obtain log W_g, and in these repeated measurements of the same threshold, the wedge was reset to a random position on each occasion. The procedure was also repeated for adaptation measurements with the adaptation gratings replaced by a uniform field of the same mean illumination level as the grating pattern, to give the threshold illumination level, log W_u. Thus two logarithmic threshold illumination levels are obtained, and a measure of the adaptation effect, associated with the grating pattern is defined as:-

$$\text{Adaptation effect}, \Delta = \log W_g - \log W_u . \qquad \text{Eq 3.1}$$

The end of one particular sequence of measurements was indicated to the observer by a buzzer signal (Appendix B), and the mean of these results gave the average value of the adaptation effect, Δ.

A.iv. Subjects

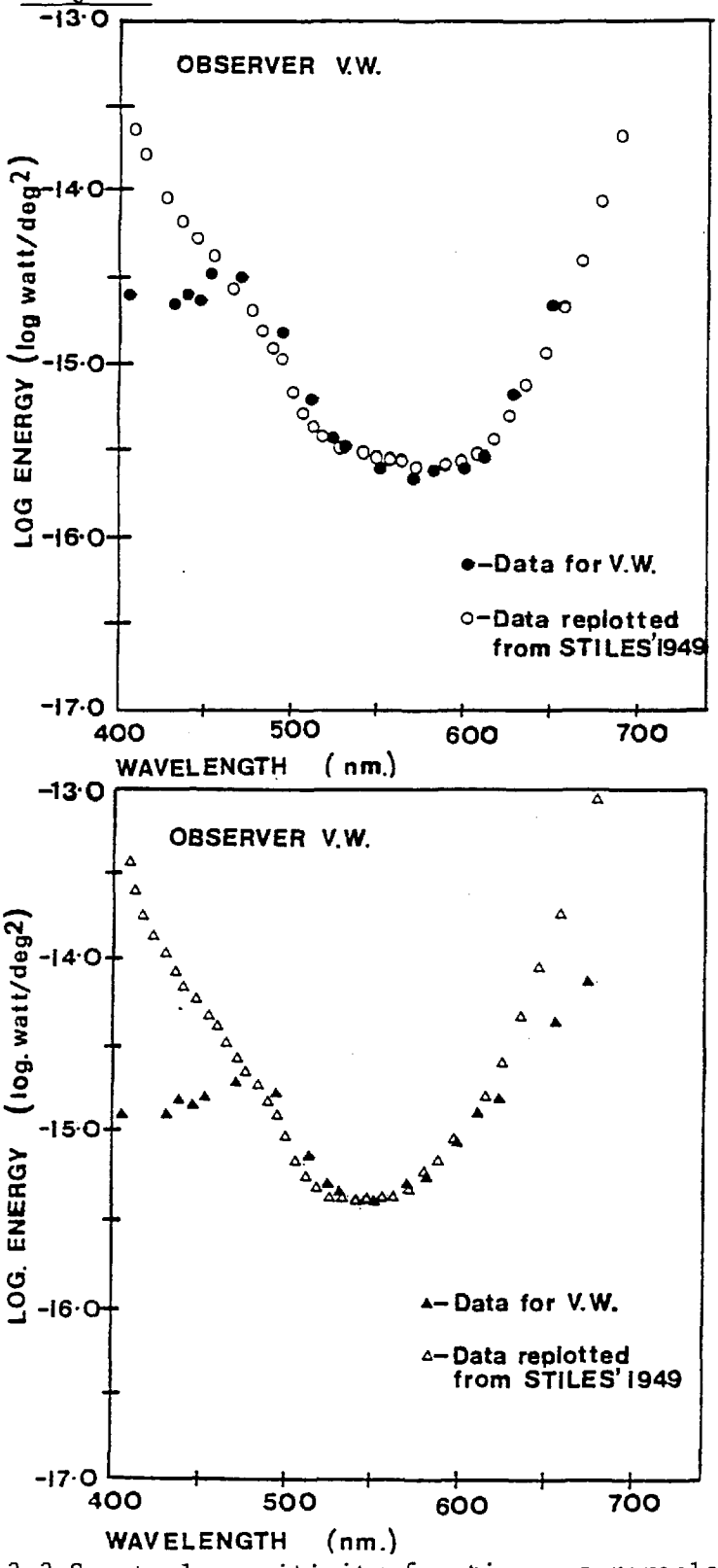

Fig. 3.3 Spectral sensitivity functions as revealed by the increment threshold technique of Stiles (1959). a. π_5 mechanism, b. π_4 mechanism. Observer V.W.

V.W., (female, aged 23 years) an emmetrope, and I.H., (male, aged 23 years) a myope, both possessing normal colour matching responses, and normal colour sensitivity as revealed by the colour matching and by the increment threshold technique of Stiles (1949, 1959, 1978), shown in fig. 3.3 and in fig. 3.4, for each observer, respectively, and in fig. 3.5.

A third subject, observer

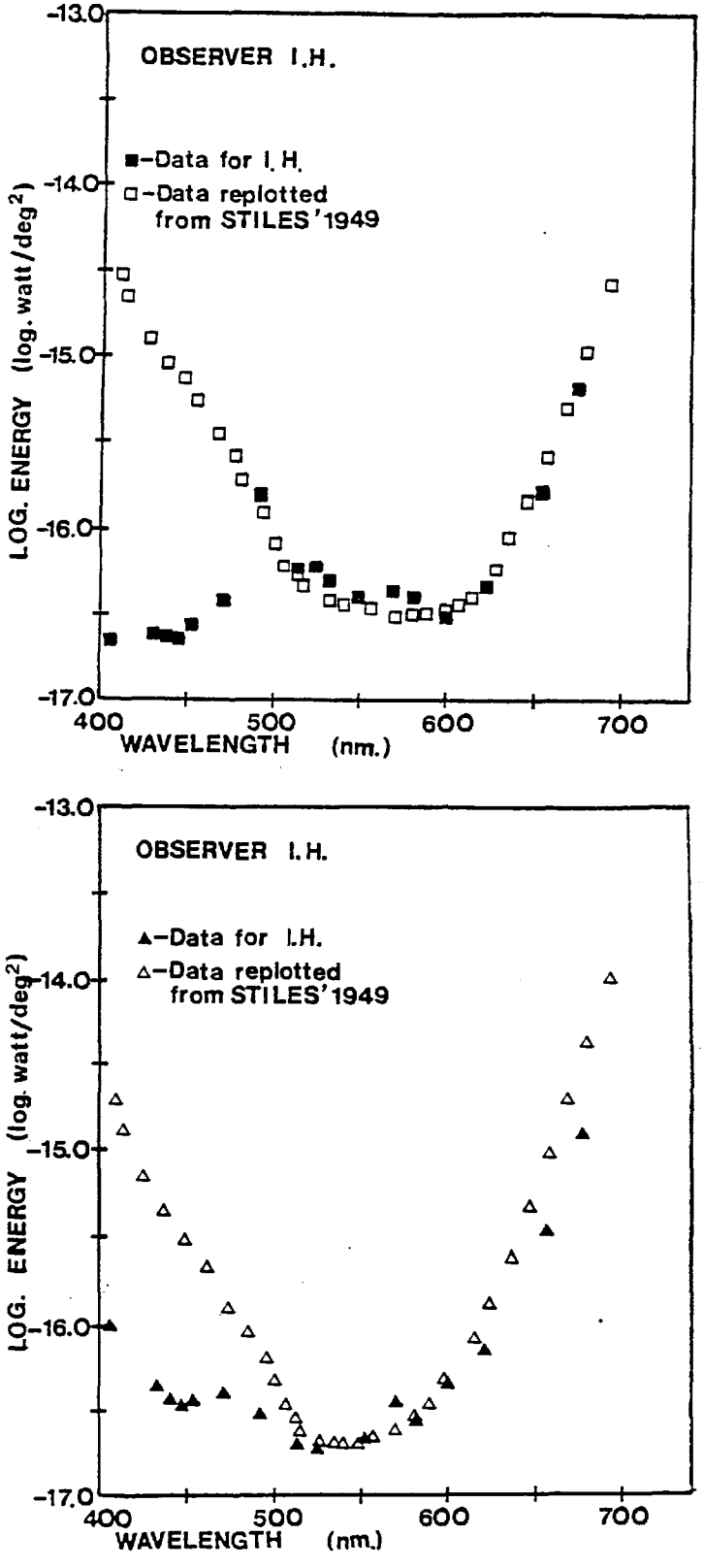

Fig. 3.4 a and b. As in fig. 3.3, but data are for observer, I.H.

C.C. (male, aged 20 years) a myope, possesses a congenital colour vision defect. His responses to the Ishi-hara Colour Vision test plates (Edition 1976) and his colour matching revealed that he is a dichromatic deuteranope. All three observers showed normal stereoscopic fusion when tested with the analglyphs (Julesz, 1971).

Unless otherwise stated, the adaptation gratings were set 4 log units

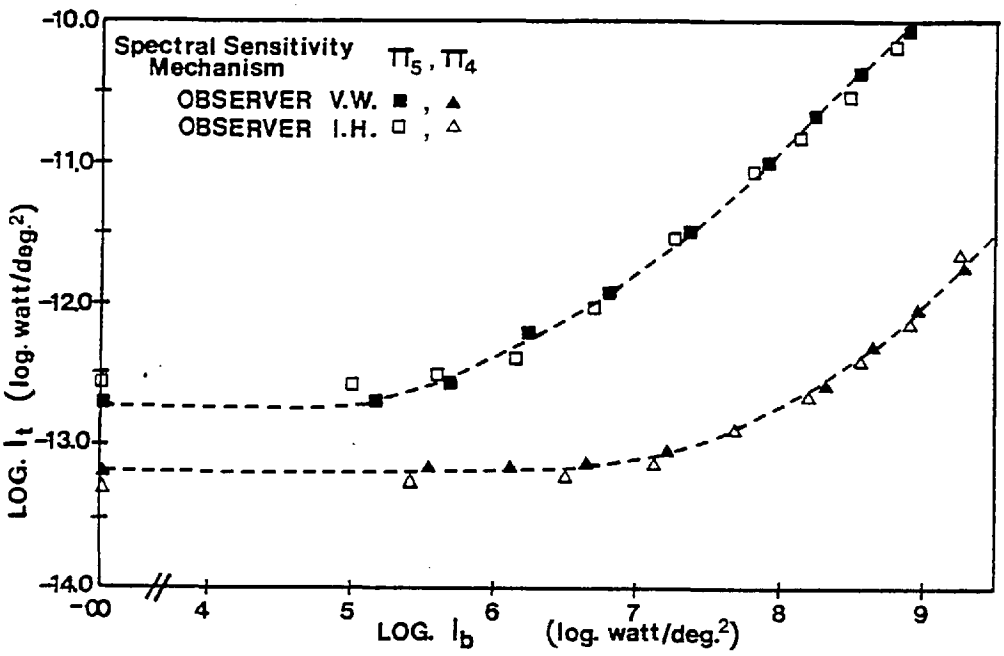

Fig. 3.5 Increment threshold data for both observer V.W. and I.H.

supra-threshold for each observer. All the data points are the mean of at least four determinations, and the mean standard error for the observers is as follows:- V.W., ≃ 0.03 log units; I.H., ≃ 0.04 log units and C.C., ≃ 0.04 log units.

B. Preliminary Results

The first experiments were designed to investigate the variation of Δ with the change in the diameter, d', and wavelength, λ, of the spot matrix. Each set of data in fig. 3.6 to fig. 3.9 refer to adaptation (AG) and test grating (TG) patterns of linear square-wave-form and bar width, d = 5.7 minutes of arc (corresponding to a fundamental spatial frequency of 5.2 c/^{o}), but of different wavelengths (i.e., fig. 3.6, 636 nm; fig. 3.7, 577 nm; fig. 3.8, 551 nm and fig. 3.9, 435 nm). The broken horizontal line in each diagram represents the values of Δ obtained in the absence of the

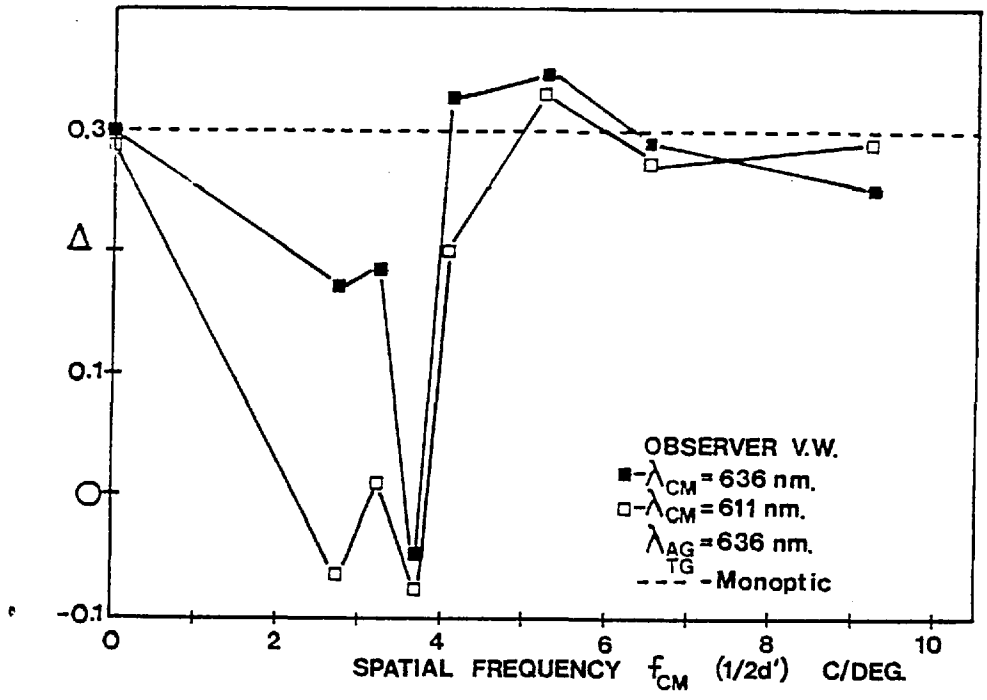

Fig. 3.6 Adaptation, Δ, plotted as a function of spatial frequency of conditioning matrix, f_{CM}, for the field configuration shown in fig. 3.2. AG and TG are presented in a wavelength of 636 nm, whereas CM is in 636 nm (■) and 611 nm (□). The dotted line represents adaptation produced in the absence of CM. Data are for observer V.W.

matrix presented to the left eye, and represents the adaptation effect associated with the simple contrast threshold elevation effect (see fig. 3.1a). The magnitude of the adaptation effect, Δ, is plotted against $(2d')^{-1}$, expressed in cycles per degree, and it is apparent that, in each case, values of Δ are minimum for large matrix spots of diameter in the range 0.8' to 6' of visual angle. If, however, the spot matrix wavelength is changed to 542 nm, as in fig. 3.10, values of Δ are virtually independent of the size of the spots in the matrix array, whereas if the matrix is of still shorter wavelength, 512 nm (fig. 3.11) or 470 nm and 439 nm (fig. 3.12), values of Δ increase relative to the simple contrast threshold elevation level (broken line) for coarse spots.

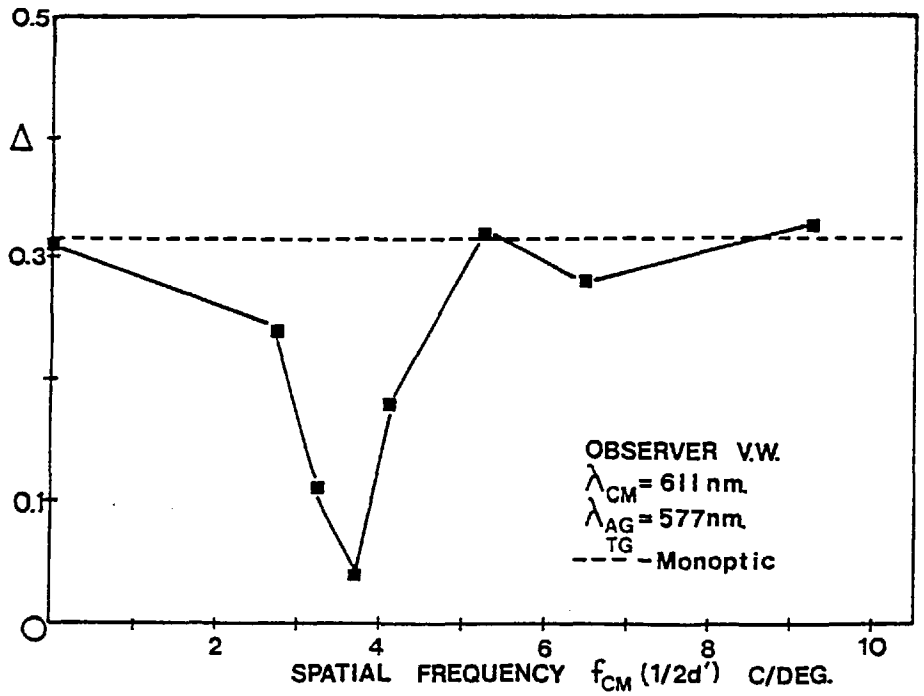

Fig. 3.7 As in fig. 3.6, but AG and TG are presented in a wavelength of 577 nm, and CM in 611 nm.

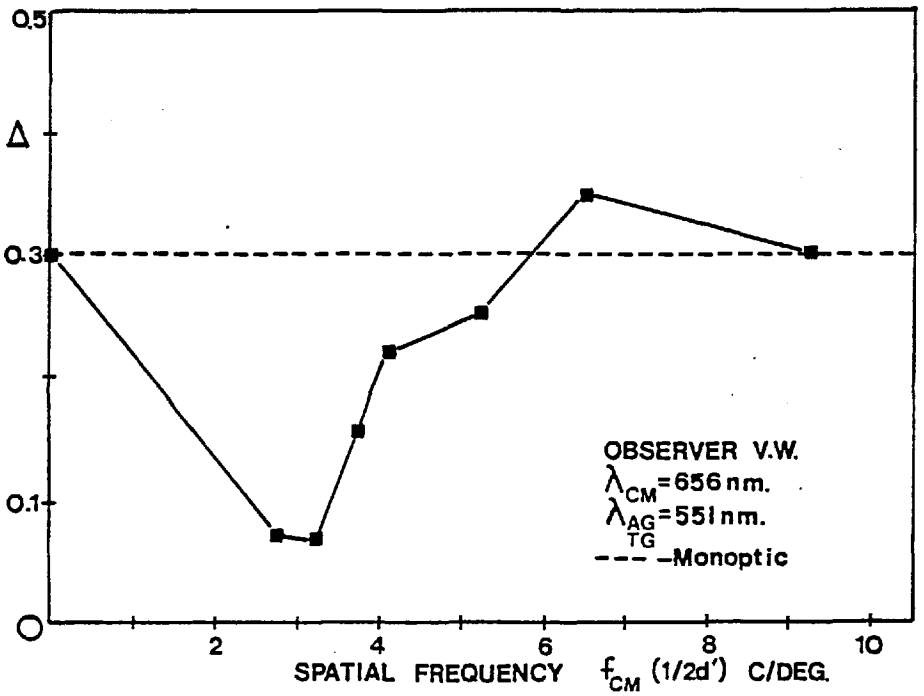

Fig. 3.8 As in fig. 3.6, but AG and TG are presented in a wavelength of 551 nm, and CM in 656 nm.

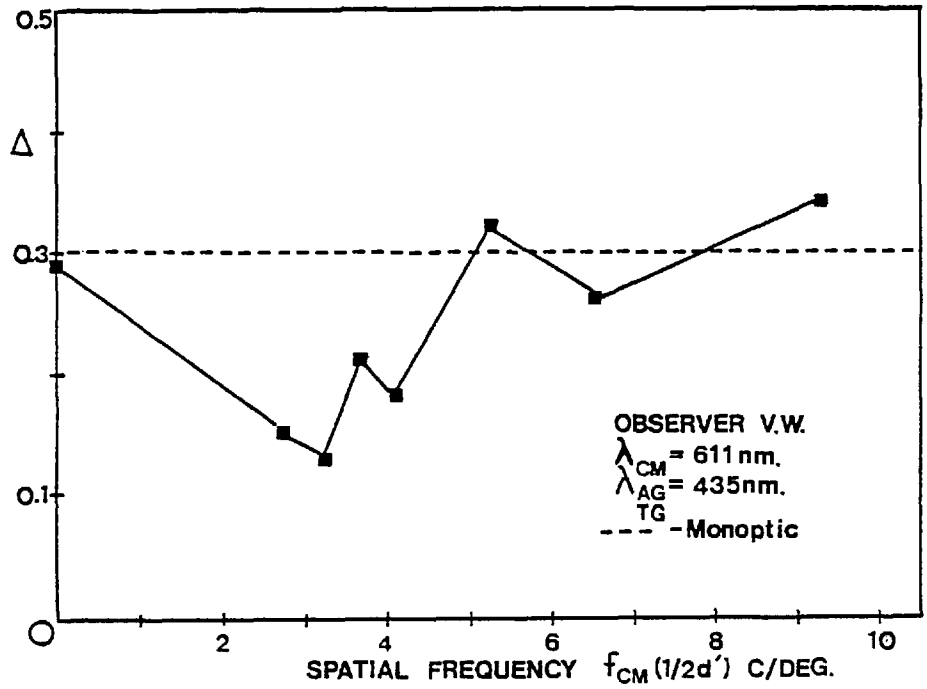

Fig. 3.9 As in fig. 3.6, but AG and TG are presented in a wavelength of 435 nm, and CM in 611 nm.

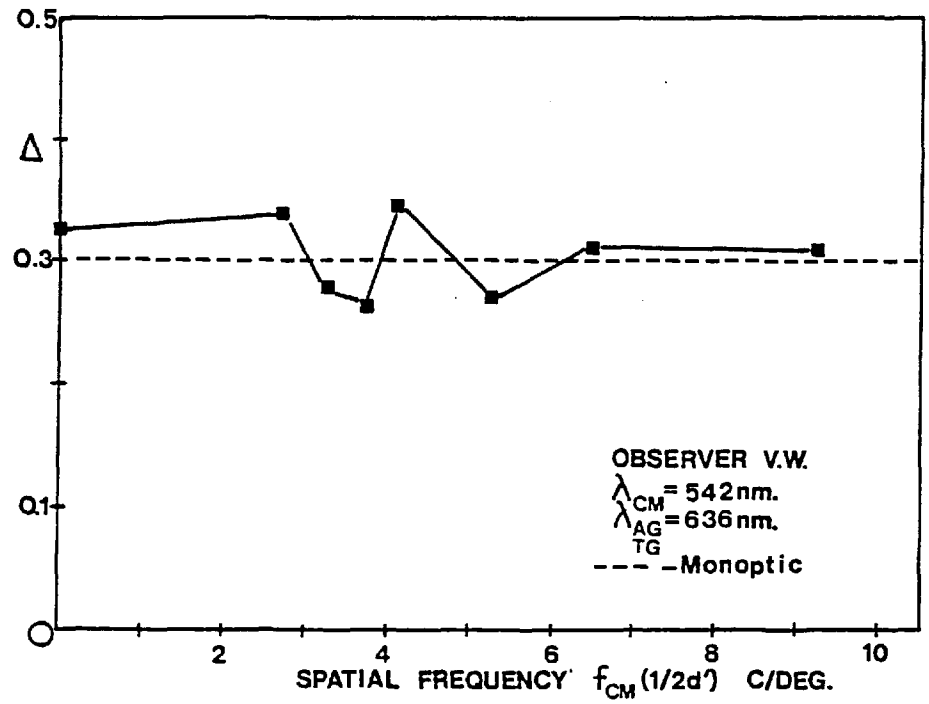

Fig. 3.10 As in fig. 3.6, but AG and TG are presented in a wavelength of 636 nm, and CM in 542 nm.

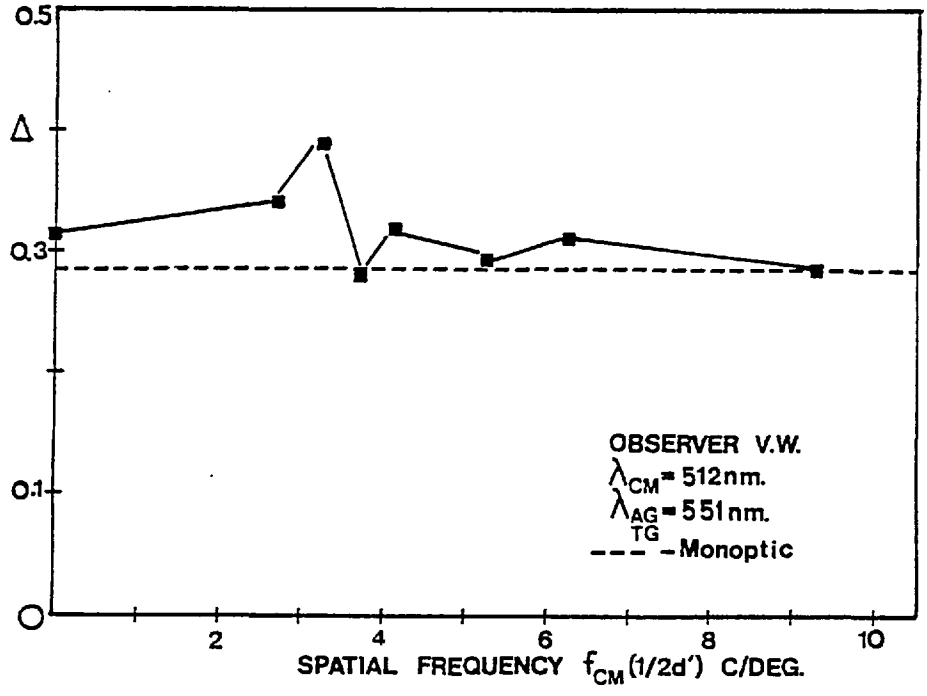

Fig. 3.11 As in fig. 3.6, but AG and TG are presented in a wavelength of 551 nm, and CM in 512 nm.

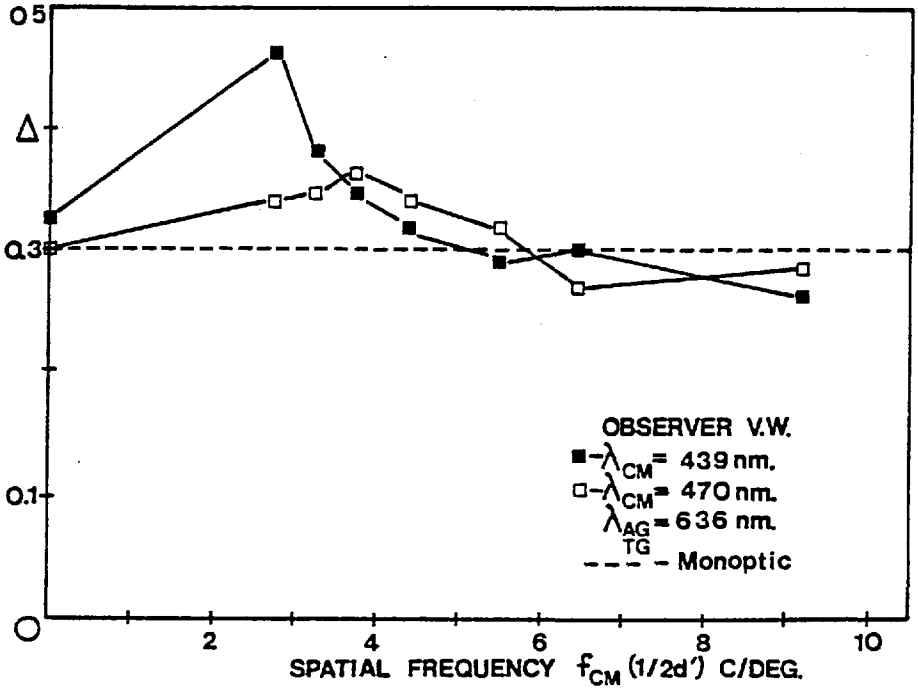

Fig. 3.12 As in fig. 3.6, but AG and TG are presented in a wavelength of 636 nm, whilst CM is in 470 nm (□) and 439 nm (■).

Measurements were also made with a reverse contrast spot matrix, that is, with black spots on a bright background. In figure 3.13, Δ is plotted against $(2d')^{-1}$, where d' is the diameter of the black spots, the adaptation and test gratings had similar spatial characteristics to those of fig. 3.6 to fig. 3.12, but were of wavelength 551 nm. Data are given in fig. 3.13, for three wavelengths of the matrix surround, namely, 636 nm, 551 nm and 439 nm. Again, the values of Δ fall significantly below the broken line, for $(2d')^{-1}$ in the range 0.8^{o} to 6' of visual angle, particularly for a matrix background of wavelength 551 nm, but much less so for wavelengths 439 nm and 636 nm. The data shown in fig. 3.14 are equivalent to those in fig. 3.13, but the test and adaptation gratings were of wavelength 636 nm. The effect is similar to that shown in fig. 3.13, and thus the results for a negative contrast spot matrix show binocular interaction, which reduces the value of Δ, for a range of spot sizes

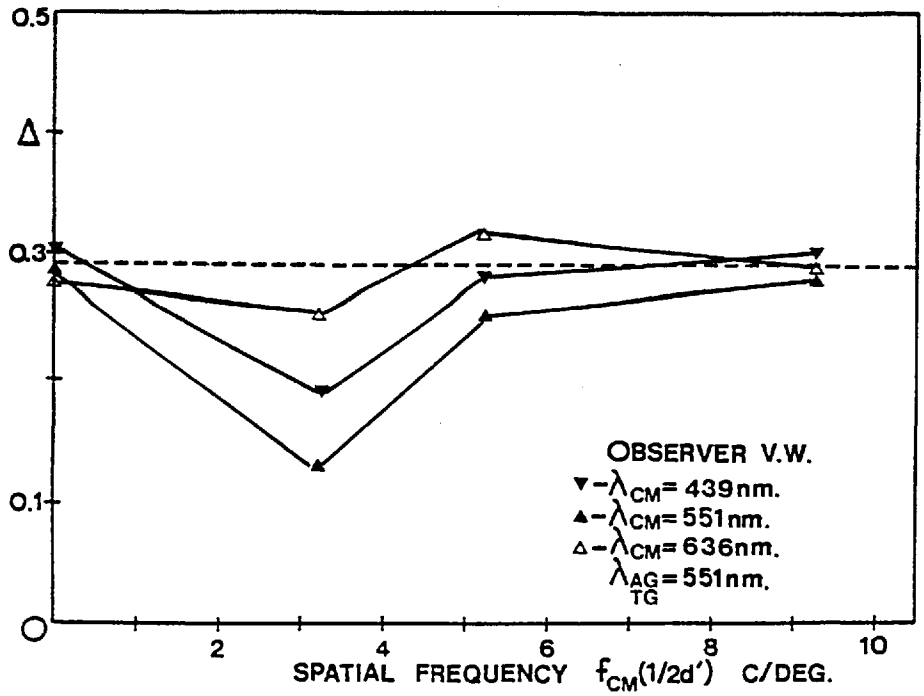

Fig. 3.13 As in fig. 3.6, but CM is of reverse contrast characteristics and presented in light of wavelength, 439 nm (▼), 551 nm (▲) and 636 nm (△), whilst AG and TG are in 551 nm.

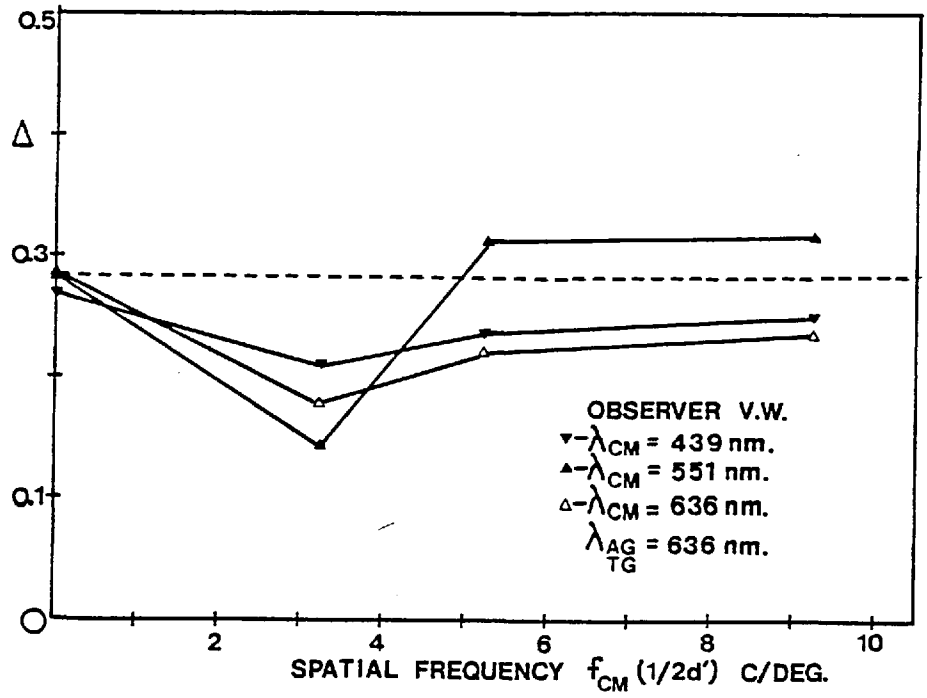

Fig. 3.14 As in fig. 3.13, but AG and TG are of a wavelength 636 nm, and CM is of 636 nm (△), 551 nm (▲) and 439 nm (▼).

similar to that found for the positive contrast spot matrix (see fig. 3.6 to fig. 3.12). In no case, however, did the values of Δ increase relative to that for the simple contrast threshold elevation effect when negative contrast gratings were employed.

Other combinations of stimuli were employed to investigate possible activity of short wavelength (blue-sensitive) mechanisms. Coarse gratings were employed, because the blue-sensitive mechanism has coarser spatial characteristics (Stiles, 1949; Brindley, 1953; Brindley, Du Croz and Rushton, 1966; Burton and Ruddock, 1972; Pugh and Mollon, 1979). Thus, the adaptation and test gratings were linear square-waveform with a bar width of some 10 minutes of arc (corresponding to a fundamental spatial frequency of 3 c/^{o}), and of short wavelength (435 nm). Further, the blue test grating was presented in simultaneous contrast, i.e., on a uniform yellow

(580 nm) background in order to enhance the isolation of the short wavelength mechanism. The illumination of this yellow background was equated, photometrically, to that of the 435 nm adaptation grating.

Results for these measurements, with Δ plotted against $(2d')^{-1}$, where d' is the diameter of the spots in the matrix array, are shown in fig. 3.15 and in fig. 3.16; the former referring to a 439 nm, and the latter to a 524 nm conditioning matrix. It can be seen that in the former case, Δ is significantly reduced for values of $(2d')^{-1}$ in the range 0.8^{0} to 8' of visual cycle, whereas there is a smaller effect in the latter case. Thus there appears to be a short wavelength effect associated with these stimulus conditions.

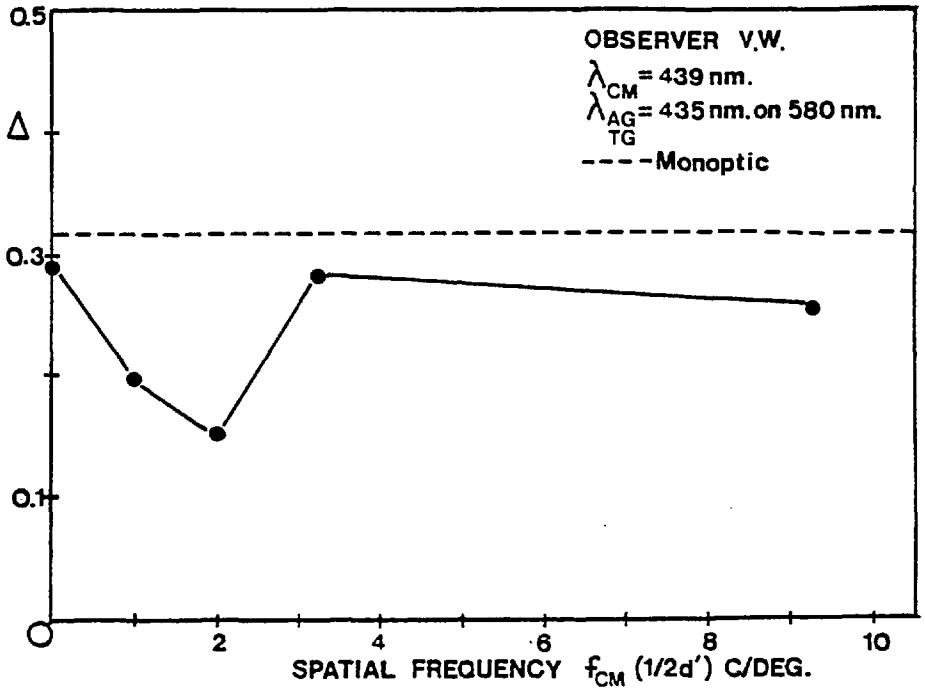

Fig. 3.15 As in fig. 3.6, but the spatial characteristics of the visual field configuration are coarser, and presented using the method of simultaneous contrast. AG and TG are presented in a wavelength of 435 nm, with CM in 439 nm.

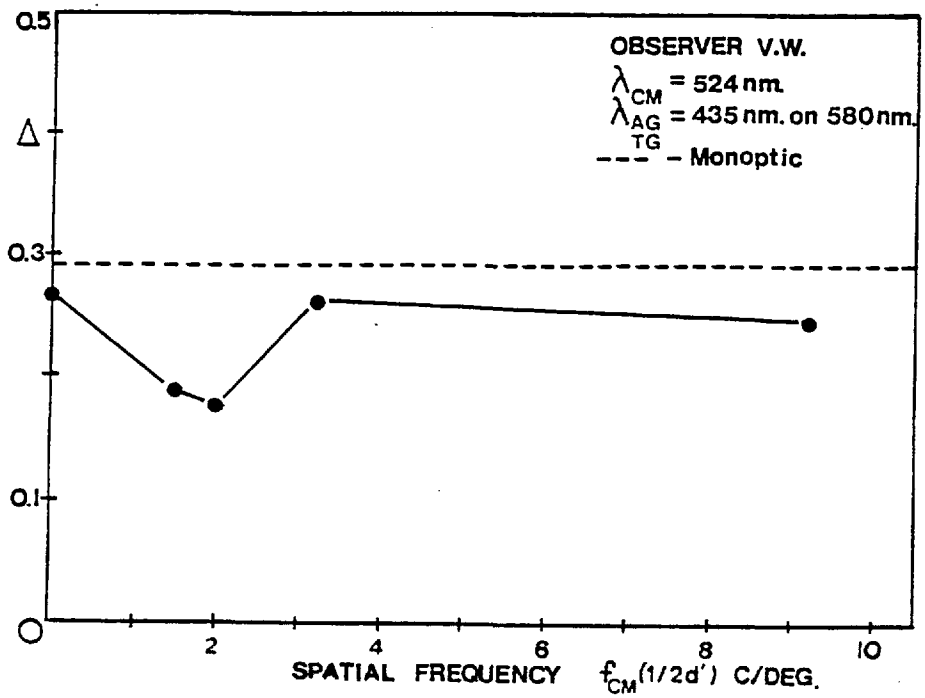

Fig. 3.16 As in fig. 3.15, but CM is presented in a wavelength of 524 nm.

The experimental data presented so far display characteristics similar to those of the binocular inhibitory interaction observed with gratings (Ruddock, Waterfield and Wigley, 1979), except that in this case, it is wavelength selective. Ruddock and Wigley (1976) report that a bar grating conditioning stimulus whose spatial frequency lies in the range 1 c/° to 4 c/° (equivalent to bar widths of 0.6° to 7' of visual angle) presented to one eye, significantly reduces the contrast threshold elevation effect exerted by a bar grating adaptation stimulus on a similar spatial frequency test grating presented contralaterally. However, they found that a blue and red conditioning grating were equally effective in suppressing the contrast threshold elevation effect associated with red adaptation and test gratings.

C.i. The Spectral Characteristics of the Three Response Mechanisms

The preceding section described a series of experiments which yielded at least three spectral classes of wavelength selective binocular adaptation. A detailed investigation of the wavelength selectivity of these three binocular adaptation mechanisms was undertaken and in this and subsequent sections results are given relating to the following:-

a. The detailed spectral properties of the three response mechanisms,

b. The magnitude of the effect as a function of the illumination level of the conditioning grating, and

c. The characteristics of the effect for a colour defective observer.

From these measurements, the spectral sensitivity of the post-receptoral mechanisms associated with these responses can be determined.

The stimulus configuration shown in fig. 3.2, section A.iii of this chapter, was used in all of the following experiments. The results of the preliminary experiments were used to select the spatial parameters appropriate to the isolation of each of the three spectral mechanisms, and in all of the experiments, the test and adaptation gratings were of the same wavelength. The experimental variable was in each case the wavelength of the conditioning matrix, λ_{CM}, a two-dimensional array of spots presented to the left eye. Data are presented for the two observers with normal colour vision, V.W. and I.H.

C.ii. Results

Values of Δ (defined by equation 3.1) are plotted against the wavelength of the spot conditioning matrix, λ_{CM}, in fig. 3.17 to fig. 3.20. Adaptation and test gratings have a bar width of 5.7 minutes of arc, and the spot diameter of the matrix was 9.3 minutes of arc. The results represent the responses of the observers V.W. and I.H., and each figure is labelled accordingly. Each figure refers to a different wavelength of the adaptation and test gratings, as defined with the figure. The broken line in each case represents the magnitude of the monoptic contrast threshold elevation effect for the gratings, measured in the absence of the spot matrix, i.e., fig. 3.1a.

Figure 3.17 and figure 3.18 refer to the data for the two observers when the conditioning grating has positive contrast, that

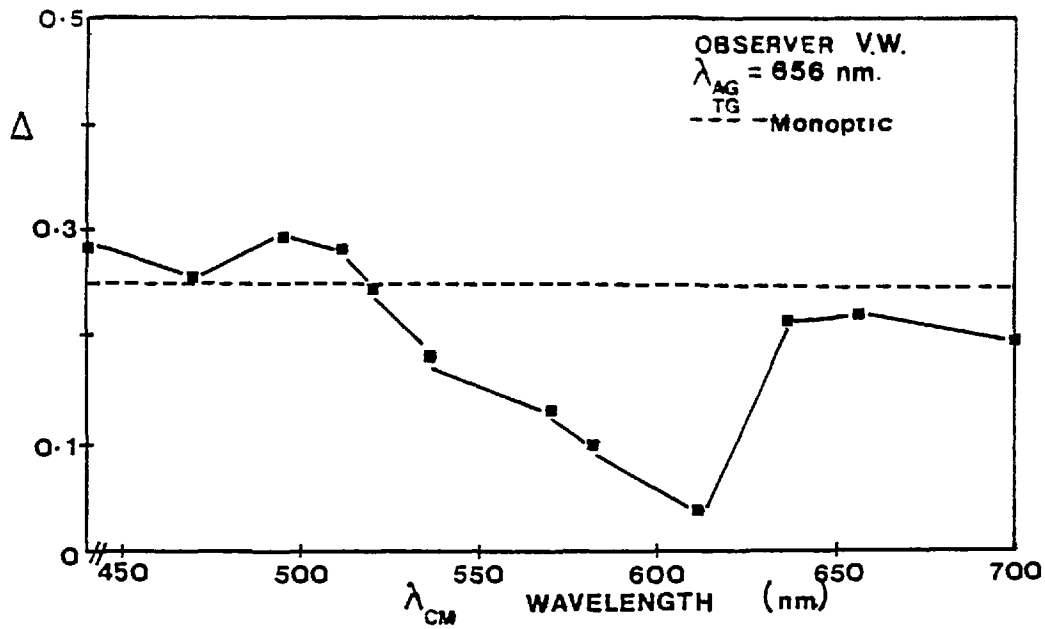

Fig. 3.17a Adaptation, Δ, plotted as a function of wavelength of conditioning matrix, λ_{CM}, for AG and TG of wavelength 656 nm. Broken line represents adaptation in the absence of CM. Data are for observer V.W.

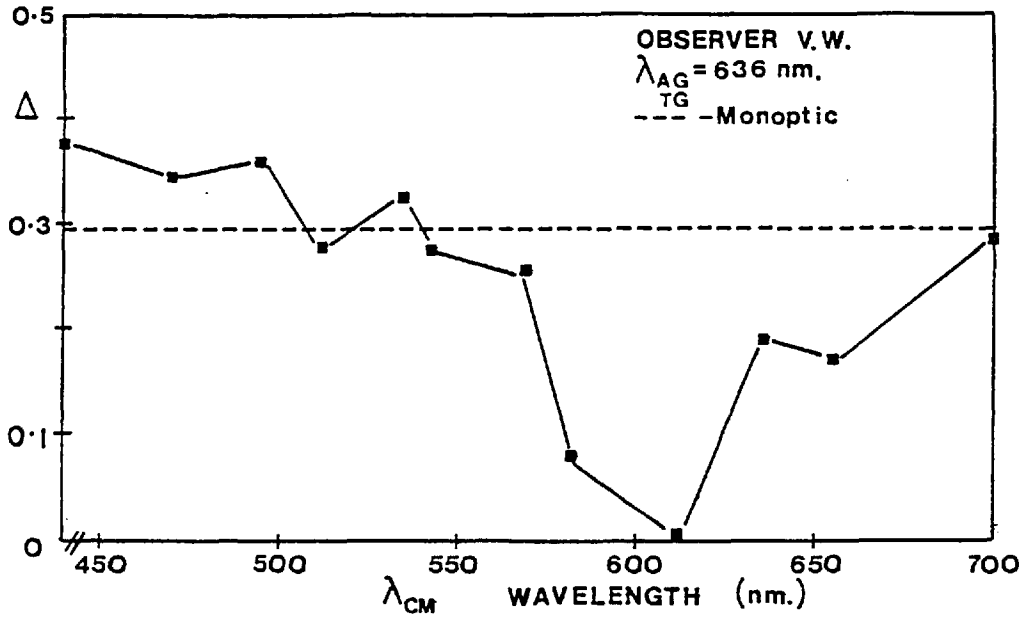

Fig. 3.17b As in fig. 3.17a, but AG and TG are of wavelength 636 nm.

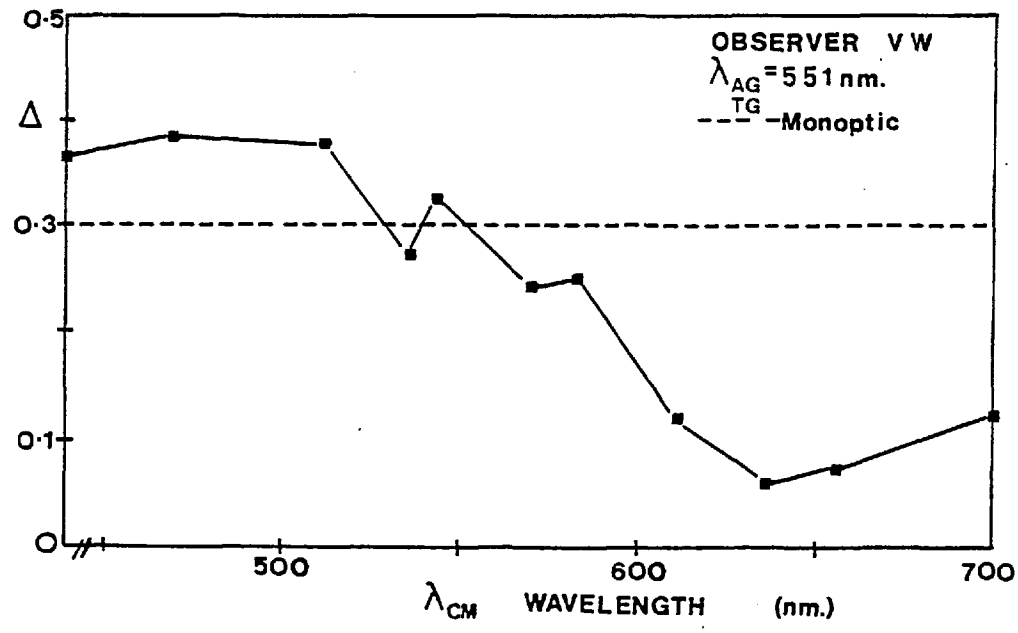

Fig. 3.17c As in fig. 3.17a, but AG and TG are of wavelength 551 nm.

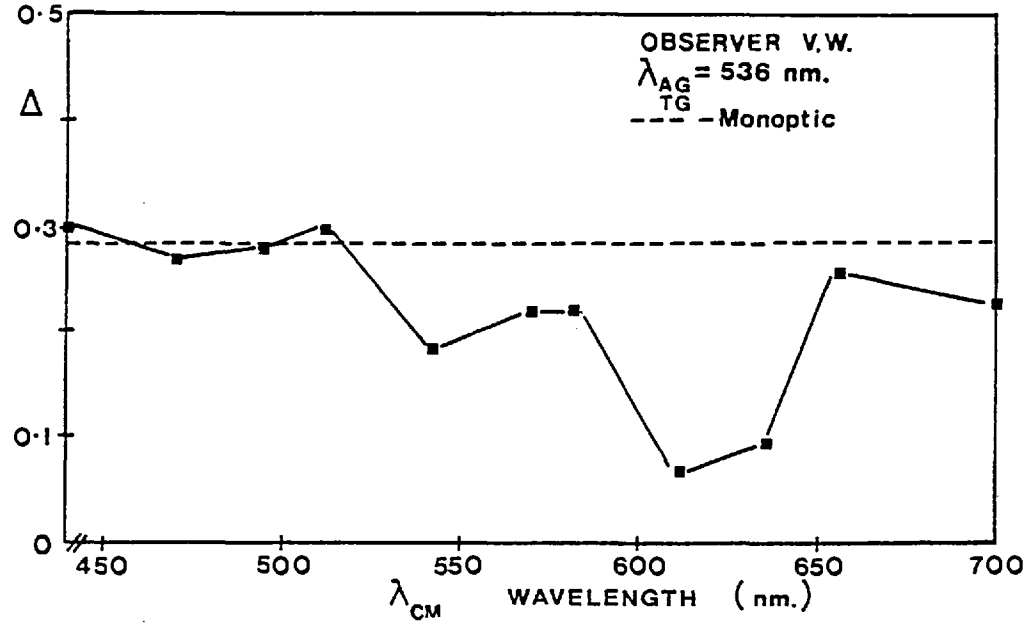

Fig. 3.17d As in fig. 3.17a, but AG and TG are of wavelength 536 nm.

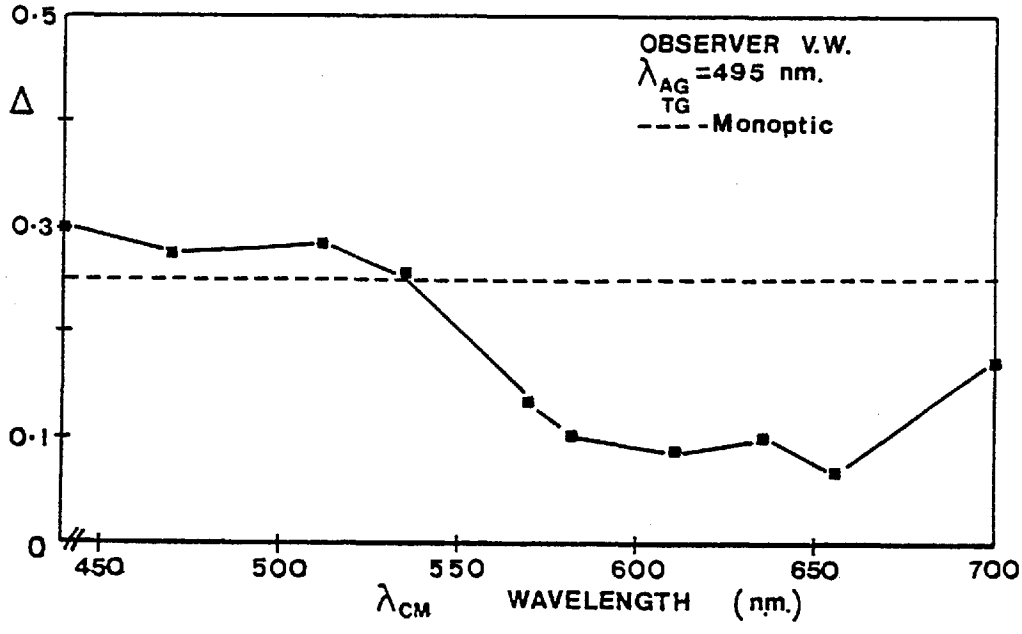

Fig. 3.17e As in fig. 3.17a, but AG and TG are of wavelength 495 nm.

is, it consists of bright spots on a dark background. The data show that in all of the cases investigated, the adaptation effect, Δ, is markedly dependent on the wavelength of the spot conditioning matrix, λ_{CM}, and the effect is similar for all adaptation and test grating wavelengths.

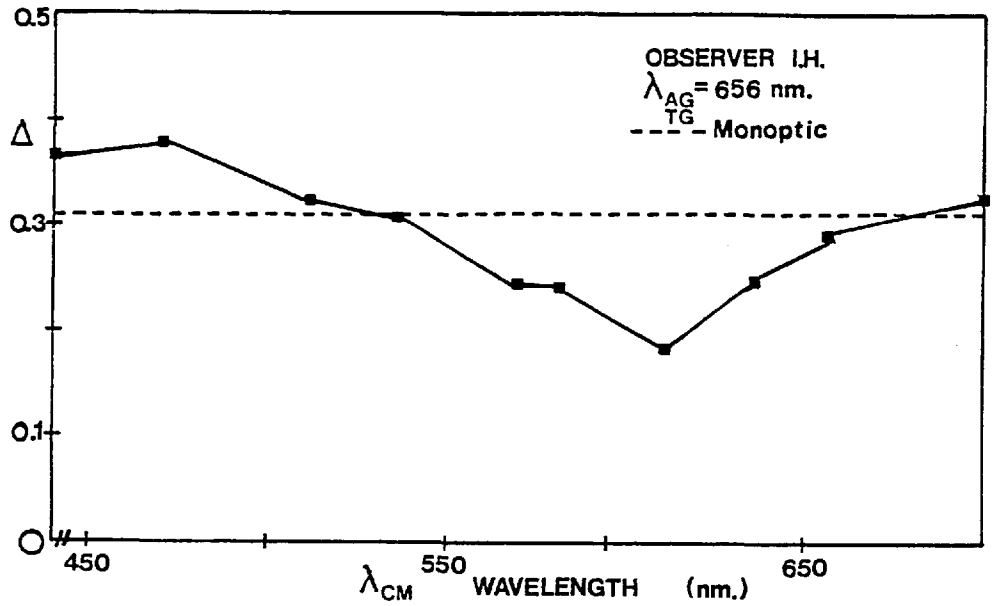

Fig. 3.18a Adaptation, Δ, plotted as a function of wavelength of conditioning matrix, λ_{CM}, for AG and TG in light of wavelength 656 nm. Broken line represents adaptation in the absence of CM. Data are for observer I.H.

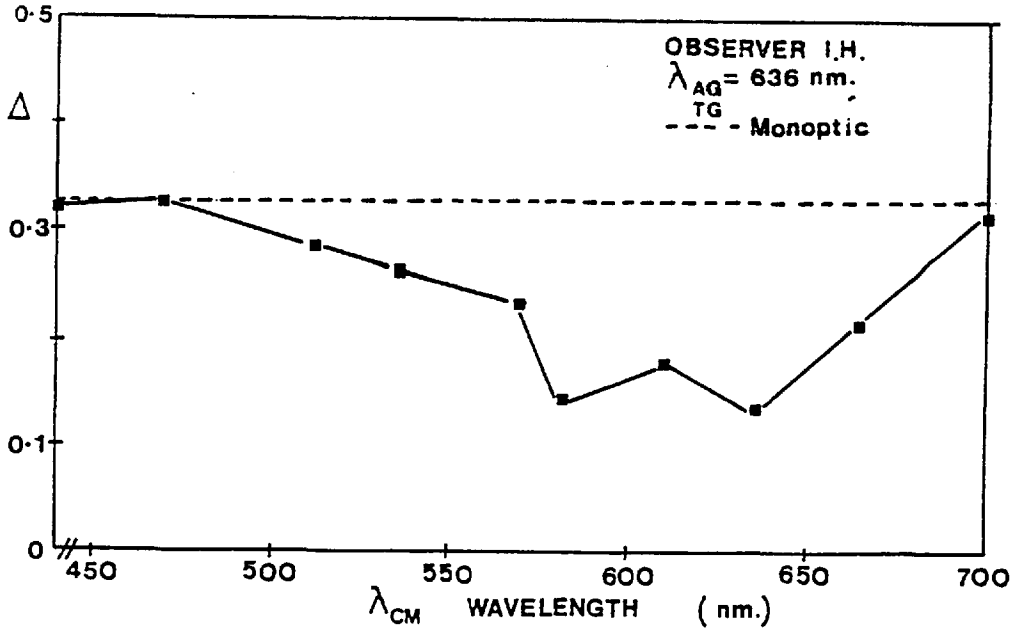

Fig. 3.18b As in fig. 3.18a, but AG and TG are of wavelength 636 nm.

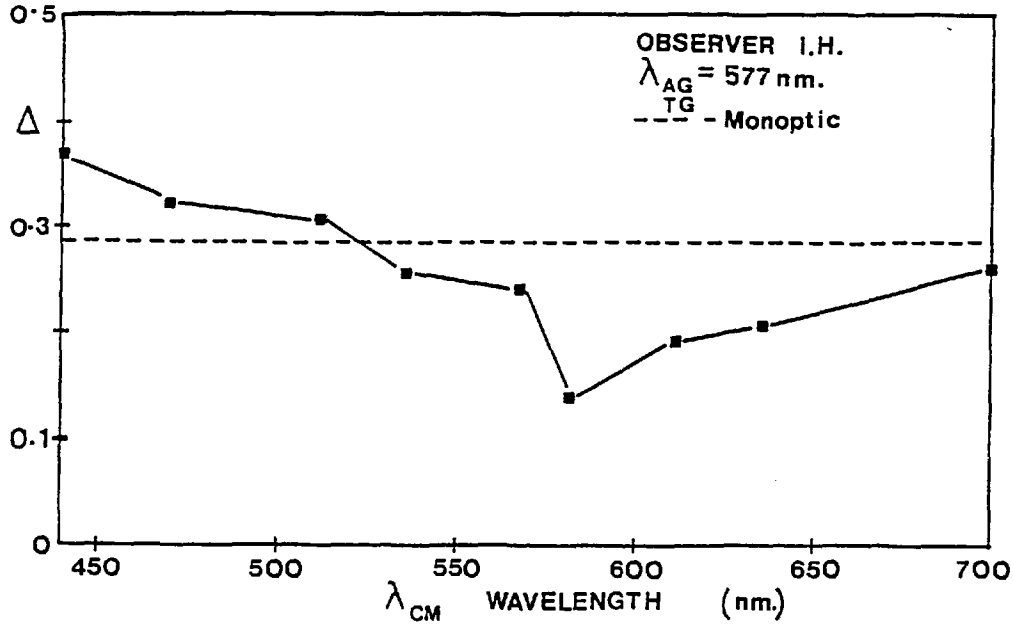

Fig. 3.18c As in fig. 3.18a, but AG and TG are of wavelength 577 nm.

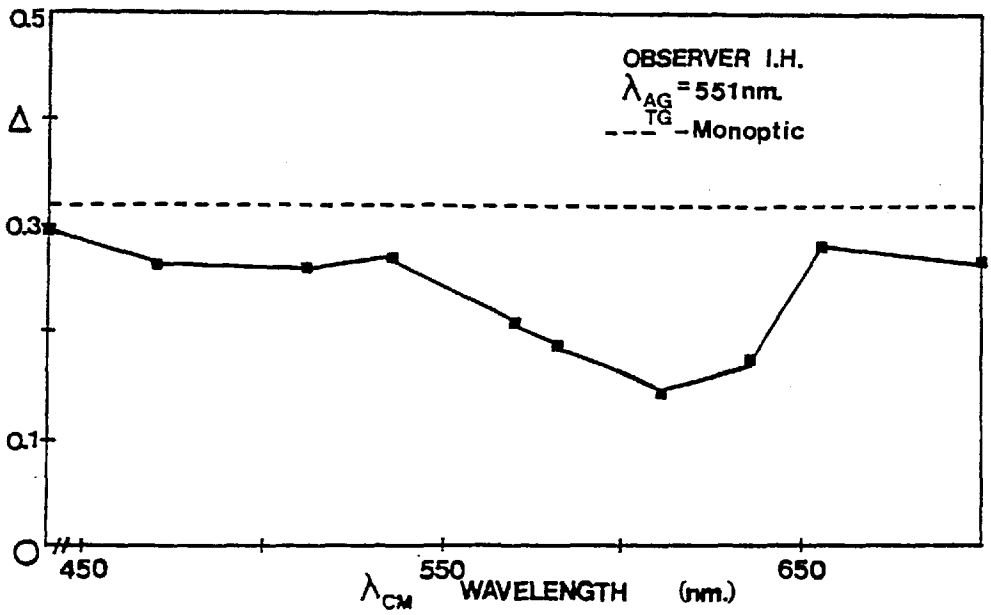

Fig. 3.18d As in fig. 3.18a, but AG and TG are of wavelength 551 nm.

For matrix wavelengths, $\lambda_{CM} > 600$ nm, the monocular contrast threshold elevation effect is virtually abolished (i.e., $\Delta \simeq 0$),

whereas for wavelengths, $\lambda_{CM} < 580$ nm, the adaptation effect, Δ, recorded in the right eye is approximately the same as that found for monoptic adaptation (shown by the broken line), and in some conditions, it is even increased (see fig. 3.17a,b,c,e and fig. 3.18a,c). Thus, there seems to be some opponent activity within the red-green regions of the spectrum. The responses of the two observers agree within experimental error, and each gives a minimum value of Δ for $\lambda_{CM} \simeq 610$ nm.

Figure 3.19 and figure 3.20 represent the responses of the two observers when the conditioning matrix is presented in negative contrast, that is, black spots of 9.3 minutes of arc diameter, superimposed upon a monochromatic background. Under these conditions, values of Δ fall significantly below the broken line for matrix

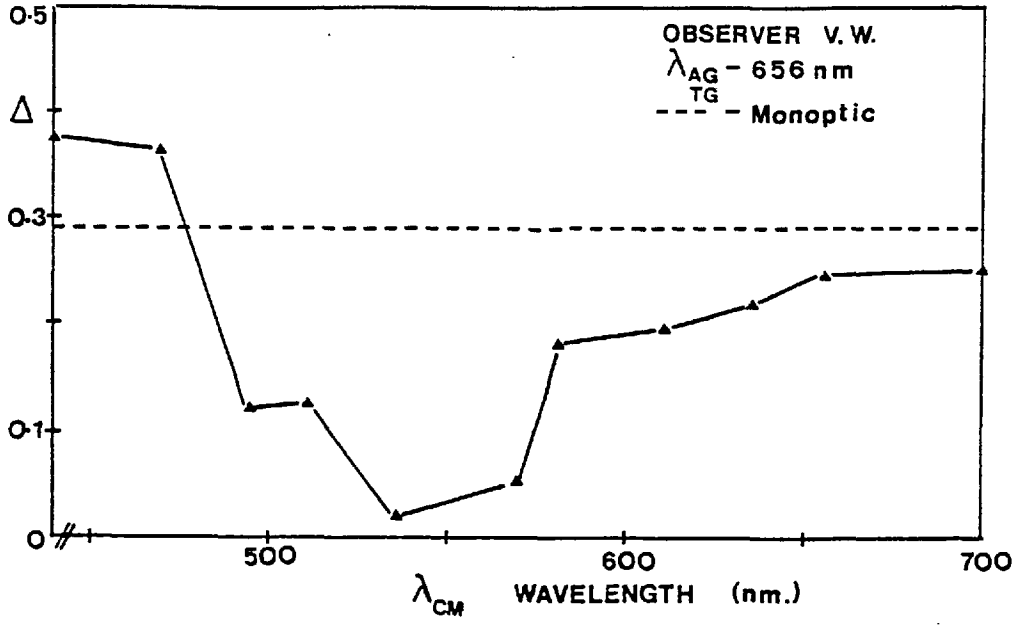

Fig. 3.19a Adaptation, Δ, plotted as a function of wavelength of conditioning matrix, λ_{CM}, (negative contrast) for AG and TG in light of wavelength 656 nm. Broken line represents adaptation in the absence of CM. Data are for observer V.W.

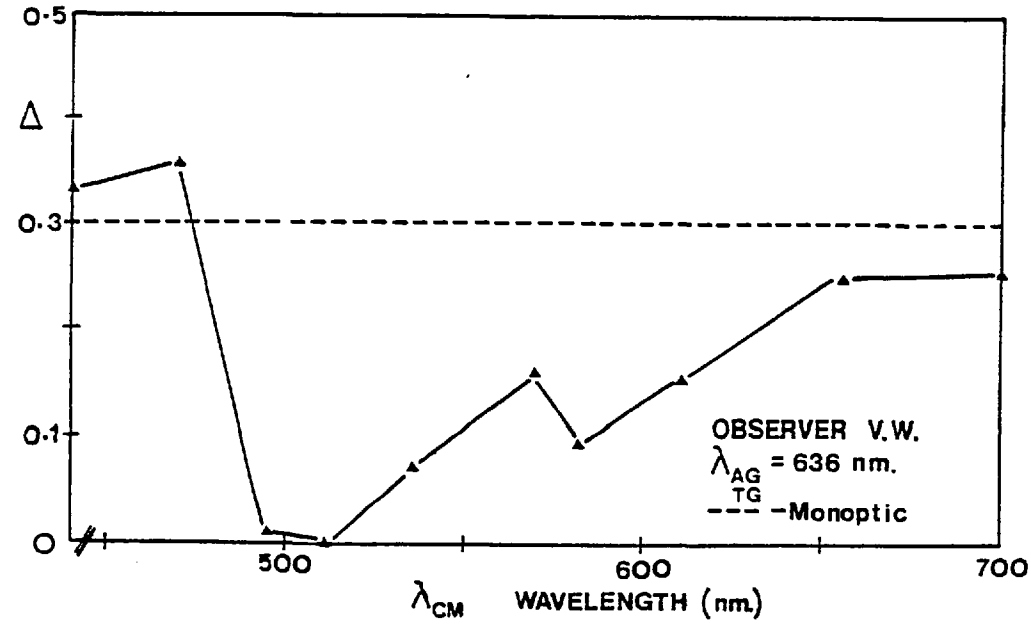

Fig. 3.19b As in fig. 3.19a, but AG and TG are of wavelength 636 nm.

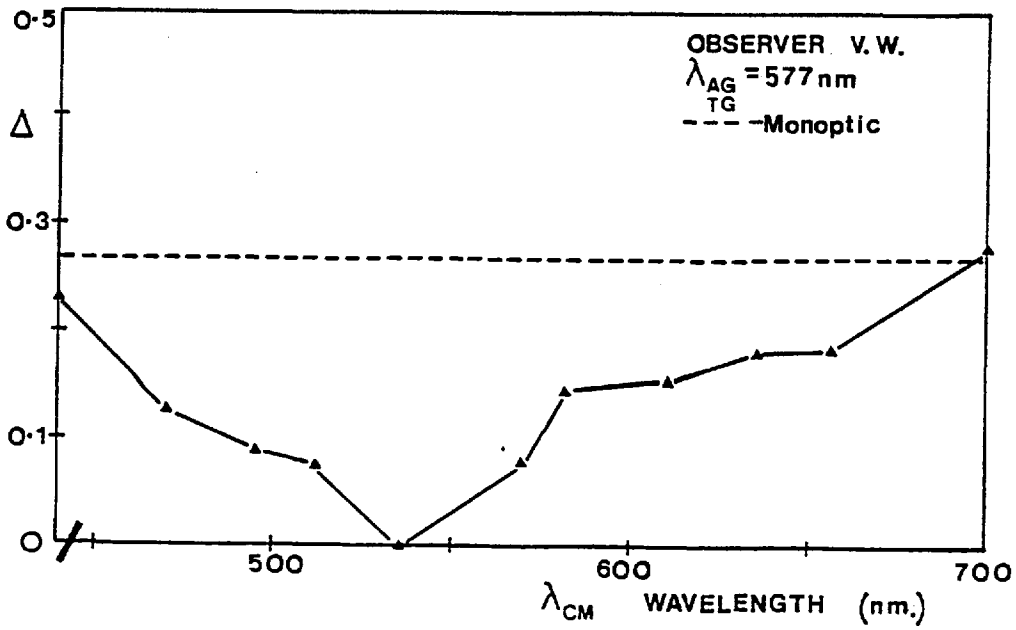

Fig. 3.19c As in fig. 3.19a, but AG and TG are of wavelength 577 nm.

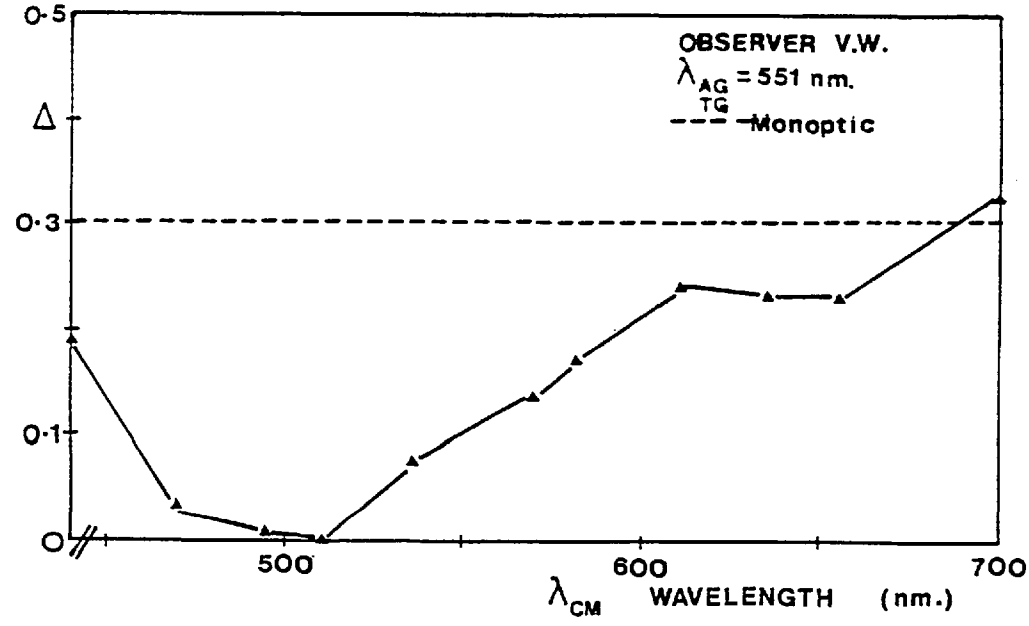

Fig. 3.19d As in fig. 3.19a, but AG and TG are of wavelength 551 nm.

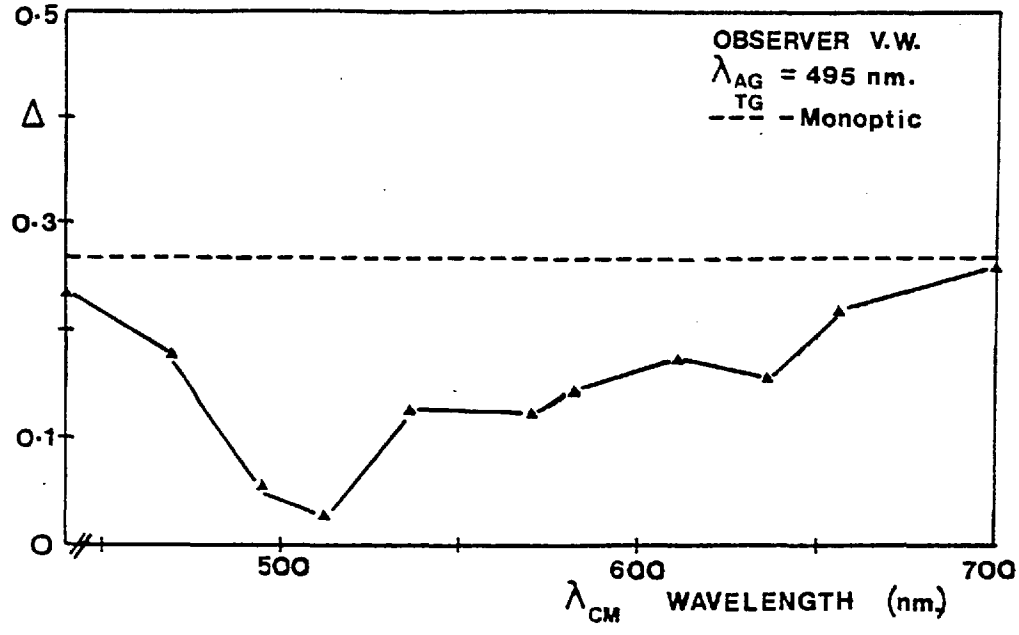

Fig. 3.19e As in fig. 3.19a, but AG and TG are of wavelength 495 nm.

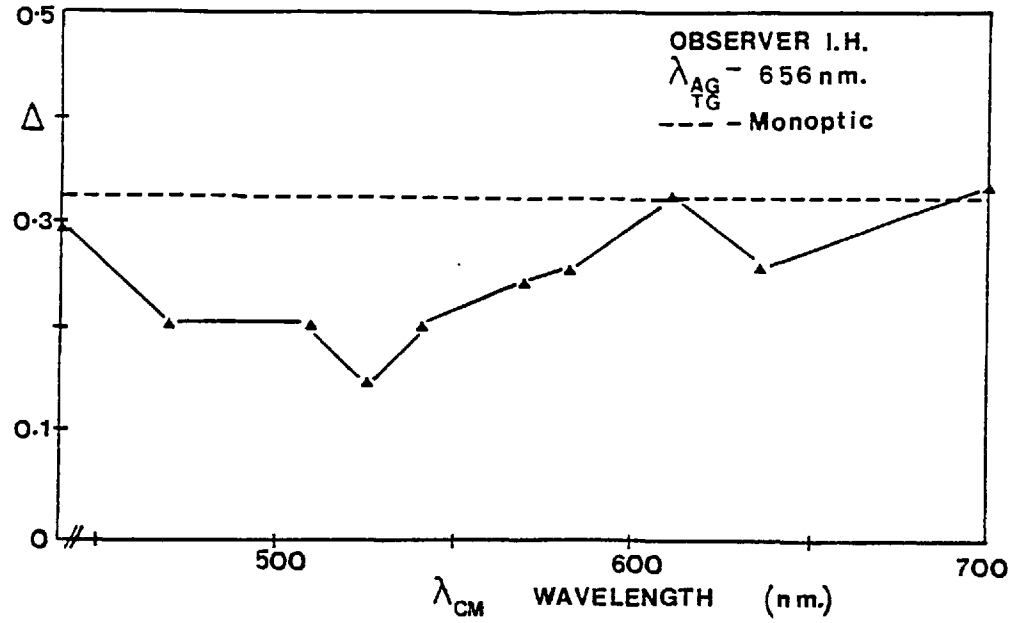

Fig. 3.20a Adaptation, Δ, plotted as a function of wavelength of a conditioning matrix of negative contrast, λ_{CM}, for AG and TG presented in light of wavelength 656 nm. Broken line represents adaptation in absence of CM. Data are for observer I.H.

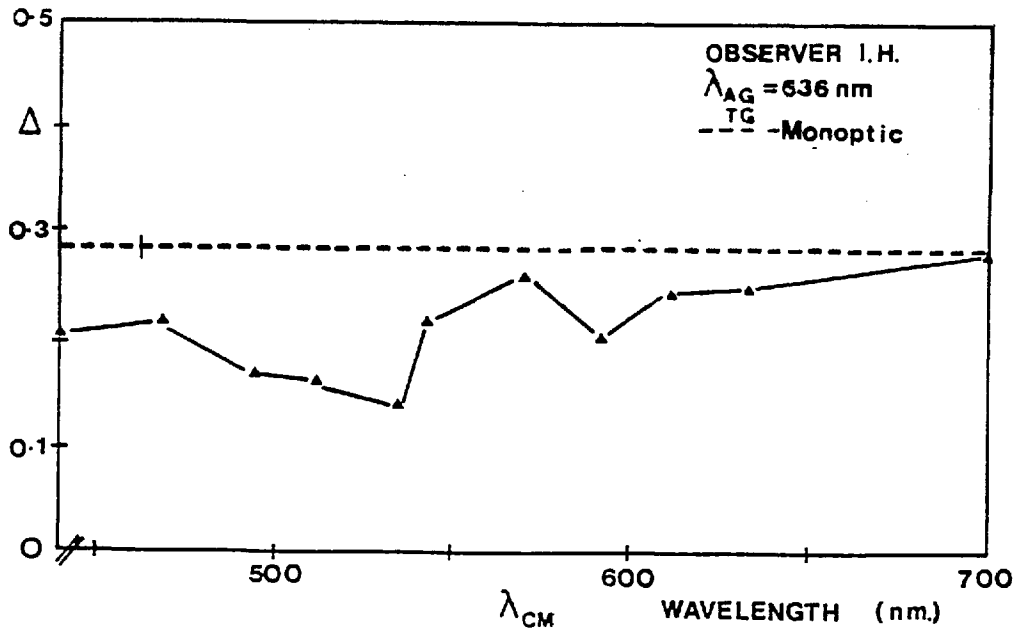

Fig. 3.20b As in fig. 3.20a, but AG and TG are of wavelength 636 nm.

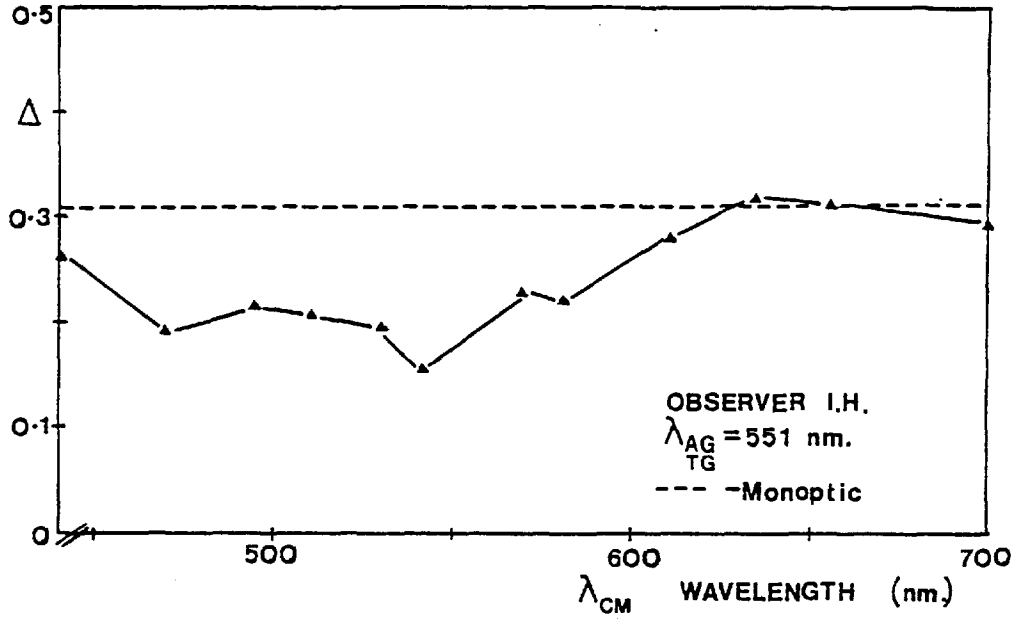

Fig. 3.20c As in fig. 3.20a, but AG and TG are of wavelength 551 nm.

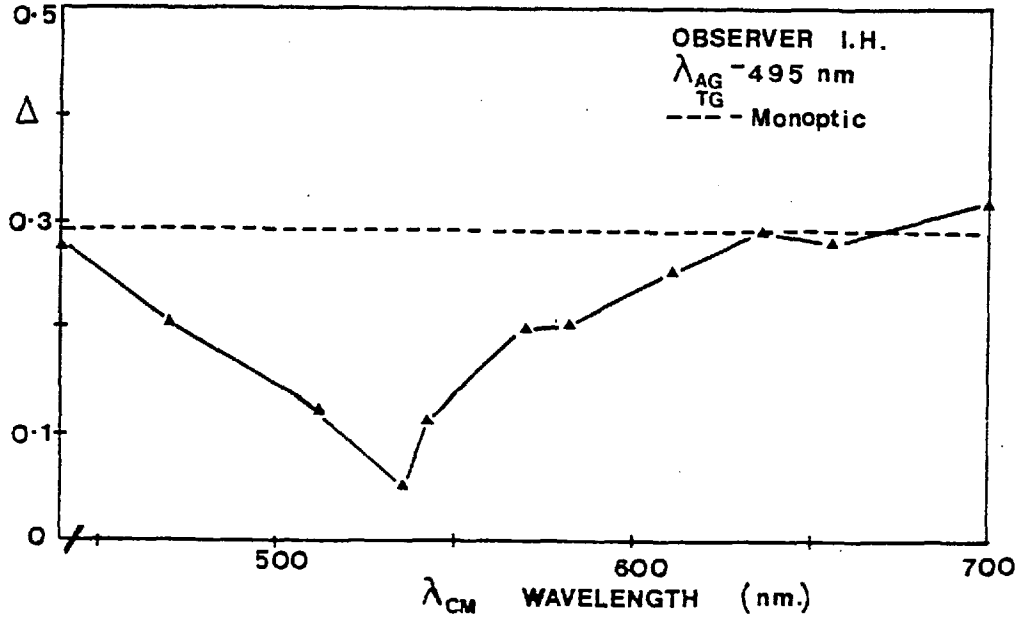

Fig. 3.20d As in fig. 3.20a, but AG and TG are of wavelength 495 nm.

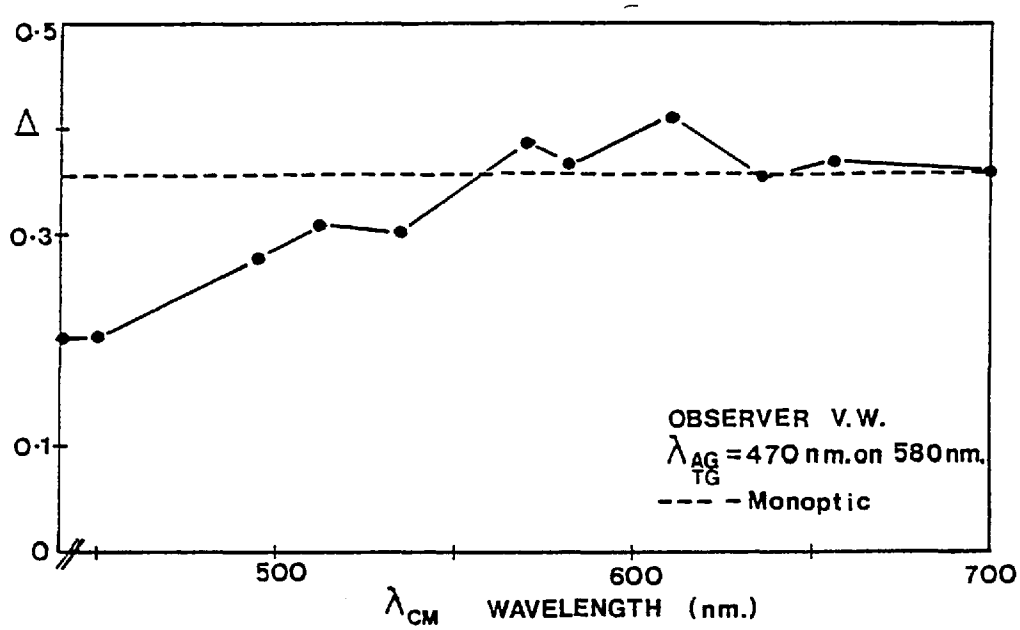

Fig. 3.21a Adaptation, Δ, plotted as a function of wavelength of conditioning matrix (coarse spatial characteristics), λ_{CM}, with AG and TG presented in a wavelength of 470 nm and in simultaneous contrast. Broken line represents adaptation in absence of CM. Data are for observer V.W.

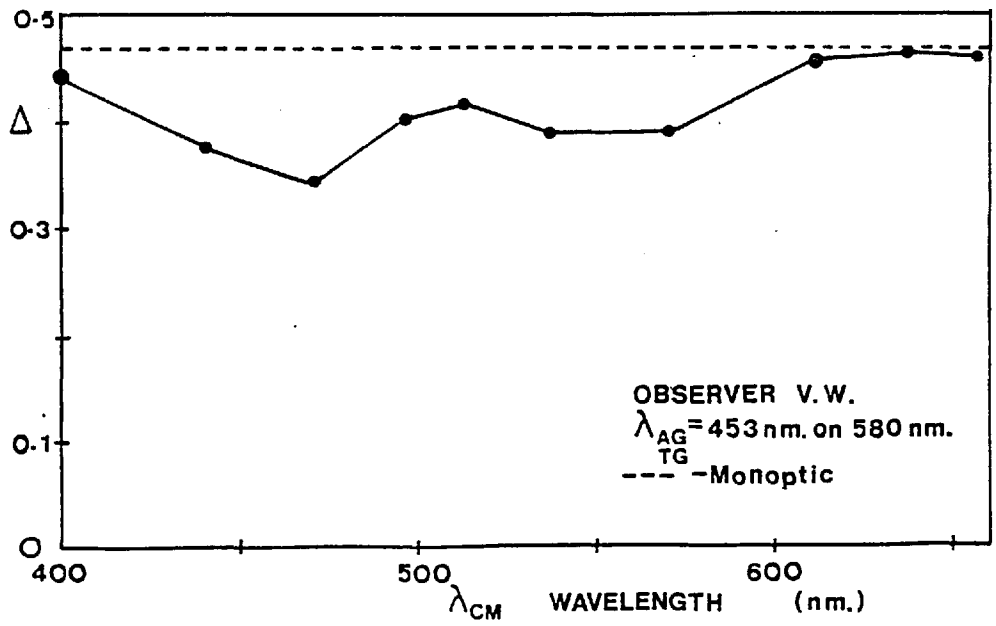

Fig. 3.21b As in fig. 3.21a, but AG and TG are of wavelength 453 nm.

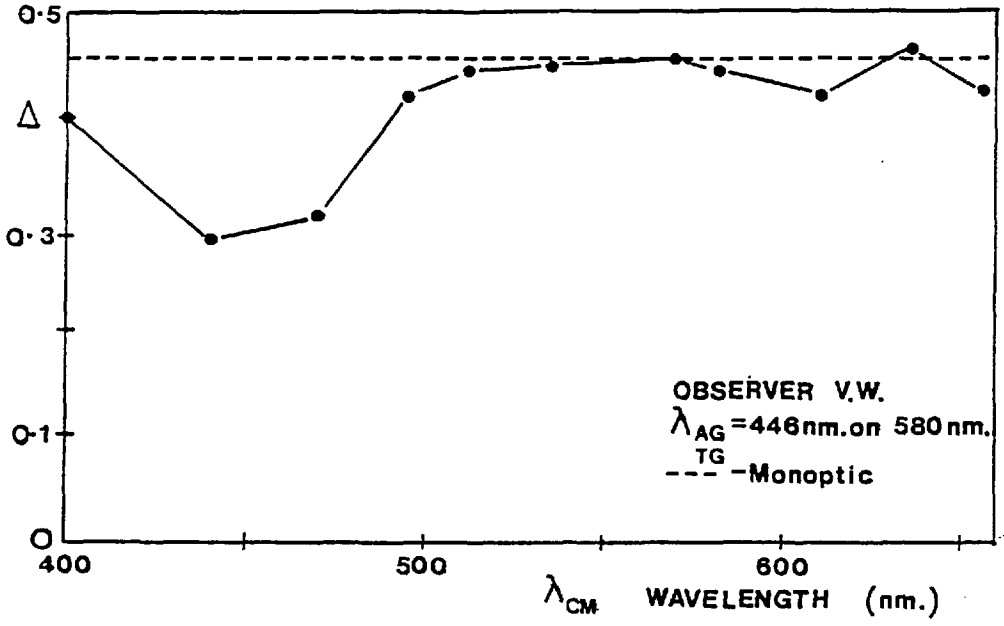

Fig. 3.21c As in fig. 3.21a, but AG and TG are of wavelength 446 nm.

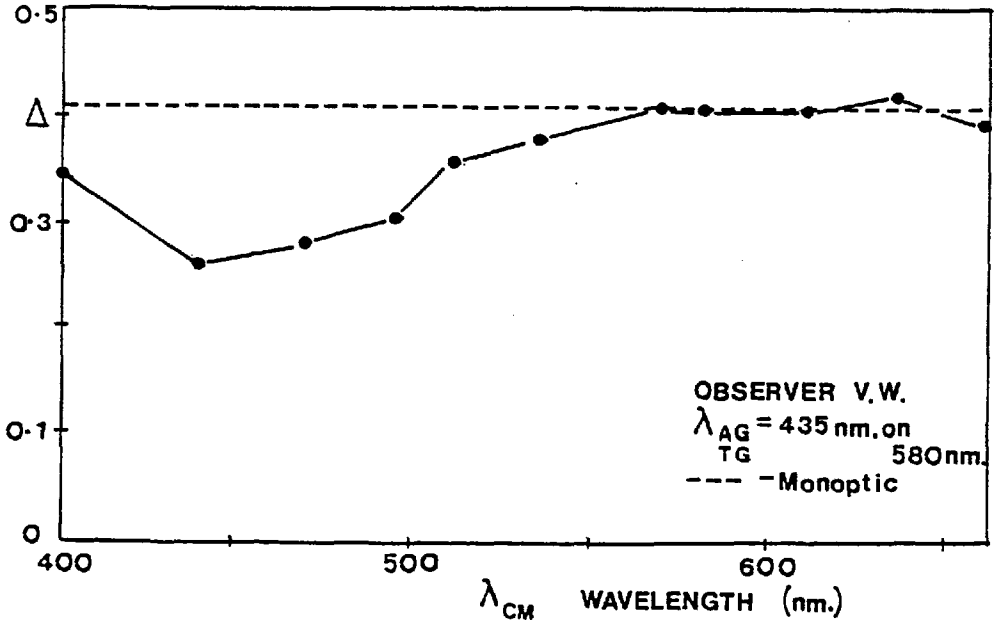

Fig. 3.21d As in fig. 3.21a, but AG and TG are of wavelength 435 nm.

wavelengths, λ_{CM}, in the range 500 nm to 580 nm, which is similar for both observers. At no wavelength, however, is there an enhancement of the effect.

The data, shown in fig. 3.21 and in fig. 3.22, represent the values of Δ obtained for adaptation and test gratings of bar width 10 minutes of arc, and a conditioning matrix of spot diameter equal to some 15 minutes of arc. As for the preliminary data (see fig. 3.15 and fig. 3.16), the test grating was presented on a yellow, 580 nm, uniform background field. Figure 3.21 and figure 3.22 show the responses for the two subjects, and again, the variation of Δ with λ_{CM} is similar for both. The values of Δ are significantly reduced below the monoptic level only for short wavelengths, λ_{CM}, in the range 400 nm to 500 nm.

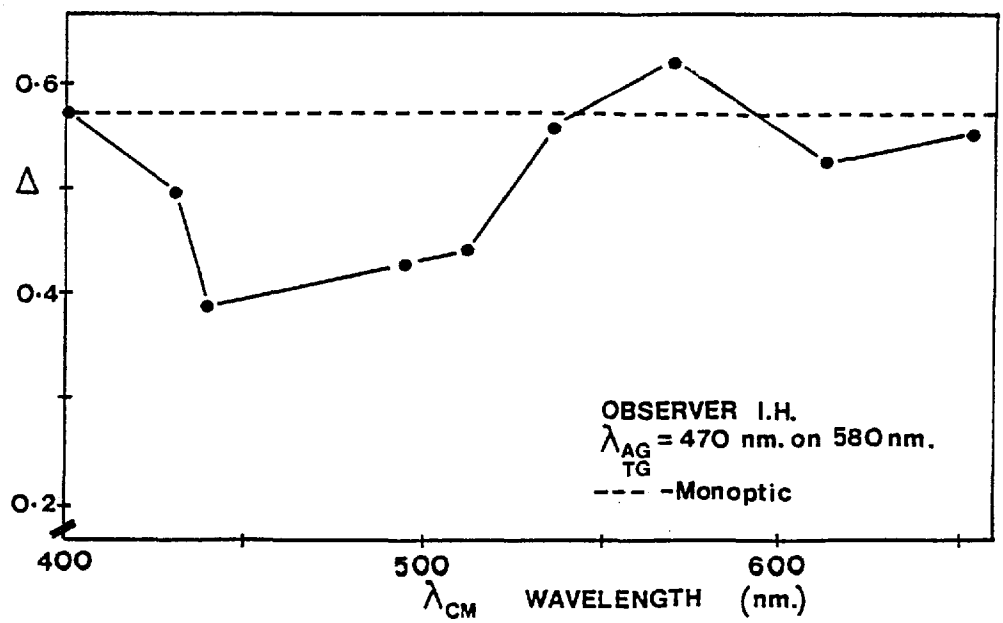

Fig. 3.22a Adaptation, Δ, plotted as a function of wavelength of conditioning matrix (coarse spatial characteristics), λ_{CM}, with AG and TG presented in light of wavelength 470 nm and in simultaneous contrast. Broken line represents adaptation in absence of CM. Data are for observer I.H.

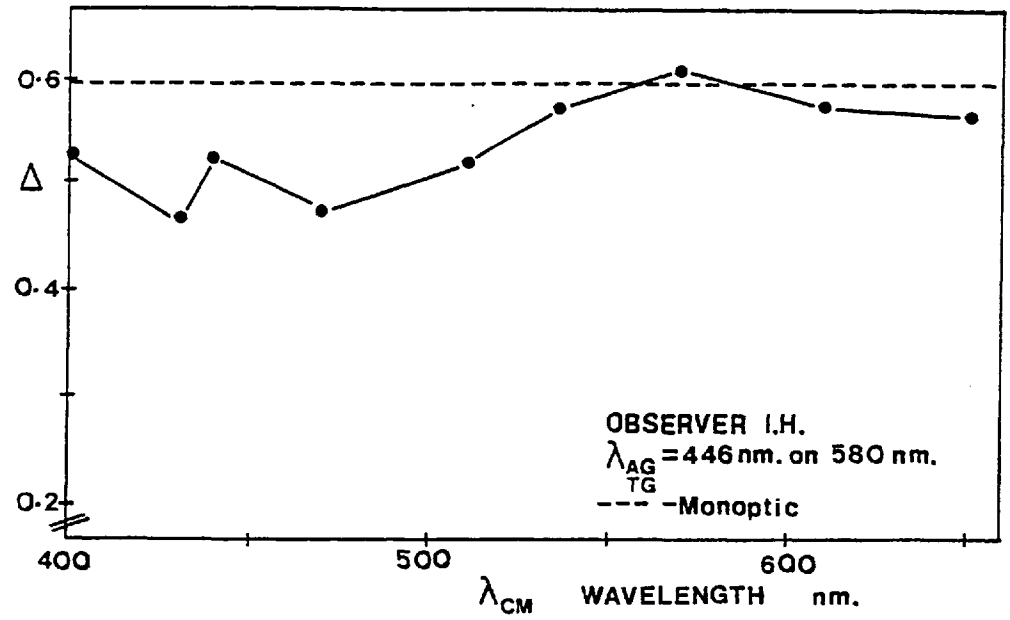

Fig. 3.22b As in fig. 3.22a, but AG and TG are of wavelength 446 nm.

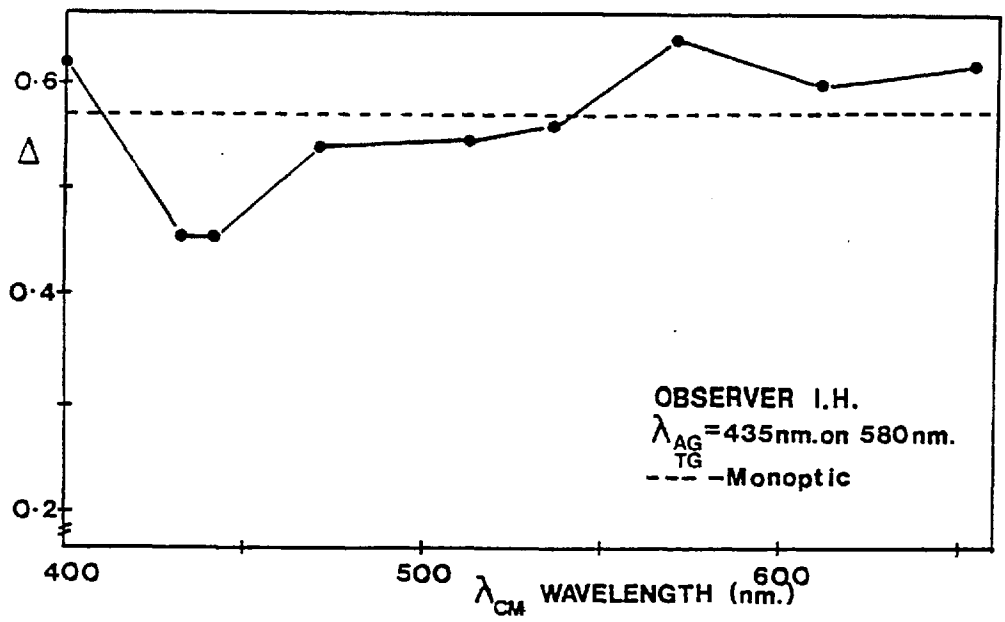

Fig. 3.22c As in fig. 3.22a, but AG and TG are of wavelength 435 nm.

C.iii. The Effect of Changing the Illumination level of the Conditioning Matrix

The data, shown in fig. 3.17 to fig. 3.22, were all obtained with the adaptation stimuli set at an illumination level 4 log units above the threshold level for their detection, thus they are equated for visual efficiency.

In the measurements to be presented here, the adaptation grating presented to the right eye was still set at an illumination level 4 log units above its threshold detection level, but the illumination level of the conditioning spot matrix, I_{CM}, presented to the left eye was the experimental variable. The spatial and spectral parameters were determined from the data of fig. 3.17 to fig. 3.22, such that they gave the maximum amplitude of Δ, either positive or negative with respect to that found for monoptic adaptation in the absence of the spot matrix. Separate experiments were performed for those conditions which increase and for those which decrease the value of Δ relative to the monoptic value. The experiments were performed for conditions which were appropriate to the isolation of each of the three mechanisms.

C.iv. Results

Results for a number of combinations of adaptation and test grating wavelengths are shown in fig. 3.23 to fig. 3.26. The magnitude of the effect, Δ (equation 3.1), is plotted along the ordinate in relative log units, as a function of the illumination level of the conditioning matrix, log I_{CM}. Figure 3.23 and figure 3.24 represent the variation of the effect under conditions which give the red-green opponent responses shown in fig. 3.17 and in fig. 3.18,

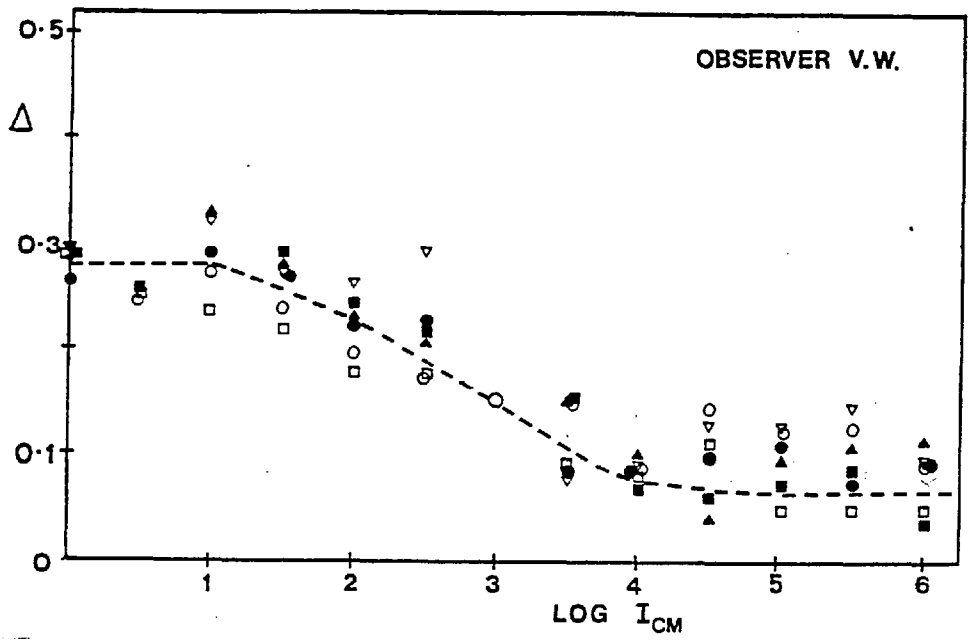

Fig. 3.23a Amplitude variation of Δ as a function of log of illumination level of CM above threshold for its detection. Data points represent a number of AG and TG wavelengths for a λ_{CM} giving maximum suppression of effect for observer V.W. from fig. 3.17.

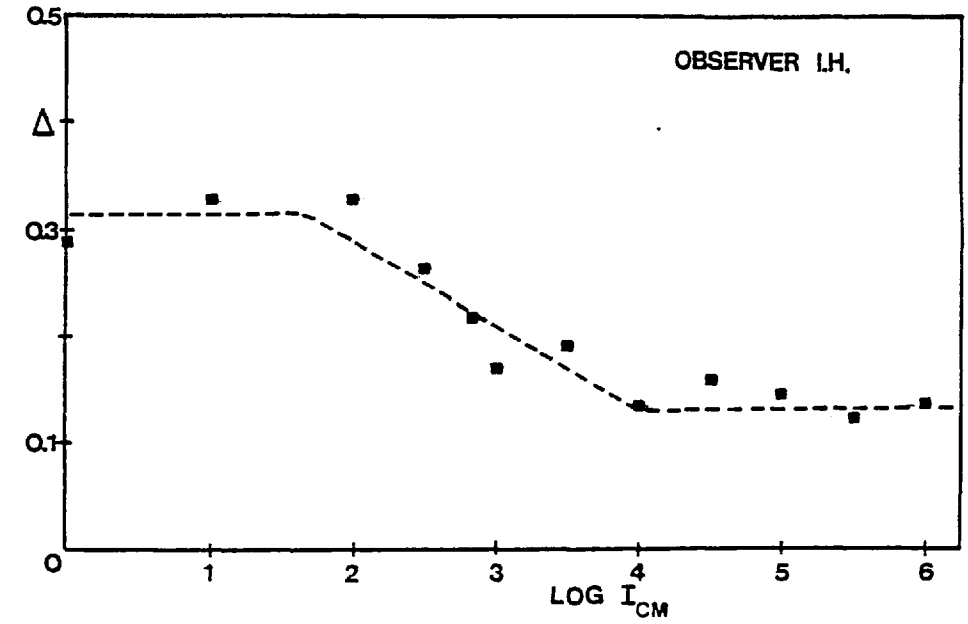

Fig. 3.23b As in fig. 3.23a, but data points are for observer I.H. (see fig. 3.18).

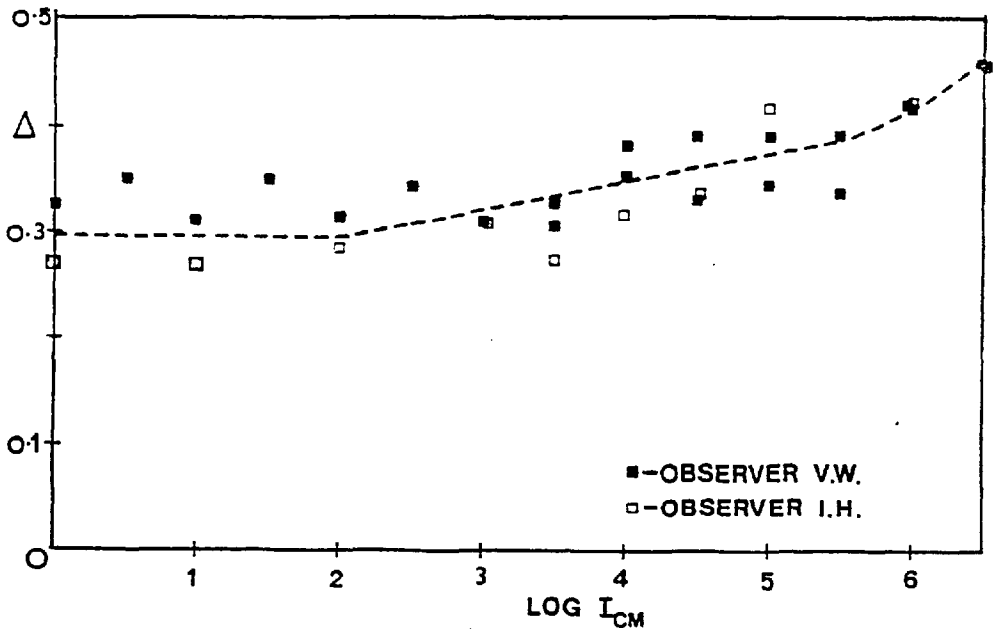

Fig. 3.24 As in fig. 3.23a, but conditions tested are those which facilitate the effect compared to the monoptic condition. Data are for observer V.W. (■) and I.H. (□). (see fig. 3.17 and fig. 3.18, respectively).

i.e., with a matrix of bright spots on a dark background. Figure 3.23a,b represent conditions under which Δ is lower than the monoptic value, and figure 3.24 conditions under which it is greater. Results for the negative contrast spot matrix, which yields the green-sensitive responses, are shown in fig. 3.25, and those obtained with coarser patterns and blue test superimposed on a yellow background (see fig. 3.21 and fig. 3.22) are given in fig. 3.26. Results are presented for two subjects, V.W. and I.H., as indicated on the diagrams.

Increase of log I_{CM}, the intensity of the conditioning matrix, is accompanied by a decrease in Δ, to a value of approximately 0.08 log units, in fig. 3.23, in fig. 3.25 and in fig. 3.26. This change

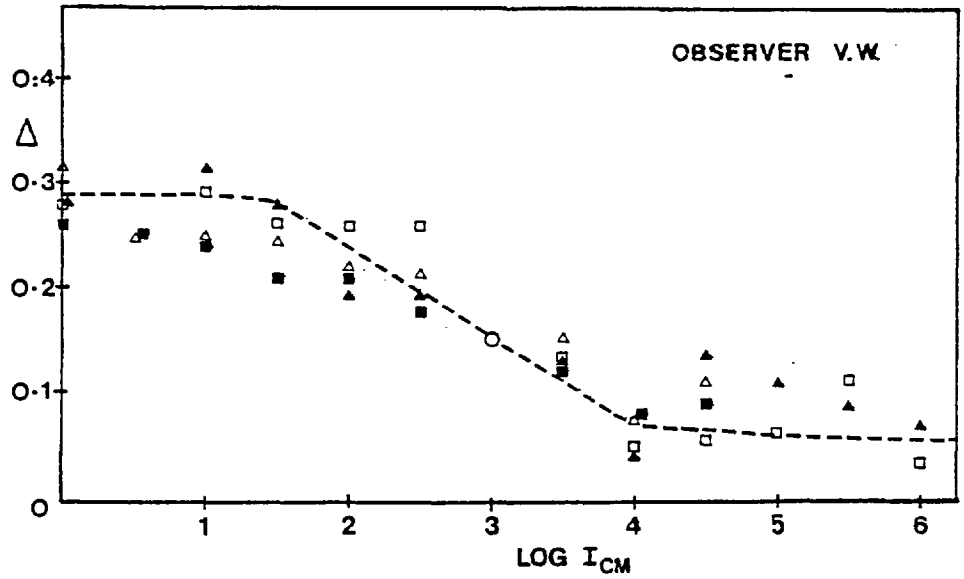

Fig. 3.25a As in fig. 3.23a, but the data points are for observer V.W. for the conditions examined in fig. 3.19.

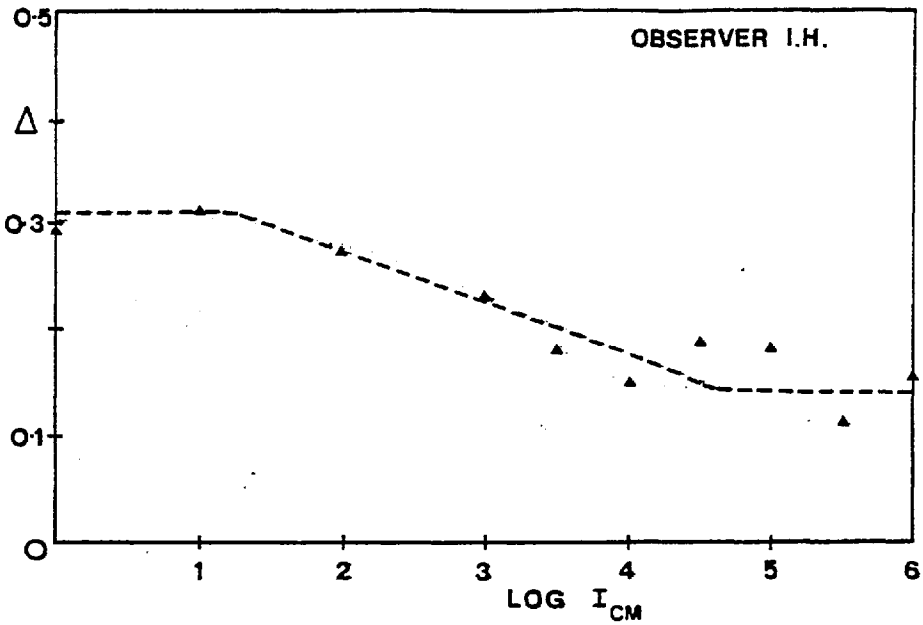

Fig. 3.25b As in fig. 3.23a, but the data points refer to observer I.H., and the conditions of fig. 3.20.

occurs in the range 1.5 to 4.5 log units above the threshold for the detection of the matrix. Further increases in log I_{CM} do not reduce Δ significantly below this value. However, in fig. 3.21, increasing I_{CM}, the intensity of the conditioning matrix, has the opposite effect. This time the value of Δ increases to a value of about 0.5 log units over the same approximate range, 1.5 to 4.5 log units above threshold.

These data can be compared with the variation with illumination level of the adaptation grating when no conditioning matrix is present, i.e., the simple contrast threshold elevation effect (see fig. 3.1a). Such data were obtained for a number of test and adaptation wavelengths, and the mean of these data is plotted together with the mean data of fig. 3.23a, in fig. 3.27. This plot shows that although the changes in the value of Δ are in the opposite direction, the adaptation grating illumination level for which the peak value of

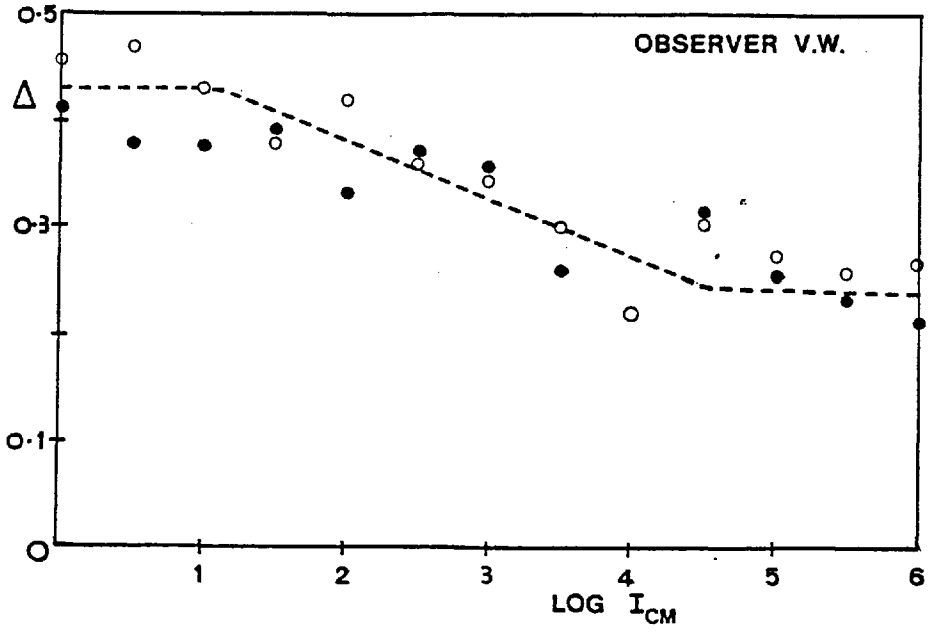

Fig. 3.26a As in fig. 3.23a; the data points are for conditions examined in fig. 3.21, and refer to observer V.W.

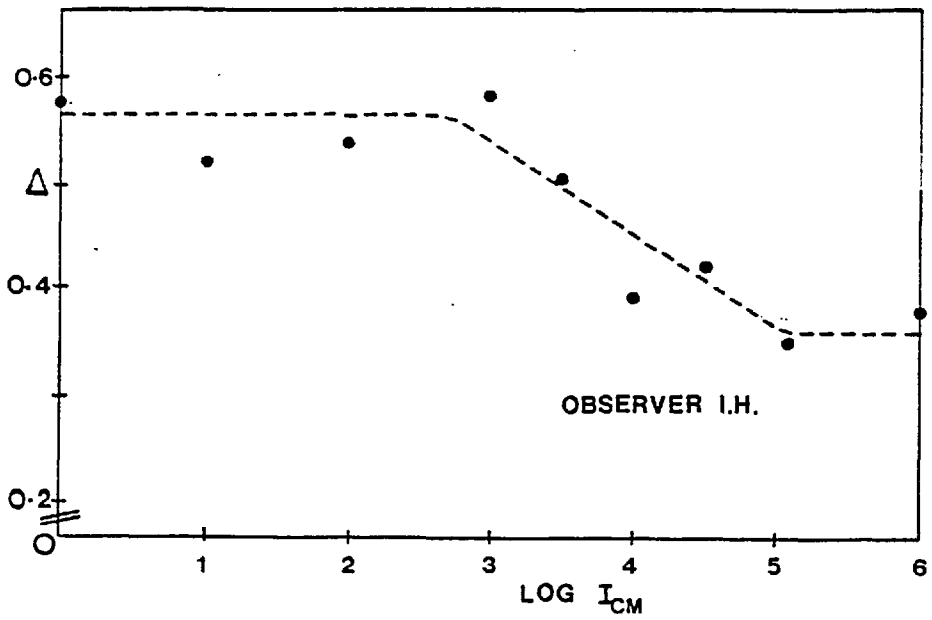

Fig. 3.26b As in fig. 3.23a, but data are for observer I.H. under the conditions of fig. 3.22.

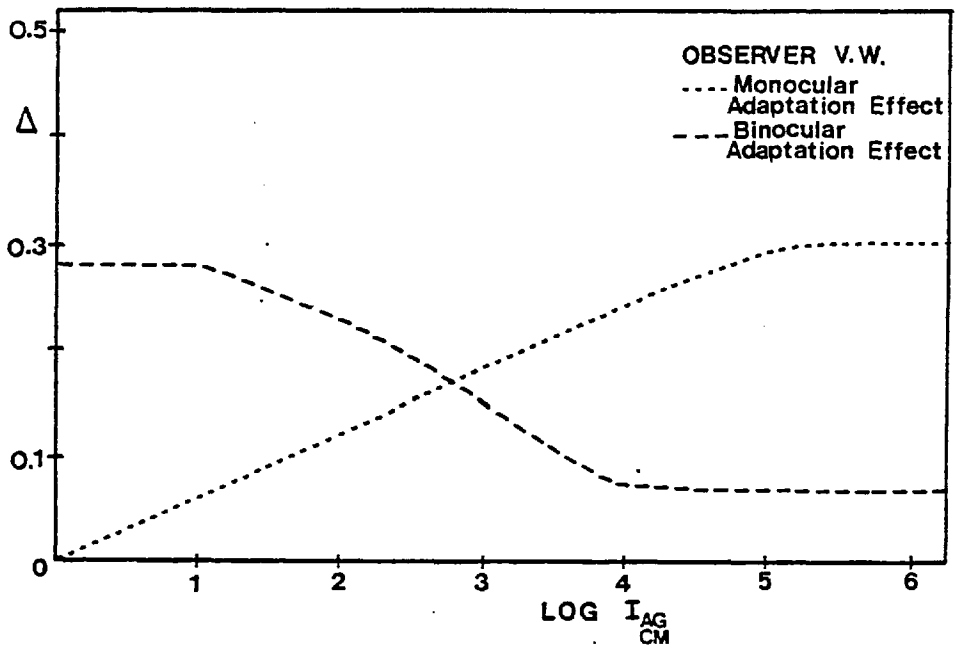

Fig. 3.27 To compare the variation in the amplitude of Δ obtained under simple monoptic conditions (···), i.e., fig. 3.1a, and under binocular conditions (——), i.e., fig. 3.1e. Observer V.W.

Δ is just attained in the contrast threshold elevation effect, is approximately the same as that of the conditioning matrix which just yields the minimum value of Δ in the binocular arrangement. For values of log I_{CM} in the range 1.5 to 4.5 log units above threshold, there is an approximate linear relationship between Δ and log I_{CM}.

C.v. Characteristics of the Effect investigated with a Colour Defective Observer

A number of the experiments carried out by the two observers with normal colour vision and described in the previous section were repeated with a congenitally colour defective subject. The experiments chosen for this subject were restricted to those involving red-green effects, as it has been shown that it is in this spectral range that deuteranopes have abnormal photopigment absorption (Rushton, 1958 and 1965), and colour discrimination (Wright, 1946), whereas the short wavelength response mechanism is apparently normal (König, 1893). The adaptation effect, Δ, (equation 3.1) was determined as for the normal observers.

The results of the measurements with observer C.C., the deuteranope, are shown in fig. 3.28. The adaptation and test gratings presented to the right eye were of bar width 5.7 minutes of arc, and the spot diameter in the matrix, d', was 9.3 minutes of arc. Data obtained for a positive contrast spot matrix equivalent to fig. 3.17 and to fig. 3.18 for the normal subjects are given in fig. 3.28. The results show that unlike the two normal observers, V.W. and I.H., the deuteranopic observer, C.C., shows no significant wavelength selectivity for the positive contrast matrix. The mean data of fig. 3.17 and of fig. 3.28 for observers V.W., and C.C., respectively, are

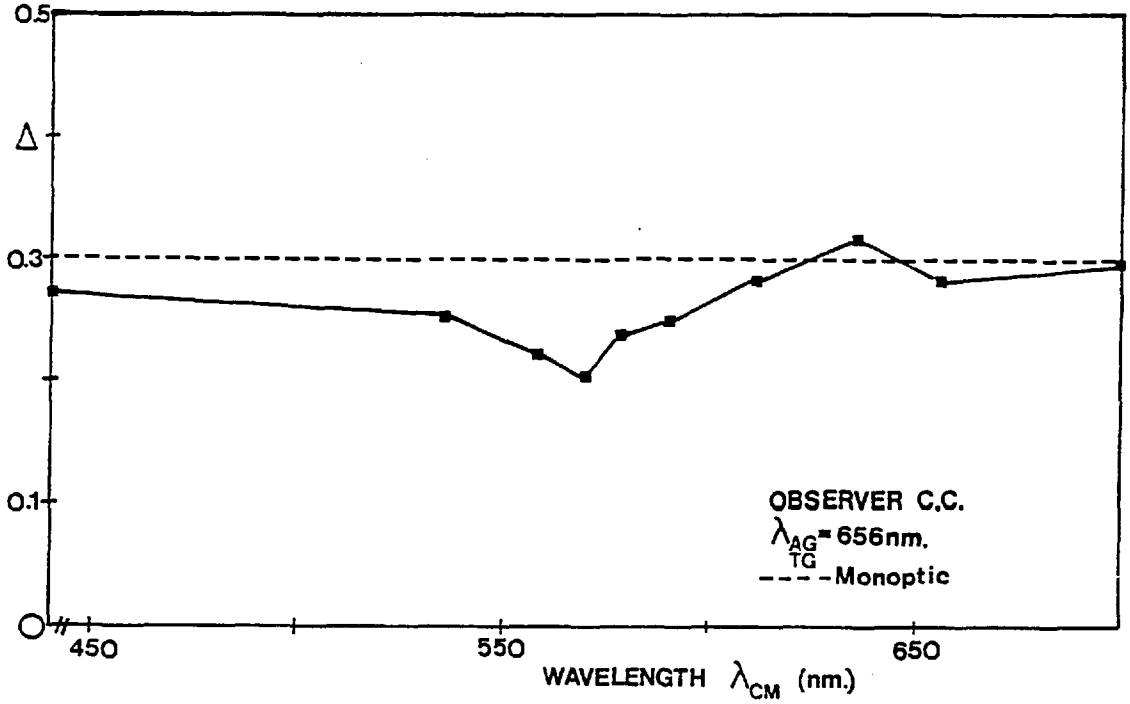

Fig. 3.28 Adaptation, Δ, as a function of wavelength of CM for a number of wavelengths of AG and TG. Data are for observer C.C. and conditions are as given in fig. 3.17.
a. AG and TG are of wavelength 656 nm.

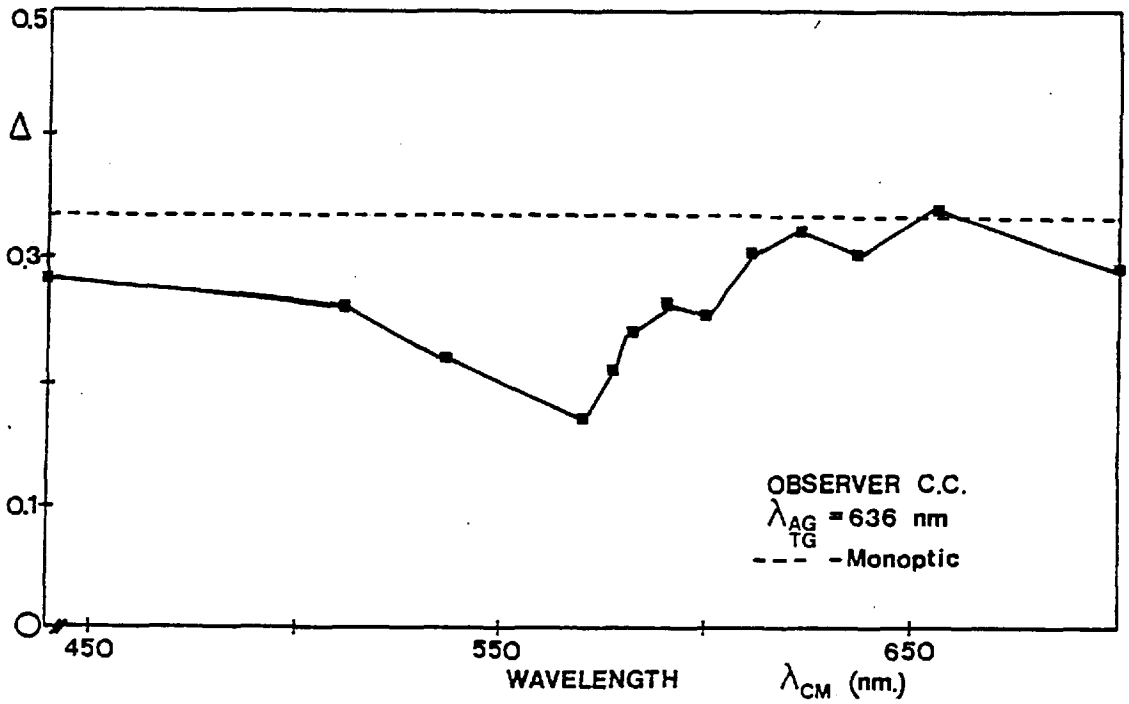

Fig. 3.28b AG and TG are of wavelength 636 nm.

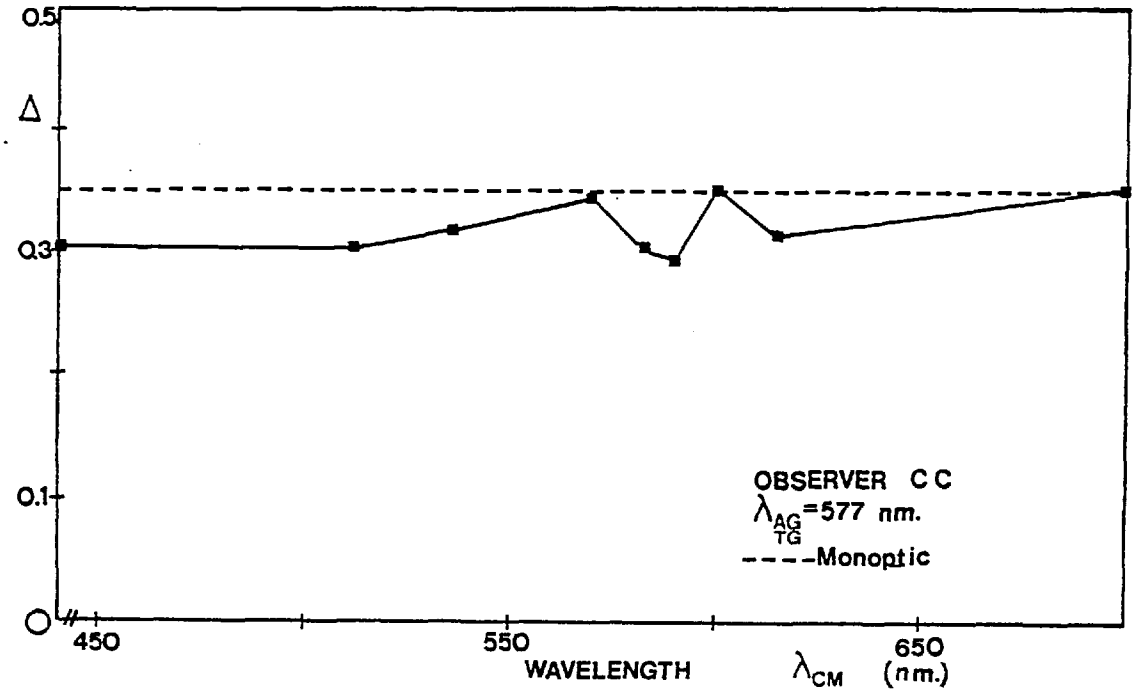

Fig. 3.28c AG and TG are of wavelength 577 nm.

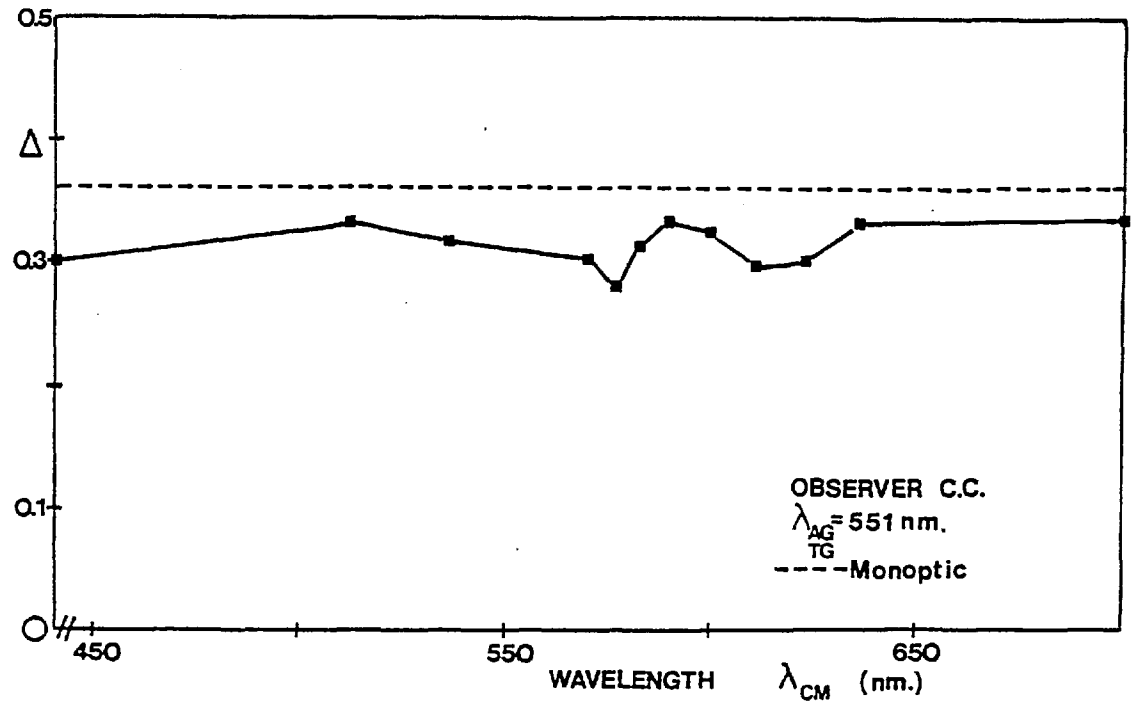

Fig 3.28d AG and TG are of wavelength 551 nm.

plotted for comparison in fig. 3.29.

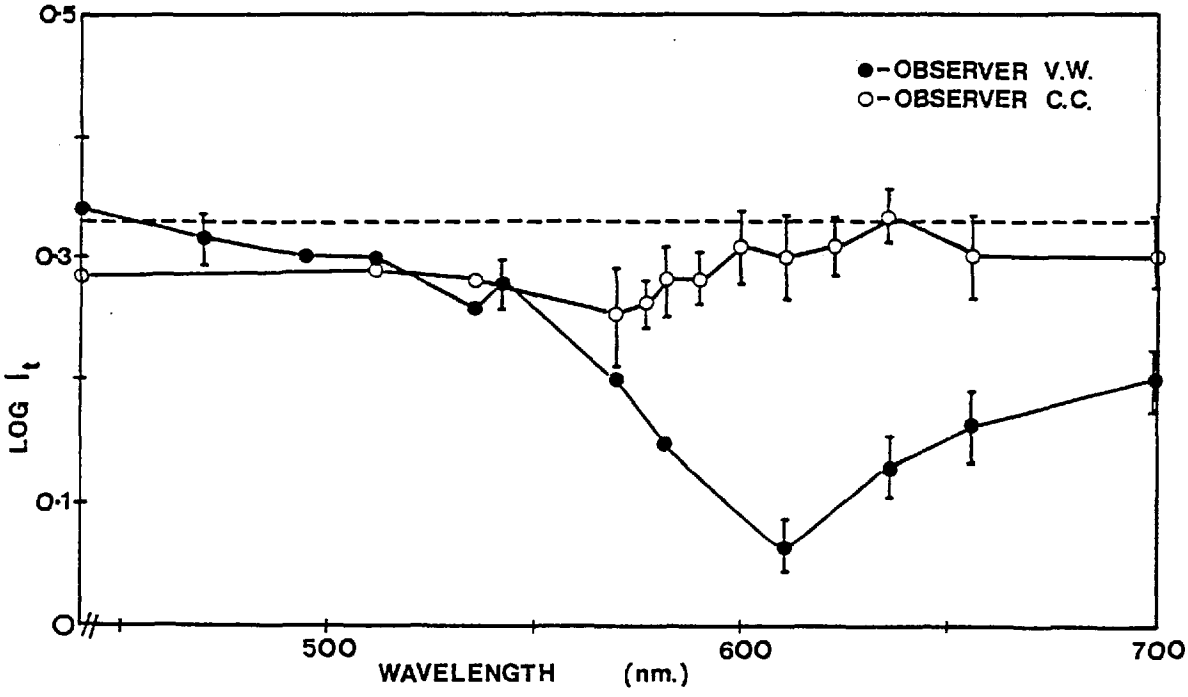

Fig. 3.29 Mean data replotted from fig. 3.17 for observer V.W. (●) from fig. 3.28 for observer C.C. (○).

D. Discussion

D.i. Derivation of the Post-receptoral Spectral Response Functions

The data, shown in fig. 3.17 to fig. 3.22, can be transformed by means of the data in fig. 3.23 to fig. 3.26 to give the sensitivity of the post-receptoral spectral response mechanisms. Adaptation, Δ, is not linearly dependent on log I_{CM}, as shown in fig. 3.23 to fig. 3.26, but over the range 1.5 to 4.5 log units above the threshold illumination level required for the detection of the conditioning matrix, there is an approximate linear relationship between the value of Δ and log I_{CM}.

The sensitivity profiles of the respective post-receptoral response mechanisms were calculated from the following expression:-

$$\log S_{\lambda} = -\log W_{\lambda} + \log I_{CM}, \qquad \text{Eq 3.2}$$

where:-

S_{λ} represents the sensitivity of the mechanism at a particular wavelength, λ,

W_{λ} is the energy in $\mu W/m^2$ of the monochromatic spot matrix at a retinal illumination 4 log units above the threshold illumination level, for which the experimental data were determined, and

Log I_{CM} corresponds to the increase in the illumination level, as measured for the data of fig. 3.23 to fig. 3.26, which would be required to make the amplitude of Δ equal for different wavelengths, λ_{CM}.

This transformation process produces the data plotted in fig. 3.30 to fig. 3.32. In each of these figures, the sensitivity of the post-receptoral spectral response function is plotted along the ordinate in terms of a normalized scale of relative reciprocal energy units with wavelength, in nanometers, plotted along the abscissa. The full symbols, squares, triangles and circles, in each of the figures respectively, represent the mean of the transformed data, whereas the open symbols in each of the figures represent the transformed psychophysical data points, each symbol representing a different test wavelength, as indicated for the relevant symbols in the legend.

Figure 3.30a,b represent the sensitivity functions for observers V.W. and I.H., respectively. The most notable feature of the sensitivity profiles plotted in fig. 3.30a,b, are the narrow-band long wavelength components, which have a peak sensitivity at approximately

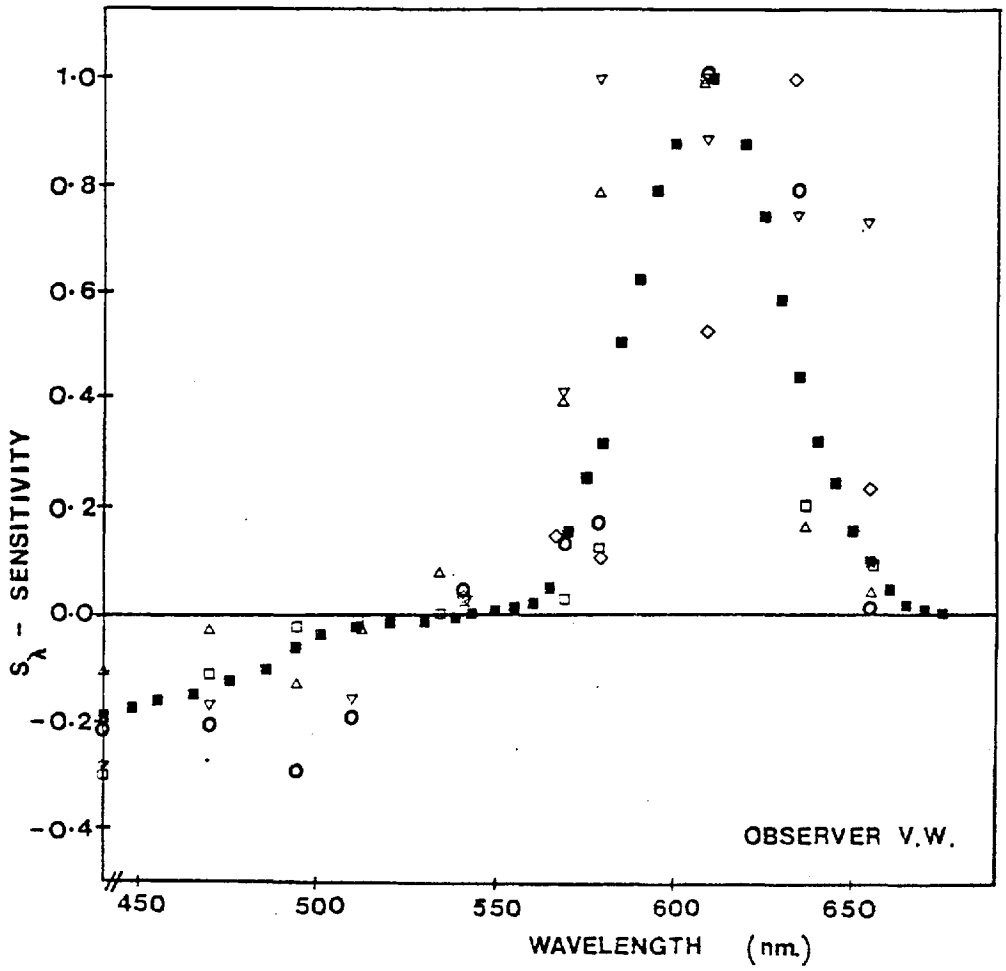

Fig. 3.30a A 'red-green' spectral sensitivity function derived from the binocular suppression of grating threshold illumination level (see fig. 3.17, observer V.W.). Each symbol is the mean of six values, with standard error 0.5, and corresponds to a different wavelength of the spot matrix [i.e., 656 nm (△); 636 nm (□); 551 (◇); 536 nm (○) and 495 nm (▽)]. The full squares (■) represent the best-fit mean curve.

610 nm, and a half bandwidth of some 50 nm. There is also a broad-band short wavelength component with polarity opposite to that of the long wavelength component. The 'neutral point', at which the sensitivity is zero, is at approximately 540 nm, and these spectral characteristics suggest a red-green opponent mechanism.

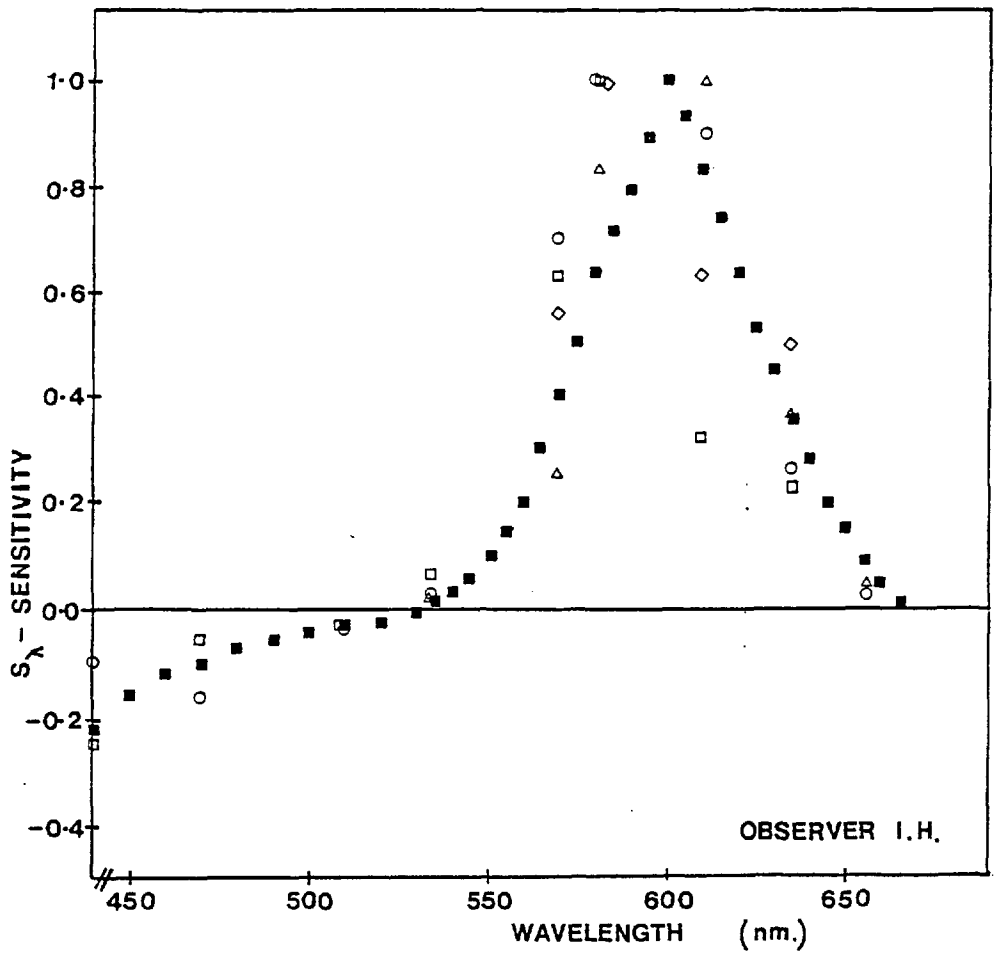

Fig. 3.30b As in fig. 3.30a, but data refer to fig. 3.18 and observer I.H.

The sensitivity profiles for the green sensitive mechanism are shown in fig. 3.31, and the broken line represents the spectral sensitivity of the Π_4 mechanism (Stiles, 1959; numerical values from Wyszecki and Stiles, 1967). For both subjects, the sensitivity profile of this mechanism has its peak response at approximately 530 nm, and a half bandwidth of some 70 nm. However, this spectral function exhibits no component with a sensitivity of opposite polarity, as shown in the mechanism of fig. 3.30.

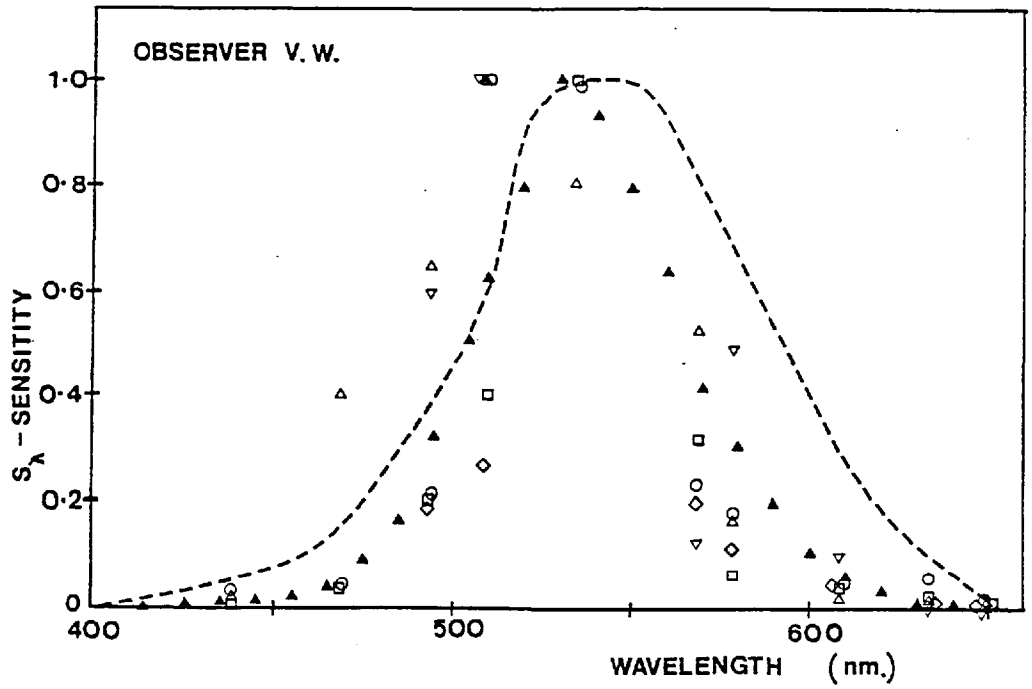

Fig. 3.31a A green-sensitive spectral response mechanism. Symbols are as in fig. 3.30, but data refer to fig. 3.19, and observer V.W. The full triangles (▲) represent the best-fit mean curve, and the broken line, the spectral sensitivity of the $\overline{rr}_4$ mechanism (Stiles, 1959; numerical values, Wyszecki and Stiles, 1967).

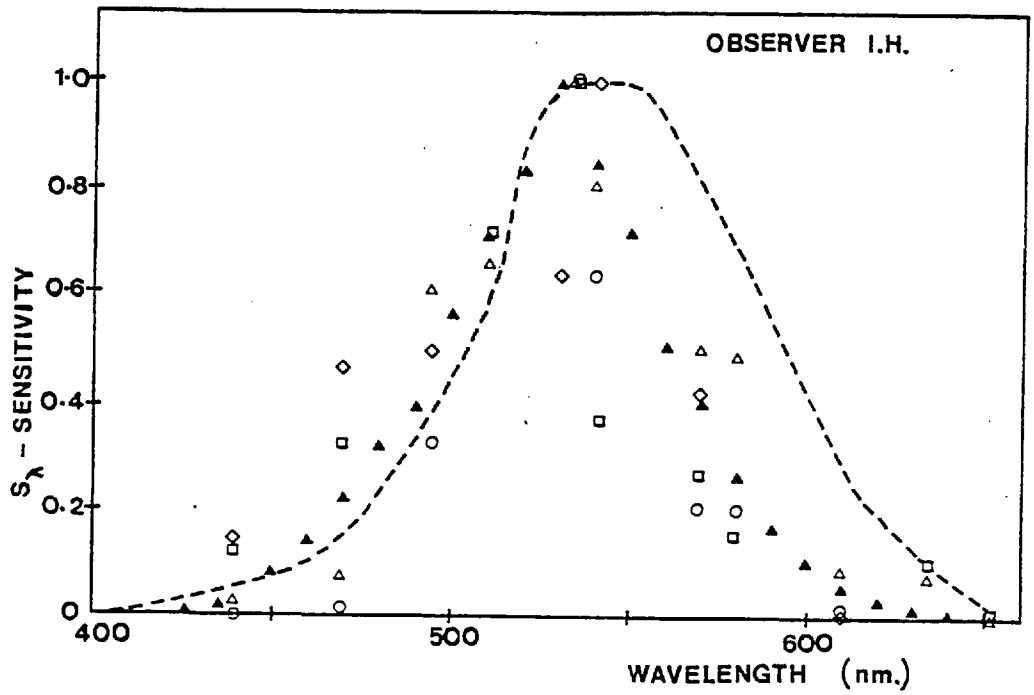

Fig. 3.31b As in fig. 3.31a, but data refer to fig. 3.20, and observer I.H.

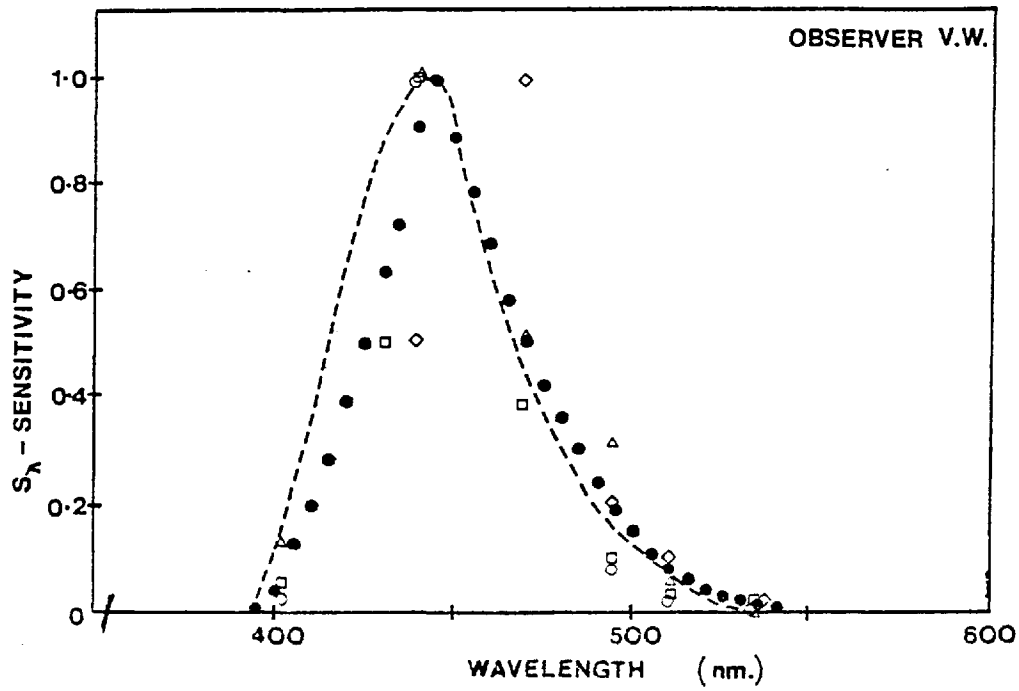

Fig. 3.32a A blue-sensitive spectral response mechanism. Symbols are as in fig. 3.30, but data refer to fig. 3.21 and observer V.W. The full circles (●) represent the best-fit mean curve, and the broken line, the π_1 spectral sensitivity mechanism (Stiles, 1959; numerical values, Wyszecki and Stiles, 1967).

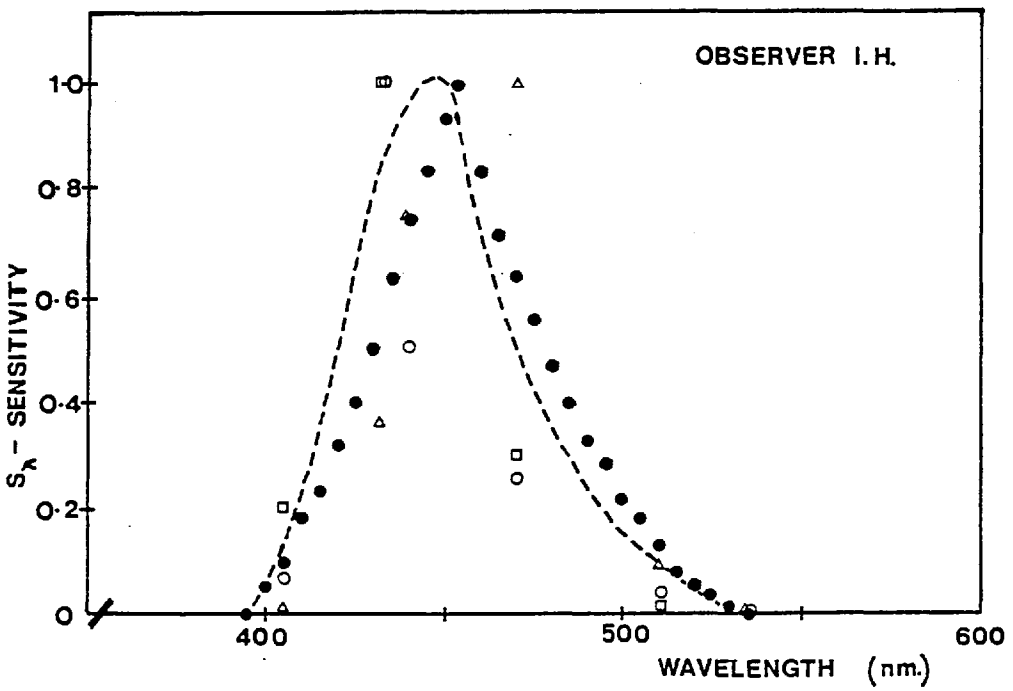

Fig. 3.32b As in fig. 3.32a, but data refer to fig. 3.22, and observer I.H.

The data of observers V.W. and I.H., shown in fig. 3.21 and in fig. 3.22, are transformed and replotted in fig. 3.32a,b, respectively, to give a third spectral response function. The sensitivity profile is very similar to that of the π_1 spectral sensitivity mechanism of Stiles, plotted as the broken line in fig. 3.32a,b (numerical values from Wyszecki and Stiles, 1967). The peak sensitivity of this response mechanism occurs at approximately 450 nm for both observers, and its half bandwidth is of the order of 50 nm.

D.ii. Mechanisms underlying the Post-receptoral Spectral Response Functions

Two models for the combination of the outputs of the different spectral classes of cones, which may yield the sensitivity of the post-receptoral spectral mechanisms are examined. These are shown in fig. 3.33, and in both cases only two receptor mechanisms are considered, namely those with relative spectral sensitivities, R_λ and G_λ, per unit irradiance of monochromatic stimulus of wavelength λ. R_λ and G_λ, are assumed equivalent to the Stiles π_5 and π_4 spectral sensitivity mechanisms, respectively (Stiles, 1939, 1949, 1953, 1959, 1978; numerical values from Wyszecki and Stiles, 1967).

The spectral sensitivity S_λ of the interaction unit is represented as a linear combination of the two separate inputs in fig. 3.33a, and defined by equation 3.3:-

$$S_\lambda = F\,[R_\lambda - \beta G_\lambda]\,, \qquad \text{Eq 3.3}$$

where the value of the coefficient β is a constant, and in fig. 3.33b, the model proposed is based on a logarithmic transformation of the two inputs before the site of the interaction mechanism, i.e., $F(R_\lambda)$ and $F(G_\lambda)$, respectively. The sensitivity is therefore predicted from the

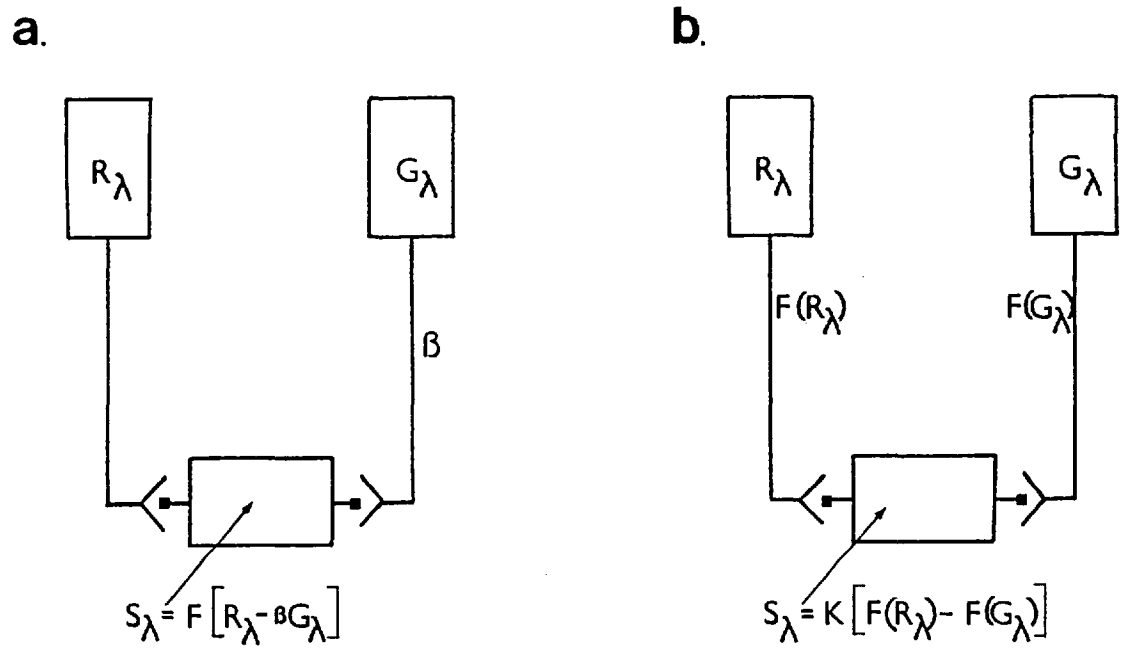

Fig. 3.33 Models proposed for the post-receptoral spectral response function a. linear and b. non-linear combination of the spectral outputs from the two types of cone photoreceptors.

equation:-

$$S_\lambda = k[\log (R_\lambda) - \log (G_\lambda)] . \qquad \text{Eq 3.4}$$

The combination of π_5 and π_4, which, on the basis of equation 3.3, gives the optimum fit to the 'red-green' opponent mechanism of fig. 3.30 is examined first. Values of π_5 and π_4 taken from Wyszecki and Stiles (1967) are plotted in fig. 3.34, with π_4 multiplied by ß equal to 0.9. Computation showed that this value gave the best agreement between equation 3.3 and the experimental data shown in fig. 3.30, and the predicted and experimental values are plotted in fig. 3.35. As the Wyszecki and Stiles data represent average values, however, the π_5 and π_4 spectral sensitivity functions were measured for the two subjects, V.W. and I.H. (see fig. 3.3, fig. 3.4 and fig.

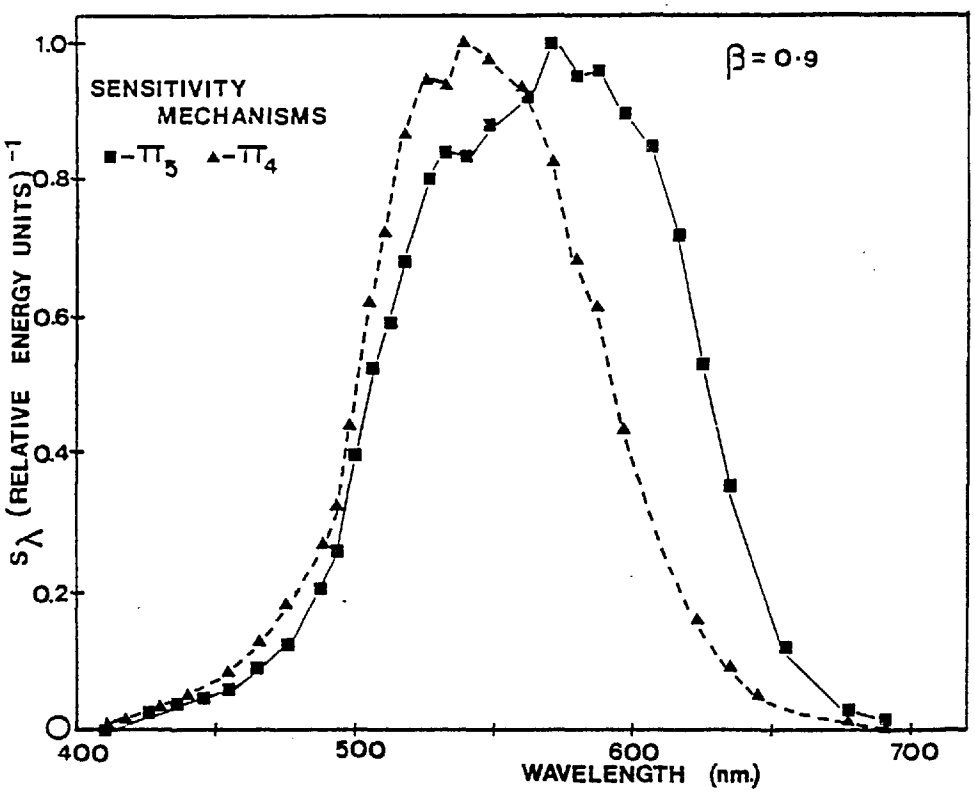

Fig. 3.34 Derivation of the post-receptoral spectral response function from a linear combination of the Stiles' spectral sensitivity mechanisms (numerical values from Wyszecki and Stiles, 1967).

3.5) and values of β determined on the basis of these individual functions. The optimum value of β for subject V.W. was 1.0, giving the computed function $(\pi_5 - \pi_4)$ (or $R_\lambda - G_\lambda$), shown in fig. 3.36, and for subject I.H., the value was 0.82, giving the computed function shown in fig. 3.37. In each of these figures, the experimental data, taken from fig. 3.30a (V.W.) and fig. 3.30b (I.H.), are plotted together with the computed values, and it is clear that in each case, the computed peak sensitivity and 'neutral point' are similar to the experimental values.

A similar computation was performed for the green-sensitive mechanism (e.g., in fig. 3.31). In this case, the functions were computed as:-

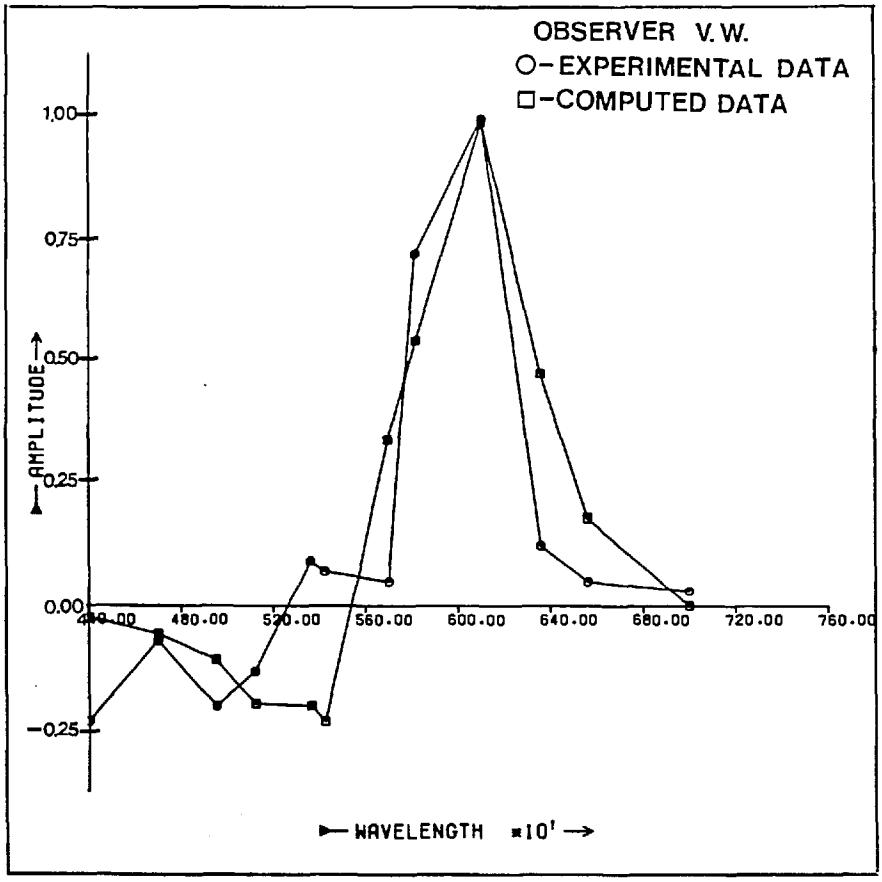

Fig. 3.35 Experimental and computed data of the 'R-G' opponent mechanism of fig. 3.30. Computation based on linear combination of Stiles' spectral mechanisms with $\beta = 0.9$.

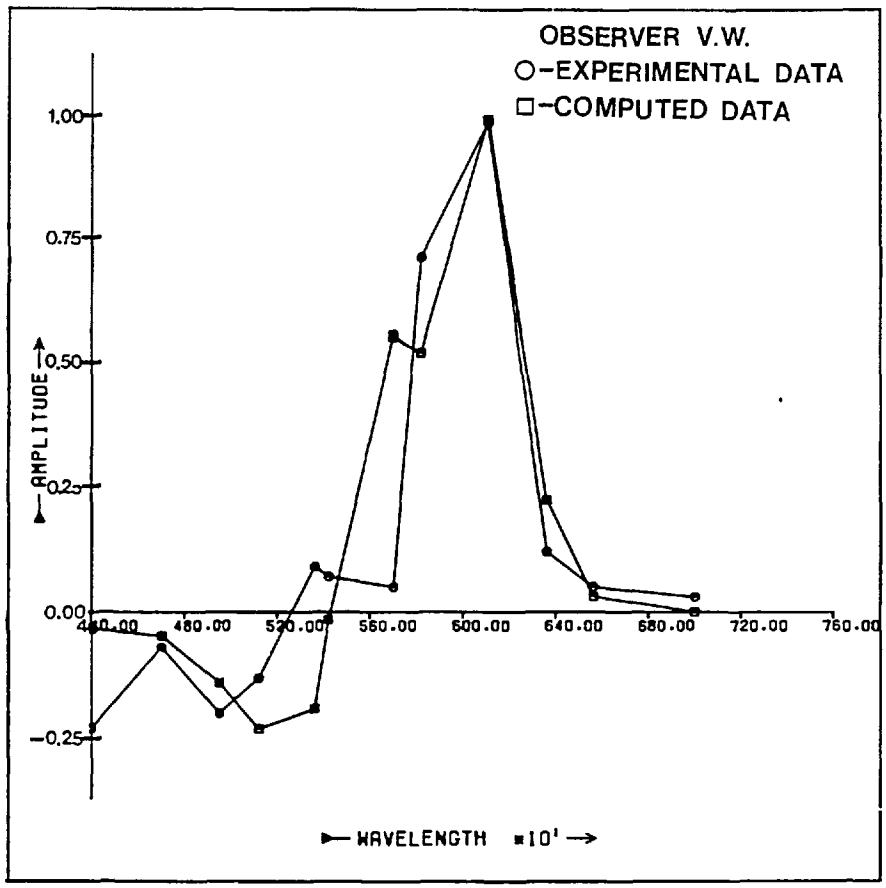

Fig. 3.36 As in fig. 3.35, but value of the coefficient $\beta = 1.0$ for observer V.W.

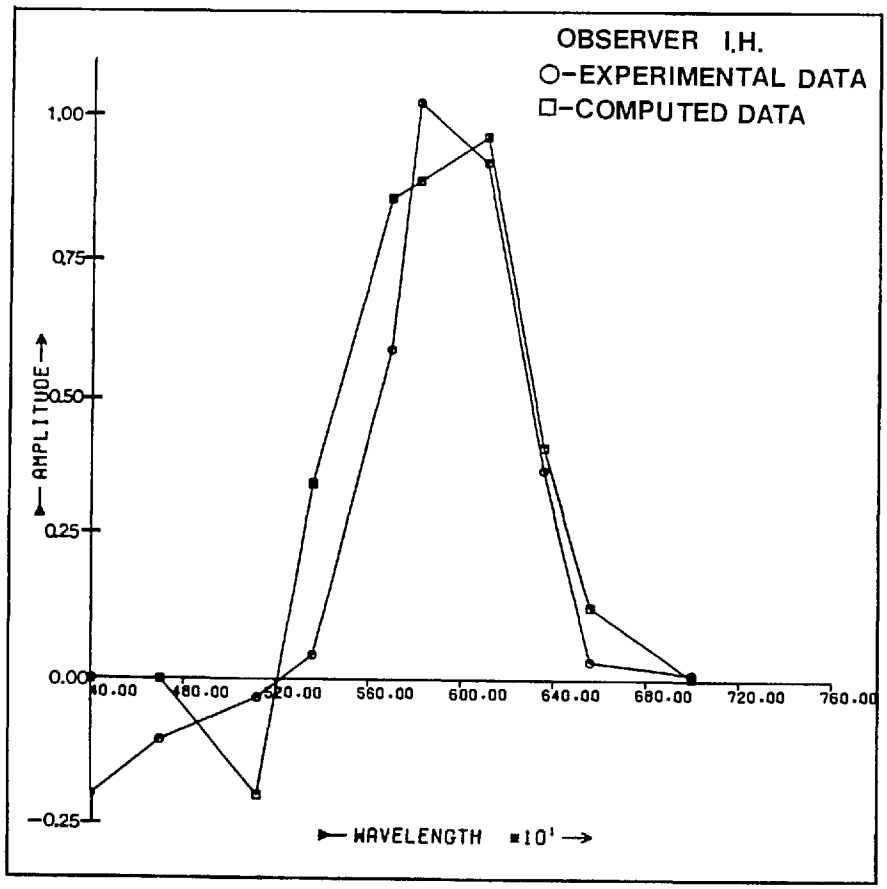

Fig. 3.37
As in fig. 3.35, β has a value of 0.82 for observer I.H.

$$S_\lambda = F[G_\lambda - \alpha R_\lambda] , \qquad \text{Eq 3.5}$$

where α is another constant coefficient. Computation, on the basis of Wyszecki and Stiles' average data, showed that the best fit was obtained with α equal to 0.33, as is illustrated in fig. 3.38, and computations using the Π-mechanism values found for each individual subject gave optimum fit values of α equal to 0.32 for subject V.W. (see fig. 3.39) and 0.30 for subject I.H. (see fig. 3.40).

Attempts were made to reproduce the red-green sensitivity functions of fig. 3.30 and fig. 3.31 from non-linear combinations of the Π_5 and Π_4 spectral response mechanisms (see fig. 3.33b and Eq. 3.4). As the contrast threshold elevation effect and its binocular suppression both yield log-linear relations between the adaptation

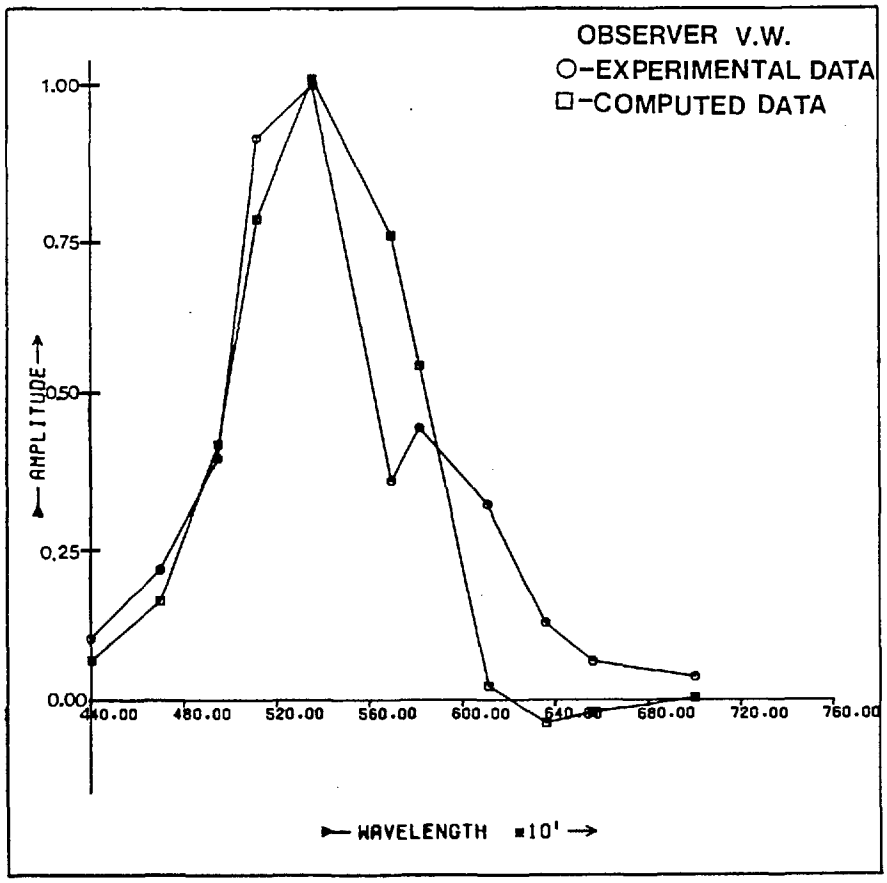

Fig. 3.38
Computed and experimental data for the mechanism in fig. 3.31. Value of the coefficient $\alpha = 0.33$ for Stiles' spectral mechanisms.

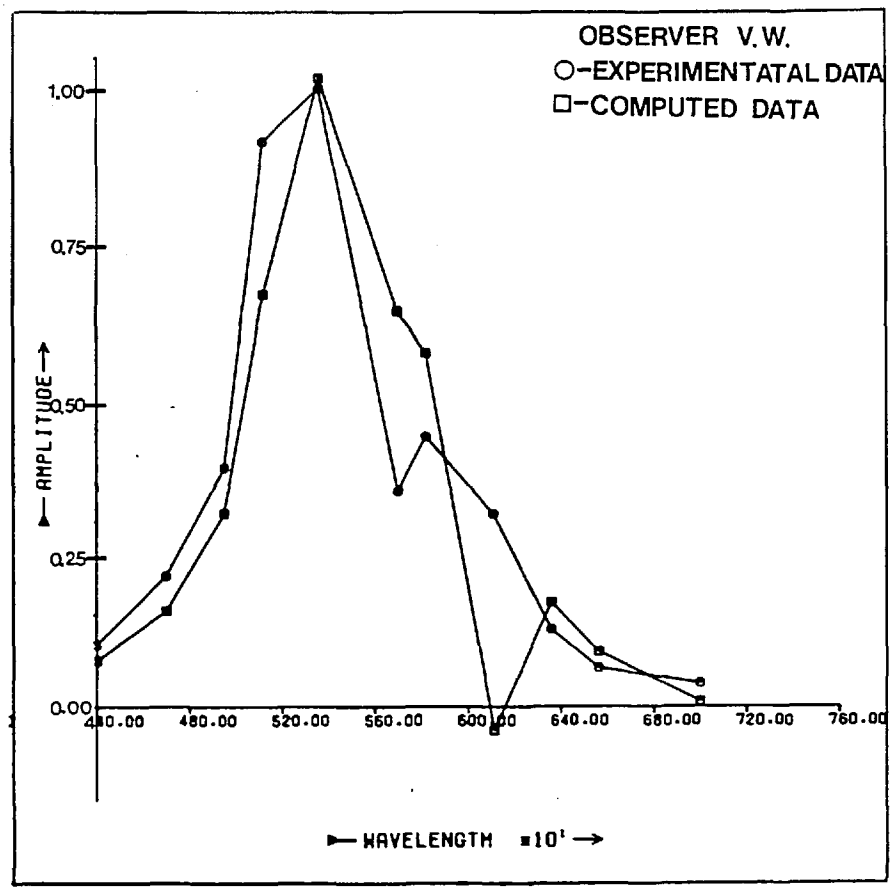

Fig. 3.39
As in fig. 3.38, but α has a value of 0.32 for observer V.W.

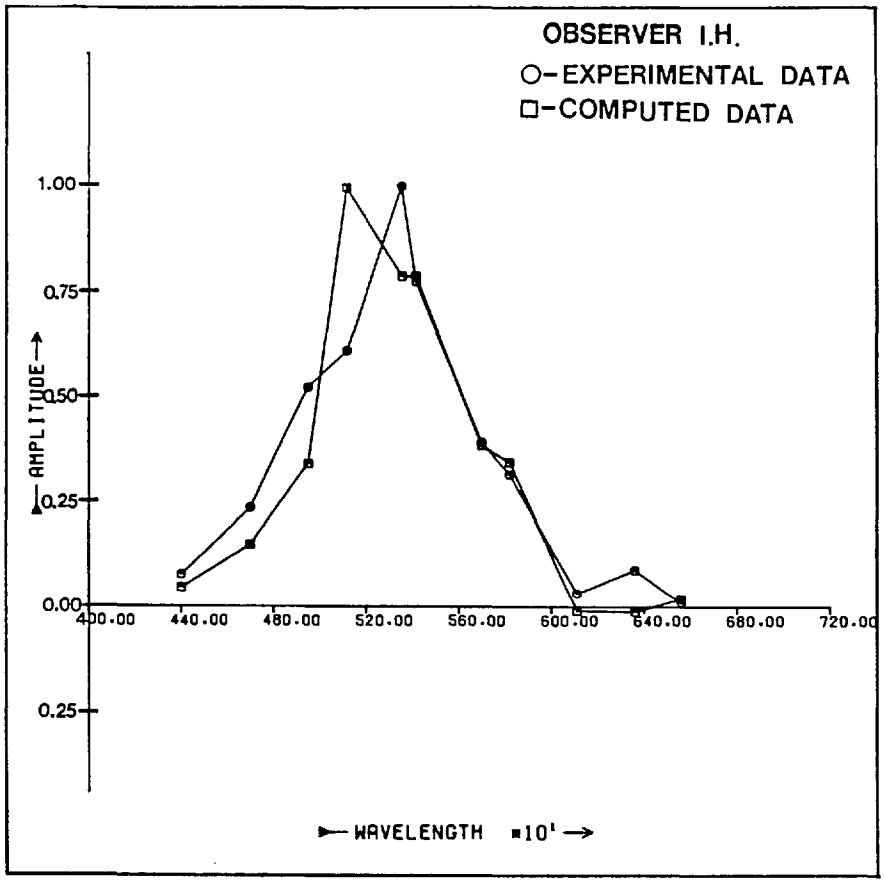

Fig. 3.40
As in fig. 3.38, except $\alpha = 0.30$ for observer I.H.

effect and illumination level (e.g., fig. 3.27), combinations of log Π_5 and log Π_4 were explored. It was found, however, that the experimental data, particularly the 'red-green' opponent mechanism (see fig. 3.30) could not be predicted in this way, because the differences of logarithmic values of Π_5 and Π_4 gave maximum sensitivity at the red end of the spectrum, i.e., in fig. 3.41.

Thus, although the experimental method involves high contrast stimuli of high mean illumination level, the resulting spectral response functions can be closely represented by linear combinations of the component spectral response mechanisms. It should be noted that the three response mechanisms derived in these measurements, one with spectral sensitivity of the Π_1 mechanism (see fig. 3.32), another

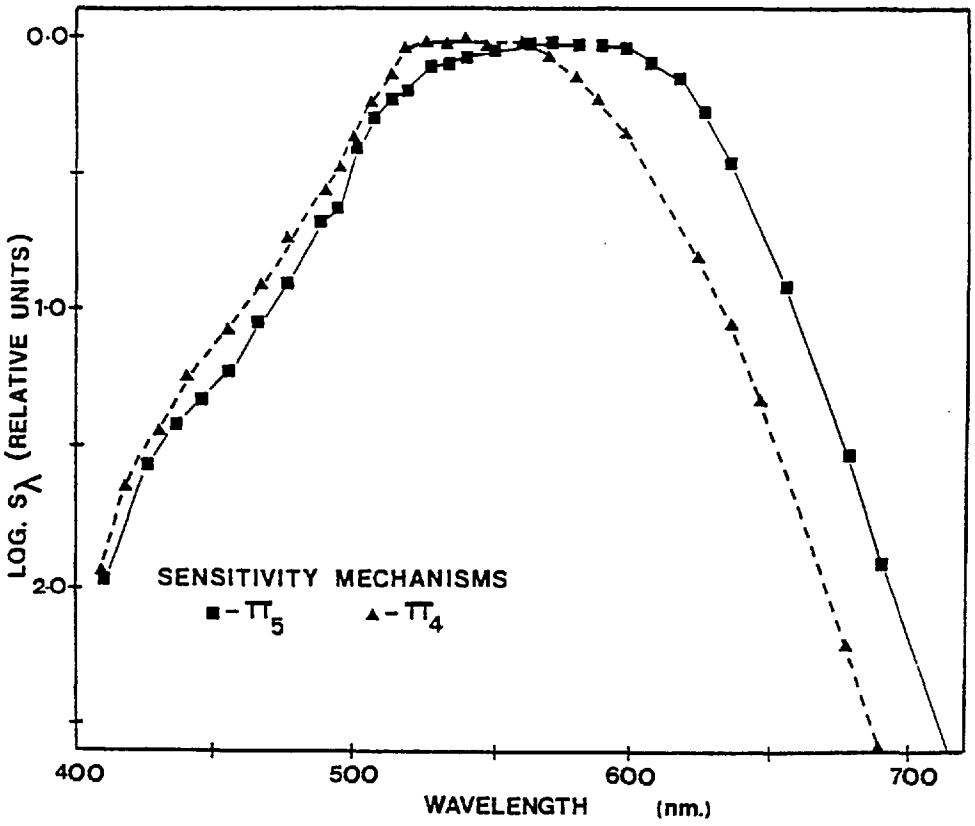

Fig. 3.41 Derivation of the post-receptoral spectral response function from a logarithmic combination of the Stiles' spectral sensitivity mechanisms (numerical values from Wyszecki and Stiles, 1967).

$\pi_5 - \pi_4$ (fig. 3.30) and a third, $\pi_4 - 0.3\,\pi_5$ (fig. 3.31) correspond closely to the three component mechanisms isolated psychophysically after high level bleaching of the macaque retina (Sperling and Harwerth, 1971).

D.iii. Spectral Sensitivity Correlations in the Visual System

All of the principal theories of colour vision postulate a trivariant organization of cone spectral responses. This is inferred from the experimental fact that three stimuli are required in additive colour matching. Hering (1875) proposed a coding scheme for colour which was based on inhibition, even though at that time he had no

direct evidence for such inhibition processes. He postulated a system based on several perceptual effects of colour coding which suggested an opponent, rather than a component, coding system. He suggested that there were three specific pairs of coded representations (see fig. 3.42), which acted in opposition; one pair was a red-green opponent system, R-G, a second, a yellow-blue, Y-B, and the third a black-white, Bk-W, channel which specifies brightness and saturation.

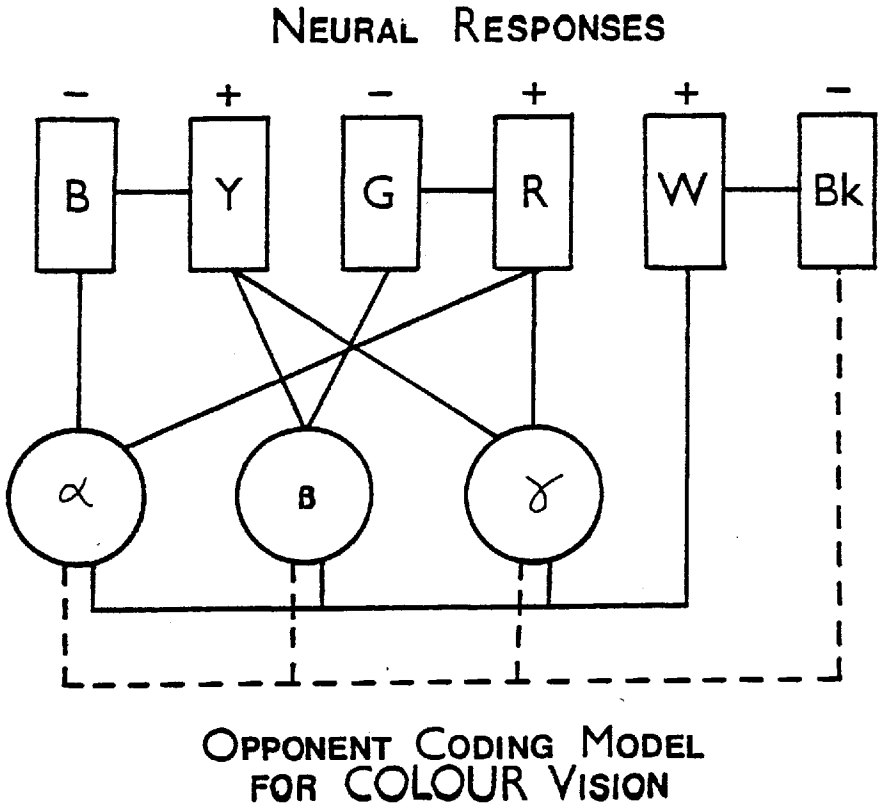

Fig. 3.42 Model based on Hering's proposals (after Hurvich and Jameson, 1957).

The model suggested that wavelengths corresponding to red and green are coded as opposites and not combinations. Thus, the red-green absorbing system will receive its inputs from red cones and green cones. If the red input dominates, then the output of the red-green channel is positive, indicated by an increase in its firing frequency over the spontaneous level of activity, while negative,

should the green input be greater, or vice versa. Red-green coding is therefore handled by one system, which is nowadays presumed to occur after the initial receptor absorption.

Later, Hurvich and Jameson (1957) derived the spectral sensitivity functions for the two opponent-colour processes, and provided a qualitative description of how variations in wavelengths lead to apparent changes of hue. The functions were determined psychophysically for an assumed opponent response system. The data were obtained by neutralizing, e.g., a blue stimulus, by the addition of a particular yellow wavelength until the stimulus appeared neither blue nor yellow. The result is regarded as fixing the null point between the balance of yellow and blue. The amount of a yellow which has to be added to a particular blue, provides a measure of the relative blue response of the yellow-blue opponent system for that wavelength of blue. This type of process is repeated for all wavelengths in the spectrum for both the Y-B and G-R systems to generate the curves shown in fig. 3.43.

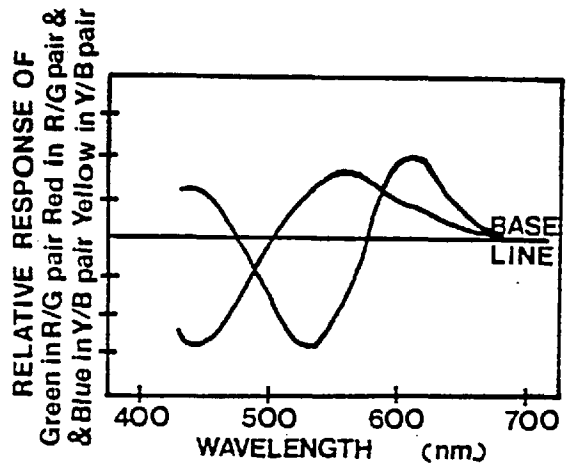

Fig. 3.43 Theoretical spectral sensitivity functions for the two opponent colour processes, one for red-green, and the other for yellow-blue, (after Hurvich and Jameson, 1957).

These distinct processes, which underly the triple nature of colour vision, can only function as a discriminating device if the quality of one physical radiation and another differ significantly on their spectral sensitivity curves. These physiological sensitivity curves are more

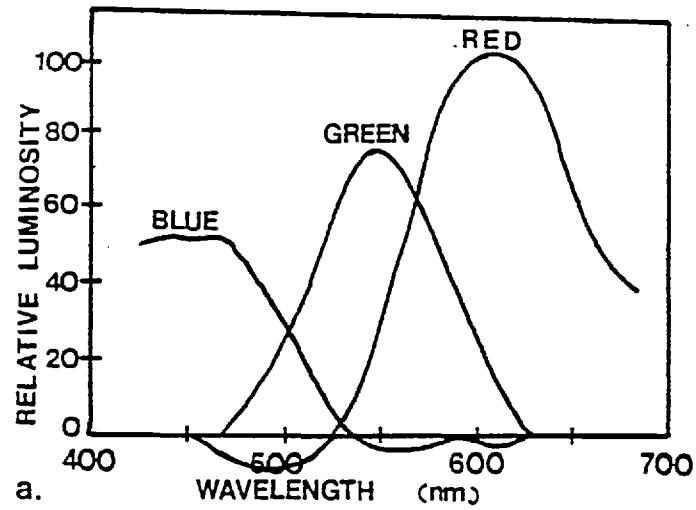

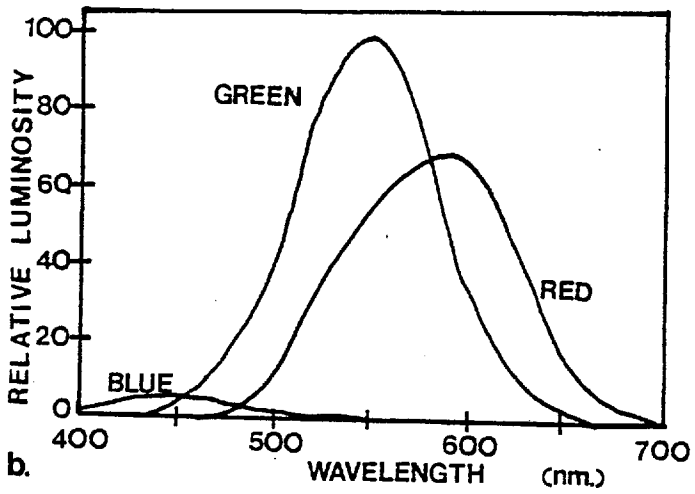

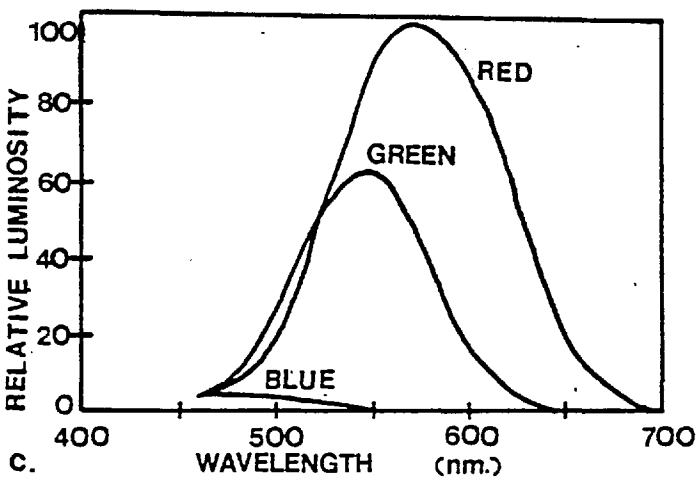

Fig. 3.44 Several derivations of the fundamental response curves,
a. after Maxwell, 1890;
b. after König, 1886;
c. after Abney, 1913;

commonly referred to as the fundamental response curves, and are primarily related to the process of light absorption in the retina. Several psychophysical methods have been suggested for the derivation of these fundamental response curves, notably Maxwell (1890) who derived a set of curves from speculations on the shape of the spectral locus in the chromaticity chart (fig. 3.44a), Helmholtz (1911), Hecht (1932) and others derived curves from the analysis of colour mixture and colour discrimination data, (see fig. 3.44d) as also did Abney (1913) but he included results on the

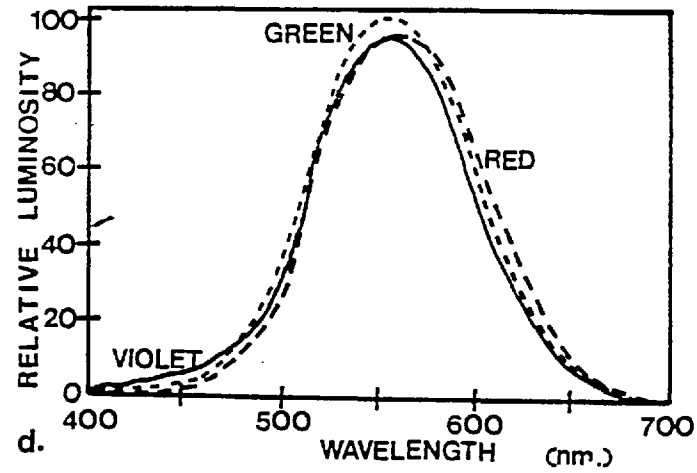

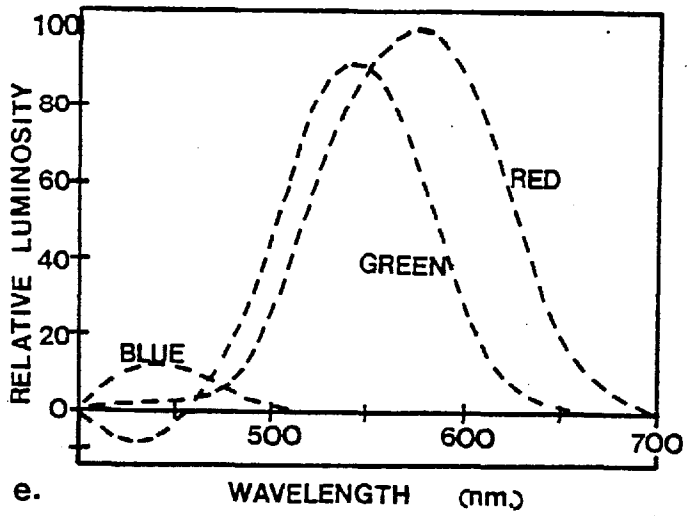

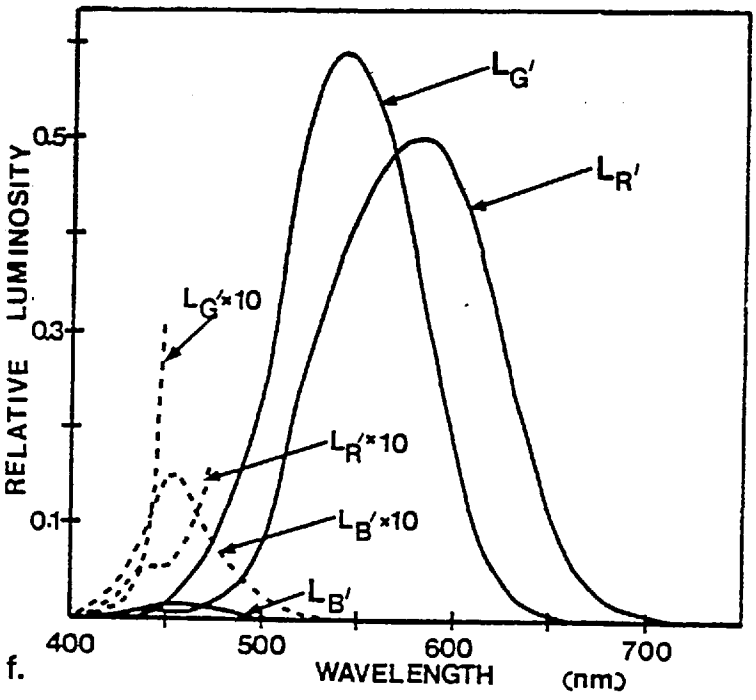

Fig. 3.44 d. after Hecht, 1932; e. after Wright, 1934; f. after Pitt, 1944.

luminosities of mixed radiations (fig. 3.44c), and König (1886), relied on the comparison of data for normal and defective colour vision (fig. 3.44b).

The spectral sensitivity mechanisms derived from the studies of Stiles (1939, 1959, 1978) on the colour thresholds under various conditions of colour adaptation have already been plotted in fig. 3.34 for π_5, and in fig. 3.31 and fig. 3.32, where the sensitivity of the π_4 mechanism and π_1 mechanism, represented by the broken lines, are shown respectively. Wright (1934) derived three

fundamental response curves, which were determined by the analysis of colour adaptation phenomena, and are shown in fig. 3.44e. Lastly, in fig. 3.44f, the curves of Pitt (1944) are shown. These were derived from the location of the fundamental stimuli from considerations of the confusion zones for colour defectives.

The fundamental response curves, shown in fig. 3.44, all have similar characteristics; the blue curve has a maximum sensitivity in the short wavelength end of the spectrum (440 to 460 nm), the green curve peaks in the green (540 nm) and the red in the yellow/orange region (580 to 600 nm). Thus, it can be seen that although the response curves of fig. 3.30 to fig. 3.32 are also derived from psychophysical data, and have similar peak sensitivities to the data in fig. 3.44, the curves are measuring a different kind of spectral sensitivity. The data of figure 3.44 appear to be closely related to the absorption spectra of single cones (e.g., Marks, Dobelle and MacNichol, 1964), whilst those of fig. 3.30 to fig. 3.32 appear to represent post-receptoral interaction mechanisms. None of the red curves, in fig. 3.44, show any opponent type process of the kind seen in the data of fig. 3.30, and it is clear that the green mechanism of fig. 3.31 does not correspond to the sensitivity mechanism of Stiles' π_4. The blue mechanism (see fig. 3.32) does, however, follow closely the spectral sensitivity of the π_1 mechanism of Stiles.

Sperling and Harwerth (1971) have obtained spectral sensitivity data from behavioural studies on both monkeys and humans in order to relate the receptor sensitivities to psychophysical response data. Their studies show that spectral sensitivity in the primate eye can be

regarded as the upper envelope of three spectral sensitivity functions, defined as follows:-

Channel 1 : $S_\lambda = \Pi_5 - \Pi_4$, Eq 3.6

Channel 2 : $S_\lambda = \Pi_4 - \Pi_5$, Eq 3.7

Channel 3 : $S_\lambda = \Pi_1$. Eq 3.8

The sensitivities of the three response channels described by Sperling and Harwerth (1971) are therefore remarkably similar to those discovered in the present studies, defined by:-

Mechanism 1 : $S_\lambda = \Pi_5 - \Pi_4$, Eq 3.9

Mechanism 2 : $S_\lambda = \Pi_4 - 0.33\,\Pi_5$, Eq 3.10

Mechanism 3 : $S_\lambda = \Pi_1$. Eq 3.11

D.iv. Mechanism underlying Colour Defective Post-receptoral Spectral Response

The data shown in fig. 3.28 for the deuteranopic observer C.C., indicate that the red-green opponent post-receptoral spectral response is non-functional. Comparison data to that in fig. 3.19 and in fig. 3.20 for normal subjects indicates that a 'type' of green-sensitive mechanism occurs in the deuteranope, and that binocular suppression is active for this subject.

Deuteranopes have dichromatic colour vision (Wright, 1946) and Rushton (1965) has shown that the lack of discrimination for the red-green spectral range is associated with the loss of the green-sensitive cone pigment, chloralabe. Thus for the deuteranope, the model of the 'R-G' opponent post-receptoral spectral response

mechanism, (see fig. 3.30), must be modified, as the green photoreceptor, G_λ, is either absent, or is replaced by the red photoreceptor, R_λ. The sensitivity of the opponent response mechanism is either equal to R_λ (if G_λ is simply absent) or approximately zero (if G_λ is replaced by R_λ), as it was shown that the value of β is approximately equal to unity.

The data for the deuteranope shows clearly that the reduction in the contrast threshold elevation effect which in normal vision arises from the 'red-green' opponent mechanism ($R_\lambda - G_\lambda$) does not occur in the case of the deuteranope (see fig. 3.29). This implies that the opponent channel responsible for this interaction in normal vision gives zero output for the deuteranope, i.e., it supports the substitution hypothesis that in deuteranopia, the green-sensitive cone response mechanism, G_λ, is replaced by the red-sensitive mechanism, R_λ.

D.v. Neural and Physiological Correlates of the Binocular Inhibitory Effect

When Hering (1875) proposed his opponent colour coding model, he had no neurophysiological evidence of opponent or inhibitory processes, nor was there any evidence to suggest that there were interactions arising in the output of three cone spectral mechanisms.

The first opponent chromatic responses were observed in the retinae of fish by Svaetichin (1953, 1956). He recorded from two classes of cell, in which the responses were amplitude modulated, but in one, the luminance, or L-type, the response was always negative, i.e., hyperpolarizing, whereas in the other, the chromatic, it was depolarizing or hyperpolarizing depending upon the light stimulus, and

two kinds were found as shown in fig. 1.9b, (chapter I); one depolarized for long wavelength stimuli, and hyperpolarized to shorter wavelength stimuli (i.e., R-G, see fig. 1.9b,a) and vice versa (i.e., Y-B, see fig. 1.9b,b). It was shown by intracellular dye injection that these signals were generated in retinal horizontal cells and similar chromatic organization was later observed in goldfish retinal ganglion cells by Svaetichin and MacNichol (1958), Daw (1968) and Spekreijse, Wagner and Wohlbarsht (1972).

In ganglion cells, chromatic signals are also organized into spatially separate centre and surround receptive field areas. For example, the receptive field centres may respond to long wavelength stimuli with a burst of spike potentials at light 'on', and the surrounds to short wavelength stimuli with a burst of spikes at light 'off'. In primates, some twenty-six different combinations of spectral and spatial receptive field organizations have been observed (De Monasterio and Gouras, 1975). The majority of these cells have concentrically arranged receptive fields and are also colour-opponent, i.e., centre and surround regions are driven by different spectral classes of photoreceptor. De Monasterio, Gouras and Tolhurst (1975) have identified three functionally distinct classes of ganglion cell in the rhesus monkey retina. Those with concentric receptive field organization possess single spectral cone input into the receptive field centre and one or two cone inputs into the antagonistic surround. In addition, there are cells with broad-band spectral responses, which exhibit transient responses and concentric, antagonistic receptive fields, with the centre and surround responses mediated by the same two cone inputs (see fig. 1.13, chapter I).

De Valois (1965) first reported direct evidence for colour opponent coding at the level of the primate lateral geniculate nucleus, and De Valois, Abramov and Jacobs (1966) measured the responses of single geniculate units in response to diffuse illumination. Their study established two types of cell; one which was classified as non-opponent, and the other as opponent. The non-opponent cell class behaved exactly like an intensity detector, but the opponent cells showed wavelength dependence in their responses. For some wavelengths, their firing rate was increased above the spontaneous level, whereas for others, it was decreased. In one of their examples, a cell yielded a positive response to long wavelengths; others showed approximately the reverse characteristics (see fig. 3.43).

Wiesel and Hubel (1966) showed that as well as being colour coded, geniculate neuronal receptive fields are also spatially organized into antagonistic concentric centre-surround regions.

Electrophysiologically, all three cone mechanisms of primate vision have been identified in the earliest visual activity of cortical neurones (Gouras, 1971, 1972; Gouras and Padmos, 1974). Further, studies of the visual cortex in primates (Gouras, 1970; Dow and Gouras, 1973; Dow, 1974) showed that some cells in this region received trichromatic input, e.g., an inhibitory input signal from the green-sensitive cones, and an excitatory input signal from both the blue- and the red-sensitive cones. This suggests a cortical trichromatic orgnization, which indicates that the subcortical organization found at the lateral geniculate nucleus level (De Valois, 1965; Wiesel and Hubel, 1966), where some cells receive only inputs

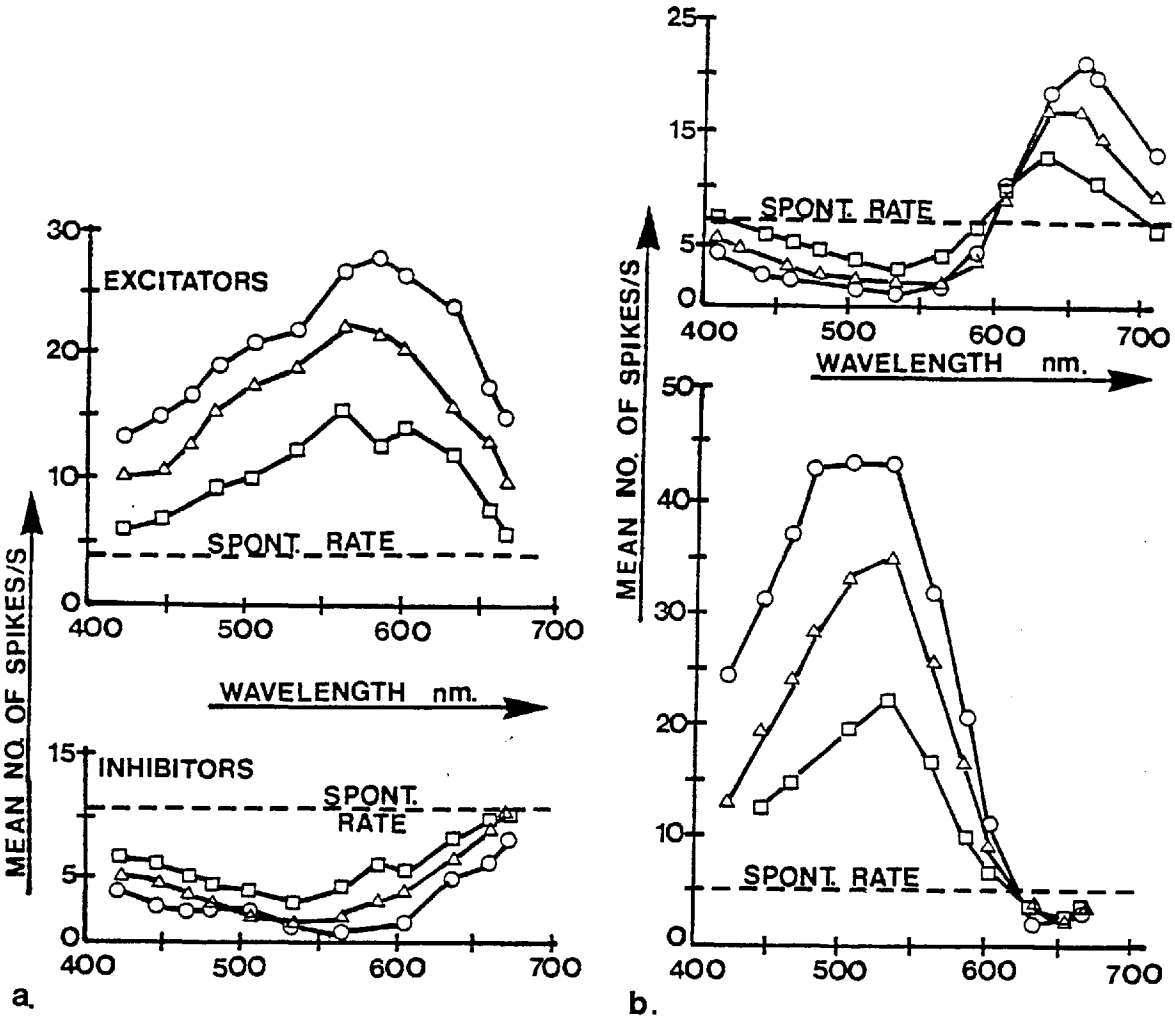

Fig. 3.43 Responses from L.G.N. in the monkey to varying wavelengths of light. These show evidence for a. non-opponent, b. opponent coding of colour information (after De Valois, Abramov and Jacobs, 1966).

from the green- and the red-sensitive cones, and others only from the blue- and the green-, or from the blue- and the red-sensitive cones, must undergo a central reorganization for the cortical processing of colour information.

Gouras (1974) classified the majority of the cells in layer IVB of the visual cortex as possessing opponent-colour properties, a classification based upon finding a particular wavelength which

separates the response polarity (excitation or inhibition) for a particular cell, and defines its 'neutral point'. Most cells in layer IVB exhibit neither orientation nor direction selectivity (Gouras, 1974) but layer IVB and layer IIIB receive a large input from the optic radiations (Hubel and Wiesel, 1972) and therefore colour-opponency plays a major role at the early stage of visual processing in the foveal striate cortex. Monkeys are found to possess more non-oriented receptive fields for cortical cells than the cat (Hubel and Wiesel, 1962 and 1965), which correlates with the reduced colour vision observed in cats compared with that in the monkey (Poggio, 1972; Dow and Gouras, 1973).

The difference between the receptive field organization of the opponent-colour cells in the L.G.N. and in the cortex may provide the additional neural processing which is required to produce the spatial specificity in colour vision. In the monkey, the opponent-colour cells in the L.G.N. receive direct excitation from one cone mechanism and inhibition from another (Hubel and Wiesel, 1968; De Valois and Pease, 1971 and Daw, 1973). These cells have spectral opponency without any spatial opponency at one end of the spectrum at least, and are therefore insensitive to colour contrast and have only poor spatial contrast. Many of the opponent-colour cells in the foveal striate cortex, however, have a centre, surround, antagonistic receptive field organization, both of which may receive inputs from the same cone mechanism. This has already been observed by Hubel and Wiesel (1968) who report a similar situation for several opponent-colour cells in the non-foveal striate cortex (10%).

The opponent-colour cells with non-directional specificity are

also particularly sensitive to simultaneous colour contrast effects, because an appropriate wavelength which excites the surround, disinhibits the centre's response. The psychophysical data presented in fig. 3.22 (section C of this chapter) are consistent with the findings of Gouras (1974). In his study, the cells with a weak surround antagonism have a lower spatial frequency sensitivity than those with a strong surround, and cells with different degrees of spectral antagonism result in response channels with different spectral bandwidths.

Michael (1978,a,b,c) studied electrophysiologically cells in the primate's striate cortex which were specifically sensitive to colour. The cells which he defines as concentric, namely ones where both the field centres and surrounds receive opposite types of input from the red- and the green-sensitive cones, have similar properties to those termed opponent-colour cells by Gouras (1974). Michael's concentric cells, as the Gouras opponent-colour cells, were also driven only by one eye, and their laminar distribution was restricted to layer IV and its sub-divisions. Further evidence (Michael, 1978a) suggests that the concentric cells receive direct input from the geniculate cells, and therefore they represent the first cortical stage in the integration of colour contrast information.

The experimental data of section C of this chapter in which colour-selective central responses have been obtained psychophysically with two-dimensional spot stimuli rather than one-dimensional linear square-wave gratings, is consistent with the neurophysiological evidence which shows that the cortical neurones which possess colour-selective properties, are those which have non-oriented receptive

field profiles. The cells which have oriented receptive field profiles are usually non-colour-selective in their response properties (Hubel and Wiesel, 1968; Gouras, 1974; Schiller et al., 1976).

In the pre-striate cortex of the monkey, Cragg (1969) and Zeki (1969, 1970, 1971a) have shown there are multiple anatomical areas, which suggest a division of labour within the area as a whole, and differential wiring to each area dictates the aspect of the visual stimulus which will be emphasized, generalized or de-emphasized. Zeki (1978) has systematically compared the receptive field properties of neurones in the pre-striate areas, and has shown that although ocular dominance shows very little or no variation, orientation specificity is much more common in the areas he defines as visual areas V2, V3 and V3A than in V4 (in the anterior bank of the lunate sulcus) and STS (a region in the medial part of the inferior bank of the superior temporal sulcus); opponent-colour coding also appears to be virtually absent from all but areas V4 and the lateral STS. A picture emerges, therefore, of a mosaic of areas, each with a different functional emphasis, and presumably the visual information analyzed in these areas will be further assembled at an even more central cortical area.

The post-receptoral spectral response functions, derived in section D.i, correlate very closely with the overall responses measured by Sperling and Harwerth (1971) (see section D.ii) and Regan (1974). Their spectral response channels combine data from behavioural and electrophysiological studies, and show that a linear subtractive interaction between the response of cones containing the photopigments with peak sensitivity at 575 nm and 535 nm accounted for the threshold sensitivity of the primate's eye. They account for the

peak sensitivity near 445 nm by the action of a single class of cones containing a photopigment with maximum sensitivity at 445 nm, and which has no interaction with any other class of cone.

D.vi. Psychophysical Evidence regarding Colour Selectivity in Central Mechanisms

Psychophysical evidence does exist which suggests colour selectivity is present in central mechanisms, notably the McCollough effect (McCollough, 1965), and several colour after-effects (i.e., Anstis et al., 1978). The McCollough effect has been used to indicate the presence of neural channels not only selective to colour, but also to other spatial variables (Harris and Gibson, 1968) and more recently different modulation transfer functions for the mechanisms which underly overall pattern appearance, and those which govern the establishment of the McCollough effect (White and Mandler, 1978).

The experimental data presented in this chapter have shown that with a suitable choice of stimulus parameters, binocular adaptation effects associated with the perception of spatially structured stimuli exhibit selected bandwidth spectral response functions. Only three independent spectral response mechanisms were observed, but it may be that other combinations of the stimulus parameters might reveal further post-receptoral spectral response mechanisms.

The method described in this chapter, may provide a useful technique for the analysis and classification of acquired colour vision defects which arise from abnormal post-receptoral responses and it may also, as demonstrated in section C, help to elucidate the origins of congenital red-green colour vision deficiencies (Nunn and Ruddock, 1978; Alpern, 1979).

CHAPTER IV

Visual Organization in a Subject with a Central Colour Vision Defect

A.i. Introduction

Congenital colour vision defects are caused by abnormal photopigment absorption (Rushton, 1963 and 1965) and are characterized by reduced wavelength discrimination and abnormal colour matching. Such defects do not, however, give rise to loss of other visual functions such as form perception, spatial resolution, stereoscopic depth perception and motion perception. In this chapter, data are presented for a subject with an unusual colour vision defect, which affects other visual responses.

The male subject, M.W., was 26 years of age during the period of the investigation. Ophthalmoscopic investigation reveals that M.W.'s fundus and ocular media are normal, and his visual acuity, measured with test charts, is 6/5. He has no medical history of any serious diseases or injuries, nor treatment with any unusual drugs. In preliminary tests with the Ishi-hara Colour Vision test plates (Edition 1976), he was unable to identify correctly any but the first, which is an orange figure twelve on a blue background. This is identified by all subjects except those with monochromatic colour vision. Nevertheless, M.W.'s performance with the remaining plates was still inconsistent with those of the standard forms of defective colour vision. Both maternal and paternal sides of the family have a history of defective colour vision. His father gives deutan responses to the Ishi-hara plates, whilst the male members of his mother's

family give responses which are classified by the Ishi-hara plates as red/green defective. He also has a sister whose responses to the Ishi-hara plates are classified as mildly red/green defective. His colour vision has been subject to previous extensive investigation (Bender and Ruddock, 1974), the main results of which are briefly reviewed.

Wavelength discrimination data for observer M.W. measured for a bipartite 80' x 80' visual field are given in fig. 4.1. There is virtually no discrimination for wavelengths below 500 nm, and the discrimination step is minimum, with a value of some 15 nm, at around 620 nm. The logarithm of the absolute threshold sensitivity for a 1° circular test field is shown as a function of stimulus wavelength in fig. 4.2 M.W.'s absolute threshold sensitivity is very low compared to that of a normal observer, especially for long wavelength stimuli. The most unusual feature to emerge from this study, however, is the form of the increment

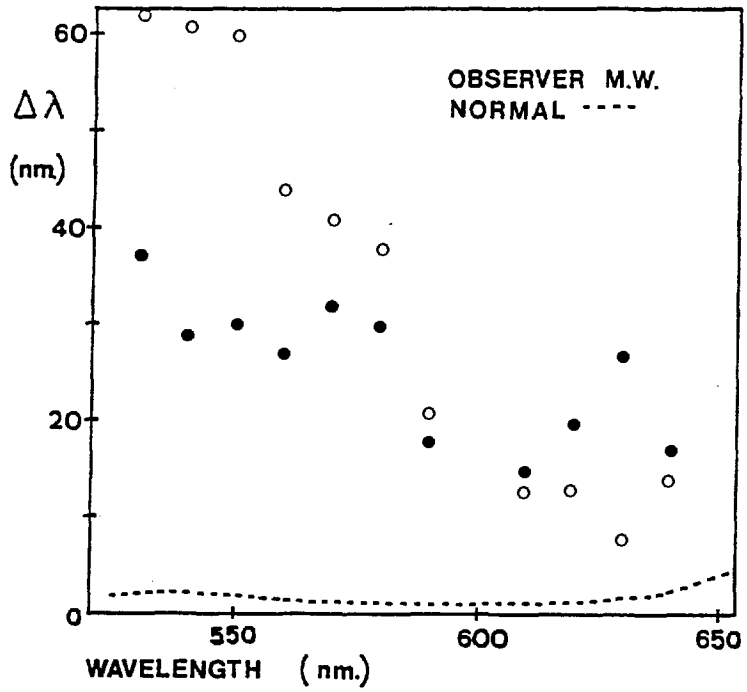

Fig. 4.1
The 'just noticeable' difference steps of wavelength discrimination for observer M.W., established between two halves of an 80' x 80' bipartite field in the Wright Colorimeter.
(after Bender and Ruddock, 1974)

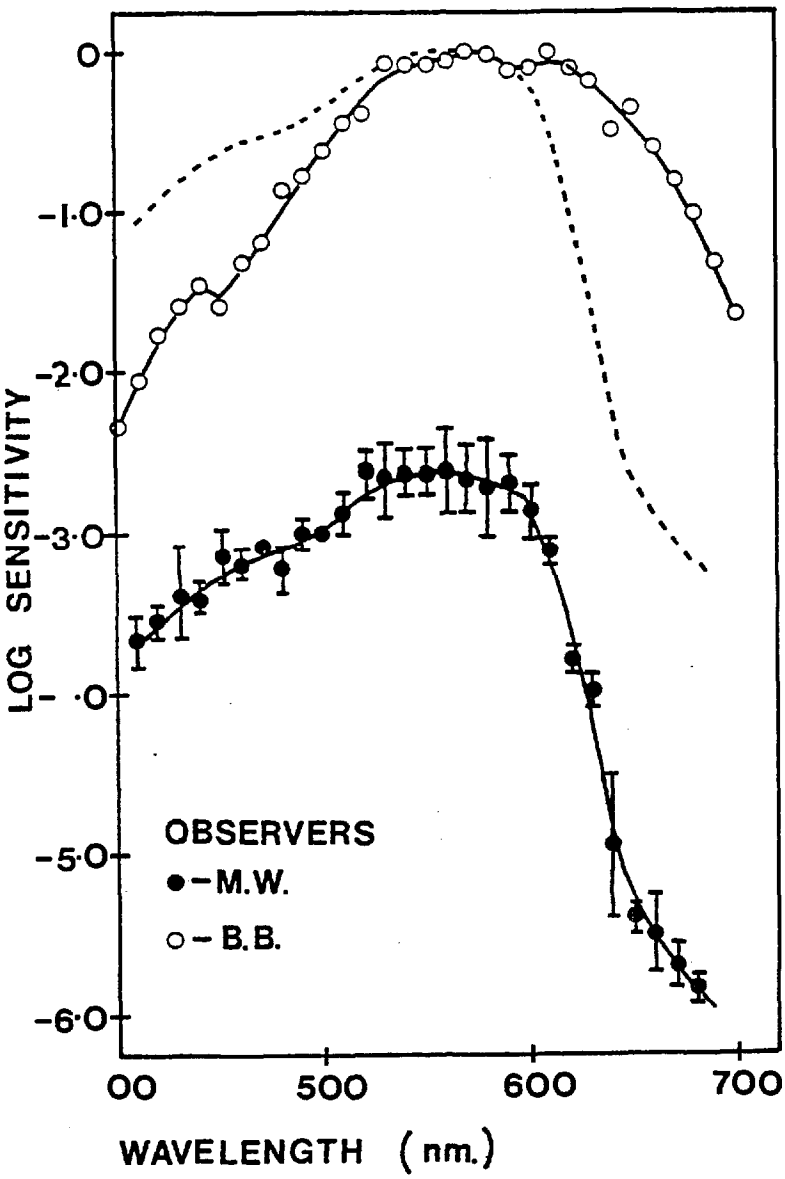

Fig. 4.2
Logarithm of the absolute threshold sensitivity plotted as a function of stimulus wavelength. The continuous lines are drawn by eye and the broken curve represents M.W.'s data shifted upwards along the sensitivity axis for comparison with those of the normal trichromat, B.B. (after Bender and Ruddock, 1974)

threshold sensitivity for long wavelength (red) stimuli. Figure 4.3 shows increment threshold values, I_t, for a 1° diameter test stimulus, superimposed on a background field of illumination level, I_μ, measured for M.W. and for two subjects with normal colour vision, B.B. and G.J.B. The stimulus wavelength, 650 nm, was the same for both the test and the background fields. The most significant feature of this data is the sudden fall in the threshold illumination level of the test stimulus, I_t, which occurs as the illumination level, I_μ, of the background field is increased beyond a

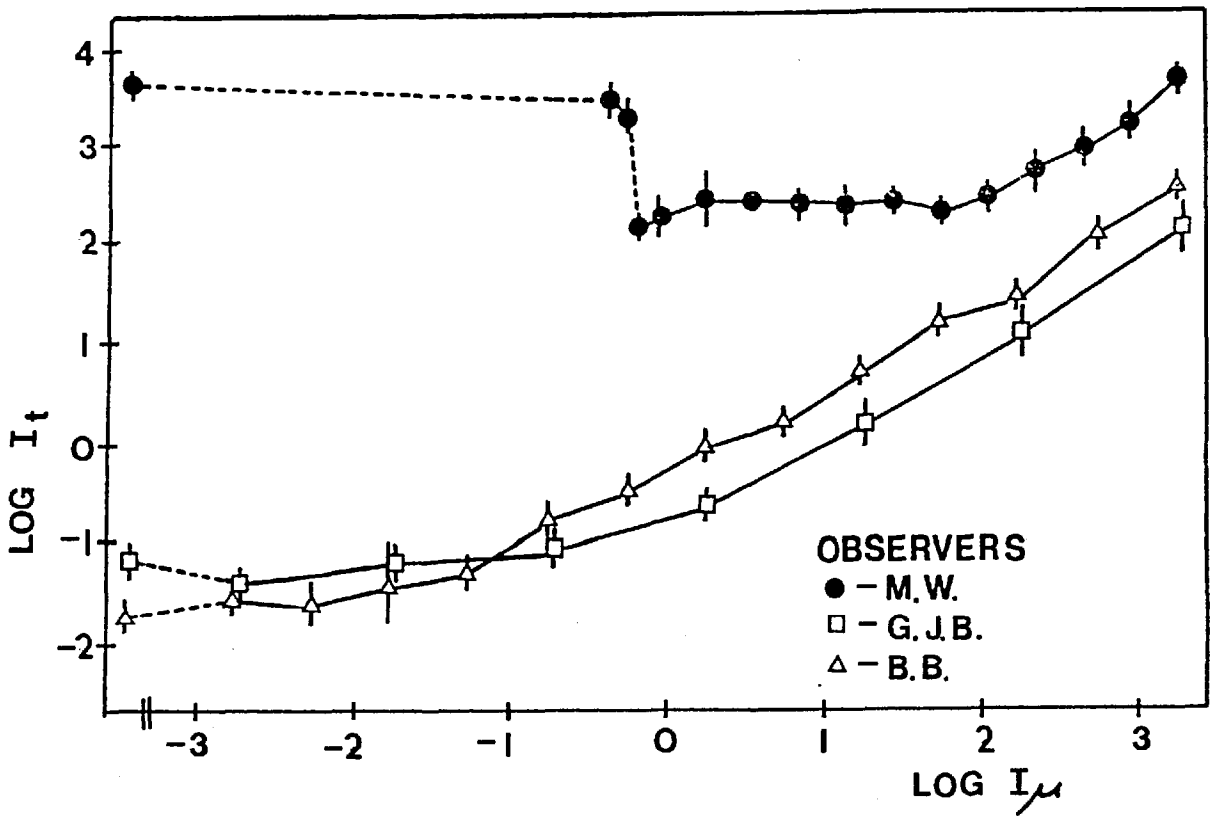

Fig. 4.3
Logarithm of threshold retinal illumination levels, log I_t, expressed in log trolands, plotted against the logarithm of the background field, log I_μ, in log trolands.
(after Bender and Ruddock, 1974)

critical value. This critical value of background illumination level coincides approximately with that at which the background field just becomes visible to M.W. In addition to M.W.'s low threshold sensitivity for zero background field, which is some 10^5 log units below that of the normal observers, the variation of I_t is restricted to a range of values in the upper part of the normal response range.

The principal feature of M.W.'s subjective response is his almost total failure to detect red objects. Light stimuli of wavelength $\lambda > 610$ nm are described by him as black when viewed in day-light, or 'silvery-grey' in the dark adapted state, and devoid of any well defined structure. In red light, he is able to resolve only gross spatial structures which subtend a visual angle of 1 to 2^o, and his

grating acuity, measured with 100% modulated, high illumination level sinusoidal interference fringes, derived from a 632.8 nm Spectra Physics helium-neon laser beam, was less than 0.5 c/^{o}, compared with 60c/^{o} for normal observers. Nevertheless, as stated previously, his white light acuity is normal, with 6/5 vision in either eye. Two-colour-increment threshold measurements (Stiles, 1959) provide evidence for the activity of two of the normal π mechanisms; one corresponding to the normal π_5 (red-sensitive) mechanism, and the other, an interaction mechanism with a long and short wavelength component from which the π_1 mechanism can be isolated with an auxilliary background field. Thus, although his responses to long wavelength stimuli are grossly abnormal, the long wavelength sensitive increment threshold mechanism appears to function. Further, a normal pupil reflex action was obtained for long wavelength stimuli using the apparatus shown schematically in fig. 4.4. Table 1 tabulates the values of the observer's pupil diameter for a range of wavelengths of light and under four intensity conditions. The pupil reflex behaves normally under all illumination conditions, even for the long (red) wavelength lights which he is unable to perceive.

The fact that M.W. exhibits a normal π_5 increment threshold mechanism implies that he possesses the red-sensitive cone mechanism. Further, the pupillary response to red lights implies that signals elicited by red lights are transmitted beyond the retina. In the present investigation, visual functions dependent on central processing have been studied. These are:-

a. The contrast threshold elevation effect for linear grating stimulus patterns (Gilinsky, 1968; Pantle and Sekuler, 1968;

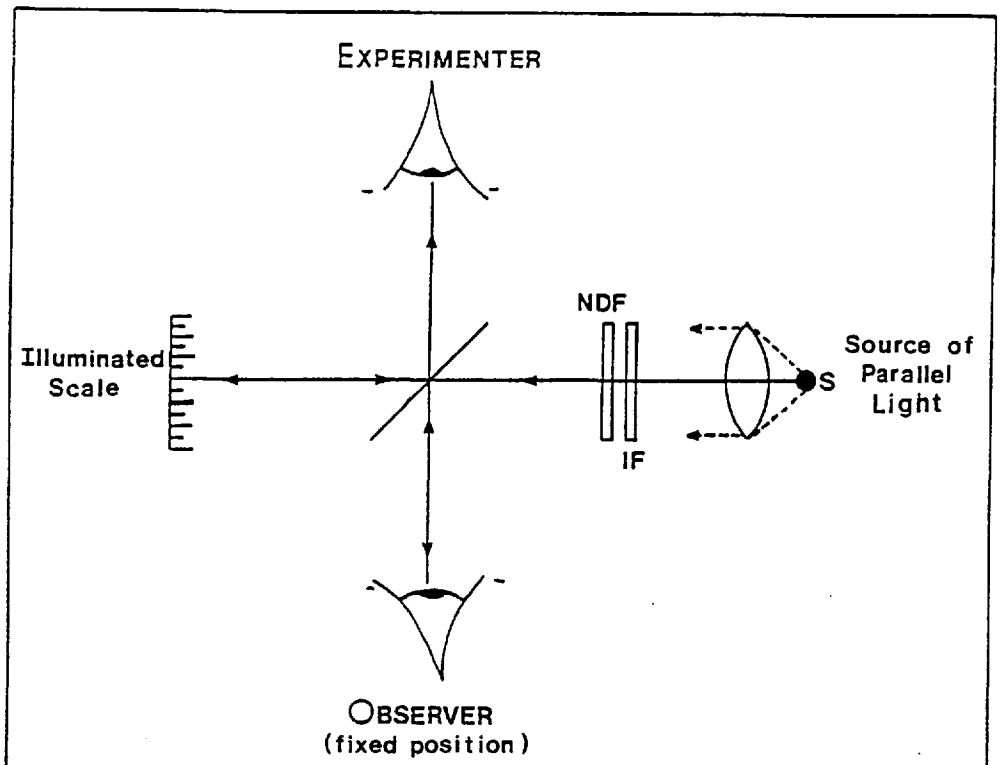

FIG.4.4 Schematic arrangement of apparatus for PUPIL SIZE Determination

Fig. 4.4

Table 1

WAVE-LENGTH nm.	LIGHT INTENSITY $I = I_{max}$			
	I	$I/2$	$I/6$	$I/10$
700	6			
656	4	5	6	6·5
636	4	5	5·5	6
623	4	5	5·5	6
611	4	5	5	6
582	4	4·5	5·5	6
570	3·5	4·5	4·5	5·5
551	4	5	5·5	5·5
530	4	5	5·5	5·5
495	4·5	5	6	6·5
471	4·5	5·5	6	6·5
453	4·5	5·5	6	6·5

PUPIL DIAMETER in mm.

Blakemore and Campbell, 1969b). This effect is interocularly transferred, and therefore, most probably arises in neuronal responses of the primary visual cortex (Maffei, Fiorentini and Bisti, 1973).

b. Stereoscopic image perception with two coloured, random dot stereograms, called analglyphs (Julesz, 1971). Stereoscopic fusion can only be accomplished by the convergence of neural signals from the two eyes. Cortical neurones have been identified which are capable of stereoscopic depth discrimination (Barlow, Blakemore and Pettigrew, 1967; Hubel and Wiesel, 1970).

c. Binocular rivalry between crossed linear gratings. Rivalry occurs only after the signals from the two eyes have converged, and there is evidence to suggest that this particular function is therefore mediated at a level in the visual system central to the mechanism responsible for the contrast threshold elevation effect (Blake and Fox, 1974; Ruddock and Wigley, 1976).

In the experiments with M.W., these three functions, all of which are associated with spatially structured stimuli, were measured with long wavelength ($\lambda > 610$ nm) stimuli, for which he has very low spatial resolution. This long wavelength stimulus was obtained by filtering a white light-source (colour temperature $\simeq 3 \times 10^3$ K) through narrow band interference filters (Balzer, Type B40) with a peak transmission at 630 nm and ± 5 nm half-bandwidth. Although it was not possible in all experiments to position the interference filter in a parallel light beam, measurements with a Beckmann DK2 recording spectrophotometer established that for a $\pm 7^{o}$ angle of incidence, equal to the maximum value employed in the experiments, the filter transmission spectrum was shifted by only some 5 nm to the shorter wavelengths.

In addition to these measurements, data are also given for some general visual functions, namely visual acuity and motion perception.

A combination of the signals elicited by the retinal image transmitted to the cortical centres from the eye, and the association of these transmitted signals with known objects is required for pattern recognition in human observers. The mechanisms responsible for the transmission of the signals have been studied both psychophysically and electrophysiologically, and are shown to exhibit responses which are highly specific for different stimulus attributes. The stage at which the 'association' takes place for pattern recognition has not been analysed, but the illusory appearance of certain stimulus parameters has been used to infer a mechanism involving the formation of central (cognitive) hypotheses concerning the structure of retinal images (Gregory, 1963, 1966 and 1970). A contrary view is that the visual illusions are the result of inherent distortions introduced during transmission of the signals along the visual pathways, and indeed some of the illusory effects can be explained by computation from the basis of known spatial filters which simulate visual response characteristics (Ginsburg, 1971, 1973 and 1975). Observer M.W. provides a valuable means of isolating the functions at the 'association' stage in visual pattern recognition. His responses can be used to test whether illusions have to be perceived in order to be detected (the perceptual hypothesis) by presenting to him the illusory patterns printed partly, or wholly, in red. Thus M.W. will not perceive some elements of the pattern, although they will be transmitted along his visual pathway as far as the level at which his defect occurs. If the illusory effects arise

before the site of the defect, they may be detected by him, but if they require perception of the whole image, they will not be detected.

A.ii. Experimental Apparatus

The Maxwellian viewing system, described in Section A, Chapter II, was used to determine visual acuity and for measurement of the contrast threshold elevation effect.

A.iii. Subjects

The subjects involved in this investigation were the observer M.W. and two observers with normal colour vision and stereoscopy, V.W. (female, aged 23 years) and K.H.R. (male, aged 38 years).

B. Measurements

B.i. Visual Acuity

Visual acuity was measured in terms of the resolution of linear gratings, consisting of alternate dark and coloured bars, with a light:dark ratio of one (see fig. 4.5). The gratings were produced as

FIG 4.5

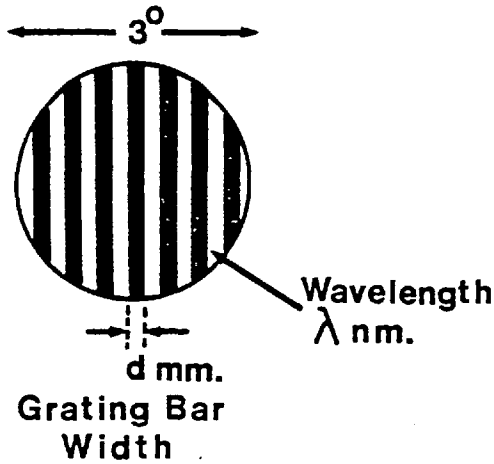

Schematic Representation of Linear Gratings

described in section A.vi, Chapter II, and were viewed by the subject through an artificial, 2 mm diameter, pupil in the Maxwellian viewing system. An arrangement designed for automatic random stimulus selection (Barbur, 1979) was used to present the linear gratings to the observer in beam 4 of the optical system (see fig. 2.3, Chapter II). The observer's head position was maintained by the use of a dental bite bar, and normal accommodation throughout stimulus presentation was obtained by means of a 0.2^{o}, 530 nm fixation spot derived from beam 3 (see fig. 2.3). Beams 1 and 2 were prevented from entering the eyepieces by means of suitably placed stops. The illumination level of the grating was controlled by a neutral density wedge, and their spectral composition by narrow band interference filters (Balzer, type B40, $\pm$ 5 nm half-bandwidth). The retinal illumination level at which a grating of given bar width and wavelength could 'just-no-longer' be resolved by the observer was measured, and thus, the grating visual acuity was determined as a function of illumination level and wavelength.

B.ii. Motion Perception

Motion perception was investigated using apparatus specifically designed for such experiments (Barbur, 1980) and the observer's responses to target movement measured by recording the threshold illumination level required for detection of a 3.5^{o} diameter, circular target, moving at constant velocity along the horizontal meridian. The target moves through 10^{o} of visual angle positioned centrally within a 17.5^{o} diameter, 2^{o} wide, white light annulus (see insert, fig. 4.8). The observer maintained correct accommodation by focusing

this annulus, which also provided a guide to the position at which the moving target would appear. Both the annulus and the circular target were produced photographically, and viewed through the 3.5mm diameter pupil of a Maxwellian optical system, which comprised the motion detection equipment. Threshold illumination levels were obtained for the detection of the moving target for several target velocities and for monochromatic stimuli, one red (630 nm), and the other green (540 nm). In the latter case, the target was seen against a 540 nm, 18^{o} diameter, circular background field, located centrally with respect to the annulus.

B.iii. The Contrast Threshold Elevation Effect

The contrast threshold elevation effect was measured for linear square-waveform grating patterns, produced as decribed in section A.vi, Chapter II. Suitable adaptation and test grating stimuli were placed in beams 1 and 3, respectively, of the Maxwellian viewing system of fig. 2.3 (section A, Chapter II) and presented dichoptically to the subject. A high contrast adaptation grating (beam 1, fig. 2.3), which was either red (630 nm) or blue (436 nm), was presented to the left eye and the test grating (436 nm), superimposed on a uniform 436 nm background field of illumination level equal to the average level of the adaptation grating, was presented to the right eye.

The experimental procedure was outlined in section A, Chapter II, and also section A, Chapter V. The adaptation effect produced by the high contrast grating is defined by equation 2.19 (Chapter II). The magnitude of the adaptation effect, Δ, represents the logarithmic change in threshold levels between uniform and grating adaptation.

The 436 nm square-wave test grating was of fundamental spatial frequency, f_t, equal to 5.6c/^{o}, and a series of adaptation gratings of fundamental spatial frequency, f_a, and in a wavelength of 630 nm or 436 nm were presented to the left eye.

B.iv. Stereoscopic Vision

Two colour random dot stereograms, called analglyphs (Julesz, 1971), were used to test M.W.'s stereoscopic function. The analglyphs were printed in red and green inks, and in this investigation were viewed with a stereo viewer which had interference filters (Balzer, Type B40) incorporated into the eye pieces, with a red (630 nm) filter in front of one eye, and a green (530 nm) before the other. The measurements were performed under two illumination conditions; one of artificial fluorescent lighting, and the other, Northern Daylight (approx. colour temperature 6.5×10^{3} k). Observations were made by M.W., and by the two normal subjects. A number of different analglyphs were presented in random order to each observer, and intermingled with these were examples from the series which contain different degrees of correlation between the red and the green patterns (Julesz, 1971, fig. 8.12, A to G). Observer M.W. has had no scientific training, and therefore, had not previously seen the analglyphs, but as a further precaution, the text describing the appearance of the stereo images was obscured from view.

B.v. Binocular Rivalry

Binocular rivalry was investigated with crossed vertical and horizontal, high contrast square-wave gratings, presented one to either eye, in a stereo viewer system. The high contrast gratings,

produced photographically on square cards, were of fundamental spatial frequency, $3c/^{o}$, and the side of each card subtended 10^{o} at the observer's eye. The observer was asked to indicate changes, over a five minute period, in the dominant appearance from vertical to horizontal bars, or vice versa, by pressing a buzzer.

B.vi. Pattern Recognition

A series of illusory patterns were printed either in red or in red and black on white card. The reflection spectrum of the red ink (measured with a Beckmann DK2 recording spectrophotometer) was effectively restricted to wavelengths greater than 620 nm, so that it fell well within the abnormal response range of M.W.

Each series of patterns consisted of approximately forty copies of each, together with the related 'null' patterns (fig. 4.6). The elements of these patterns which were printed in red are denoted 'r' in fig. 4.6, except for the patterns B.i, which were printed entirely in red. The first series shown in fig. 4.6 A.i.a. consists of the Kanizsa triangle illusion (Kanizsa, 1955), which appears as a bright triangle whose apices are formed by the missing segments of the circles. The 'created' object has sharp contours, which bound a large region of enhanced brightness. Figure 4.6 A.i.b,c, shows other patterns which were used in the test, and the 'null' patterns were similar to fig. 4.6 A.i.a,b,c, but the left hand side of the triangle was lost. Figure 4.6 B.i.a shows Ehrenstein's effect which is perceived as a bright area in the centre of the radially distributed lines. In fig. 4.6 B.i.b,c,d, the presence of the additional contours, or misaligned components, eliminates the effect, at least, in part. The Poggendorf illusion is shown in fig. 4.6 c, for which

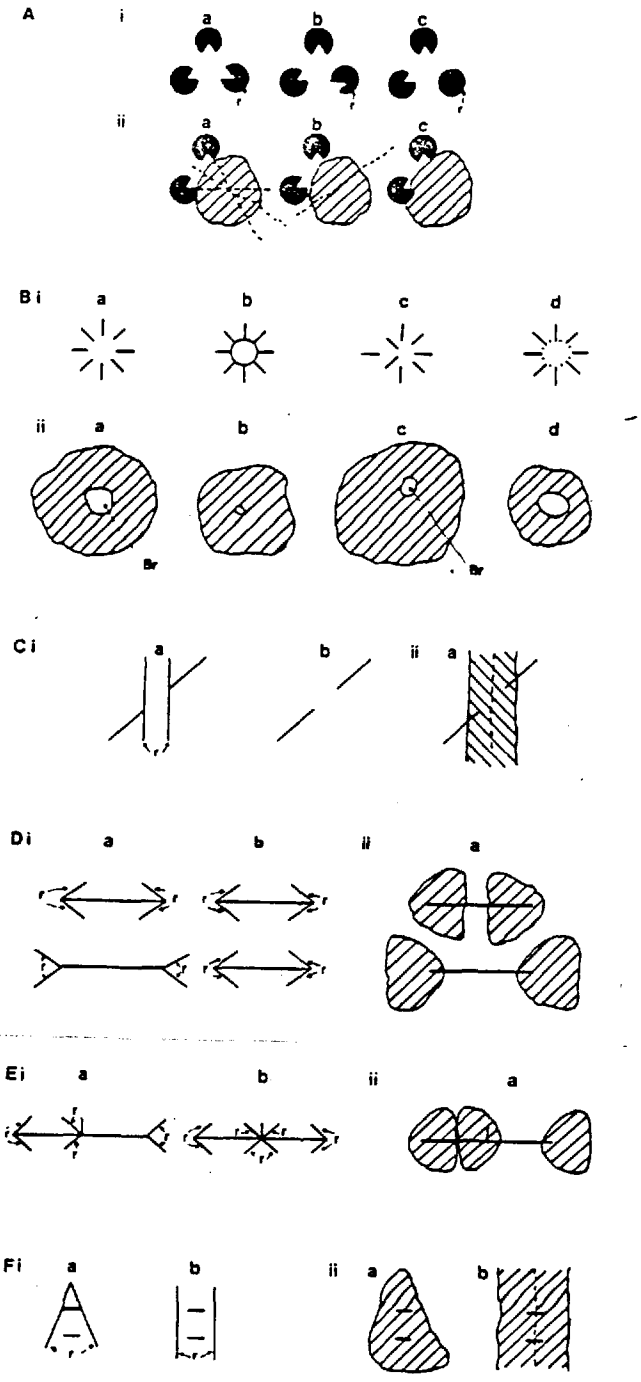

Fig. 4.6
To illustrate the illusory patterns used for pattern recognition.

normal subjects report that the two diagonal lines appear displaced parallel to each other, when in fact they are parts of the same straight line. The 'null' pattern of fig. 4.6 C.i.b shows that the effect is attributable to the presence of the parallel vertical lines. A number of representations and forms of the well known Müller-Lyer illusion are shown in fig. 4.6 D.i and E.i. Normal observers report a length difference between the two horizontal lines, which are physically equal in length, and a displacement of the short central vertical line to the left in fig. 4.6 E.i.a. These effects are lost in the 'null' patterns (see fig. 4.6 D.i.b and E.i.b). Similarly in the last series, the Ponzo illusion shown in fig. 4.6 F.i.a., normal observers report that the upper of the two horizontal lines appears longer, although

physically they are the same length. This effect is lost in the 'null' printing (see fig. 4.6 F.i.b).

The visual illusions presented in the red and black format were readily identified by normal observers, and M.W. was able to identify the illusions correctly when they were shown to him printed in black and white. Forty copies of each pattern relating to a single defect were presented in random sequence and orientation to M.W. At the end of each test series, M.W. was asked to draw his perceived image for each of the printed illusions.

C. Results

C.i. Visual Acuity

Grating visual acuity, expressed as d^{-1}, where d is the bar width in minutes of arc of the linear square-wave test gratings, is plotted against the logarithm of the mean grating illumination level (relative absolute units) in fig. 4.7. Data are given for observer V.W. by open (O-540 nm) and full (●-610 nm) circles; all of the other data points refer to observer M.W.

The data in fig. 4.7 show that M.W. suffers a marked loss of visual acuity for stimulus wavelengths, $\lambda \geq 580$ nm, and for $\lambda \geq 600$ nm, he is able to resolve only the coarsest gratings, with a bar width of about 1^{o} of visual angle. It seems, therefore, that the wavelengths for which M.W. has markedly subnormal visual acuity are those for which he also has low detection sensitivity, and those which appear 'silvery-grey' to him. In other regions of the spectrum, $470 \text{ nm} \geq \lambda \leq 540$ nm, his results are much more comparable to those of the normal observer V.W., and they also establish that M.W.'s visual system is capable of high spatial resolution.

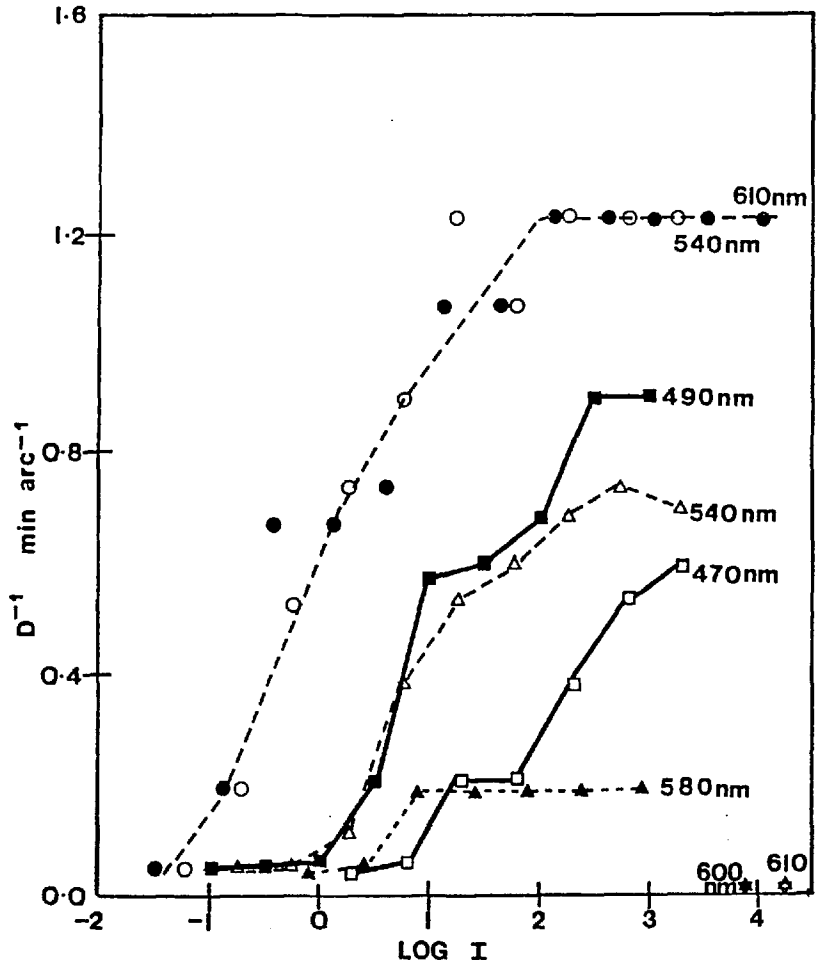

Fig. 4.7 D^{-1}

Grating visual acuity, expressed as d^{-1}, where d is the bar width in minutes of arc of the linear square-wave test gratings, plotted against the logarithm of the mean grating illumination level (in relative absolute units). The modulation depth of the test grating images is $>95\%$, and the wavelength for each set of data is denoted in nm.

C.ii. Motion Perception

Threshold illumination levels for the detection of a 3.5^{o} diameter, circular target moving at constant velocity, V $s^{o\,-1}$, across a uniform background field are plotted in fig. 4.8. Data are presented in fig. 4.8 for the two observers, M.W. and V.W.; the squares refer to a green (540 nm) target moving against a 540 nm, 18^{o} diameter, circular background field of mean illumination level 1.3 log troland

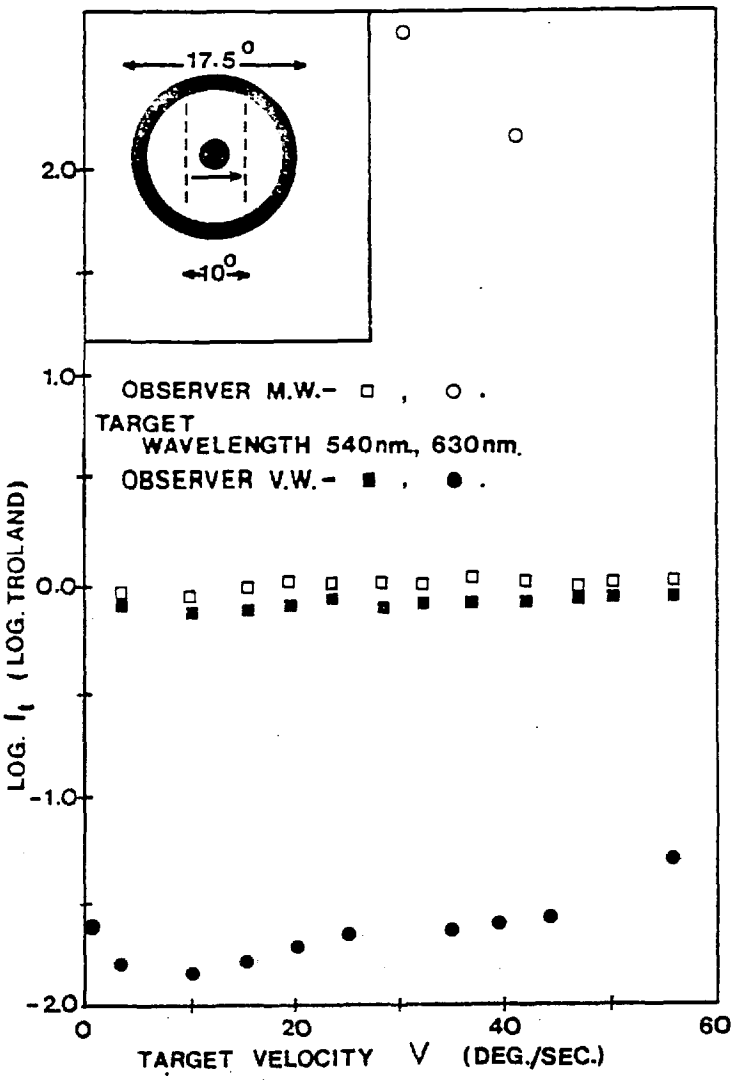

Fig. 4.8
Log threshold illumination level, log I_t (log trolands), for detection of a 3.5° circular target moving with a velocity, $V^{o}s^{-1}$, along the horizontal meridian.

(□-M.W., ■-V.W.), whereas the circles refer to a 630 nm target moving against a dark background field (○-M.W., ●-V.W.).The data are given for a number of target velocities, and all data points are the mean of four observations with a typical standard error of 0.04 log trolands.

The experimental data of fig. 4.8 shows that M.W.'s threshold sensitivity for the 540 nm target is similar to that of the normal subject V.W. over the full range of velocity. However, for the 630 nm target, his detection is limited to the high illumination levels, and the higher range of velocities. Thus, as in the case of visual acuity, M.W.'s sensitivity to motion is markedly wavelength selective, being near normal for green, but highly abnormal for red targets. This result confirms the gross abnormality which exists in M.W.'s visual system for stimulus wavelengths, λ , $\geq$ 610 nm.

C.iii. The Contrast Threshold Elevation Effect

The value of Δ (equation 2.19, Chapter II) obtained for a 436 nm square-waveform test grating presented to the right eye and square-waveform adaptation gratings presented to the left eye, are shown in fig. 4.9 and in fig. 4.10. The fundamental spatial frequency of the test grating was 5.6c/^{o}, and that of the adaptation grating was f_a c/^{o}, the experimental variable. Data are given in fig. 4.9 and in fig. 4.10 for observers V.W. and M.W., respectively, and each data point is the mean of four observations with the error bars denoting the standard error. In each figure, the magnitude of the adaptation effect, in log units, is plotted along the ordinate as a function of the adaptation spatial frequency, f_a, in cycles per degree. In fig. 4.9, the full squares represent the data obtained for observer V.W.,

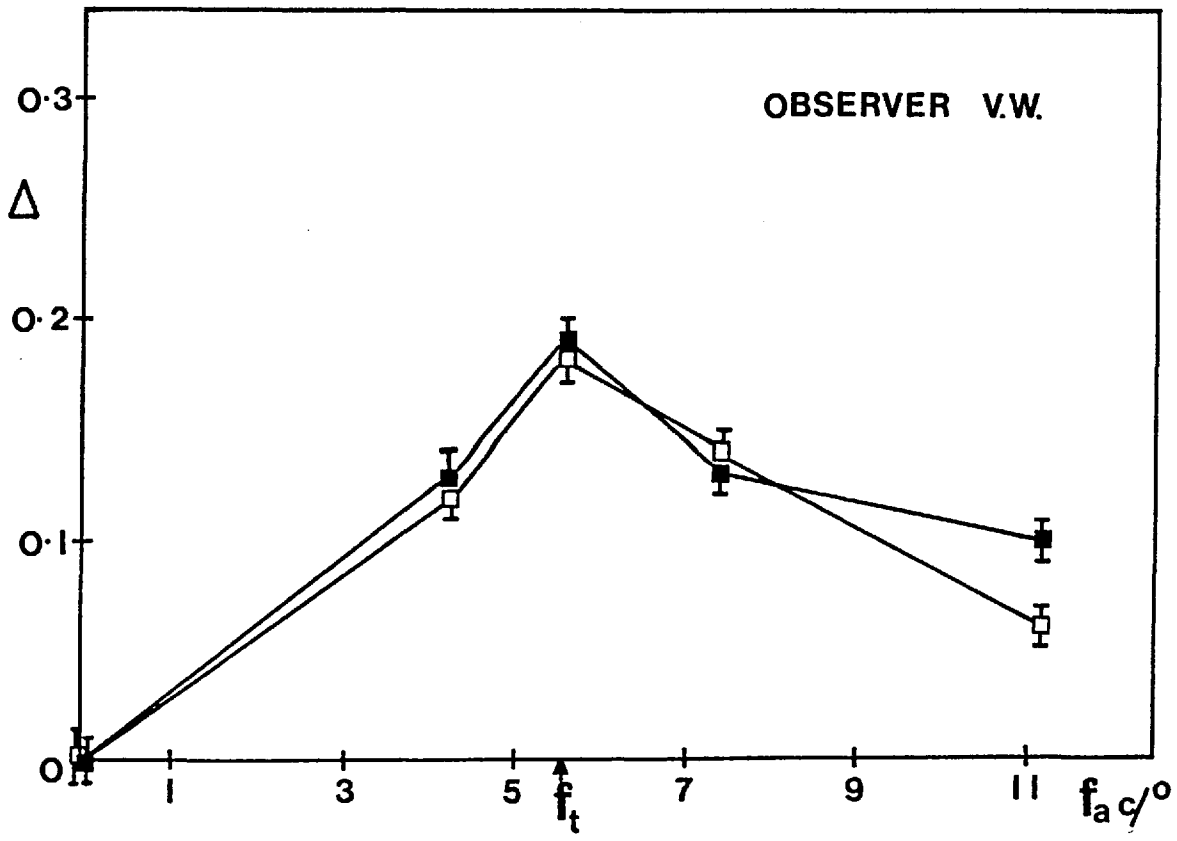

Fig. 4.9 Contrast threshold elevation, Δ, measured for a blue (436 ± 15 nm) test grating and both red (630 ± 5 nm) and blue (436 ± 15 nm) adaptation grating for observer V.W.

when the adaptation grating is presented in red light (630 nm), and the open squares, when it is presented in blue (436 nm). This data shows that the amplitude of the effect, Δ, is a maximum for $f_a = f_t$ (i.e., 5.6c/^{o}); it falls to an insignificant value when $f_a = f_{t/2}$ or $f_a = 2f_t$, and is similar for both adaptation wavelengths. Thus, it is consistent with that reported previously by Blakemore and Campbell (1969b) and Maudarbocus and Ruddock (1973a).

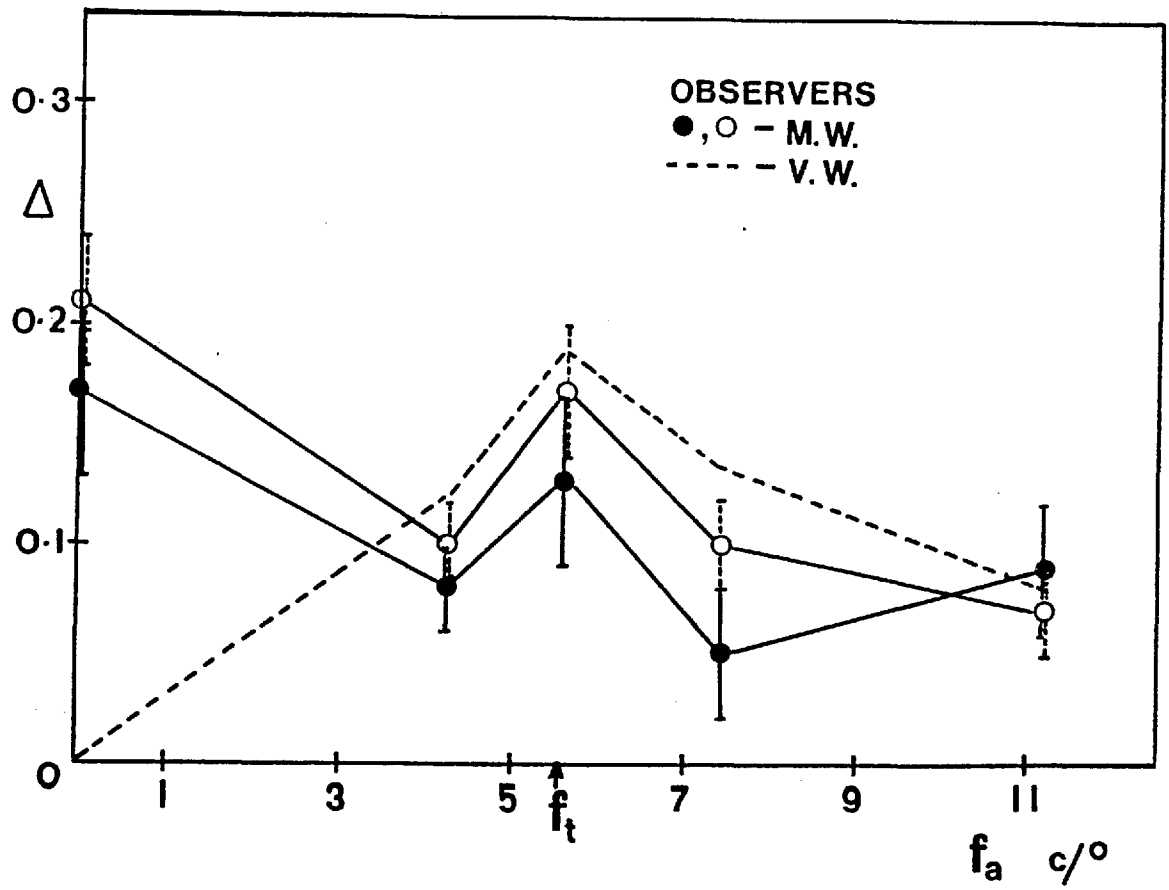

Fig. 4.10 Contrast threshold elevation, Δ, measured for a blue (436 ± 15 nm) test grating and both red (630 ± 5 nm) and blue (436 ± 15 nm) adaptation gratings, for observer M.W. Also shown superimposed (broken line) are the mean data for observer V.W.

The data for observer M.W., obtained under similar experimental conditions to those of fig. 4.9, are shown in fig. 4.10, where the

full circles refer to the red (630 nm), and the open circles to the blue (436 nm) adaptation grating. The broken line in this figure represents the mean data of observer V.W. superimposed from fig. 4.9.

The experimental results plotted in fig. 4.10 display similar characteristics for both adaptation wavelengths, but are significantly different from those of the normal observer V.W., in fig. 4.9, following adaptation to a uniform (f_a = 0c/^{o}) field, which has the same mean illumination level as the high contrast adaptation grating. Subjectively, M.W. is unable to resolve any of the red adaptation gratings; he perceives all of them as a uniform 'silvery-grey' area. The results establish, however, that these unresolved structures are capable of inducing the same contrast threshold elevation effect as the blue adaptation gratings which he could resolve. The point corresponding to f_a = 0c/^{o} was repeated some fourteen times with each adaptation wavelength, in order to confirm the high Δ values obtained by M.W. Despite the intrinsic difficulties involved in making such threshold measurements, the data seem to establish that M.W.'s data deviate significantly from the normal response pattern for this adaptation condition.

C.iv. Stereoscopic Vision

The responses of each observer to the analglyphs (Julesz, 1971) were similar for both of the illumination conditions. Observer M.W.'s visual acuity through the 630 nm filter in the stereo viewer was such that he could identify the edge region of the high contrast, bar shape patterns, whose width exceeded 2^o of visual angle, and could detect some variation in contrast for bars of width greater than 1^o of

visual angle (see fig. 4.7, section C.i). He could detect no spatial structure in the analglyphs when viewing through the red interference filter alone, but the elements of the analglyphs, the width of which subtend approximately 12' at the observer's eye, were resolved successfully through the green (530 nm) filter. Nevertheless, observer M.W. was able to identify correctly, in both stereo-perspectives, the analglyphs containing graded correlations at 100% and 90%, and could partially identify that at 80%. Observer K.H.R. gave very similar results, and observer V.W. could identify completely the pattern with 80% correlation, and identified in part that at 70%. In general, therefore, M.W.'s ability to identify the different analglyphs is similar to that of the reference observers with normal vision.

In an attempt to simulate M.W.'s responses, the observers with normal vision placed either neutral density filters or a diffuser before the red filter, in order to reduce their visual acuity. Under neither condition, however, could they correctly identify the analglyphs when their grating visual acuity fell below $5c/^{o}$, compared with M.W.'s maximum acuity of $0.5c/^{o}$. This implies that M.W.'s stereo acuity is not impaired by the functional abnormality which causes the loss of acuity associated with red patterns.

C.v. Binocular Rivalry

Under daylight illumination, observer M.W. reported that he was readily able to resolve the gratings used to produce binocular rivalry. His responses, over a five minute period, indicated that he detected the horizontal bars for 31% and the vertical bars for the remaining 69% of the presentation period. When the horizontal grating

was viewed through the red (630 nm) interference filter, and the vertical grating through the green (530 nm) interference filter, he detected the vertical grating for 68% of the presentation time, but for the remaining 32% of the time, reports that it was suppressed, and that no clear structure was visible. In both of these measurements, the vertical grating was seen for periods of some 8s duration, and suppressed for periods of 3.5s. With the horizontal grating viewed through the green filter, and the vertical grating through the red filter, M.W. reported detection of the horizontal grating for 58% of the presentation period, with no clear resolvable structure present during the other 42% of the time. (This corresponded to average detection periods of some 11s and 8s, respectively.)

The results of the final test, when the horizontal grating was replaced by a uniform white card, showed that M.W. experiences no binocular suppression when viewing the field configuration of a vertical grating and white card presented in the stereo viewer in day-light nor through the green and red filters, respectively. This final observation establishes, therefore, that binocular rivalry depends upon the presentation of crossed grating structures to the two eyes. Thus, although M.W. was unable to perceive the 3c/^{o} grating, when viewing through the red filter alone, it still produced the effects of rivalry when the green grating was seen by the other eye.

C.vi. Pattern Recognition

This next section describes the results obtained from the series of illusory patterns, designed to investigate the activity of cognitive mechanisms in visual pattern recognition. Figure 4.6.Ai-Fi,

section B.vi of this chapter, shows the illusory and 'null' patterns used in this investigation, and A.ii to F.ii are examples of the drawings made by M.W. to illustrate the appearance of the patterns. The percentage of presentations on which each respective illusion was correctly identified by M.W. are summarized in Table 2.

TABLE 2

FIGURE 4.6	PERCENTAGE of CORRECT RESPONSES a.	b.	c.	d.
A.i.	100	0	0	
B.i.	100	5	100	10
C.i.	100	0		
D.i.	5	0		
E.i.	20	0		
F.i.	0	0		

The results in Table 2 show that on 100% of the occasions of the presentation of the Kanizsa triangle series, M.W. was able to identify correctly fig. 4.6 A.i.a, and as indicated by his drawing in fig. 4.6 A.ii.a, the bright lines depict a triangular structure for this form. However, he does not detect the triangular region in the other patterns.

In the series representing Ehrenstein's effect, M.W. was asked to locate any region on the test card which he perceived as significantly brighter than the general white background. M.W. was able to identify correctly the bright area in fig. 4.6 B.i.a and c. However, the subject was not misled by the brightness contrast between the centre and the surround, as he failed to report a central region brighter than the surround, under the conditions which are known to destroy the

illusion, shown in fig. 4.6 B.i.d,e, for normal observers.

When asked to report the relative disposition of the two diagonal lines, in the Poggendorf illusion (fig. 4.6 C.i.a), M.W.'s responses were as expected from normal subjects on 100% of the presentations, whereas, he did not see the illusion for the 'null' patterns.

In contrast, M.W. could identify correctly neither the Müller-Lyer illusion (fig. 4.6 D,E), nor the Ponzo illusion (fig. 4.6 F). The effect of the contrast of the red ink was varied in the last series, by increasing its saturation. It was found that not until the saturation was so great that the lines appeared almost black to normal observers, was M.W. able to correctly identify any of the illusions.

These results indicate that the illusions fall into two groups; those which merely involve a distortion in brightness or shape can be identified although all the pattern's elements are not perceived, whereas those which involve a change of metric cannot be identified unless all the components are resolved.

D. Discussion

The results of these separate investigations will now be considered as a whole. Essentially they indicate that despite M.W.'s inability to resolve spatial patterns, presented in long (red) wavelength light, signals elicited by them contribute to pattern dependent responses. It is necessary, however, to consider whether or not M.W.'s inability to 'see' red coloured patterns is truly an attribute of his visual sensory system, or whether it is due to some psychological block in perception. In view of his very unusual dichromatic colour matching characteristics, and his increment

threshold responses, (see fig. 4.1 and fig. 4.3, in the Introduction to this chapter), it seems logical to associate the abnormal responses with a malfunction of the primary visual pathways. Both of these response functions have remained stable over a period of at least eight years, and there is no simple way in which an observer can manufacture consistent responses of this kind.

M.W.'s visual response characteristics do not apparently correspond to any recorded previously, but they may belong to a class of defects referred to as 'colour aphasias' (Duke-Elder, 1949). The defect is, nevertheless, non-progressive, and M.W. has been aware of his colour vision deficiency from an early age. At the age of four or five years, he reports suffering burns from a failure to detect the red glow of heated objects. He has also incurred many educational and employment difficulties as a result of the deficiency.

The investigations, described in this chapter, show that observer M.W. possesses a visual defect which severely impairs his detection of red-coloured spatial patterns, but does not interfere with his stereoscopic fusion, nor binocular rivalry elicited with long (red) wavelength stimuli, (sections C.iv,v). It should be noted that Lu and Fender (1962) found that Julesz analglyphs could not be fused to give stereoscopic images if they gave only chromatic contrast, suggesting that colour mechanisms do not contribute to this response. The fact that M.W., a subject with a colour vision defect, is able to perceive the stereoscopic image is consistent with this conclusion. The contrast threshold elevation effect can also be induced for red patterns which he cannot perceive (fig. 4.10, section C.iii), but these results do exhibit some abnormality in their dependence upon the

spatial frequency of the adaptation grating.

M.W.'s visual acuity is markedly wavelength selective. He exhibits near normal acuity for a certain spectral range, 480 nm $\geq \lambda \leq$ 580 nm, but has very poor acuity for long wavelength stimuli, especially $\lambda \geq$ 600 nm (see fig. 4.7). This is reflected in his response to motion (fig. 4.8), in which his sensitivity to a green (540 nm) target is normal, whereas that to a red (630 nm) target is grossly abnormal.

The visual defect of this subject, therefore, is restricted to certain functions which involve the detection of red light stimuli. This implies that either the neural pathways which process stereoscopic function and binocular rivalry are organized in parallel with the defective pathways, or the defect arises at a stage of processing central to the mechanisms responsible for these normal responses. If the absorption in M.W.'s red-sensitive cones were abnormal, it would account for his general malfunction in response to all long wavelength stimuli. The fact that he displays the Π_5, (red-sensitive) increment threshold mechanism implies, however, that the red-sensitive cones function normally. Another possibility is that the defect arises at a post-receptoral level, and affects pathways other than those which project to the visual centres dealing with stereoscopy, which is normal even for red light. Although electrophysiological studies indicate that groups of ganglion cells are specialized for form or motion perception (Enroth-Cugell and Robson, 1966; Hubel and Wiesel, 1970), there does not appear to be any special group associated with disparity sensitive cortical neurones. Thus, it cannot be argued that the retinal projection which elicits

global stereoscopic vision is separate from the other projections.

The experimental data presented in sections C.i-vi of this chapter provide evidence of colour selective functional losses in M.W.'s vision. The human visual system signals information about a variety of stimulus parameters, and the results of recent neurophysiological investigations suggest that the visual cortex may be organized in such a way that different attributes of the visual image are processed in different areas of the cortex. In other words, there is evidence for multiple projection maps of the visual field, each map having a specific associated response, i.e., colour discrimination, stereoscopic function and increment detection (Hubel and Wiesel, 1970; Zeki, 1973, 1978a,b,c, and Cowey, 1979). Neurones, which respond selectively to a given stimulus parameter localized in each map, tend to be sensitive only to changes in the parameter encoded by that map. Such multiple representation of the field with associated division of function requires extensive interconnections between the different visual areas. Gilbert and Kelly (1975) have described highly organized nerve fibre projections which exist between the different visual areas, and which could account for such interconnections.

The anatomical and electrophysiological data have been interpreted as evidence that different stimulus parameters are processed separately by the central visual pathways. M.W.'s data shows, however, that a defect involving only long wavelength (red) light, i.e., a colour vision defect, selectively influences spatial acuity and detection of movement (see fig. 4.7 and fig. 4.8, section C.i and ii, respectively). It has already been argued that

the effect arises after the site of binocular fusion, so that it must be cortical in origin. M.W.'s responses imply that central processing of colour, form and motion are interdependent, because malfunction in one affects the other two. This does not provide support for the view that these parameters are processed independently, although the interactions may occur at a point beyond the level of separate processing, for example, in the synthesis of the final perceived image.

The study of visual illusions with observer M.W., described in section C.vi of this chapter, could provide an insight into the significance of visual illusions. As described in the Introduction to this chapter, there are two hypotheses regarding visual illusions. One proposal is that the identification of a particular pattern is derived on the basis of the available visual information, which can lead to a misinterpretation of the image and produces 'false' images, termed visual illusions. This constitutes the cognitive hypothesis (Andrews, 1964; Gregory, 1963, 1966 and 1970 and Hoptopf, 1966). On the other hand, there is the view that visual illusions are caused by distortions introduced during signal transmission along the visual pathways (e.g., Ginsburg, 1973). The experimental data of section C.vi, obtained from the presentation of illusory patterns, printed in red or in red and black on a white background, to the observer, M.W., has produced some new evidence which can be related to these two hypotheses. M.W. is unable to perceive the red components of the patterns, but he could nevertheless describe and identify correctly some of the visual illusions. In contrast, some illusions were not detected unless all of the components of the pattern were perceived.

Thus, he perceives those illusions, i.e., Group A - the Kanizsa triangle, Ehrenstein's effect and the Poggendorf illusion, which involve the distortion of apparent brightness or shape, even though all the components of the patterns are not perceived, whereas those illusions which include a change of metric, i.e., Group B - the Müller-Lyer and the Ponzo illusion, he cannot detect unless all the components of the pattern are perceived. These results imply that the illusions in Group A are the result of distortions occurring in the visual system, prior to the stage of the abnormal functional response in M.W.'s visual pathways, whereas those in Group B may be produced as a result of signal distortion which occurs in the transmission mechanisms, at a site more central than the defect of the observer allows, or may indeed be due to some cognitive activity in the visual system.

CHAPTER V

Colour and Spatial Pattern Discrimination in an Albino

A. Introduction

In this chapter, abnormal visual function which occurs as a result of albinism is examined. Albinism is an anomaly created by an 'inborn error of metabolism'. It provides a good example of an inherited trait which is dependent on a rare recessive gene. This is an abnormal X-linked allele with an autosomal recessive character, and has an incidence of 1 in 2×10^4. Homozygosity of this gene is responsible for the absence, or inactivity, of an enzyme. This enzyme participates in the transformation of an amino acid, tyrosine, into a precursor of melanin. Its absence, therefore, creates a block in the reaction (Duke-Elder, 1964; Lentau and Montagu, 1971; Stern, 1973). Non-albinotic individuals have numerous microscopically small granules deposited in their skin, hair and iris, which contain melanin pigment, and give rise to their colour. However, the block in the conversion of tyrosine to melanin for albinos prevents them from possessing this pigmentation, and as a result they are very light skinned, have white/light hair and their eyes are pinkish, because any reflected light will pass through the blood vessels in the eye. Occasionally, they have pale blue/green eyes, when some pigment has formed in the iris.

In animals, including primate apes, albinism is associated with a projection from the retina to the lateral geniculate nucleus and the visual cortex, which differs from the normal pattern beyond the optic chiasma. There is a total crossing of fibres in the albino, and,

consequently, each hemisphere in the visual cortex receives a mapping of the complete visual field (Kaas and Guillery, 1973; Guillery, 1974). To counteract diplopia, which will result from such a mapping, albinos tend to suppress one eye, which leaves them with monocular vision rather than stereovision.

Albinism in humans is the result of an X-linked autosomal recessive gene, but two types have been identified and are classified by the hair bulb incubation test. One of these types possesses quite normal sized melanosomes in the epithelium, yet still exhibits a significant hemispheric asymmetry in the visual evoked potentials (VEP) elicited by monocular stimulation. The retino-geniculo-striate projections are, therefore, thought to be organized in a way similar to that previously reported for albino mammals, and this suggests that these abnormal optic nerve projections are associated with a lack of ocular pigment, and not with any specific generalized pigment defect (Creel et al., 1978). A squint, so often associated with albinism, maybe a useful functional adaptation to this mis-routing of optic fibres (Guillery et al., 1974).

Numerous studies have been conducted to investigate albinism in a variety of species, e.g., rats, cats and mink, with particular reference to the anatomical and functional organization of their visual systems. In albino mammals, the absence of pigmentation in the eyes is associated with abnormalities of the visual pathways (Creel et al., 1978), and recent research on siamese cats has shown that they possess very similar abnormalities in their visual systems to those associated with the albino gene. In siamese cats, however, there is more than one pattern of abnormality of the visual pathways, which

results in a scrambled input to the visual centres of the brain, and likewise the visual cortex has more than one way of dealing with its selection of this abnormal input (Guillery, Cassagrande and Oberdorfer, 1974; Shatz and Levay, 1979).

There appears to be a great deal of literature relating to albinism in all species except man. Most of the recent investigations of human albinism have been connected with the method of visual evoked potentials (VEP), which attempts to analyse the behaviour of albinos' visual systems. This method does reveal an asymmetry between evoked potentials recorded from each hemisphere of monocularly illuminated human albinos, relative to those of normally pigmented subjects (Creel, Witkop and King, 1974; Regan, 1975), so indicating that there is a mis-routing of the signals in the visual pathways. These measurements can sometimes prove difficult for albinos, due to an associated characteristic of nystagmus, created by an optokinetic anomaly (Collewijn, Winterson and Dubois, 1978).

B.i. Experimental Apparatus and Methods

The Wright colorimeter and the interferometer used in this investigation have been described in detail in section C and B, Chapter II, respectively.

a. The Wright Colorimeter

Colour matches were established for a 80' x 80' bipartite field (fig. 5.1), in which the top half consists of an additive mixture of the three 'matching' stimuli, whilst the lower half consists of the test stimulus to be matched. The observer makes his match between the two fields by varying the amounts of the red (R), green (G) and

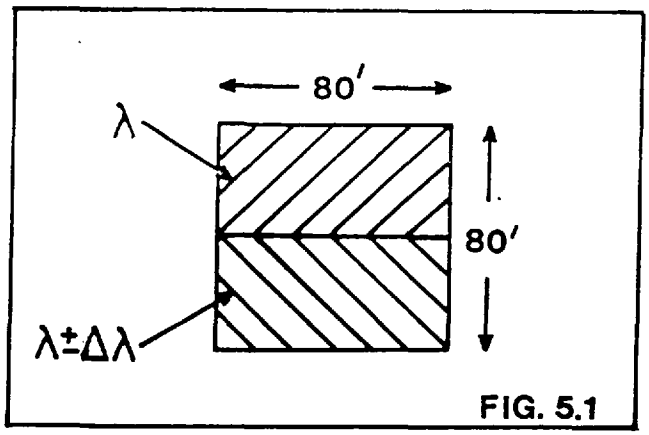

Fig. 5.1
Colour matches were established for a 80' x 80' bipartite field.

blue (B) with R = 650 nm, G = 530 nm and B = 460 nm.

Relative spectral sensitivity was determined by brightness matching methods for which the two halves of the field consist of monochromatic stimuli of wavelength λ_1 (derived from the W1 spectrum, fig. 2.20, Chapter II), and λ_2 (derived from the W2 spectrum) respectively. The brightness of the λ_1 field is controlled by neutral density filters, which are inserted into the W1 spectrum, whereas the brightness of the λ_2 field is continuously varied with the photometer wedge. The observer adjusted the brightness of the λ_2 field with this wedge until it appeared to be of equal brightness to that of the λ_1 field, under the given conditions of observation. This was repeated for values of λ_2 throughout the spectrum, and in spite of the difference in colour, which exists between the two halves of the field, consistent matches were achieved. In particular, at the lower brightness levels, the subject found colour differences less obtrusive, and thus less disturbing to the accuracy of the match.

Critical flicker fusion frequency can also be found with the colorimeter by insertion of a 90^o sector, whose front surface is coated with magnesium oxide. This surface was illuminated by a parallel light beam from the lamp source, S2 (fig. 2.20, Chapter II). As the sector rotates, the observer sees alternately the light from

the sector, and the light from the colorimeter (fig. 2.20). The observer was instructed to adjust the intensity of the test stimulus, by the photometer wedge in the W2 spectrum, until he has established the condition of minimum flicker between the white light and the matching stimuli. The rotating speed of the sector was adjusted to the critical frequency by means of a controlling rheostat, and similar measurements were repeated for several matching stimuli throughout the spectral range.

Stray light was occluded by matt black card and black curtaining. Fifteen minutes dark adaptation was allowed before the observer commenced measurements, and his head positioning was maintained steady by a dental bite bar. This eliminated any colour fringing, caused by the chromatic aberrations of the eye, when the colorimeter exit pupil is located to one side of the optical axis of the eye, and also because the pupil function changes with point of entry of the light (Stiles and Crawford, 1933).

Measurements of spectral sensitivity and foveal colour matching are made to investigate the colour vision characteristics of an albino observer. A previous investigation of the colour vision characteristics of three human albinos (Pickford, 1958), using a Nagel anomaloscope, indicated that compared with normal vision, albinos possessed abnormal colour vision with matches equivalent to those of a protanomalous observer. There is, however, no other evidence to support this hypothesis, and so the aim of these measurements was to compare the colour matching responses of the albino with those of a normal subject.

b. The Interferometer

i. Contrast Thresholds for Single Sine-Waves

Grating acuity measurements can be obtained using the interferometric arrangement (fig. 2.15, Chapter II), which provides 100% modulated high contrast sinusoidal fringes. A potentially more useful measurement of acuity, however, is the determination of contrast threshold, which requires the superposition of a test stimulus on a uniform background field. The interferometric apparatus achieves this (fig. 2.15, Chapter II), by deriving the uniform background as a single beam from laser 1, and with both beams from laser 2 forming the interference fringes. All beams were diverted into the right eye, and the left eye was occluded. The arrangement of the apparatus allows the maximum, Imax, and minimum, Imin, illumination levels present in the visual field to be adjusted without altering the mean retinal illumination level, and therefore the retina is maintained in a state of constant light adaptation. The contrast, C, and contrast sensitivity, M, of the stimulus are defined as follows:-

$$C = \frac{Imax - Imin}{Imax + Imin} , \qquad \text{Eq. 5.1}$$

and

$$M = 1/C . \qquad \text{Eq. 5.2}$$

The variation of the contrast threshold sensitivity of the stimulus with spatial frequency defines the modulation transfer function (MTF) for threshold detection of the gratings.

The interferometer provides a circular visual field of some 30^{o} in diameter. If Io represents the mean retinal illumination level, and f, the spatial frequency of the sinusoidal grating superimposed

upon a uniform background field, the variation of retinal illumination, I, with visual angle x, is given by:

$$I = Io\ (1 + C\ \mathrm{Cos}\ 2\pi fx)\ , \qquad \text{Eq. 5.3}$$

where C defines the contrast of the grating, and has a maximum value of 1.

The contrast sensitivity M, is defined as in equation 5.2.

The observer adjusts the visual stimulus, represented by equation 5.3, to contrast threshold level by moving the wedge, W (fig. 2.15, Chapter II), thus increasing the optical neutral density in the beam and thereby reducing the value of C (equation 5.3), until the sinusoidal grating could 'just-no-longer' be distinguished from the background field. This procedure was repeated several times for each spatial frequency value, and also for a number of spatial frequencies.

ii. Contrast Thresholds for Beat Frequencies derived from two sinusoids

When two sinusoidal gratings of similar frequencies, h and k, are superimposed, the result is a sine-wave of frequency $\frac{(h+k)}{2}\ c/^{o}$, which is modulated in amplitude with a periodicity of (h-k), equation 5.5.

$$I = \mathrm{Cos}\ 2\pi hx + \mathrm{Cos}\ 2\pi kx\ , \qquad \text{Eq. 5.4}$$

then:-

$$I = 2\mathrm{Cos}\ 2\pi \frac{(h+k)x}{2}\ \mathrm{Cos}\ 2\pi \frac{(h-k)x}{2}\ . \qquad \text{Eq. 5.5}$$

The modulation has a periodicity given by (h-k), because in order to define the periodicity of the beats, the distance required is that between corresponding points on the waveform, i.e., 1/(h-k).

When such a waveform is seen, it is the low frequency modulation of spatial periodicity (h-k) which is observed. This is termed the

first difference beat frequency (Burton, 1973). If h is changed to be equal to 2k, second difference beating is observed which has a periodicity of (h-2k).

For the determination of contrast threshold sensitivity to the beat frequencies, the 30^{o} visual fields were composed of a mixture of two high contrast ($C \simeq 1.0$) sinusoidal gratings of different spatial frequencies, h and k, one derived by interference of two beams from laser 1, and the other from laser 2 (fig. 2.15). The two laser beams were polarized at right angles to each other, thus ensuring that they were incoherent and could not interfere. The values of h and k were chosen to produce either first or second difference beating, appropriately. In this situation, there is no background field, and the 'beat' contrast threshold level was found for the observer by moving the wedge, W (fig. 2.15), to increase the optical neutral density in the beam from laser 2. This increases simultaneously the mean illumination level of the higher frequency component, h, in comparison to the lower frequency component, k, until the threshold criterion of 'just-no-longer' detect beats is reached. In this situation the total average retinal illumination will remain unchanged, and its profile is given by:-

$$I = Io\,[(1+C_B)\,\mathrm{Cos}\,2\pi hx + (1-C_B)\,\mathrm{Cos}\,2\pi kx]\,, \qquad \text{Eq. 5.6}$$

where C_B defines the 'beat' contrast and is determined from the increase in the optical density required to reach the threshold level. The beat contrast sensitivity, M_B, is defined:-

$$M_B = 1/C_B\,. \qquad \text{Eq. 5.7}$$

The contrast threshold for first order beating was determined by maintaining one of the component sine-wave gratings in the pattern at

a fixed value, $h\,c/_{o}$, whilst the other component was set at various frequencies, $k\,c/_{o}$, thus producing a beat frequency of $(h-k)c/_{o}$. Contrast thresholds were also determined for first difference beats, produced from combinations of different pairs of component frequencies, h and $k\,c/_{o}$, and for a fixed beat frequency generated from different contributions of spatial frequencies.

In each case, the contrast thresholds were determined several times for each 'beat' frequency, and the wedge reset to a random position between every setting. The change in the optical density recorded by the wedge position gives a measure of the contrast threshold level of the visual system to a particular grating stimulus, and the reciprocal provides the relative log contrast sensivity of the visual system. The contrast threshold function for sine-waves was determined with a uniform background field derived from a single laser beam, so that it is comparable to the beat patterns. In this way, both sets of measurements were obtained against a speckle background.

Measurements of visual acuity and MTF's for both single sine-waves and first difference beating were to quantify and examine the effect of the very poor restriction on the entry of light into the albino's eyes, and its subsequent impairment of visual acuity. Beats arise only from a mixture of two sinusoidal frequencies when they pass through a non-linear device, and Burton (1973) suggested that this non-linear device occurred prior to the mechanisms in the visual system where the spatial interaction occurs which defines the shape of the MTF's. Thus, beat measurements are used to investigate the level at which an albino's anomalous acuity is determined.

iii. The Contrast Threshold Elevation Effect (section C.vii, Chapter I)

The contrast threshold elevation effect (section C.vii, Chapter I) is the increase in the threshold illumination level required for the detection of a test target after adaptation to a high contrast structure of identical spatial frequency, compared to that required after adaptation to a uniform field of the same mean illumination level as the structure. The effect applies to both linear square or sine-wave gratings, and has been described extensively in the introduction to Chapter III.

The field configurations used to measure the contrast threshold elevation effect in this investigation are shown in fig. 5.2 for sine-

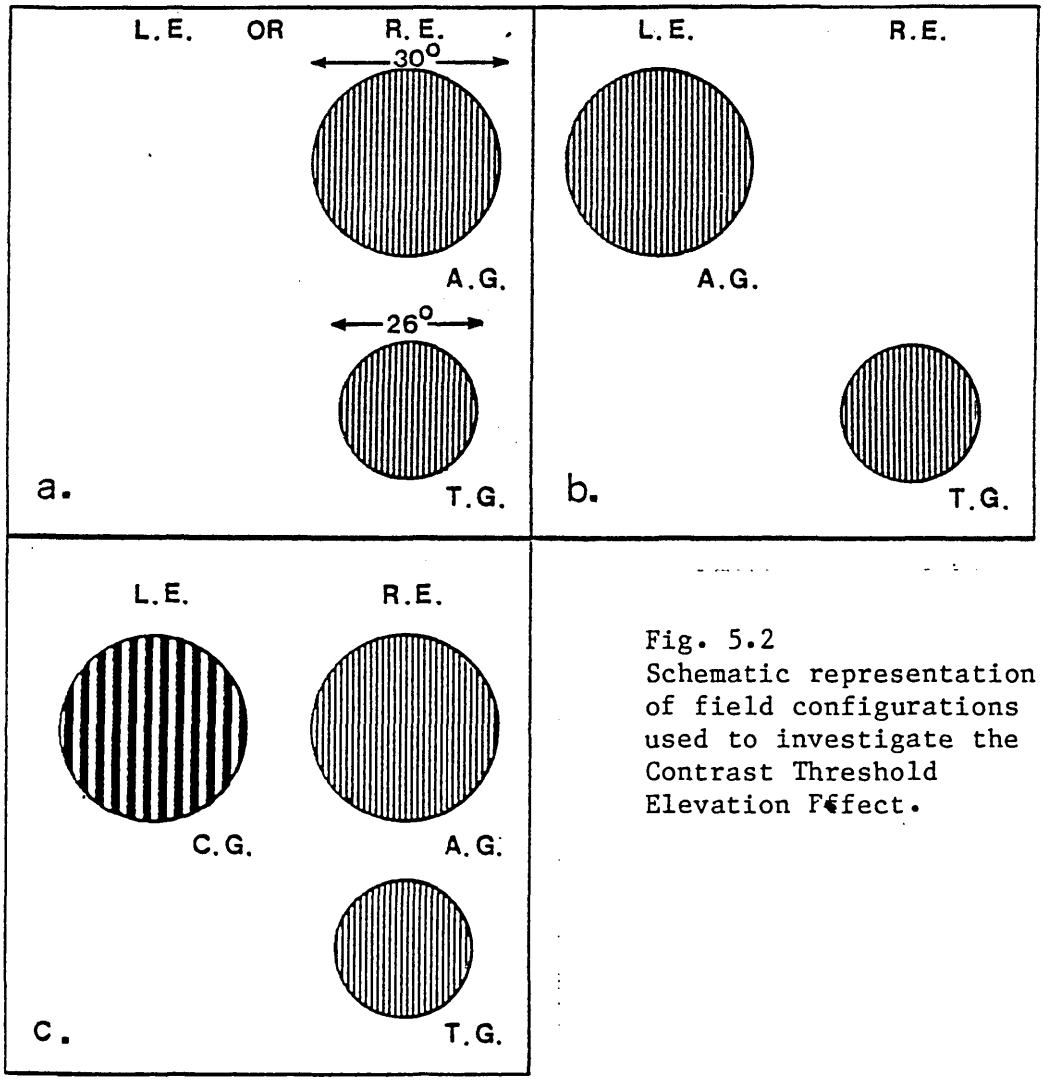

Fig. 5.2
Schematic representation of field configurations used to investigate the Contrast Threshold Elevation Effect.

wave gratings produced by the interferometer (section B, Chapter II). Figure 5.2a illustrates the configuration for monoptic presentation of the stimuli, in which the adaptation (AG) or test (TG) gratings are presented to either only the right eye (RE) or the left eye (LE) by positioning stops in front of the appropriate eyepiece in the interferometer. The high contrast adaptation grating was derived from the light beam of laser 1, as also was the uniform adaptation field. In the latter case, one of the two interfering beams was masked, and a 0.3 log unit neutral density filter was removed from the other beam so that the uniform field's illumination level was equal to the average level of the interference fringes. The test grating was derived by the interfering beams from laser 2, which pass through the wedge, W. It is by means of this wedge that the test grating can be adjusted to the threshold criterion. These measurements are designed to test the symmetrical adaptation responses of the two eyes in the albino subject, who possesses monocular vision and shows a right eye dominance.

As described in the Introduction (section C.vii, Chapter I) the contrast threshold elevation effect can be interocularly transferred. This effect is tested by the stimulus configuration shown in fig. 5.2b, which results in dichoptic presentation, that is the high contrast adaptation grating is presented to the left eye (stop in position before exit of beam to right eye, fig. 2.15, Chapter II) with the subsequent presentation of the test grating to the right eye (stop to prevent lower beam entering the left eye). Measuring this effect with an albino subject investigates the means by which such an effect is transferred. As a result of the total decussation of the optic fibres at the optic chiasma, and thus unlike a normal subject, the

albino has a complete mapping of the visual field presented to each eye in the contralateral hemisphere in the visual cortex. The two hemispheres are connected by the transcallosal fibres of the corpus callosum (Choudhury, Whitteridge and Wilson, 1965), but their precise function is not yet known. Measurements of the interocular transfer of the contrast threshold elevation effect will show whether in fact they do serve as the interconnecting pathway between the two separate visual representations in the two hemispheres of the visual cortex in albino subjects.

Figure 5.2c represents the field configuration used to study the binocular inhibitory effect of the contrast threshold elevation effect (Ruddock and Wigley, 1976; see section A.i, Chapter III). In this case, the high contrast adaptation and test grating presented to the right eye have identical spatial frequencies, whilst the high contrast adaptation grating, defined the conditioning grating (CG) presented to the left eye, is varied through a range of spatial frequencies. In normal observers, the presence of this conditioning grating inhibits the monocular contrast threshold elevation effect, and the data suggest that the effect arises at a post-chiasmal location where the signals from the two eyes come together, i.e., in the visual cortex (Hubel and Wiesel, 1967). As was discussed in the Introduction to this chapter, albino animals do not possess the normal retino-geniculate-striate projections, and so it is of interest to find whether or not this binocular interaction occurs in subject D.C. (an albino).

The experimental procedure for determining the change in the threshold illumination level, produced as a result of adaptation to these grating configurations, and measured in terms of the parameter

Δ, has been described in detail (section B, Chapter II). In all three experiments, measurements represent the mean of at least three determinations, with standard mean errors of $\simeq$ 0.05 log units. Unless otherwise stated, the retinal illumination levels were set 4 log units above the subject's threshold level for the detection of the test grating presented against a dark background field.

B.ii Subjects

The principal observer was a male albino, D.C., aged 33 years (Cameron, 1979). He is classified as a complete albino with nystagmus in all positions, due to the non-formation of a fovea, which is a distinct characteristic of human albinism. The iris of his eyes are translucent, and pale blue-grey, but D.C. has no other fundus abnormality, apart from it being albinotic (Pickford and Taylor, 1968). He suffers from another albino characteristic, which is attributable to the low pigmentation, and that is photophobia. He has a right convergent squint, and attended an oculist at an early age to be fitted with tinted spectacles in order to correct a moderate degree of hypermetropic astigmatism. His external albino features are all a consequence of his low pigmentation. He has snow-white hair, a rough, folded hyper-keratotic milk-white complexion, and from the results of the hair bulb incubation test, he belongs to the group of albinos classified as Tyrosinase negative (Dr. Winder, Ins. of Ophthal.). In view of his suppression producing monocular vision, and strabismic history, it is not surprising to find that he lacks any form of stereoscopic vision as tested by the Julesz anaglyphs (Julesz, 1971; Wigley, 1977; Abadi, 1974). Under two lighting conditions, he could

fuse neither the two random dot patterns printed in black and white, nor identify the stereo image hidden in the patterns printed in red and green ink, and his performance did not improve for increased viewing distance (Mollon et al., 1979).

Comparison results for most of the investigations are also given for a normal observer, V.W., (female, aged 23 years, an emmetrope).

C. Results

C.i. Colour Discrimination

The results of brightness matching and flicker determination of the spectral sensitivity function both for the albino subject, D.C., and for the normal subject, V.W., are shown in fig. 5.3. In this figure, the relative luminosity is plotted along the ordinate as a function of wavelength, in nanometers, along the abscissa.

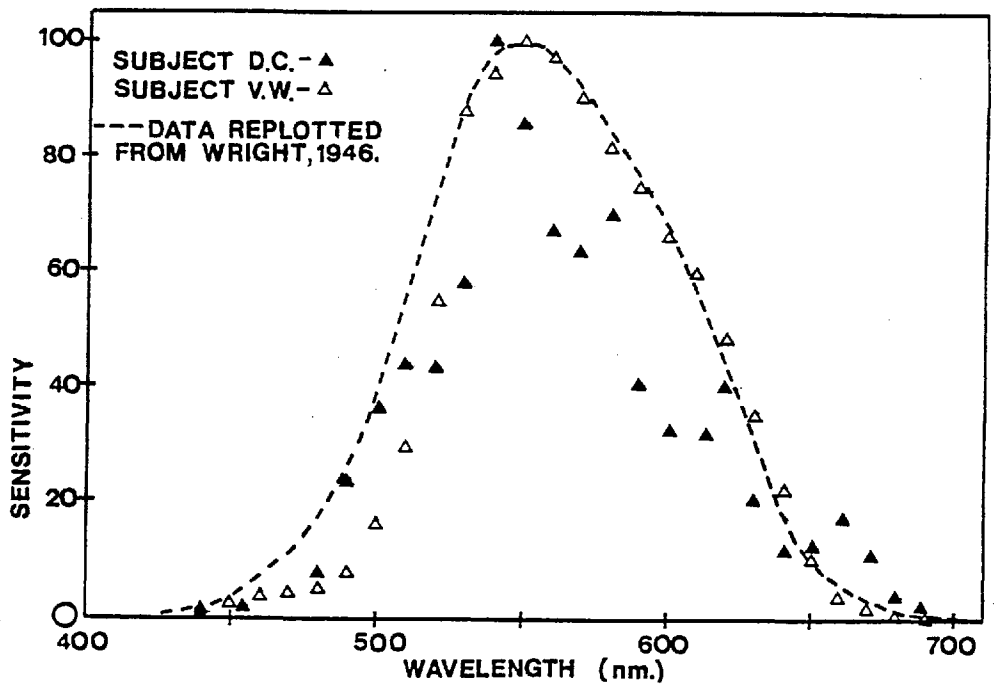

Fig. 5.3 The spectral sensitivity function as determined for the albino, D.C. and the normal subject, V.W., by brightness matching and flicker determination (see text for details).

Flicker determination and brightness matching proved difficult for

the albino due to nystagmus, especially in the short wavelength region of the spectrum, but nevertheless the experimental results shown in fig. 5.3 are not significantly different from those of a normal observer, under similar conditions. There is, however, a slight shift of the albino's peak spectral sensitivity towards the shorter wavelength regions.

Figure 5.4 shows subject D.C.'s colour matching coefficients, and also for comparison the broken line represents those of a normal

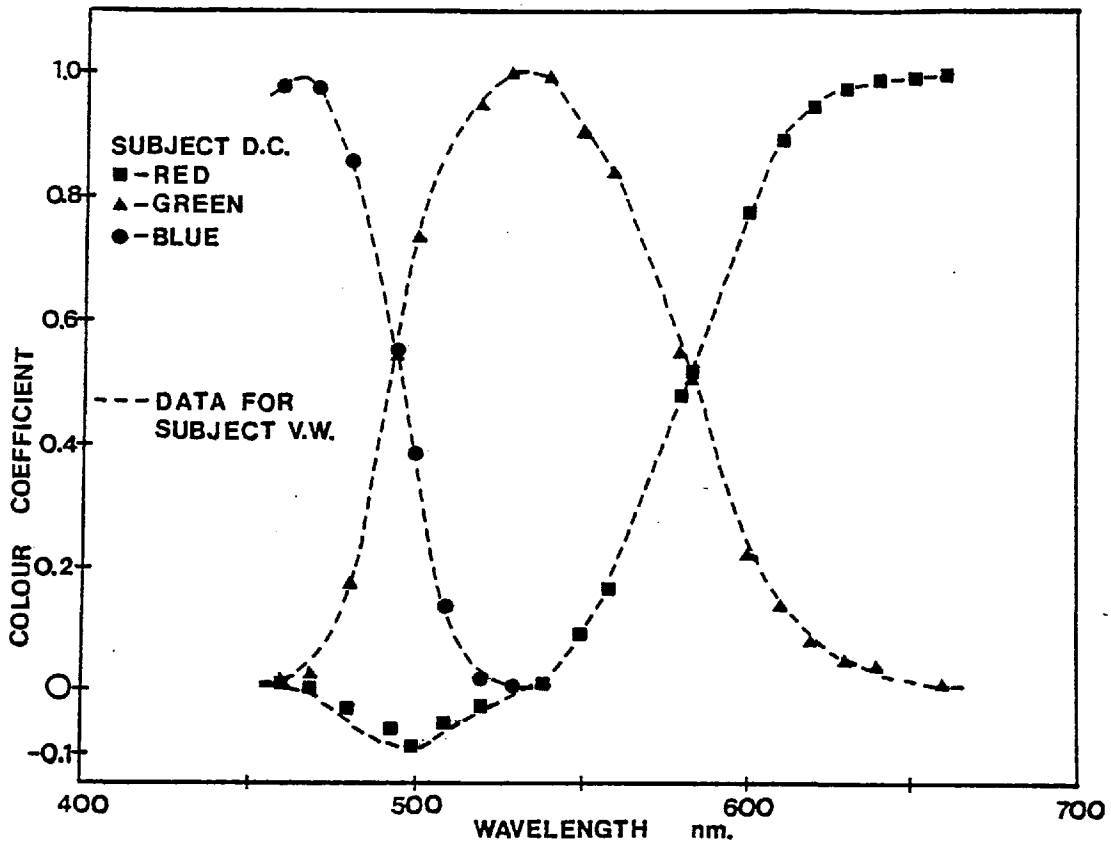

Fig. 5.4 Spectral coefficient curves for observer D.C. The broken line represents those of the normal observer V.W.

subject, V.W. This figure shows that within the limits of the experiment, the two sets of data are very similar.

C.ii. Visual acuity and MTF's

Probability of detection curves obtained for twenty-five presentations of 100% modulated, 632.8 nm, sine-wave gratings of various spatial frequencies are shown in fig. 5.5. Data are given for two illumination levels; one, at the albino's absolute threshold for a uniform field of wavelength 632.8 nm, measured after forty minutes of dark adaptation (□), and the other, 3 log units above this threshold level for the uniform field (■). These data show that in comparison to the normal observer, the albino, D.C., suffers a severe reduction in visual acuity. The increase in retinal illumination improves his acuity limit, but even so, it is still considerably lower than that of a normal observer, with maximum cut-off at 4 c/^{o}, compared to 60 c/^{o} for the normal observer under the same conditions.

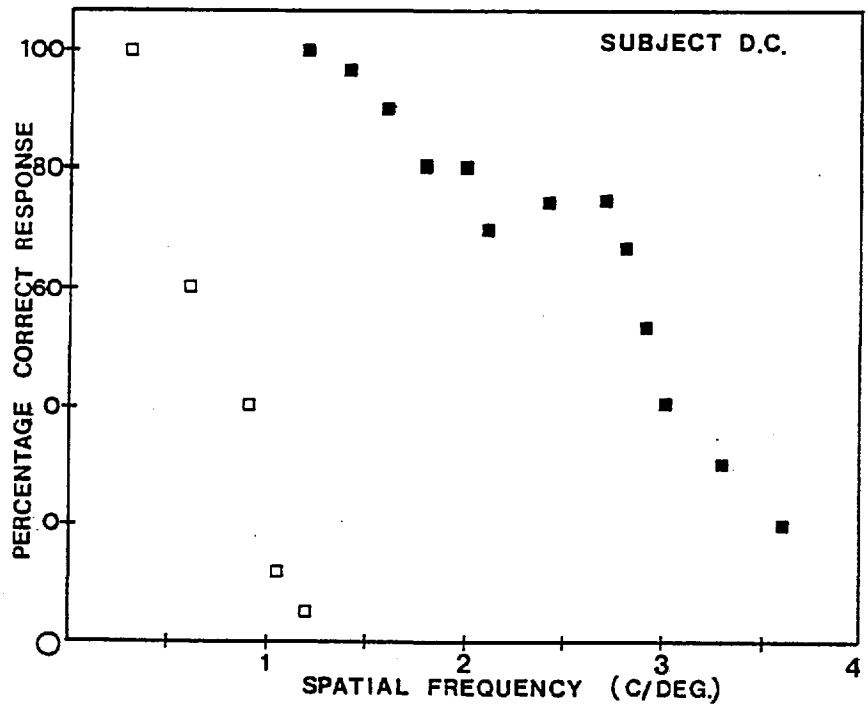

Fig. 5.5 To show the probability of detection as a function of spatial frequency for the albino subject, D.C.

Contrast threshold sensitivity data for single sine-wave and beat detection are given in fig. 5.6 and in fig. 5.7 for the albino subject, D.C., and the normal observer, V.W., respectively. Both sets

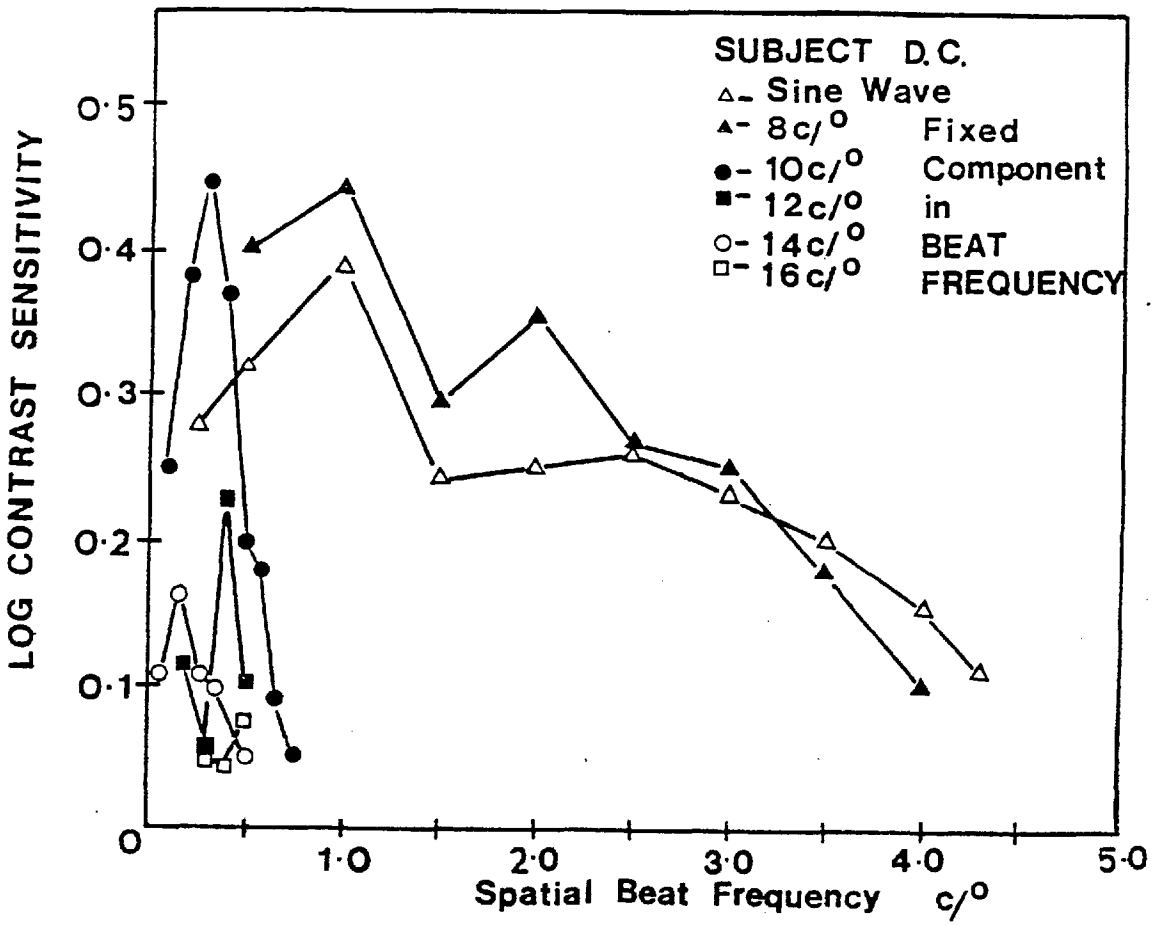

Fig. 5.6 Contrast threshold sensitivity functions for single sine-wave and beat detection determined using the interferometric arrangement for the albino subject, D.C.

of data were obtained at a retinal illumination level 3 log units above the threshold level for the albino's detection of a 632.8 nm uniform field. In each figure, the ordinate denotes the logarithm of the contrast sensitivity with the spatial frequency, or the perceived beat frequency, plotted along the abscissa in cycles per degree of visual angle. Each data point represents the mean of at least three determinations, and the mean standard error was typically 0.05 log units.

The MTF for a single sine-wave grating is shown as open triangles (△) both in fig. 5.6, for the albino, D.C., and in fig. 5.7, for the

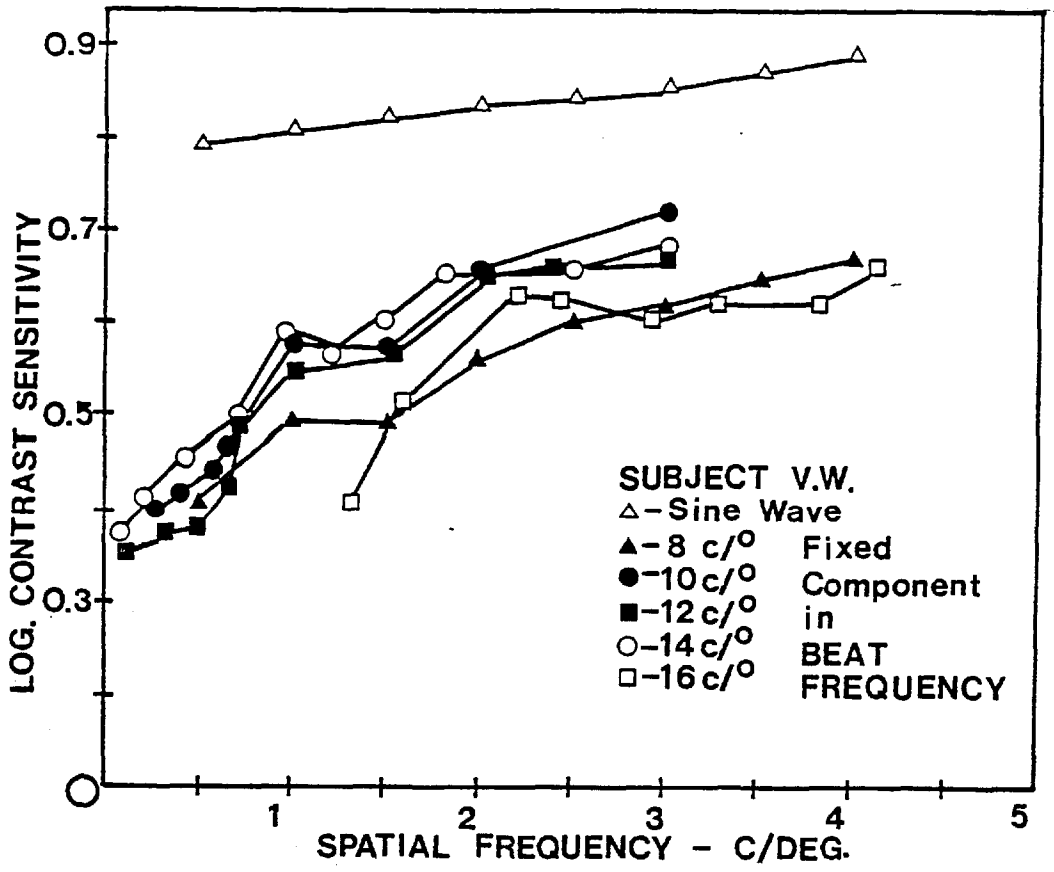

Fig. 5.7 As fig. 5.6, but data are for the normal subject, V.W.

normal observer, V.W. The logarithmic contrast sensitivity curve of the normal observer, V.W., for the single sinusoidal test grating, presented against a laser generated background field, agrees for this range of spatial frequencies and retinal illumination level with those reported by Burton (1973), (see fig. 5.8a). The data show a gradual increase in the log contrast sensitivity as the spatial frequency increases up to a value of 4 c/^{o} to 6 c/^{o}. The data for the albino, D.C., (fig. 5.6), however, lie within a narrower range of spatial frequencies with the cut-off at 4 c/^{o}. (N.B., This is the value which represents the limit of his visual acuity.) His peak sensitivity occurs at a spatial frequency of some 0.5 c/^{o}. Both of these values

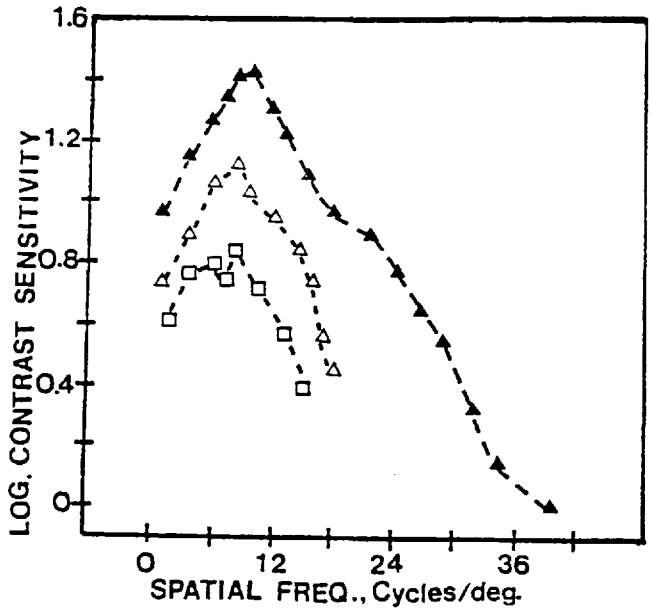

Fig. 5.8a
Modulation transfer functions for a single sine-wave (▲), first difference 'beating' (△) and second difference beating (□). (Replotted from Burton, 1973).

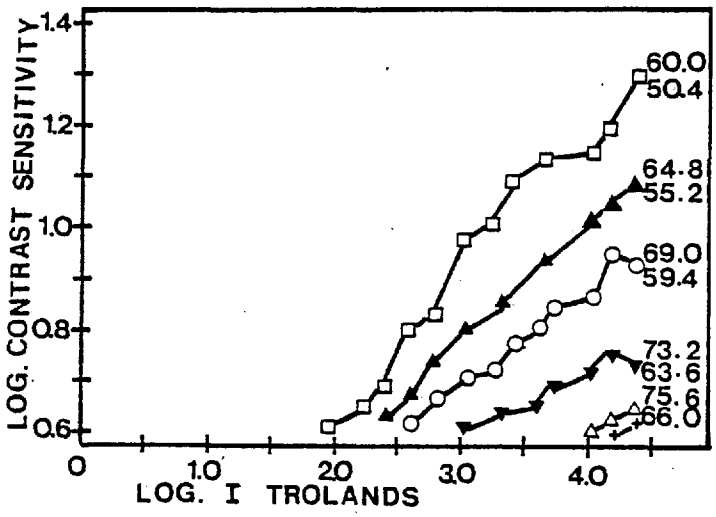

Fig 5.8b
Log contrast sensitivity functions for a first difference 'beating' of 9.6 c/° with respect to mean retinal illumination levels for several pairs of component frequencies, shown alongside the relevant curve in c/°. (Replotted from Burton, 1973).

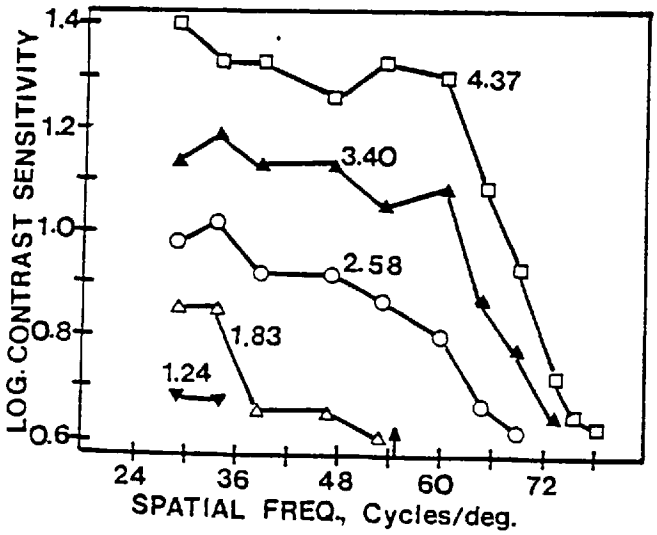

Fig. 5.8c
Log contrast sensitivity functions for first difference beats with respect to the higher frequency components, at five mean illumination levels, which are shown next to the corresponding curve in log trolands. (Replotted from Burton, 1973).

are significantly lower than for a normal observer, whose peak sensitivity occurs at some 5 c/^{o} and shows a cut-off point at some 60 c/^{o}.

Log contrast threshold sensitivities obtained for first difference beats are shown in fig. 5.6, for observer, D.C., and in fig. 5.7, for observer, V.W. This time, in each case, the abscissa represents the perceived beat frequency, (h-k) c/^{o}, which was obtained by maintaining one of the component sinusoids at a fixed spatial frequency, h c/^{o}, whilst the other was set at different frequencies, k c/^{o}. The value of the fixed component frequency is shown alongside the corresponding curve. These results show significant variation in the contrast sensitivity for the albino, D.C., as the fixed frequency component, h c/^{o}, changes, yet for the normal subject V.W., there is very little difference between data for different h values and the contrast sensitivity data for simple sinusoidal gratings. Burton's (1974) data for a normal subject also show that when component frequencies produce a beat frequency within the frequency range, 0 c/^{o} to 10 c/^{o}, the results are not critically dependent on the component frequencies. Burton (1974) shows also that there are two factors which influence beat detection in normal vision, the mean retinal illumination level, and the frequency of the upper fixed component sinusoid. If the latter exceeds a critical value, then immaterial of the illumination level, the subject observes no beats. This situation exists for the albino when the fixed component of the beat frequency is 16 c/^{o}, a value which significantly exceeds the limit of his spatial resolution under normal conditions. A possible explanation for the fact that reduction in sensitivity occurs at 16 c/^{o}, as

opposed to the usual 60 c/^{o} to 70 c/^{o} for normal vision, is that in the albino, contrast reduction may occur in the two component sinusoids, as their frequencies are increased. This is caused primarily by light scattering effects in the optical media and eye movements, both of which are significant features of albino vision.

Contrast threshold sensitivity was also measured for a fixed beat frequency, 0.5 c/^{o}, as a function of retinal illumination level. (N.B., The spatial frequency of 0.5 c/^{o} was chosen because the maximum sensitivity of the albino's contrast sensitivity function occurs at this spatial frequency (see fig. 5.65).) Data are given for the two subjects, the albino, D.C. and the normal, V.W., in fig. 5.9 and in fig. 5.10, respectively. In both of these figures, the ordinate denotes log contrast threshold sensitivity for beat detection and the abscissa, the relative change in the log retinal illumination level of the beats, where log I equal to zero corresponds to threshold level

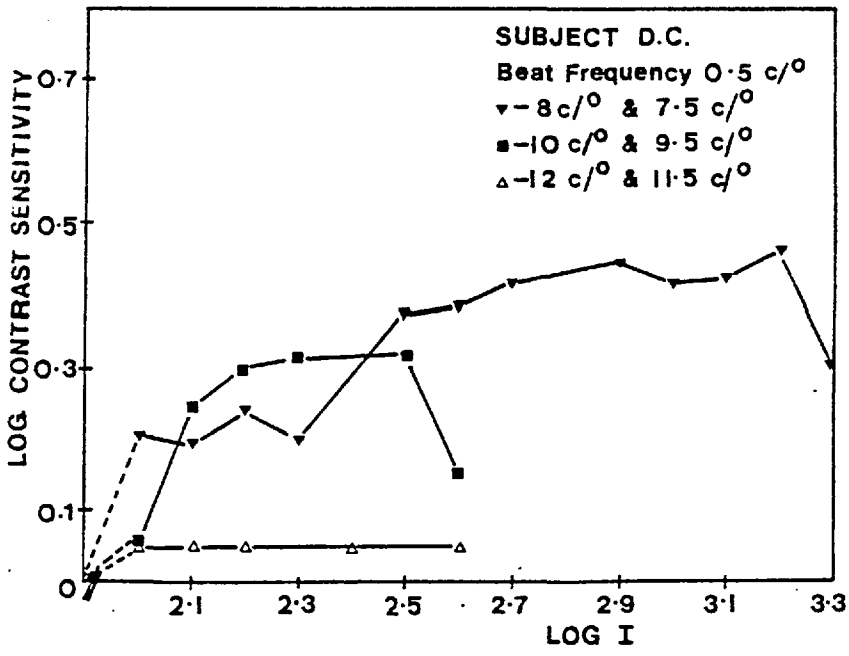

Fig. 5.9 Log contrast sensitivity functions for a first difference beating of 0.5 c/^{o} with respect to mean retinal illumination levels for several pairs of component frequencies, shown alongside the relevant curve in c/^{o}. Data are for the albino subject, D.C.

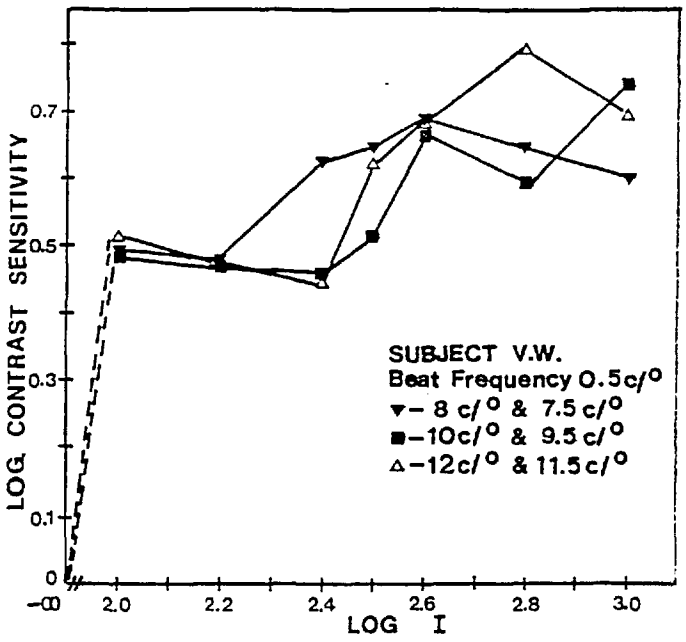

Fig. 5.10
As fig. 5.9, but data are for the normal observer, V.W.

for the albino's detection of a 0.5 c/° sine waveform grating. The two spatial frequencies, from which the constant beat frequency was derived, are shown at the side of the relevant curves in cycles per degree. Each of the curves in fig. 5.10 can be represented by a single function of retinal illumination level. The effect produced by changing the spatial frequencies of the component gratings, whilst maintaining a constant beat frequency of 0.5 c/°, translates this function along the ordinate axis, without significantly changing its shape (c.f., fig. 5.8b).

C.iii The Contrast Threshold Elevation Effect

The experimental data, given in fig. 5.11 and in fig. 5.12, show the contrast threshold elevation effect for the albino observer, D.C., under the three stimulus configurations illustrated in fig. 5.2. In each case, the value of Δ, determined from equation 2.19 (chapter II) is plotted as a function of spatial frequency, expressed in cycles

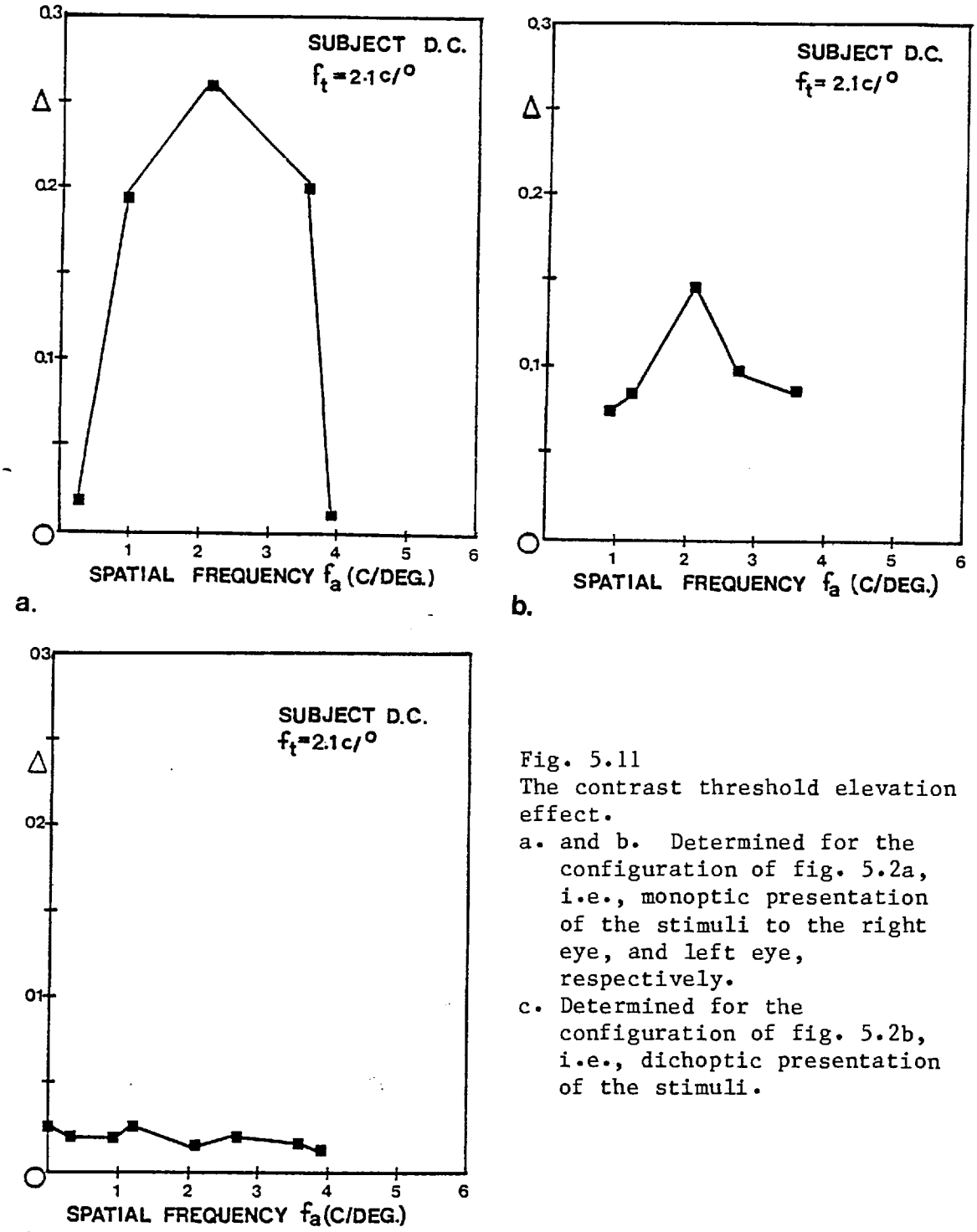

Fig. 5.11
The contrast threshold elevation effect.
a. and b. Determined for the configuration of fig. 5.2a, i.e., monoptic presentation of the stimuli to the right eye, and left eye, respectively.
c. Determined for the configuration of fig. 5.2b, i.e., dichoptic presentation of the stimuli.

per degree of visual angle, of the sinusoidal adaptation grating (fig. 5.11), and of the conditioning grating (fig. 5.12).

Data, shown in fig. 5.11a and b, are the results of the contrast threshold elevation effect determined for monoptic presentation of the

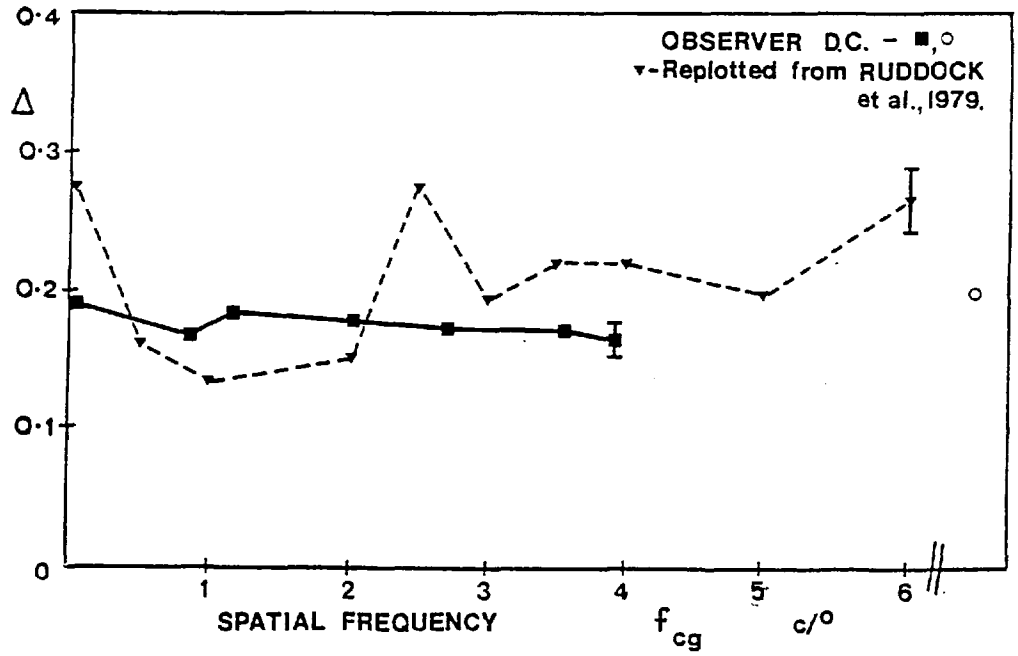

Fig. 5.12 The contrast threshold elevation effect determined for the stimulus configuration of fig. 5.2c, in which the two eyes are adapted to gratings of two different spatial frequencies.

grating to either the right (fig. 5.11a) or the left (fig. 5.11b) eye of the albino, D.C. The spatial frequency of the test grating, f_t, remained constant at 2 c/°, and was chosen to lie within the albino's range of resolution. This spatial frequency value allowed the spatial frequencies in the adaptation grating, f_a, to be varied through a range with a bandwidth of $\pm$ 1 octave around the test value. The data establish that the contrast threshold elevation effect occurs for each eye of the albino subject with appropriate low frequency gratings. The tuning curve obtained with the right eye (fig. 5.11a) exhibits similar bandwidth selectivity to that of normal observers with the maximum Δ value for $f_a = f_t = 2$ c/°, falling to an insignificant value of Δ when $f_a = f_t/2$ or $f_a = 2f_t$. A more unusual result is shown in the experimental data obtained with the albino's left eye, (see fig.

5.11b), which is of smaller amplitude compared to the values for the right eye. This may be due to the albino's right-eye dominance, accompanied by suppression of the left eye.

Data obtained for dichoptic presentation of the test and adaptation stimuli are given in fig. 5.11c. These data show that adaptation of the left eye fails to produce any significant change in the threshold illumination level required for the detection of the test grating in right eye.

The binocular inhibition associated with the contrast threshold elevation effect was measured using the stimulus configuration of fig. 5.2c. In this experiment, the spatial frequency of both the adaptation and test grating presented to the right eye was fixed at $2\ c/^{o}$, whilst that of the grating presented to the left eye was varied over the range, $0\ c/^{o}$ to $5\ c/^{o}$. The experimental data are plotted in fig. 5.12, and show that the magnitude of the adptation effect, Δ, for the albino subject is constant for all spatial frequencies of the conditioning grating, thus no inhibitory interaction occurs between the two eyes, in contrast to the results found for a normal subject (full triangles, fig. 5.12).

D. Discussion

D.i. Colour Vision and Discrimination

Evidence from previous investigations (Pickford, 1951, 1958; Pickford and Taylor, 1968) suggests that there may be a protanomalous deficiency associated with the colour vision characteristics of albinos. The data given in section C.i of this chapter indicate, however, that the albino, D.C., possesses normal colour matching

responses, and therefore has normal trichromatic colour vision. This is not to say that albinos are exempt from the other sex-linked colour vision deficiencies which may be inherited, but there is no intrinsic colour vision deficiency associated with albinism, as suggested by Pickford (1951, 1958). As explained in the introduction, albinos lack pigmentation, but the experimental data (see fig. 5.4) indicate that in spite of this, the pigments of the three types of cone are produced in the normal way, and it is concluded that they themselves are not, therefore, melanin based pigments.

D.ii. Visual Acuity

Albinos suffer a gross impairment in their visual acuity as is shown in fig. 5.5, section C.ii of this chapter. This is brought about in part by the lack of pupillary restriction on the entry of light into their eyes, caused by the low or zero iris pigmentation. Further, it has been suggested that this reduction in visual acuity is due to abnormally large receptor size, or to receptor density differences, or that it is a consequence of the poor imaging qualities of the eyes due to an excess of scattered light in the optical media and the low pigmentation (Blake and Antoinetti, 1976).

The experimental data, shown in fig. 5.6, indicate that the severe reduction in visual acuity must occur at a post-receptoral stage in the visual system. Responses of the normal visual system to sinusoidal grating profiles and first difference beats have been reported by Burton (1973). Burton suggests that the normal contrast threshold sensitivity function, associated with first difference beats, which is similar in both shape and form to that for a single

sine-wave stimulus, indicates that near threshold the beating between two sine-waves has similar properties to that of the single sine-wave, and can thus be considered as a difference frequency. This will only arise from a mixture of two sinusoidal frequencies if they pass through a non-linear device. Burton's data suggests that this non-linear device occurs at a level in the visual system prior to that mechanism where the spatial interaction occurs to define the shape of the MTF.

The similarity between the sine-wave and 'beat' contrast sensitivity values in fig. 5.6, indicate that the albino possesses and detects the two by a similar mechanism. Thus the two conditions for the detection of beats, that firstly, the beats are only detected if the visual resolution limit is not at the photoreceptor level, and secondly, a non-linear processing of the illumination level must occur in a mechanism prior to that which sets the resolution limit, must apply to the albino, D.C. His spatial resolution is, therefore, limited neither by nystagmus, nor by abnormal receptor distribution. His abnormal low-pass filter appears to be located at post-receptoral level.

Another visual response in which the albino's low-pass spatial filter characteristic is exhibited is in the motion sensitive IMG response function (Barbur and Ruddock, 1980a,b). This function is a spatial frequency tuning curve obtained from the threshold detection of a moving target over a structured background of different spatial frequencies. The albino subject, D.C., has an abnormal IMG function as shown in fig. 5.13, (Barbur, Halliday, Ruddock and Waterfield, 1980), which differs greatly from the normal functions obtained under

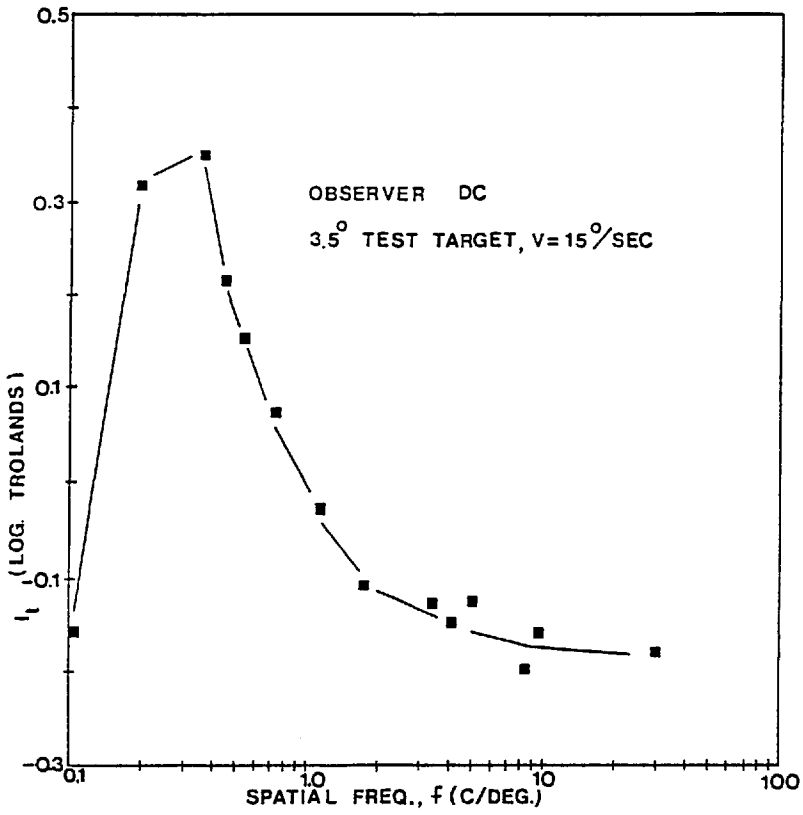

Fig. 5.13
Log threshold illumination level, log I_t, for foveal detection of a 3.5° circular test target moving at $15°s^{-1}$ along the horizontal meridian with a square wave-form background grating of spatial frequency fc/°, and mean illumination level 1 log troland. Each data point is the mean of five readings with typical standard deviation 0.06 log units. Subject D.C. (replotted from Barbur et al., 1980).

similar experimental conditions (Barbur and Ruddock, 1980a). D.C.'s IMG function exhibits similar low-pass characteristics to those of his contrast sensitivity function, i.e., with a peak at a spatial frequency of $\sim$ 0.4 c/° and being insignificant for frequencies $\geq$ 4 c/°. Thus both responses must be subject to the same abnormal low-pass spatial filter.

D.iii. The Contrast Threshold Elevation Effect

Experimental data, shown in fig. 5.11 and in fig. 5.12, indicate that due to the abnormal input to visual cortex, the albino's adaptation responses are significantly restricted. His resolution capacity restricts the range over which adaptation responses occur, but the suppression and consequent deprivation of visual input to the non-dominant left eye significantly affects its responses, (see fig.

5.11b). This is consistent with the hypothesis that a specific deficiency of features in early visual input alter the organization and connections in the visual pathways (Freeman and Thibos, 1973; Barlow, 1975; Hess and Howell, 1977; Eggers and Blakemore, 1978) especially when connected with the albino's astigmatism. Pickford and Taylor (1968) also noticed a reduction in the number of early components in VER recordings when taken over D.C.'s right hemisphere, compared with those measured over the left hemisphere.

As stated in the introduction to this chapter, in contrast to normal animals, albinos have abnormal retino-geniculate-striate projections produced by the total decussation of the optic nerve fibres at the optic chiasma. Thus each hemisphere of the visual cortex receives a complete mapping of the contralateral visual field. Daniel and Whitteridge (1961) and Zeki (1978e) have shown that normally, the two separate hemifield maps in the two hemispheres are re-united by the fibres of the corpus callosum. Von Bonin, Garol and McCulloch (1942), Myers (1962) and Zeki (1970) showed that the transcallosal fibres of the corpus callosum in the cat synapse into area 18 of the visual cortex, and from there establish short axon connections into area 17, which borders area 18. This border region of area 17 has been shown to contain the cortical representation of the vertical meridian of the visual field (Choudhury, Whitteridge and Wilson, 1965; Zeki, 1978e). This has led to the hypothesis that the transcallosal fibres are responsible for joining the two halves of the visual field together, and are therefore responsible for interactions which take place between the two eyes.

The experimental data indicate a 'null' effect both for the

dichoptic contrast threshold elevation effect and for the binocular inhibitory effect. In the albino, therefore, the visual signals elicited in the two hemispheres of the visual cortex are not transmitted by the transcallosal fibres of the corpus callosum, and thus there is no interaction between the two hemispheres. Ruddock and Wigley (1976) suggest that the binocular inhibitory effect associated with the contrast threshold elevation effect may be induced by the transcallosal fibres, in order to suppress the effect of two non-matching inputs in the visual field. The effect appears to occur only for vertically oriented gratings and may, therefore, aid the fusion of the two visual half-fields when they are matched. Alternatively, the inhibitory signals, which arise from the conditioning grating, may subserve stereoscopic vision, since Mitchell and Blakemore (1970) and Blakemore (1970) have shown that the callosal fibres may be necessary for stereoscopy at the fovea. In the albino, however, neither of these functions occurs; there is a complete mapping of the visual field in the contralateral hemisphere, and therefore, it is not necessary to suppress a non-matching input along the vertical meridian. Also, the albino has monocular vision, and exhibits no stereoscopic fusion in any part of his visual field. Thus in the albino, the transcallosal fibres show no compensatory function to aid his deficiency with respect to the separation of the visual input, and as a result, may even have become functionally redundant.

The rather unusual spatial frequency tuning shown in the adaptation responses of the albino's left eye is quite different from the symmetrical adaptation responses reported for the two eyes of two other monocular visioned subjects, who suffered from congenital

strabismus (Ruddock, Waterfield and Wigley, 1979). The results shown in Table 3 indicate that both of their eyes show symmetric adaptation, even though they are stereoblind and they show no binocular inhibition (see fig. 6.10, chapter VI).

Table 3

SUBJECT	ADAPTATION, Δ (log units)	
	RIGHT EYE	LEFT EYE
A.C.	0.30	0.35
D.P.	0.28	0.30
D.C.	0.20	0.15
	Mean error $\simeq \pm$ 0.05 log units	

D.iv. Electrophysiological correlates of Albinism

The experimental data of this chapter has established that the albino observer, D.C., responds to most visual stimuli, but many of his responses exhibit abnormal properties when compared to normal ones, especially as they are restricted to lie within his visual acuity range.

Stone and Dreher (1973), and Ikeda and Tremain (1979) have shown that in cats which experience a retinal image blur, there is abnormal development of the X and the Y pathways. In particular, cats, which suffer abnormal visual development, have X- and Y-type ganglion cells which exhibit broader receptive fields with smaller inhibitory surrounds than in normal cats. Ikeda and Tremain (1979) have also shown that cats which lose the use of the area centralis as the normal

visual axis during their early post-natal development, consequently develop amblyopia. Loss in the ability to fixate produces inadequate stimulation of the central retinal ganglion cells because of the habitual presence of blurred images at the area centralis, which arrests their full development during the critical period of 4 to 12 weeks after birth. Such abnormal development does not occur if alternating fixation between the normal and the squinting eyes can be achieved. A large contribution to the reduction in the visual acuity of human albinos may be attributed to a similar inability to fixate, due to a non-forming fovea, and a prominent characteristic of the group is nystagmus, which creates continual retinal blur, and therefore abnormal visual input, during the critical period. Thus, the abnormal development of X- and Y-type ganglion cells could arise in the same manner as described by Ikeda and Tremain (1979) for the cats. The conclusion from the 'beat' frequency experiments that resolving power is set at post-receptoral level is consistent with this view.

CHAPTER VI

Colour and Spatial Pattern Discrimination in an Observer with a Right Field Hemianopia

A. Introduction

Hemianopia is defined as the loss of vision in one half of the visual field (see fig. 1.6, Chapter I), and the characteristics of a number of cases have been given by Teuber, Battersby and Bender (1960). Hemianopia may be complete or there may be sparing of the macular region; in the latter case, it is usually caused by damage to the terminal projection of the optic radiation, whereas other cases in which there is no macular sparing, either the optic tract or optic radiation has been interrupted prior to this point. The visual field and retina are mapped topographically into the optic radiation and visual cortex. This produces an ordered retino-topological mapping of each half-field on either side of the cortex with the visual field divided along the vertical meridian. The upper half-field is mapped into the lower portions of the optic radiation and striate cortex, and vice-versa for the lower half-field. From examination of cross sections taken from the optic radiation, Polyak (1957) suggests that the macula fibres which subtend a visual field of some 9^{o}, with the central 2^{o} representing the fovea centralis, are concentrated at an intermediate level with the more peripheral fibres from the visual field segregated above and below (Polyak, 1932 and 1933).

A schematic view of the arrangement within the optic radiation, in fig. 6.1, shows that throughout its entire course, it carries all the fibres which correspond to the upper peripheral quandrants of the

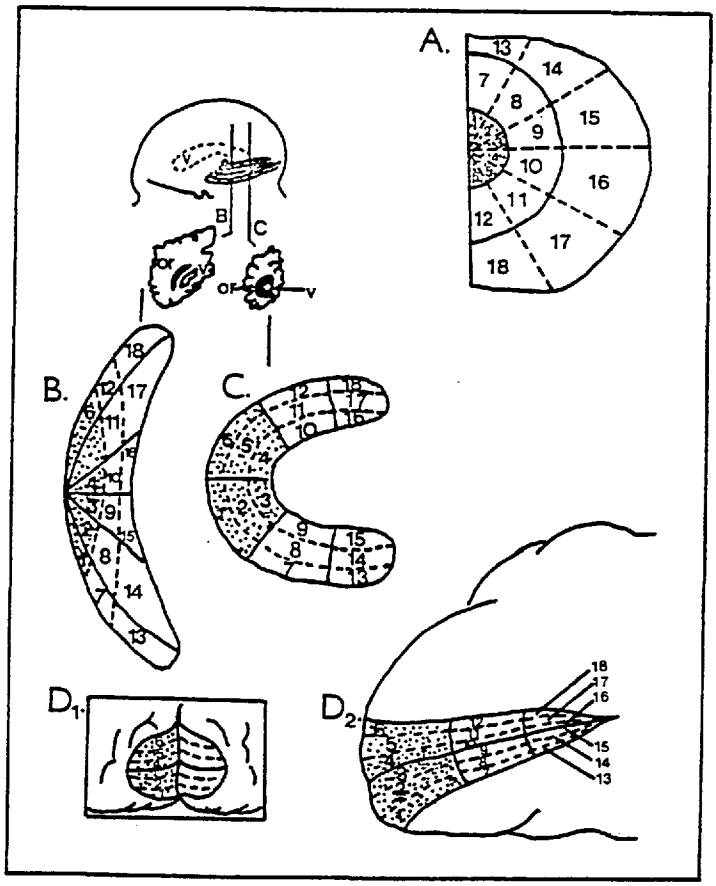

Fig. 6.1
Schematic representation illustrating the mapping of different sectors and concentric zones of the right homonymous half field (A) in the anterior part of the left optic radiation (B), the posterior part of that radiation (C), the lip of the left calcarine fissure (D_1), and the depth of the fissure (D_2). (Stippling indicates the macular and perimacular regions). The diagram on the upper left schematically indicates the two planes of cross section (B and C) of the optic radiation (ON) in relation to the ventricle (V). The macular fibres in the anterior part of the radiation (B) do not completely separate the more peripheral fibres (postulated by Polyak, 1957), but are concentrated at the lateral margin of the radiation. Only in its posterior plane (C) does the radiation have a distribution which conforms to Polyak's view. (after Spalding, 1952).

field in its ventral portion, whereas the fibres which correspond to the lower quadrants are carried in the most rostral portion. It is believed that the bundle of fibres which represent the homonymous halves of the macula are interposed between these peripheral

representations (Rønne, 1914 and 1919; Polyak, 1957).

Hughes (1954) proposed a standard form for this scheme. He suggested that a cross section of the optic radiation in its course from the posterior horn of the ventricle followed the shape of a 'C'. The uppermost segment of the C contains the lower quadrantic portion of the corresponding contralateral monocular crescent in the field of view, whilst the lowermost segment contains the upper quadrantic portion of the monocular crescent. Above and below these segments, the representations of the lower and upper peripheral quadrants are found, and it is in the middle of the C that the lower and upper quadrants of the macula are represented. Macula sparing is, therefore, very probable when the optic radiations are severed in the occipital lobe. At this stage it seems the central field has a lower vulnerability to damage because of the widespread macula representation in the optic radiation and cortex, and also the cortical macula has an improved vascular supply (Polyak, 1957). However, for man, at least in the anterior parts of the optic radiation, the macula fibres overlap with some peripheral representations.

The subject of this investigation is G.Y., a male, aged 21 years, who possessed normal vision, as far as is known, until the age of 7 years, when he was involved in a car accident. The results of subsequent medical examinations showed that the optic radiations in the left hemisphere had been severed. Consequently, the subject has a right field hemianopia with macula sparing. At the time of the accident, the subject suffered a strabismic squint, but this was eventually corrected using the 'patching' technique.

The homonymous hemianopia of subject G.Y. creates a visual field loss in the right hemifield of both right and left eyes, which means that it is in the temporal half of the visual field in the right eye, but on the nasal half of the visual field in the left eye. The temporal defect of the right eye will be more obvious to the subject than the corresponding nasal field defect in the left eye. The asymmetry in a defect of this kind parallels the asymmetry in the fibre spectrum of the optic nerve. Chacko (1948) reports that the fibres from the nasal retina have a different diameter to those in the temporal retina.

The aims of the present experiments were to examine possible visual field interactions between the normal and the 'blind' hemifield, and to examine the possibility of surviving responses within the 'blind' hemifield. Brindley, Lewin and Gautier-Smith (1969) have shown that patients who are blind as a result of general damage to the visual cortex, can achieve a brightness discrimination response, and other investigators have reported residual functions in the 'blind' hemifield of hemianopes such that they can even locate moving or flashing targets presented within their 'blind' hemifield (Pöppel, Held and Frost, 1973; Sanders et al., 1974; Weiskrantz et al., 1974; Perenin and Jeannerod, 1975 and 1978). It was suggested that such responses may arise in the pathway to the superior colliculus, which is the older (phylogenetically) visual system and has much coarser discrimination responses. Twenty per cent of the optic fibres pass directly to this structure (Wurtz and Mohler, 1976) and its cells have properties similar to those found in the visual cortex (Goldberg and Wurtz, 1972; Schiller and Vollman, 1974), except

that they are not orientation selective.

A.ii. Experimental Apparatus and Methods

Standard tests, the Ishi-hara Colour Vision test plates (Edition 1976) and the Julesz analglyphs (1971), were used to investigate G.Y.'s colour vision and stereoscopic fusion, respectively. The interferometer, which has been described in detail in section B, Chapter II, was used to investigate the responses of G.Y.'s visual system to monoptic and dichoptic presentation of spatially structured stimuli. The apparatus designed especially for motion detection experiments (Barbur, 1980) was used to determine G.Y.'s responses to flashed and moving targets presented to his right 'blind' hemifield.

B. Measurements

B.i. Preliminary Measurements

The measurements made to determine G.Y.'s stereoscopic fusion were performed in a manner similar to that described in section C.v, chapter IV, using the Julesz analglyphs. These figures test 'global' stereoscopy (Cowey and Porter, 1978) which appears to be mediated by mechanisms different from those responsible for 'fine' stereoscopy. G.Y.'s 'fine' stereoscopic discrimination was also tested with two rods, displaced in depth relative to the observer.

B.ii. Residual Functions in the 'Blind' Hemifield

Although G.Y. was clinically blind for stimuli presented to the right half-field, he could detect flashed and moving targets presented to the 'blind' visual field area. The visual fields of the subject

were investigated by measuring the threshold illumination level required for the detection of a white light, 1.2° diameter, circular target presented on a 48° diameter, circular, white light background field of illumination level 2.1 log trolands, presented to the observer in a Maxwellian view system (Barbur, 1980). Measurements were made with the target located at several different randomly selected locations within the 48° background field. The observer fixated voluntarily on a central 2° annular target, and reduced the illumination level of the target until it could 'just-no-longer' be detected. The target's position, defined relative to the fixation annulus, was noted, and a new test location presented by slowly moving the target across the field. These measurements were also repeated with the target presented in a 250 ms flash, at selected retinal locations.

Threshold illumination level required for the detection of flashed and moving targets by the 'blind' hemifield were measured as a function of background field illumination level, I_B, using the same apparatus. Two background field configurations were employed in these measurements. One consisted of a 17.5° diameter circle, of illumination level, I_B, surrounded by a larger 48° background field (see fig. 6.5) illumination level 0.05 I_B, and the second consisted of a circular 48° circular field of illumination level, I_B (see fig. 6.6). The circular target was 5.7° in diameter, presented either in a stationary mode for 250 ms, every 2.5s, or moving at a constant velocity of 39.8 s^{-1} along the horizontal meridian of the visual field. The target was presented 30° off-axis along the horizontal.

B.iii. Responses to spatially structured stimuli

The contrast threshold elevation effect (Blakemore and Campbell, 1969b; Maudarbocus and Ruddock, 1973b), and its binocular inhibition (Ruddock and Wigley, 1976) were both determined for G.Y. using the interferometric apparatus, described extensively in section B, chapter II, to produce the grating stimuli. The experimental procedure for these measurements has also been described previously in section B (chapter II) and in section B.ii,b.iii (chapter V). In all of these measurements, the magnitude of the adaptation effect, Δ, is calculated from equation 2.19 (section B, chapter II).

The visual field size and configurations for the three experiments are shown in fig. 5.2 (chapter V). The field subtended a visual angle of 30^{o} at the observer's eye. Figure 5.2a shows the adaptation field used in the monoptic experiments, performed with the right eye. Adaptation measurements were made with a test grating of fixed spatial frequency and a series of adaptation frequencies, covering a range between 0 and 12 cycles per degree. Figure 5.2b shows the dichoptic arrangement. In this case, the adaptation grating was presented to the left eye, and the test to the right eye. Figure 5.2c illustrates the field configuration used for the determination of the binocular inhibitory effect. The right eye views the adaptation and test grating pattern, which were of the same fixed frequency, whilst the left eye was stimulated by a grating, whose spatial frequency was set at different values in the range 0 to 12 $c/^{o}$. All of the data points represent the mean of at least three determinations, and were obtained for an illumination level set 4 log units above the threshold for the detection of the test grating.

C. Results

C.i. Preliminary Results

With each eye separately, or with both eyes together, observer G.Y. gave normal responses to the Ishihara Colour Vision test plates, thus establishing that the hemiopic condition has not impaired any properties associated with colour vision processes. His responses were far from normal to the Julesz analglyphs (Julesz, 1971), and under neither of the illumination conditions (section C.i, chapter IV) nor for different observation distances (Mollon et al., 1979) could observer G.Y. perceive any of the stereoimages contained in the analglyphs. This indicates that observer G.Y. possesses no 'global' stereoscopic function (Cowey and Porter, 1978). Fine stereoscopic function, i.e., the displacement of two images relative to one another, suffers no impairment, and is comparable to that of normal subjects. A similar case, involving a split brain patient (a technique used to relieve epilepsy), has been reported by Mitchell and Blakemore (1970) (see section C.vii, chapter I). This demonstrates that although 'global' stereoscopy can be retained in some subjects with cerebral lesions, it appears to be directly related to where the lesion has occurred in the visual pathways. G.Y., however, reports no difficulty in sporting activities, where a discrimination of distance and speed are essential. The car accident occurred when he was 7 years of age, and may therefore have been after the critical period for the formation of the binocularly driven cortical neurones (Hubel and Wiesel, 1970; Dews and Wiesel, 1970).

C.ii Visual Field Map

Figure 6.2 shows a plot of G.Y.'s threshold illumination levels, I_t, for different retinal locations over the centre $47^o \times 47^o$ visual field. This figure shows that there is a sharp increase in the threshold values at the vertical meridian, reflecting G.Y.'s inability to detect targets presented to the right hemifield. The plateau region on the right in this figure indicates the value of $\log I_t$ is equal to 4.5 log trolands, which is the maximum illumination setting available in the system (Barbur, 1980), and at this level G.Y. reports that he is unable to detect the target. There is an area of some 3^o to 4^o which extends around the fovea into the right hemifield, where G.Y. is able to detect the target. This represents macular sparing, which is not an uncommon characteristic of hemiopia (Teuber, Battersby and Bender, 1960), and although eye movements could account for this spread of sensitivity into the blind hemifield, sharpe changes in sensitivity

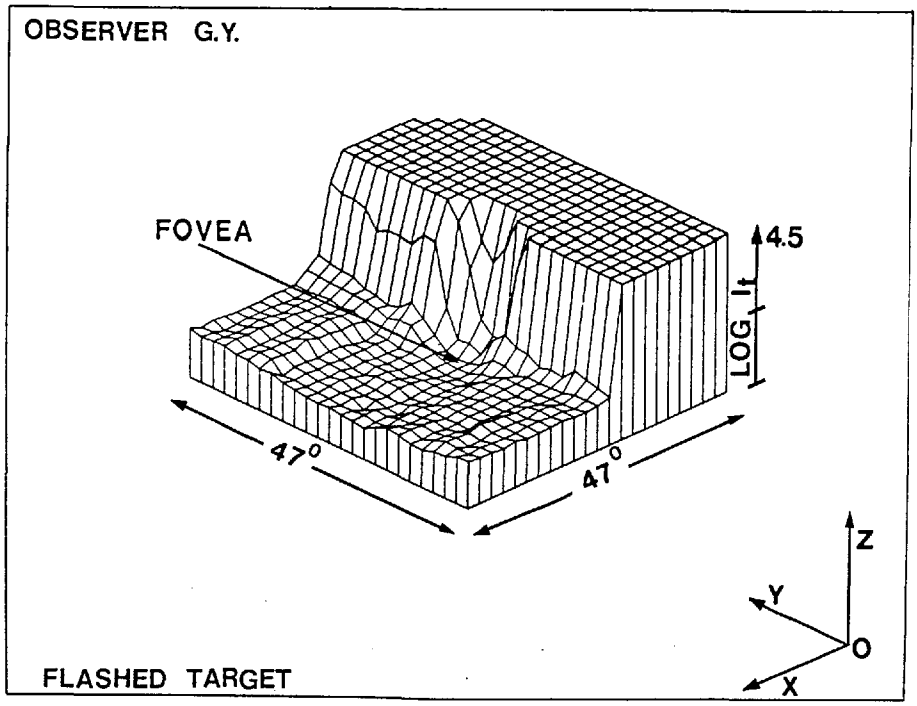

Fig. 6.2 A 3-D map of the visual field of observer G.Y. The Z co-ordinate is proportional to the log of the stimulus luminance.

along the vertical meridian are shown in fig. 6.2, at non-foveal locations. G.Y. does, however, report an awareness of some visual sensitivity extending into his blind hemifield when he is fixating centrally on a small target. Comparison data for a normal subject, J.B., are shown in fig. 6.3, and the most notable feature of his data is the increase in the threshold level, I_t, around the blind spot.

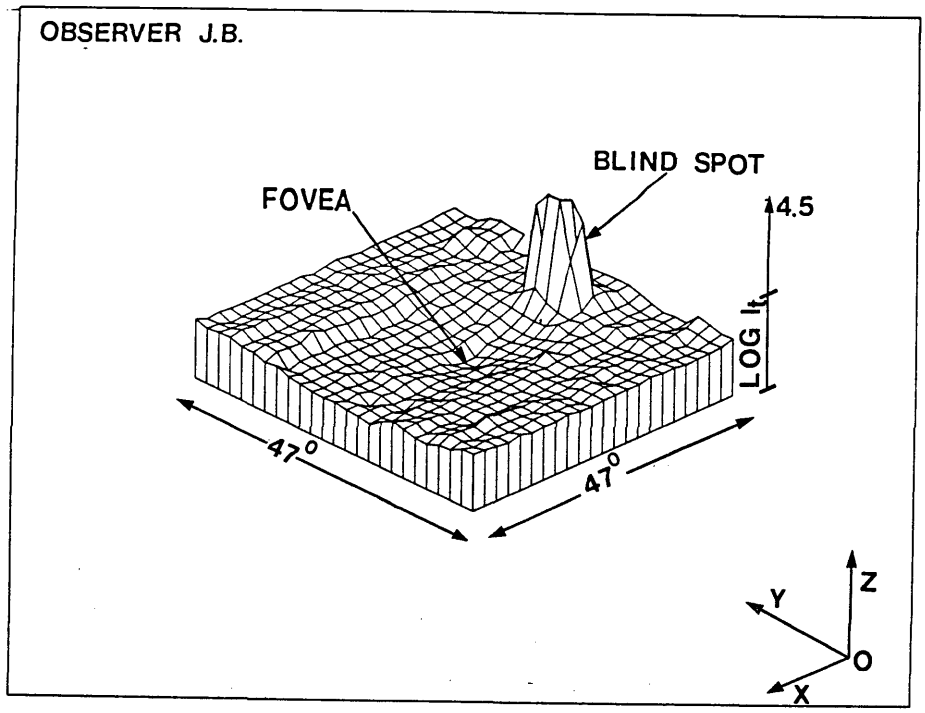

Fig. 6.3 A 3-D map of the visual field of observer J.B., for comparison to that of observer G.Y. (fig. 6.2).

Data obtained with a flashing target are shown in fig. 6.4 and shows G.Y. is able to detect a <u>flashed</u> target deeper into the 'blind' hemifield, up to some 10^{o}, but he is unable to detect stationary targets at any point in the 'blind' hemifield. The blind spot was not revealed in any of these measurements with G.Y., because of the relatively large targets used. G.Y. reports, subjectively, that a flashed target of near threshold illumination level appears as a 'dark' shadow, located in the 'blind' hemifield, whereas at higher illumination levels, its appearance changes to that of a localized, bright flash. The following tests were made in an attempt

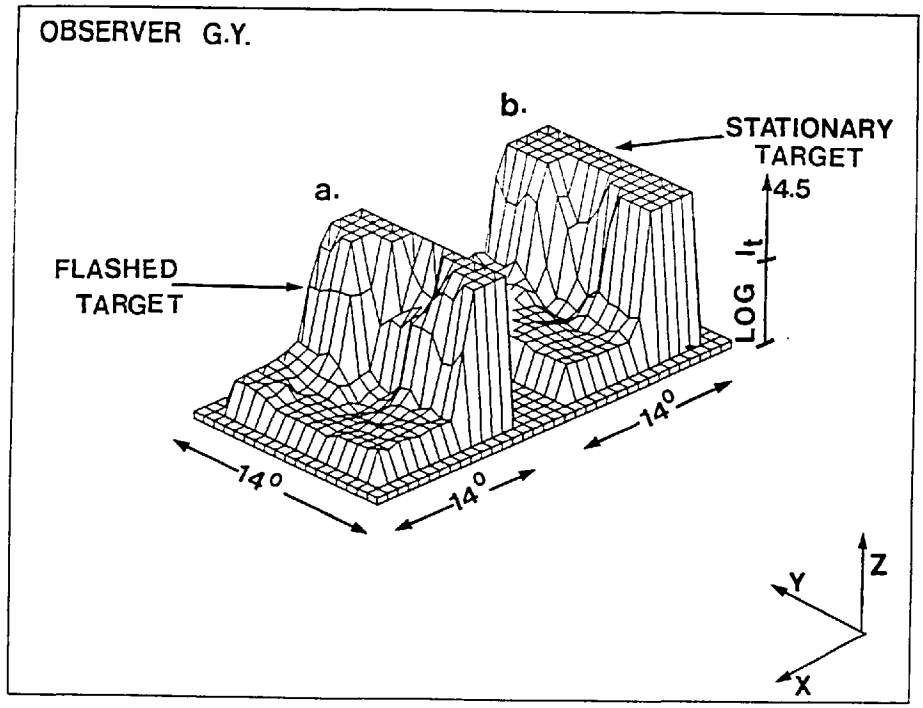

to examine the possible contribution of scattered light to G.Y.'s detection of flashed targets.

Fig. 6.4 Two 3-D maps of the visual field of observer G.Y. (centre 14^{o} x 14^{o}). The Z co-ordinate is proportional to the log of the stimulus luminance required for the threshold detection of a. a flashed target, b. a stationary target, of similar dimensions.

Increment threshold sensitivity curves obtained for G.Y.'s 'blind' hemifield to flashed and moving targets, presented 30^{o} off-axis are plotted in fig. 6.5. The ordinate shows the logarithm of the threshold sensitivity, log I_t, as a function of the logarithm of the background illumination level, log I_B. The results for the stationary targets are represented by squares (□), and those for the moving target by triangles (△). The full squares (■) represent the comparison data for G.Y.'s normal hemifield obtained with a stationary flashed target similarly located. The relationship between log I_t and log I_B, in fig. 6.5, is similar for all three sets of data; the values obtained in the 'blind' hemifield are increased by some 2 log units compared to those obtained for the normal hemifield. The results

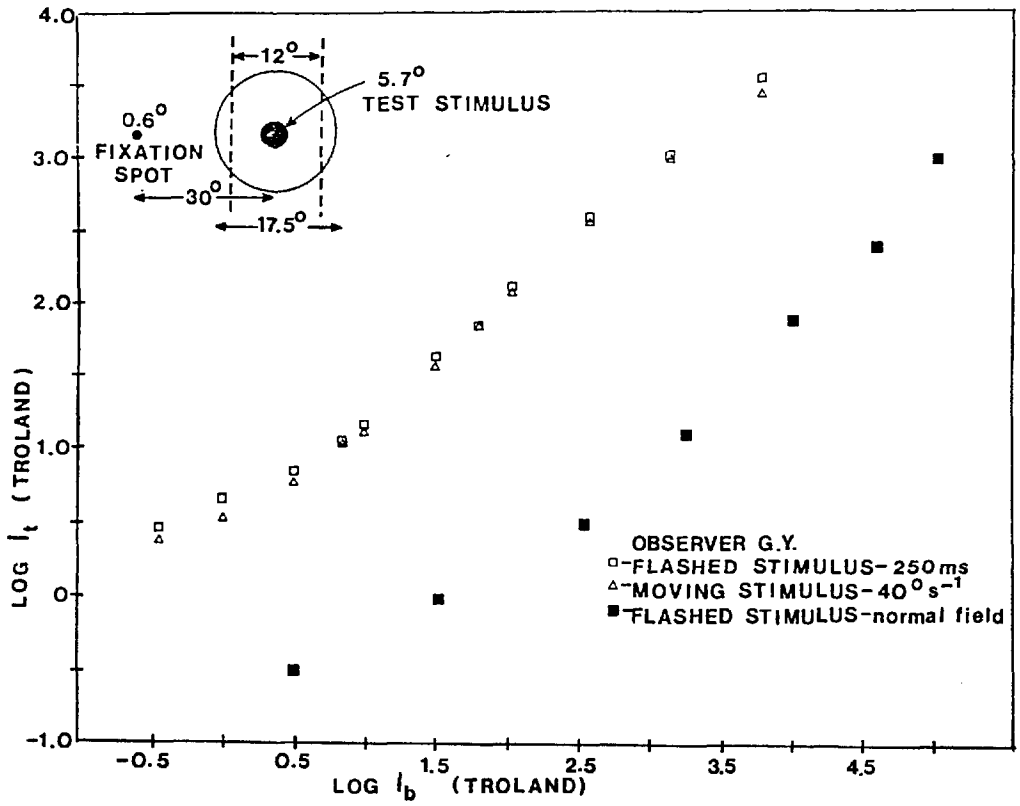

Fig. 6.5
Increment threshold sensitivity curves for G.Y.'s 'blind' hemifield for targets presented 30° off-axis; □ - for stationary targets, △ - for moving targets, ■ - for flashed targets 30° off-axis in G.Y.'s normal hemifield.

obtained for the full 48° background field are plotted in fig. 6.6, and these results are very similar to those for the smaller background field, except that when $I_B \leq 0.5$ log troland, the thresholds for the moving targets are greater for the 48° background field. This implies that raising the illumination level of the 48° field from 0.5 to 2.0 log trolands, i.e., by a factor of 30, does not influence G.Y.'s threshold for detection, even though the field covers the parafoveal region of the normal hemifield, where it is most likely that scattered light would be detected. The data of fig. 6.5 provides evidence to indicate that G.Y. is not detecting light scattered into the normal

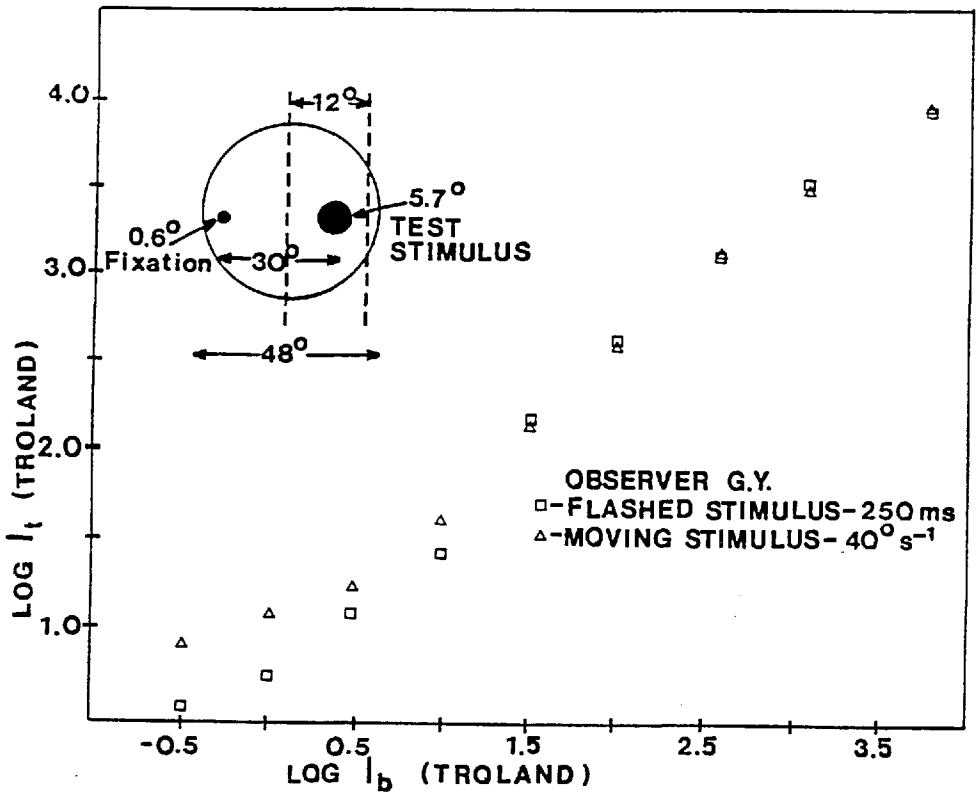

Fig. 6.6 Increment threshold sensitivity curves for the full 48° background field.

hemifield, except possibly when detecting moving targets against background fields of very low illumination levels.

C.iii. Binocular Adaptation to Grating Stimuli

The contrast threshold elevation effect for the monoptic presentation of the test and adaptation gratings is shown in fig. 6.7.

The effect of adaptation on the threshold illumination level, measured in terms of Δ, is plotted against the spatial frequency of the adaptation grating, f_a, expressed in cycles per degree. The spatial frequency of the test grating stimulus is fixed at 7 c/°. Equivalent data for dichoptic presentation of the test and adaptation gratings are plotted in fig. 6.8.

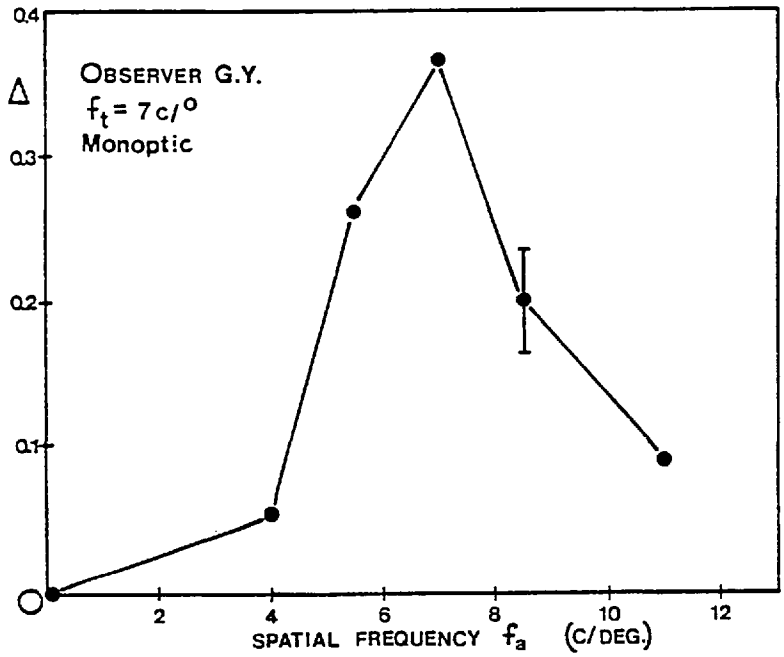

Fig. 6.7 Contrast threshold elevation effect for monoptic presentation of test and adaptation gratings. The test grating has a fixed spatial frequency of 7 c/°, and the bar denotes the typical standard error. Observer G.Y.

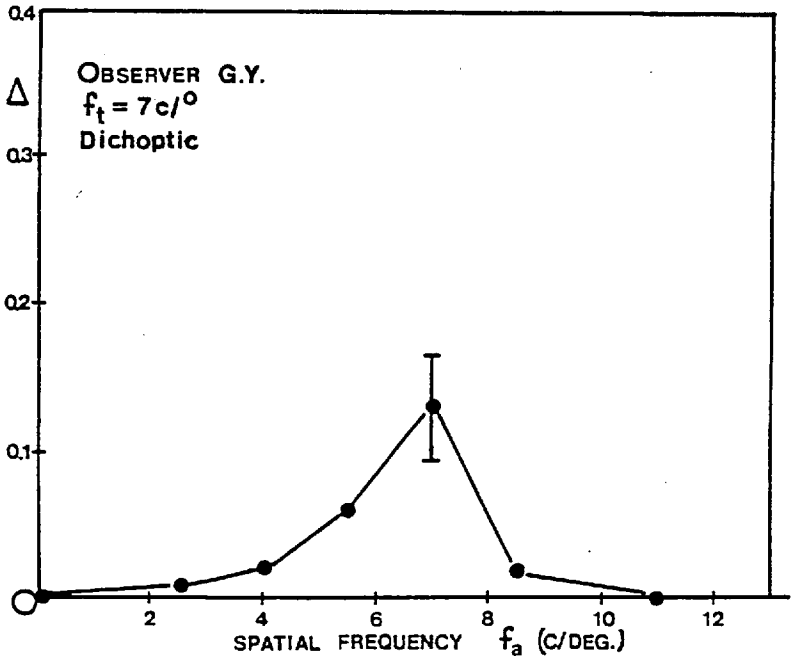

Fig. 6.8 As in fig. 6.7, but for dichoptic presentation of adaptation and test grating stimuli. Observer G.Y.

Data for the adaptation of both eyes (see fig. 5.2c and section B.ii, b.iii, chapter V) are given in fig. 6.9. In this case, both the test and adaptation gratings presented to the right eye were of spatial frequency 7 c/°, and the spatial frequency of the adaptation grating in the left eye (the conditioning grating) was the experimental variable.

Values of Δ for different conditioning grating frequencies are plotted in fig. 6.10a. In addition to the data for

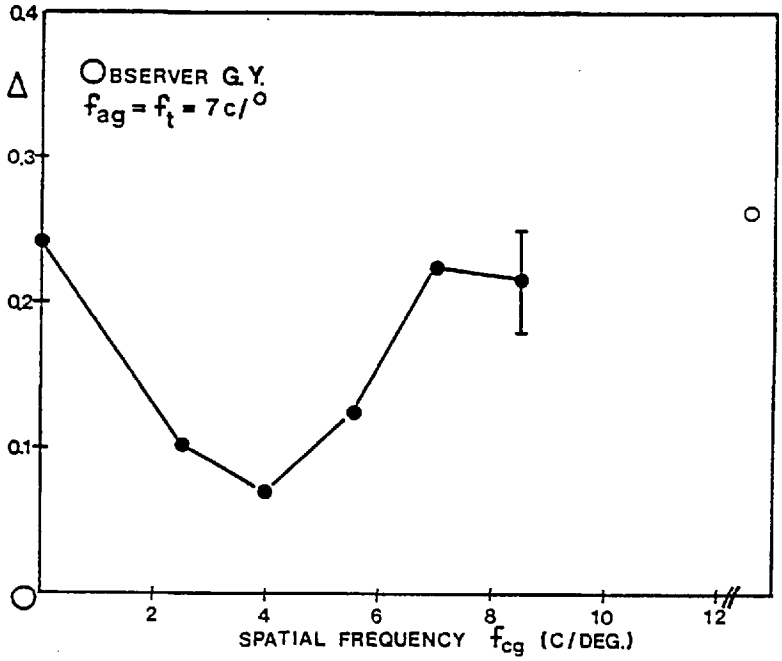

Fig. 6.9 Adaptation effect, Δ, plotted against fcg, the spatial frequency of the conditioning grating. Error bar denotes the typical standard deviation of at least four readings. The separate data point to the right of the ordinate scale denotes the values of Δ obtained in the absence of the conditioning grating presented to the left eye. The test and adaptation gratings, of spatial frequency 7 $c/^o$, were presented to the right eye.

G.Y., who possesses 'fine' but not 'global' stereoscopy, data are given for three other subjects. Two of these subjects (A.C., male, aged 24 years and D.P., male, aged 21 years) have stereoblind vision, the result of congenital strabismus, and the third is the albino subject D.C. (see fig. 6.10b), whose visual characteristics have been described in chapter V, and who also lacks stereoscopic vision. None of these last three subjects show stereoscopy of either kind.

The experimental data, in fig. 6.7, shows that the maximum contrast threshold elevation effect for monoptic presentation of the grating field occurs when the spatial frequencies of the test and adaptation are identical. There is no significant effect when the ratio of the test and adaptation frequencies falls below 0.5 or is increased beyond 2.0. The data is comparable to that found in previous investigations (Blakemore and Campbell, 1969b; Maudarbocus

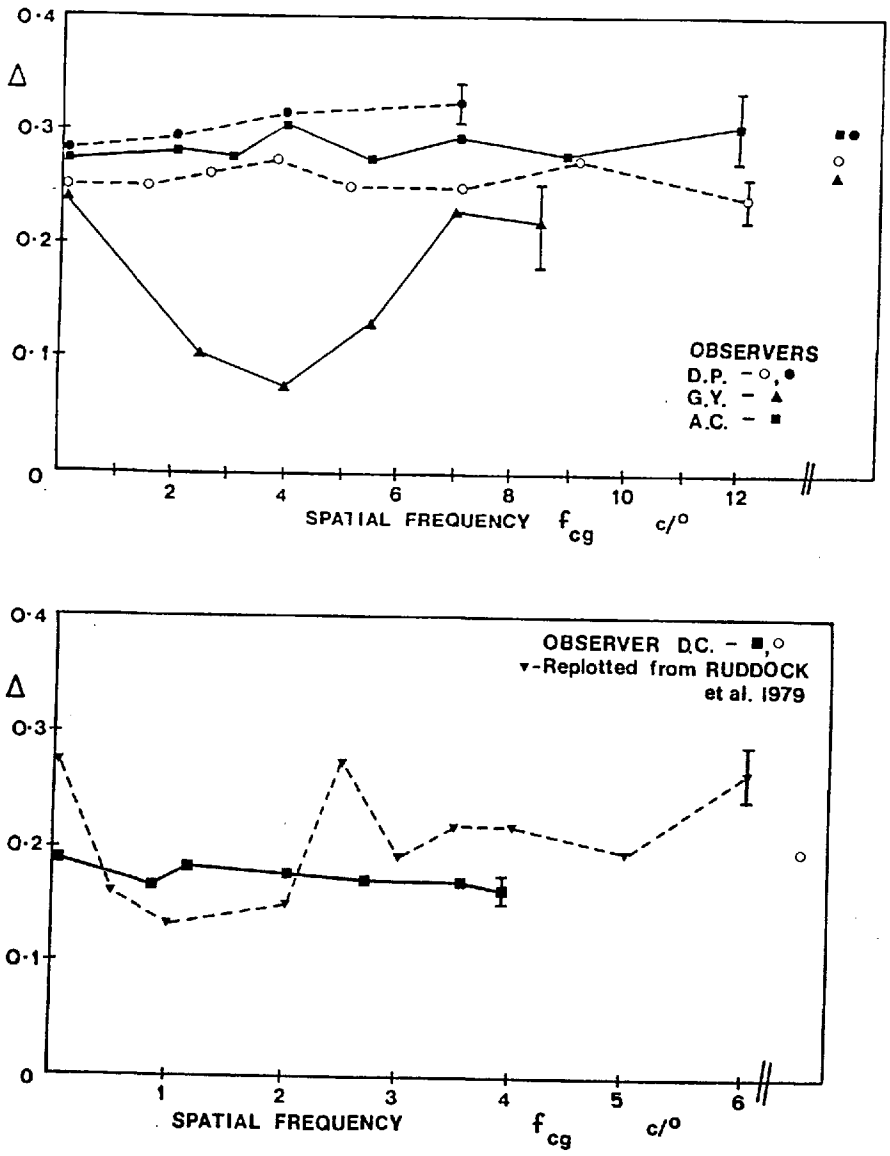

Fig. 6.10
As in fig. 6.9; a. data for stereo-blind subjects D.P. (○, ●) and A.C. (■), and for the subject with fine but not global stereoscopy, G.Y. (▲), b. data for the albino subject, D.C. (■,○), and for a normal subject, E.W. (▼). The spatial frequency of the test and adaptation gratings, in this case, was 2 c/° (D.C.) and 2.5 c/° (E.W.), with other stimulus parameters as before.

and Ruddock, 1973b). In contrast, the data obtained under the dichoptic stimulus configuration (see fig. 6.8) differs significantly both in magnitude and bandwidth selectivity from the experimental data obtained with normal subjects. This deviation from normal visual responses can probably be attributed to the disturbance of the visual pathways incurred as a consequence of the road accident.

Data for the binocular inhibitory effect, shown in fig. 6.9,

reveal a normal response for observer G.Y., with suppression of the adaptation effect for conditioning gratings with spatial frequencies in the range 0 c/^{o} to 6 c/^{o}. Thus, although G.Y. has one optic radiation severed, the two eyes interact to produce binocular suppression of the contrast threshold elevation effect. In contrast, the data for the stereo-blind observers, shown in fig. 6.10a and b, yield an insignificant binocular inhibition of the contrast threshold elevation effect when compared with the normal response data, in fig. 6.10b. This reflects the lack of interaction between their two eyes.

D. Discussion

The visual field maps, shown in fig. 6.2 and fig. 6.4, emphasize the influence of the mode of stimulus presentation on G.Y.'s visual responses. Many other cases of macular sparing involving hemiopic vision have been reported (Teuber, Battersby and Bender, 1960), and the responsiveness of the 'blind' hemifield is not entirely unexpected in view of the previous studies (Riddoch, 1917; Pöppel, Held and Frost, 1973; Weiskrantz, Warrington, Sanders and Marshall, 1974; Perenin and Jeannerod, 1978). The field map also shows that he has relatively high sensitivity to flashed targets.

The change in the increment threshold level with increasing background illumination level is similar to that found for the normal eye. The threshold values, log I_t, are, however, approximately 100 times greater for G.Y.'s 'blind' hemifield responses than for normal vision (see fig. 6.5), which implies that the projection pathway responsible for the responses arising in the 'blind' hemifield require

signals of a much higher level for target detection than are required by the pathways leading directly to the visual cortex.

Investigations, using ablation techniques on the visual cortices of animals, have shown that they are still capable of performing visual discriminations, provided the superior colliculus remains intact (Sprague, 1966; Pasik and Pasik, 1965; Schneider, 1969; Weiskrantz, 1972; Mohler and Wurtz, 1977). As a consequence, this implies that in humans with cortical lesions, the visual responses which can be elicited from the visual field areas, which should project to the damaged cortical region, reflect activity in the collicular pathways. The response characteristics of G.Y.'s blind hemifield correlate well with those of the collicular units, since electrophysiologically, it has been shown that collicular units are selectively sensitive to flashed or moving targets (Wurtz and Goldberg, 1972).

Despite the loss of cortical input from one optic radiation, G.Y. shows normal responses for binocular adaptation stimuli. His two eyes do interact to produce a binocular suppression of the contrast threshold elevation effect. This may simply reflect the fact that this binocular interaction is restricted to the region around the fovea (Ruddock, Waterfield and Wigley, 1979) and, as is shown by his threshold sensitivity data (see fig. 6.5 and fig. 6.6), normal foveal vision is present in both half fields.

It is noteworthy, however, that G.Y. possesses 'fine', but not 'global', stereoscopy, and it was originally suggested, when the binocular suppression of the contrast threshold elevation effect was first discovered (Ruddock and Wigley, 1976), that it may reflect

activity of the mechanism responsible for fine stereoscopic discrimination. Figure 6.10 shows the data for all four subjects compared to the results of a normal observer E.W. (replotted from Ruddock and Wigley, 1976) and this demonstrates that G.Y. shows normal binocular suppression of the contrast threshold elevation effect, although with slightly wider bandwidth selectivity compared to E.W. The data of subjects who lack any stereoscopic function, show an insignificant binocular suppression of the contrast threshold elevation effect. Thus, it may be concluded that in fact the binocular inhibitory effect is a function mediated by the same mechanism as that which produces 'fine' stereoscopic discrimination. It further establishes that the two kinds of stereoscopic vision can be functionally differentiated.

Chapter VII

Summary and General Conclusion

The aim of the experimental work, in this thesis, has been to investigate the mechanisms of colour and spatial pattern discrimination in human subjects who possess both normal and abnormal visual pathways. The major part of the investigation has used adaptation methods, with both one- and two-dimensional spatially structured stimuli. The study falls into two discrete parts, the first of which describes a new experimental method for the derivation of post-receptoral spectral response functions (see chapter III). The other is concerned with different aspects of visual responses in subjects with abnormal visual function.

In chapter III, it has been shown that by a suitable choice of stimulus parameters, adaptation effects associated with the perception of spatially structured stimuli exhibit narrow-band spectral response curves. The method is derived from the contrast threshold elevation effect (Blakemore and Campbell, 1969b) and the associated inhibitory binocular interaction effect (Ruddock and Wigley, 1976). The essential differences between the adaptation effects relating to elongated bar-shaped and non-elongated spot-shaped stimuli, in orientation selectivity and binocular organization, had already been found (Burton and Ruddock, 1978; Naghshineh and Ruddock, 1978) and the method, (see chapter III), establishes that the adaptation effects, employing non-elongated stimuli, are colour selective in their binocular interaction during adaptation.

The experimental method allows the post-receptoral spectral response functions to be determined, without any pre-assumption about the nature of the post-receptoral neural organization. Three independent response mechanisms have been found, and are shown in fig. 3.31, in fig. 3.32 and in fig. 3.33. Figure 3.31 represents an 'R - G' opponent mechanism, and has a narrow-band long wavelength component, with a peak spectral sensitivity at 610 nm, and a half-bandwidth of some 50 nm. It also shows a broad-band short wavelength component of opposite polarity, with a 'neutral point' (representing the change-over from an excitatory to an inhibitory response) at 530 nm. The second mechanism, shown in fig. 3.32, represents a broad-band response mechanism with spectral characteristics similar to those of the photopic spectral response mechanism. It has a peak spectral sensitivity at 530 nm, a half-bandwidth of some 70 nm, and can be modelled by a 'G - R' type mechanism, although the experimental data failed to show any opponency. Figure 3.33 shows the third mechanism, a blue-sensitive response function. This has a peak spectral sensitivity at 450 nm, and it exhibits spectral characteristics very similar to those of the π_1 spectral sensitivity mechanism of Stiles (1959). In addition to these, there is a broad-band interaction, revealed in experiments conducted entirely with bars or entirely with spots, which has a spectral response equivalent to the normal photopic spectral sensitivity curve. Although exhaustive measurements were performed with different stimulus parameters, the possibility exists that yet other spectral response mechanisms could be revealed with other stimulus parameters and configurations.

The spectral response functions, shown in fig. 3.31, in fig. 3.32

and in fig. 3.33, are consistent with the following functional model of colour vision at the post-receptoral level of the human visual system. The signals from the three spectrally independent classes of receptor are encoded by two independent classes of neural channel, a colour-opponent channel and a luminance channel. The spectral sensitivities of the three sensitive receptors, red, green and blue, can be identified with the Π_5, Π_4 and Π_1 spectral sensitivity mechanisms, respectively (Estévez and Cavonius, 1977; Pugh and Mollon, 1979), and the signals from the red- and green-sensitive receptoral classes are processed linearly prior to the site of the threshold interaction in the central colour-opponent unit.

The post-receptoral spectral response curves, shown in fig. 3.31, in fig. 3.32 and in fig. 3.33, are of the kind observed electrophysiologically in the activity of lateral geniculate and visual cortical neurones (De Valois, Abramov and Jacobs, 1966; Wiesel and Hubel, 1966 and Gouras, 1974). The fact that these colour dependent central responses have been observed with two-dimensional spot patterns, rather than purely one-dimensional grating patterns, is also consistent with the electrophysiological observation that cortical neurones, which yield colour selective responses, usually have non-oriented receptive fields, whereas those with oriented receptive fields are usually non-colour selective in their response characteristics (Hubel and Wiesel, 1968; Gouras, 1974).

The experimental data, shown in fig. 3.28, reveal that measurements with a subject possessing a congenital dichromatic colour vision defect, deuteranopia, yield significant modification of the normal response pattern (see fig. 3.17). Thus, the method described

could be particularly useful in the analysis and classification of acquired colour vision defects, and may also help to resolve the conflicting interpretations of congenital red-green colour defects (Nunn and Ruddock, 1978; Alpern, 1979).

Investigation of the central colour vision defect in subject M.W. (see chapter IV) confirmed his gross insensitivity to red light stimuli, and demonstrated that although he is unable to perceive red spectral patterns, they can contribute to his visual responses, such as stereoscopic vision and binocular rivalry. He also exhibits the contrast threshold elevation effect with grating patterns, although figure 4.11 shows that, in his case, there is some abnormal bandwidth selectivity. In comparison with normal data, M.W.'s visual acuity is greatly reduced for stimulus wavelengths, $\lambda \geq 580$ nm, for which he also has low response sensitivity, and which appear 'silvery-grey' to him. In the other regions of the spectrum, 470 nm $\geq \lambda \leq$ 540 nm, his acuity is comparable with that of a normal observer, under similar experimental conditions, and therefore his visual system is capable of high spatial resolution. This is also true for motion detection, where M.W. gives near normal response to green light, but grossly abnormal ones to red light (Barbur, Ruddock and Waterfield, 1979).

The data for M.W. has also been examined in relation to the proposed structural and functional organization of the visual cortex. Recent electrophysiological and anatomical studies of primate visual systems (Hubel and Wiesel, 1968, 1970; Zeki, 1978c,d; Cowey, 1979) have shown that single cortical neurones possess a high degree of specificity in response to the various stimulus attributes, and that

the multiple projection maps of the visual field, each has a specific associated response, i.e., colour discrimination (area V4, Zeki, 1978d), or motion detection (superior temporal sulcus (STS), Zeki, 1978d). The experimental data of chapter IV do not support the hypothesis that different parameters, of the retinal image, are independently analysed in the separate visual areas of the cortex, but suggests that the central mechanisms responsible for colour, motion and spatial structure are interdependent, since a colour anomaly within the central visual pathways seems to affect all three of these functions.

M.W. has also provided evidence on the nature of visual responses to visual images, which produce distortions, termed visual illusions. It has been proposed both that these arise from distortions introduced into the signals as they are relayed along the visual pathways (Ginsburg, 1975), and that they are due to some central cognitive processing (Gregory, 1966, 1972). The experimental results of chapter IV establish that it is possible to divide the illusions into two groups; those such as the Kanizsa triangle, which can still be perceived by M.W., even though he fails to resolve all the elements in the pattern, and those such as the Müller-Lyer illusion, which require perception of all the pattern's elements for the illusion to be perceived. It is concluded that the first group of illusions (Group A, chapter IV) cannot be dependent upon the activity of cognitive mechanisms, and must result from distortions introduced into the signals during transmission along the visual pathways. The second group of illusions (Group B, chapter IV) may be the result of signal distortion arising in the transmission mechanisms, located more

centrally than the site of M.W.'s defect, or, indeed, may result from cognitive processing of visual images (Gregory, 1972).

The analysis of the visual responses of the albino subject (see chapter V) suggest, in contrast to previous reports (Pickford, 1958), that albinos do not exhibit any intrinsic colour vision anomaly. The gross impairment of his visual acuity is reflected in all of his visual responses, which are all confined to a very low and limited range of spatial frequencies. His threshold responses to 'beat' detection lead to the conclusion that this abnormal low-pass filter must be situated at a post-receptoral level in the visual system, such that the conditions for 'beat' detection (Burton, 1973) are satisfied. These are that beats can only be detected on the assumption that visual resolution is not set at the photoreceptor level, and also that non-linear processing of the illumination must occur in a mechanism, prior to that which sets the limit of D.C.'s resolving power. It seems likely that the abnormal post-receptoral responses are caused by abnormal development in response to blurred images on receptive fields associated with ganglion cells and lateral geniculate neurones, as has been described electrophysiologically by Ikeda and Tremain (1979).

Measurements of inhibitory binocular interaction suggest that in contrast to normal subjects, where the transcallosal fibres of the corpus callosum perform the function of linking together the two half-field representations in the two hemispheres of the visual cortex (Zeki, 1978e), there is no such function in the albino because there is mapping of the whole visual field onto each hemisphere. The data also suggests that any interocular transfer is absent, and there is no

inhibitory binocular interaction between the two eyes. This can be taken to imply one of two things; either the transcallosal fibres, if present, are devoid of any functional capacity, or that they are not responsible for transmitting signals interocularly, nor the inhibitory effect of the conditioning grating (Ruddock and Wigley, 1976).

The study of hemianopic vision (see chapter VI) has established that the retino-cortical pathway does not carry all of the afferent signals relating to the retinal image, and some response can be elicited by stimulation of the non-cortical pathways. Psychophysical analysis of the responses in these pathways is not usually possible, because the cortical pathway dominates in such studies. Understanding of these pathways is none-the-less of great consequence, because they serve important functions in the visual orientation of animals in space (Sprague, 1966; Schneider, 1969; Mohler and Wurtz, 1976).

The investigation described in this thesis has revealed a number of new functional aspects of central visual processing in man. The new method for the investigation of central colour vision organization should find further application in the study of congenital and acquired colour vision deficiencies, and the 'beat' method analysis of the albino's visual acuity is the first application of this potentially powerful method in the study of abnormal visual pathways. Extension of the methods used in these studies should provide further insight into the organization of central visual processes in man. The reliability and invariant nature of visual processing under change of image magnification, rotation, displacement and distortion require powerful analysis which has yet to be demonstrated by psychophysical experiments.

A P P E N D I C E S

A P P E N D I C E S

APPENDIX A

A1: Timer Control Unit

Visual psychophysical experiments require the presentation of one or more visual stimuli for durations ranging from a few milliseconds to several seconds. The timing pulses for such experiments were derived from a set of precision timing elements (Ferranti, No. ZN 1034E), which were used to drive electromagnetic shutters (see fig. 2.3 and fig. 2.15, SH1 to SH4, chapter II) via Darlington amplifiers. A circuit diagram which illustrates schematically the timing elements and the shutter circuitry is shown in fig.A.1.

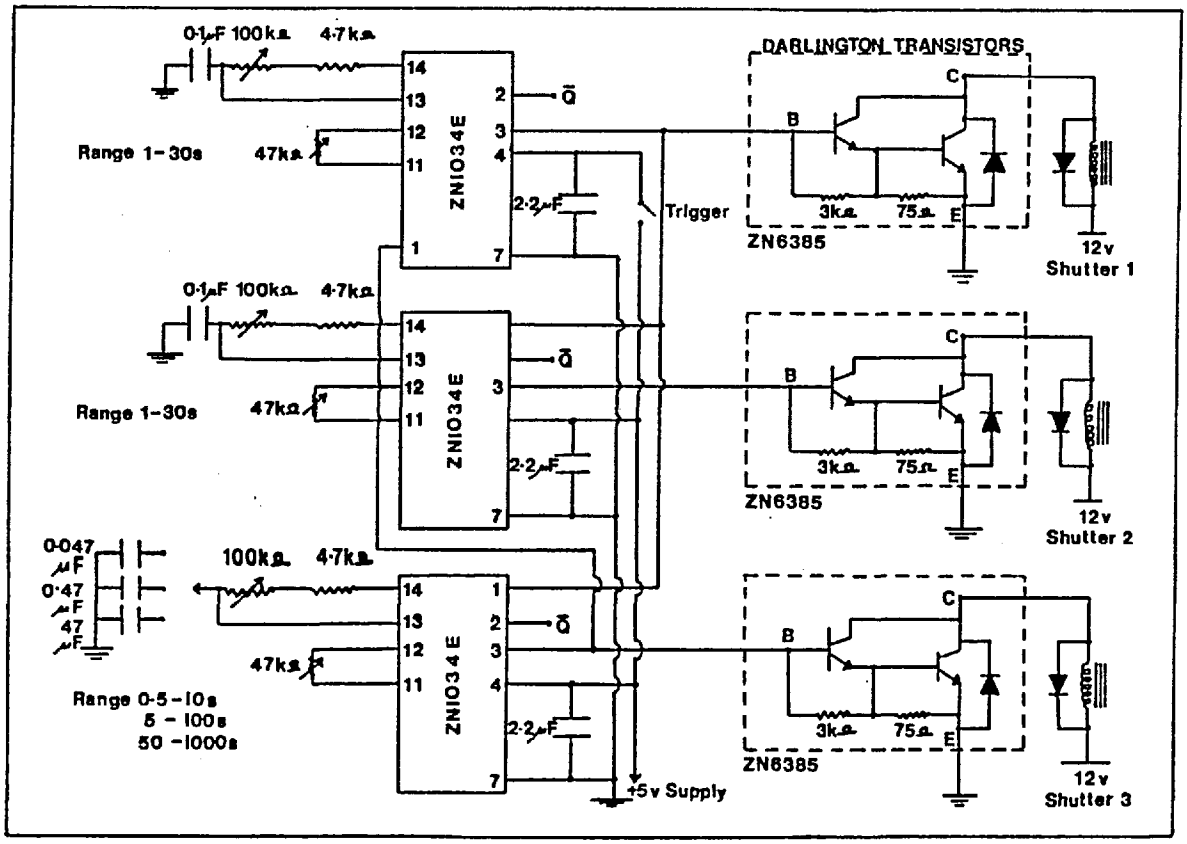

Fig. A.1 Schematic representation of the electronic circuit used for generation of timing pulses and the driving of electromagnetic shutters. (See text for details).

The duration of the pulses generated is fixed by the frequency of an interval oscillator (Unit, No. ZN 1034E) which can be altered either in steps, by means of externally connected capacitors, or continuously, by means of a 100 kilo-ohm ten-turn precision potentiometer. The duration of the output signal was measured digitally to the nearest millisecond for each potentiometer setting of interest and a typical potentiometer calibration curve is shown in fig. A.2.

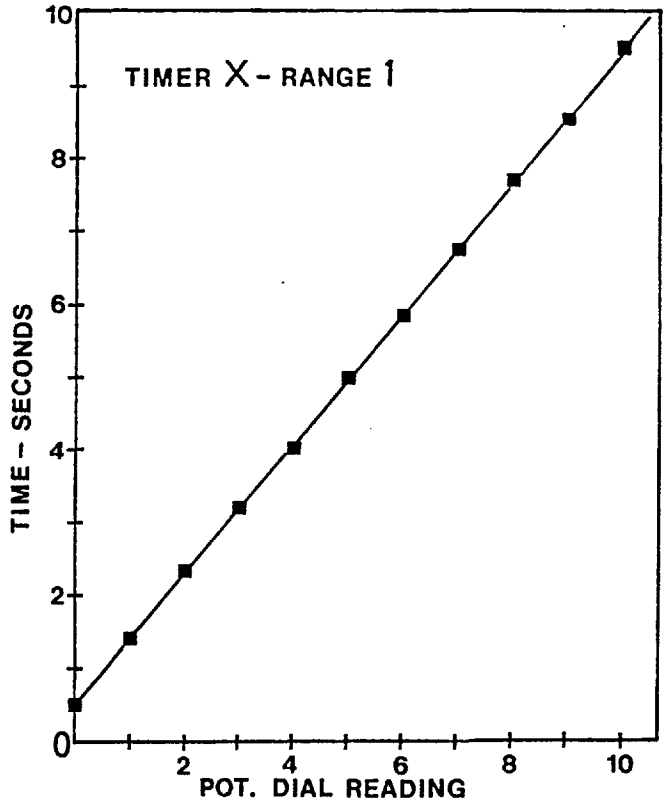

Fig. A.2 Pulse duration measurements plotted against potentiometer setting for an externally connected capacitor of 0.047 uF. The duration of the timer signals was measured digitally, to the nearest millisecond, using a commercial digital timer unit (DEVICES Digitimer).

The timing sequence is initiated by pressing the trigger switch (see fig. A.1), and the inverted ($\bar{Q}$) and the non-inverted (Q) outputs of the timing elements can be arranged so as to produce sequential presentation of four stimulus channels (see section A.ii, chapter II). The duration of each stimulus presentation is set by the choice of the external capacitor and the appropriate adjustment of the ten-turn potentiometer. The shutter driving circuitry was activated by the inverted or non-inverted voltage outputs of the timing elements via Darlington power

transistors (see fig. A.1, No. ZN 6385).

The arrangement described in this appendix provided facilities for the sequential presentation of three/four stimulus channels. It is simple to construct and eliminates the need for expensive commercial digital timing units.

APPENDIX B

B1: Counter Unit and Buzzer Circuitry

The size of measurement errors in psychophysical experiments is primarily determined by the precision of the apparatus and the judgement consistency of the observer in achieving a threshold criterion. The mean value of a finite number of independent measurements represents an unbiased estimate of the population mean from which the measurements are taken. The number of measurements in the sample determines the accuracy of the estimate, and extensive measurements of threshold illumination level required for the detection of a flashed target (e.g., the most common form of measurement in the experiments) indicate that six to seven measurements are required for a ± 0.04 log unit range in the estimate of population mean at the 95% confidence level. If the effects measured are large, a smaller number of measurements may provide a sufficiently accurate estimate of population mean.

The buzzer unit, shown in fig. B.1, was designed to count a set number of measurements, which was specified from a B.C.D. switch setting made at the beginning of the experimental session, and to produce an audible 20 ms signal at the end of each set of measurements. The signals generated on the pressing of the detection switch (see Chapter II, Section A) were countered by a Decade Counter (SN7490). The counted pulses were continuously compared with the output of a B.C.D. switch, which was used to specify the number of measurements required for an estimation of the population mean. The comparator unit was made from NAND gates (SN7400) and its output

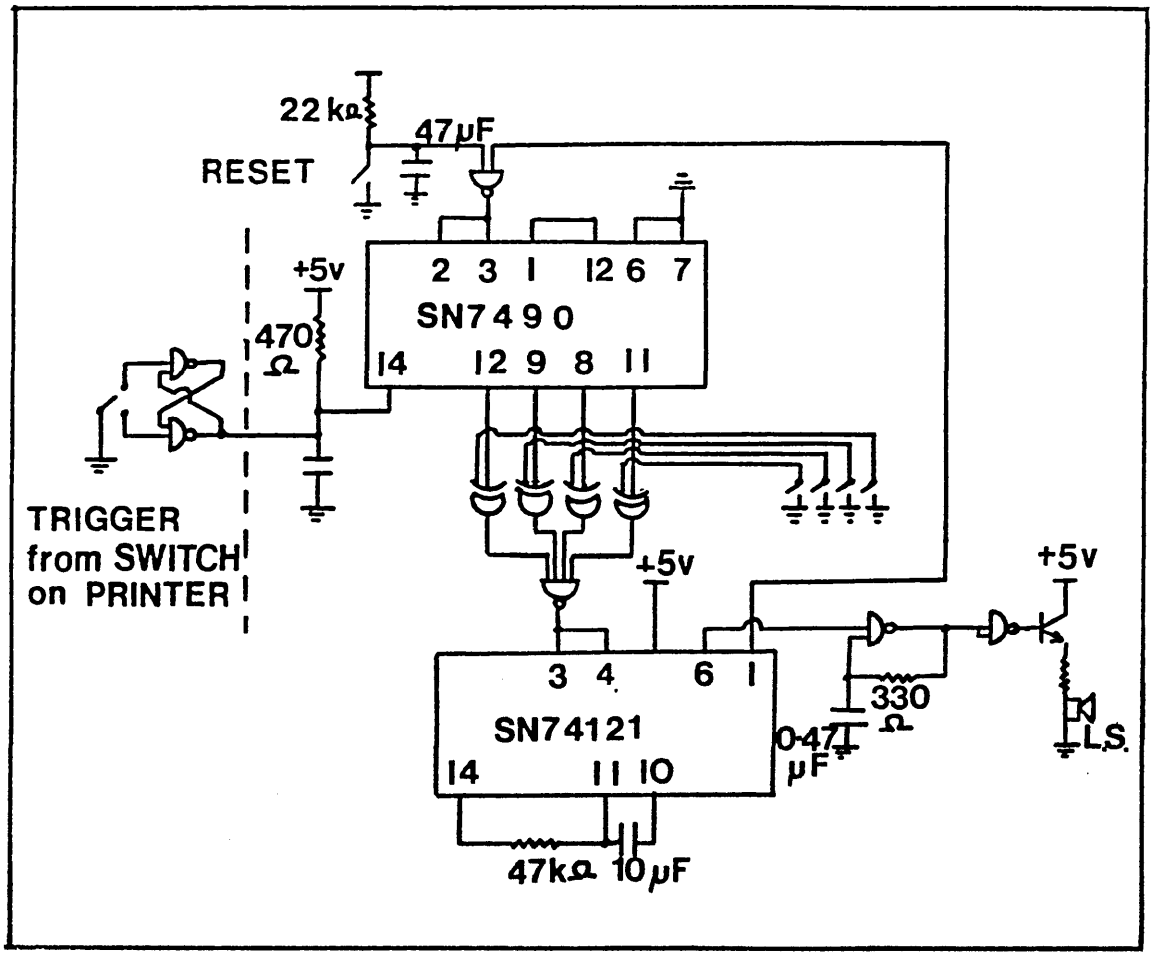

Fig. B.1 Counter Unit and Buzzer Circuitry

triggered a monostable multivibrator (SN74121) which produced a 20 ms pulse. The generated signal was used to drive a small loudspeaker (L.S., fig. B.1) via a BC184 transistor. The un-inverted output of the multivibrator was used to zero the decade counter as required for a new set of measurements.

Most experimental results were obtained by averaging at least six or seven measurements. In some long experimental sessions, however, and in particular in experiments with defective subjects, averages were made for three or four measurements, because in these cases the time for measurements was restricted.

APPENDIX C

Computer Programmes

This appendix contains details of the computer programmes which were written in order to produce some of the stimulus patterns, and also to compute meaningful results from the psychophysical data.

C1: Stimulus Pattern Generation

Several FORTRAN programmes were written to allow circular or linear patterns to be produced on the face of a high resolution terminal connected to the University of London computer centre. The generated patterns were photographed on 35 mm binary film, and the resulting negatives were copied photographically onto high contrast film, for which the optical density difference between the light and the dark areas is at least 3 log units.

A typical programme which was written to produce two-dimensional arrays of spots of various diameters and interspot separations (as required for the experimental investigations described in Chapter III) is listed below:-

```
PROGRAM DOTS(DATAVW,OUTPUT,TAPE5=DATAVW, TAPE6=OUTPUT,TAPE62)
CALL START(2)
DO60I=1,10
DELTA=0.005
READ(5,*)R
N=R/DELTA+0.01
RSTEP=4.0*R
ROWNO=10.0/RSTEP
M=ROWNO
X=0.0
DO 10 I=1,M
Y=0.0
X=X+RSTEP
DO 20 J=1,M
Y=Y+RSTEP
DO 30 K=1,3
RXY=R-(K-1)*DELTA
```

```
CALL CIRKL(X,Y,RXY)
30 CONTINUE
JJ=N-3
DO 40 L=1,JJ
P=1.8*(RXY-(L-1)*DELTA)
CALL SYMBOL(X,Y,P,1,0.0,-1)
40 CONTINUE
20 CONTINUE
10 CONTINUE
CALL NEW PAGE
60 CONTINUE
CALL ENPLOT
STOP
END
```

C2: Calculations of the Post-Receptoral Spectral Response Functions

A short computer programme was written to calculate the sensitivity of the post-receptoral spectral response functions from both the $\Pi 5$ and $\Pi 4$ spectral sensitivity mechanisms of the standard CIE observer (Stiles, 1949; numerical data from Wyszecki and Stiles, 1967) and also from the $\Pi 5$ and $\Pi 4$ spectral sensitivity mechanisms of the observers, V.W. and I.H., involved in the experimental investigation of Chapter III. The programme computes either the value of β (red-green opponent mechanism, fig. 3.30 see fig. 3.35) or α (green broad-band mechanism, fig. 3.31, see fig. 3.38) and plots both the computed and the experimental data. A listing of the programme is given below:-

```
PROGRAM VICKI (DATAVW,TAPE3=DATAVW,TAPE62,OUTPUT,TAPE6=OUTPUT)
DIMENSION RL (16),GL(16),DV(16),W(40),S(40),NUM(6)
CALL START(2)
CALL INTENSE(20)
NUM(1)=10
SMIN=1000.0
VMIN=1000.0
N=2
LINTYP=1
DO 10 I=1,10
READ(3,20) RL(I),GL(I),DV(I),W(I)
20FORMAT(3(F6.2,1X),F5.1)
IF(DV(I).LT.VMIN)VMIN=DV(I)
```

```
10 CONTINUE
DO 17 I=1,10
DV(I)=DV(I)/ABS(VMIN)
17 CONTINUE
B=0.82                                          A=0.26
DO 30 I=1,10
B=B+0.02                                        A=A+0.02
DO 40 J=1,10
S(J)=RL(J)-B*GL(J)                              SLJ)=GLIJ)-A*RLIJ
IF(S(J).LT.SMIN)SMIN=S(J)
40 CONTINUE
DO 60 K=1,10
S(K)=S(K)/ABS(SMIN)
S(K+10)=DV(K)
W(K+10)=W(K)
60 CONTINUE
NUM(2)=10
CALL GRAPH (W,S,NUM,N,LINTYP,10HWAVELENGTH,10,9HAMPLITUDE,9)
SMIN=1000.0
30 CONTINUE
CALL ENPLOT
STOP
END
```

B I B L I O G R A P H Y

BIBLIOGRAPHY

Indexes in this bibliography are after the Harvard system.

ABADI, R.V. (1974), The effect of early anomalous visual inputs on orientation selectivity, Perception, 3, 141 - 150.

ABADI, R.V. (1976), Induction masking - a study of some inhibitory interactions during dichoptic viewing, Vision Res., 16, 269 - 275.

ABNEY, Sir W. de W. (1913), Researches in colour vision and the trichromatic theory, Longmans: London.

ALPERN, M. (1979), Lack of uniformity in colour matching, J. Physiol., (Lond.), 288, 85 - 105.

ANDERSON, V.O., BUCHMANN, B., LENNOX-BUCHTHAL, M.A. (1962), Single cortical units with narrow spectral sensitivity in monkey (Cercocebus torquatusatys), Vision Res., 2, 293 - 307.

ANSTIS, S., ROGERS, B. and HENRY, J. (1978), Interactions between simultaneous contrast and after-images, Vision Res., 18, 899 - 911.

ARNULF, A., and DUPUY, O. (1960), La transmission des contrastes par le système optique de l'oeil et les seuils de contrastes rétiens, C.R. Acad. Sci., Paris, 250, 2757 - 2759.

BAGRASH, F.M. (1973), Size-selective adaptation: psychophysical evidence for size-tuning and the effects of stimulus contour and adapting flux, Vision Res., 13, 575 - 598.

BAGRASH, F.M., KERR, L.G. and THOMAS, J.P. (1971), Patterns of spatial integration in the detection of compound visual stimuli, Vision Res., 11, 635 - 645.

BARBUR, J.L. (1979), An arrangement for automatic random stimulus selection and variable speed of presentation in sensory physiology experiments, Photobiol. Bull., 1, 138 - 142.

BARBUR, J.L. (1980), Spatial organization of motion detection in subjects with normal and abnormal visual pathways, Ph.d. Thesis, Univ. of London.

BARBUR, J.L., HALLIDAY, I.E., RUDDOCK, K.H. and WATERFIELD, V.A. (1980), Spatial characteristics of movement detecting mechanisms in human vision. III. Subjects with abnormal visual pathways, Biol. Cybernetics, (in press).

BARBUR, J.L. and NUNN, B. (1978), A single 8-channel data logger: an electronic system designed for non-experts, Photobiol. Bull., 1, 40 - 50.

BARBUR, J.L. and RUDDOCK, K.H. (1980), a. Spatial characteristics of movement detecting mechanisms in human vision. I. Achromatic vision, Biol. Cybernetics, (in press). b. Spatial characteristics of movement detecting mechanisms in human vision. II. Chromatic stimuli, Biol. Cybernetics, (in press).

BARBUR, J.L., RUDDOCK, K.H. and WATERFIELD, V.A. (1979), A colour-dependent abnormality in human visual detection of stimulus motion and spatial structure, Neurosci. Letters, 15, 307 - 312.

BARLOW, H.B. (1975), Visual experience and cortical developments, Nature, (Lond.), 258, 199 - 204.

BARLOW, H.B., BLAKEMORE, C.B. and PETTIGREW, J.D. (1967), The neural mechanism of binocular depth discrimination, J. Physiol., (Lond.), 193, 327 - 342.

BARLOW, H.B., FITZHUGH, R. and KUFFLER, S.W. (1957), Change of organization in the receptive fields of the cat's retina during dark adaptation, J. Physiol., (Lond.), 137, 338 - 354.

BARLOW, H.B. and HILL, R.M. (1963), Selective sensitivity to direction of movement in ganglion cells of the rabbit retina, Science, 139, 412 - 414.

BARLOW, H.B., HILL, R.M. and LEVICK, W.R. (1964), Retinal ganglion cells responding selectively to direction and speed of image motion in the rabbit, J. Physiol., (Lond.), 173, 377 - 407.

BARLOW, H.B. and LEVICK, W.R. (1965), Mechanisms of directional selectivity in rabbit retina, J. Physiol., (Lond.), 178, 477 - 504.

BAYLOR, D.A. and FUORTES, M.G.F. (1970), Electrical responses of single cones in the retina of the turtle, J. Physiol., (Lond.), 207, 77 - 92.

BENDER, B.G. and RUDDOCK, K.H. (1974), Characteristics of a visual defect associated with abnormal response to both colour and luminance, Vision Res., 14, 383 - 393.

BLACKWELL, H.R. (1946), Contrast thresholds of the human eye, J. Opt. Soc. Amer., 36, 624 - 643.

BLACKWELL, H.R. (1963), Neural theories of simple visual discriminations, J. Opt. Soc. Amer., 53, 129 - 160.

BLAKE, R. and ANTOINETTI, D.N. (1976), Abnormal visual resolution in siamese cats, Science, 194, 109 - 110.

BLAKE, R. and CORMACK, R.H. (1979), Psychophysical evidence for a monocular visual cortex in stereoblind humans, Science, 203, 274 - 275.

BLAKE, R. and FOX, R. (1973), The psychophysical inquiry into binocular summation, Percept. and Psycho., 14, 161 - 185.

BLAKE, R. and FOX, R. (1974), Adaptation to invisible gratings and the site of binocular rivalry suppression, Nature, (Lond.), 249, 488 - 490.

BLAKEMORE, C. (1969), Binocular depth discrimination and the nasotemporal division, J. Physiol., (Lond.), 205, 471 - 497.

BLAKEMORE, C. (1970), Binocular depth perception and the optic chiasm, Vision Res., 10, 43 - 47.

BLAKEMORE, C. (1970), A new kind of stereoscopic vision, Vision Res., 10, 1181 - 1199.

BLAKEMORE, C. (1970), The representation of three-dimensional visual space in the cat's visual striate cortex, J. Physiol., (Lond.), 209, 155 - 178.

BLAKEMORE, C. and CAMPBELL, F.W. (1969), a. Adaptation to spatial stimuli, J. Physiol., (Lond.), 200, 11 - 13.

BLAKEMORE, C. and CAMPBELL, F.W. (1969), b. On the existence of neurones in the human visual system selectively sensitive to the orientation and size of retinal images, J. Physiol., (Lond.), 203, 237 - 260.

BLAKEMORE, C., CARPENTER, R.H.S. and GEORGESON, M.A. (1970), Lateral inhibition between orientation detectors in the human visual system, Nature, (Lond.), 228, 37 - 39.

BLAKEMORE, C. and HAGUE, B. (1972), Evidence for disparity - detecting neurones in the human visual system, J. Physiol., (Lond.), 225, 437 - 455.

BLAKEMORE, C., GARNER, E.T. and SWEET, J.A. (1972), The site of

size constancy, Perception, 1, 111 - 119.

BLAKEMORE, C. and NACHMIAS, J. (1971), The orientation specificity of two visual after-effects, J. Physiol., (Lond.), 213, 157 - 174.

BLAKEMORE, C., NACHMIAS, J. and SUTTON, P. (1970), The perceived spatial frequency shift. Evidence for frequency selective neurones in the human brain, J. Physiol., (Lond.), 210, 727 - 750.

BLAKEMORE, C. and SUTTON, P. (1970), Size adaptation: a new after-effect, Science, 166, 245 - 247.

BLAKEMORE, C. and TOBIN, E.A. (1972), Lateral inhibition between orientation detectors in the cat's visual cortex, Exp. Brain Res., 15(4), 439 - 440.

BOLES, J. (1971), Colour and contour detection by cells representing the fovea in monkey striate cortex, Abstracts of first annual meeting, Society Neuroscience, Washington D.C.

BORN, M. and WOLF, E. (1970), Principles of optics, Pergamon Press, (Oxford), 4th edition, 312.

BORKOFF, A. (1964), Localization of slow potential responses in Necturus retina, Vision Res., 4, 627 - 635.

BOYCOTT, B.B. and DOWLING, J.E. (1969), Organization of the primate retina: light microscopy, Phil. Trans. R. Soc., 225B, 109 - 184.

BOYCOTT, B.B. and WÄSSLE, H. (1974), The morphological types of ganglion cells in the domestic cat's retina, J. Physiol., (Lond.), 240, 397 - 419.

BRINDLEY, G.S. (1953), The effects on colour vision of adaptation

to very bright lights, J. Physiol., (Lond.), 122, 332 - 350.

BRINDLEY, G.S. (1957), Two theorems in colour vision, Quart. J. Exp. Psychol., 9, 101 - 104.

BRINDLEY, G.S. (1970), Physiology of the retina and visual pathway, Monographs of the Physiology Society, Ed. Davson, H., Greenfield, A.D.M., Writtam, R. and Brindley, G.S., Edward Arnold (Publ.), Camelot Press.

BRINDLEY, G.S., DU CROZ, J.J. and RUSHTON, W.A.H. (1966), The flicker fusion frequency of the blue-sensitive mechanism of colour vision, J. Physiol., (Lond.), 183, 497 - 500.

BRINDLEY, G.S., GAUTIER-SMITH, P.C. and LEWIN, W.S. (1969), Cortical blindness and the functions of the non-geniculate fibres of the optic tracts, J. Neurol. Neurosurg. Psychiat., 32, 259 - 264.

BRINDLEY, G.S. and LEWIN, W.S. (1968), The sensations produced by electrical stimulation of the visual cortex, J. Physiol., (Lond.), 196, 479 - 493.

BROWN, J.E. and ROJAS, A.J. (1965), Rat retinal ganglion cells: receptive field organization and maintained activity, J. Neurophysiol, 28, 1073 - 1090.

BROWN, P.K. and WALD, G. (1964), Visual pigments in single rods and cones of the human retina, Science, 144, 45 - 52.

BROWN, K.T. and WIESEL, T.N. (1959), Intraretinal recording with micropipette electrodes in the intact cat eye, J. Physiol., (Lond.), 149, 537 - 562.

BURTON, G.J. (1973), Evidence for non-linear response processing in the human visual system from measurements on thresholds of

spatial beat frequency, Vision Res., 13, 1211 - 1225.

BURTON, G.J. (1974), Factors influencing the detection of spatially structured stimuli by the human visual system, Ph.d. Thesis, University of London.

BURTON, G.J. and RUDDOCK, K.H. (1972), A lateral light adaptation effect in human vision, Vision Res., 12, 347 - 352.

BURTON, G.J. and RUDDOCK, K.H. (1978), Visual adaptation to patterns containing two-dimensional spatial structure, Vision Res., 18, 93 - 99.

BURTON, G.J., NAGHSHINEH, S. and RUDDOCK, K.H. (1977), Processing by the human visual system of light and dark contrast components of the retinal image, Biol. Cybernetics, 27, 189 - 197.

BYRAM, G.M. (1944), The physical and photochemical basis of visual resolving power. Part II. Visual acuity and the photochemistry of the retina, J. Opt. Soc. Amer., 34, 718 - 738.

CAJAL, S.R. (1911), Histologie du système nerveux de l'homme et des vertébrés (2 vols.), Paris, Maloine.

CAJAL, S.R. (1933), La rétien des Vertébrés, La cellule, 9, 17 - 257.

CAMERON, D. (1979), An albino's view, Ophthal. Optician, 19, 538 - 540.

CAMPBELL, F.W., CLELAND, B.G., COOPER, G.F. and ENROTH-CUGELL, C. (1968), Angular selectivity of visual cortical cells to moving gratings, J. Physiol., (Lond.), 198, 237 - 250.

CAMPBELL, F.W., COOPER, G.F. and ENROTH-CUGELL, C. (1969),

Spatial selectivity of visual cells of the cat, J. Physiol., (Lond.), 203, 223 - 235.

CAMPEBLL, F.W., COOPER, G.F., ROBSON, J.G. and SACHS, M.B. (1969), The spatial selectivity of visual cells of the cat and squirrel monkey, J. Physiol., (Lond.), 204, 120P.

CAMPBELL, F.W. and GREEN, G. (1965), Optical and retinal factors affecting visual resolution, J. Physiol., (Lond.), 181, 576 - 593.

CAMPBELL, F.W. and GUBISCH, R.W. (1966), Optical quality of the human eye, J. Physiol., (Lond.), 186, 558 - 578.

CAMPBELL, F.W. and MAFFEI, L. (1970), Electrophysiological evidence for the existence of orientation and size detectors in the human visual system, J. Physiol., (Lond.), 207, 635 - 652.

CAMPBELL, F.W. and MAFFEI, L. (1971), The tilt after-effect: a fresh look, Vision Res., 11, 833 - 840.

CAMPBELL, F.W. and ROBSON, J.G. (1968), Application of Fourier analysis to the visibility of gratings, J. Physiol., (Lond.), 197, 551 - 566.

CHACKO, L.W. (1948), An analysis of fibre-size in the human optic nerve, Brit. J. Ophthal., 32, 457 - 461.

CHAN, R.Y. and NAKA, K. (1976), The amacrine cell, Vision Res., 16, 1119 - 1129.

CHOUDHURY, B.P., WHITTERIDGE, D. and WILSON, M.E. (1965), The function of the callosal connections of the visual cortex, Quart. J. Exp. Psychol., 50, 214 - 219.

CLARKE, Le Gros, W.E. and PENMAN, C.G. (1934), The projection of the retina in the lateral geniculate body, Proc. Roy. Soc.,

(Lond.), 114B, 291 - 313.

CLELAND, B.G. and LEVICK, W.R. (1974), a. Brisk and sluggish concentrically organized ganglion cells in the cat's retina, J. Physiol., (Lond.), 240, 421 - 456. b. Properties of rarely encountered types of ganglion cells in the cat's retina and an overall classification, J. Physiol., (Lond.), 240, 457 - 492.

COBB, P.W. (1914-15), The influence of pupilliary diameter on visual acuity, Amer. J. Physiol., 36, 336 - 346.

COLEMAN, H.S., COLEMAN, M.F., FRIDGE, D.L. and HARDING, S.W. (1949), Coefficient of specific resolution of the human eye for Foucault test objects viewed through circular apertures, J. Opt. Soc. Amer., 39, 766 - 770.

COLLEWIJN, H., WINTERSON, B.J. and DUBOIS, M.F.W. (1978), Optokinetic eye movements in albino rabbits: inversion in anterior visual field, Science, 199, 1351 - 1353.

COLTHEART, M. (1971), Visual feature analyzers and after-effects of tilt and curvature, Psychol. Review, 78, 114 - 121.

COWEY, A. (1974), Atrophy of retinal ganglion cells after removal of striate cortex in a rhesus monkey, Perception, 3, 257 - 260.

COWEY, A. (1979), Cortical maps and visual perception, Quart. J. Exp. Psychol., 31, 1 - 17.

COWEY, A. and ROLLS, E.T. (1974), Human cortical magnification factor and its relation to visual acuity, Exp. Brain Res., 21, 447 - 454.

COWEY, A. and PORTER, J. (1978), Brain damage and global stereopsis, Proc. Roy. Soc. (Lond.), Series B (in press).

CRAGG, B.G. (1969), The topography of the afferent projections in

the circumstriate visual cortex (C.V.C.) of the monkey studied by the Nauta method, (Vision Res., 9, 733 - 747.

CREEL, D., O'DONNELL, F.E. Jnr. and WITKOP, C.J. Jnr. (1978), Visual system anomalies in human ocular albinos, Science, 201, 931 - 933.

CREEL, D., WITKOP, C.J. Jnr. and KING, R.A. (1974), Asymmetric visually evoked potentials in human albinos: evidence for visual system anomalies, Invest. Opththal., 13, 430 - 440.

DAITCH, J.M. and GREEN, D.G. (1969), Contrast sensitivity of the human peripheral retina, Vision Res., 9, 947 - 952.

DANIEL, P.M. and WHITTERIDGE, D. (1961), The representation of the visual field on the cerebral cortex in monkeys, J. Physiol., (Lond.), 159, 203 - 221.

DARTNELL, H.J.A. (1957), The visual pigments, Methuen, London.

DAW, N.W. (1967), Goldfish retina: organization for simultaneous colour contrast, Science, 158, 942 - 944.

DAW, N.W. (1968), Colour-coded ganglion cells in the goldfish retina: extension of their receptive fields by means of new stimuli, J. Physiol., (Lond.), 197, 567 - 592.

DAW, N.W. (1972), Colour-coded cells in goldfish, cat and rhesus monkey, Invest. Ophthal., 11, 411 - 417.

DE MONASTERIO, F.M. (1978), Macular pigmentation and the spectral sensitivity of retinal ganglion cells of macaques, Vision Res., 18, 1273 - 1277.

DE MONASTERIO, F.M. (1978), a. Properties of concentrically organized X- and Y-ganglion cells of macaque retina, J. Neurophysiol., 41, 1394 - 1417. b. Centre and surround

mechanisms of opponent-colour X- and Y-ganglion cells of the retina of macaques, J. Neurophysiol., 41, 1418 - 1434.

c. Properties of ganglion cells with atypical receptive field organization in the retina of macaques, J. Neurophysiol., 41, 1435 - 1449.

DE MONASTERIO, F.M. (1979), Asymmetry of 'ON' and 'OFF' pathways of blue-sensitive cones of the retina of macaques, Brain Res., 166, 39 - 48.

DE MONASTERIO, F.M. and GOURAS, P. (1975), Functional properties of ganglion cells of the rhesus monkey retina, J. Physiol., (Lond.), 251, 167 - 195.

DE MONASTERIO, F.M. and GOURAS, P. (1977), Responses of macaque ganglion cells to far violet lights, Vision Res., 17, 1147 - 1156.

DE MONASTERIO, F.M., GOURAS, P. and TOLHURST, D.J. (1975),

a. Trichromatic colour-opponency in ganglion cells of the rhesus monkey retina, J. Physiol., (Lond.), 251, 197 - 216.

b. Concealed colour-opponency in ganglion cells of the rhesus monkey retina, J. Physiol., (Lond.), 251, 217 - 229.

DE VALOIS, R.L. (1965), Behavioural and electrophysiological studies of primate vision, in Contributions to Sensory Physiology, Vol. 1., ed. Neff, W.D., N.Y. Academic Press, 137 - 178.

DE VALOIS, R.L. (1969), Colour vision; colour deficiency, Stockholm Congress Report .

DE VALOIS, R.L., ABRAMOV, I. and JACOBS, G.H. (1966), Analysis of response patterns of L.G.N. cells, J. Opt. Soc. Amer., 56, 966 - 977.

DE VALOIS, R.L. and PEASE, P.L. (1971), Contours and contrast: responses of monkey lateral geniculate nucleus cells to luminance and colour figures, Science, 171, 694 - 696.

DEWS, P.B. and WIESEL, T.N. (1970), Consequences of monocular deprivation on visual behaviour in kittens, J. Physiol., (Lond.), 206, 437 - 455.

DJAMGOZ, M.B.A. and RUDDOCK, K.H. (1978), Properties of amacrine cell responses recorded from isolated fish retinae, Neurosci. Letters, 7, 89 - 93.

DOW, B.M. (1974), Functional classes of cells and their laminar distribution in monkey visual cortex, J. Neurophysiol., 37, 927 - 946.

DOW, B.M. and GOURAS, P. (1973), Colour and spatial specificity of single units in rhesus monkey foveal striate cortex, J. Neurophysiol., 36, 79 - 99.

DOWLING, J.E. (1968), Synaptic organization of the frog retina: an electron microscopic analysis comparing the retinae of frogs and primates, Proc. Roy. Soc. (Lond.), 170B, 205 - 228.

DOWLING, J.E. and BOYCOTT, B.B. (1966), Organization of the primate retina: electron microscopy, Proc. Roy. Soc. (Lond.), 166B, 1639 - 1641.

DREHER, B., FUKADA, Y. and RODIECK, R.W. (1976), Identification, classification and anatomical segregation of cells with X-like and Y-like properties in the L.G.N. of old world primates, J. Physiol., 258, 433 - 452.

DUFFIEUX, P.M. (1946), L'intégrale de Fourier et ses applications à l'optique, Rennes.

DUKE-ELDER, W.S. (1949), Text-book of Ophthalmology, Vol. IV. The neurology of vision. Motor and optical anomalies, Henry Kimpton, London, Chapter 43.

DUKE-ELDER, W.S. (1964), System of Ophthalmology, Vol. III. Normal and abnormal development: part II, congenital deformities, Henry Kimpton, London.

EGGERS, H.M. and BLAKEMORE, C. (1978), Physiological basis of anisometropic amblyopia, Science, 201, 264 - 267.

ENROTH-CUGELL, C. and ROBSON, J.G. (1966), The contrast sensitivity of retinal ganglion cells of the cat, J. Physiol., (Lond.), 187, 517 - 552.

ESTÊVEZ, O. (1979), On the fundamental data-base of normal and dichromatic colour vision, Ph.d. Thesis, University of Utrecht, The Netherlands.

ESTÊVEZ, O. and CAVONIUS, C.R. (1977), Human colour perception and Stiles' π mechanisms, Vision Res., 17, 417 - 422.

ESTÊVEZ, O., SPEKREIJSE, H., VAN DEN BERG, T.J.T.P. and CAVONIUS, C.R. (1975), The spectral sensitivities of isolated human colour mechanisms determined from contrast evoked potential measurements, Vision Res., 15, 1205 - 1212.

FINLAY, B.L., SCHILLER, P.H. and VOLMAN, S.F. (1976), Quantitative studies of single-cell properties in monkey striate cortex. IV. Corticotectal cells, J. Neurophysiol., 39, 1352 - 1361.

FIORENTINI, A. and MAZZANTINI, L. (1966), Neural inhibition in the human fovea: a study of interactions between two line stimuli, Atti. Ford. Georgio Ronchi, 21, 738 - 747.

FISHER, G.H. (1968), Gradients of distortion seen in the context of the Ponzo illusion and other contours, Quart. J. Exp. Psychol., 20, 212 - 217.

FREEMAN, R.D. and THIBOS, L.N. (1973), Electrophysiological evidence that abnormal early visual experience can modify the human brain, Science, 180, 876 - 878.

GIBSON, J.J. (1933), Adaptation, after-effect and contrast in the perception of curved lines, J. Exp. Psychol., 16, 1 - 31.

GIBSON, J.J. and RADNER, M. (1937), Adaptation after-effect and contrast in the perception of tilted lines. I: Quantitative studies, J. Exp. Psychol., 20, 453 - 467.

GILBERT, C.D. and KELLY, J.P. (1975), The projection of cells in different layers of the cat's visual cortex, J. Comp. Neurol., 163, 81 - 106.

GILINSKY, A.S. (1968), Orientation specific effects of patterns of adaptating light on visual acuity, J. Opt. Soc. Amer., 58, 13 - 18.

GILINSKY, A.S. and DOHERTY, R.S. (1969), Interocular transfer of orientation effects, Science, 164, 454 - 455.

GINSBURG, A.P. (1971), Psychological correlates of a model of the human visual system, I.E.E.E. Proc., NAECON, 283 - 290.

GINSBURG, A.P. (1973), Pattern recognition techniques, I.E.E.E., Proc., NAECON, 309 - 316.

GINSBURG, A.P. (1975), Is the illusory triangle physical or imaginary?, Nature, (Lond.), 257, 219 - 220.

GLEES, P. (1961), Terminal degradation and trans-synaptic atrophy in the lateral geniculate body of the monkey, in The Visual

System, Ed. Jung and Kornhuber, Berlin: Springer, 104 - 110.

GOLDBERG, M.E. and WURTZ, R.H. (1972), a. Activity of superior colliculus in behaving monkey. I. Visual receptive fields of single neurones, J. Neurophysiol., 35, 542 - 557. b. Activity of superior colliculus in behaving monkey. II. Effect of attention on Neuronal responses, J. Neurophysiol., 35, 560 - 574.

GOURAS, P. (1967), The effects of light-adaptation on rod and cone receptive field organization of monkey ganglion cells, J. Physiol., (Lond.), 192, 747 - 760.

GOURAS, P. (1968), Identification of cone mechanisms in monkey ganglion cells, J. Physiol., (Lond.), 199, 533 - 547.

GOURAS, P. (1969), Antidromic responses of orthodromically identified ganglion cells, J. Physiol., (Lond.), 204, 407 - 419.

GOURAS, P. (1970), Trichromatic mechanisms in single cortical neurons, Science, 168, 489 - 492.

GOURAS, P. (1971), The function of the midget cell system in primate colour vision, Vision Res., suppl. 3, 397 - 410.

GOURAS, P. (1972), Colour-opponency from fovea to striate cortex, Invest. Ophthal., 11, 427 - 432.

GOURAS, P. (1974), Opponent-colour cells in different layers of foveal striate cortex, J. Physiol., (Lond.), 238, 583 - 602.

GOURAS, P. and LINK, K. (1966), Rod and cone interaction in dark-adapted monkey ganglion cells, J. Physiol., (Lond.), 184, 499 - 510.

GOURAS, P. and PADMOS, P. (1974), Identification of cone

mechanisms in graded responses of foveal striate cortex, J. Physiol., (Lond.), 238, 269 - 281.

GRAHAM, C.H., BROWN, R.H. and MOTE, F.A. (1939), The relation of size of stimulus and intensity in the human. I. Intensity thresholds for white light, J. Exp. Psychol., 24, 555 - 573.

GRANIT, R. and SVAETICHIN, G. (1967), Principles and techniques of electrophysiological analysis of colour reception with the aid of microelectrodes, Upsala Lakareforen, Forh. N.F. Bd., XLV, 161 - 177.

GREGORY, R.L. (1963), Distortion of visual space as inappropriate constancy scaling, Nature, (Lond.), 199, 678.

GREGORY, R.L. (1966), Eye and brain, World University Library, London.

GREGORY, R.L. (1970), The intelligent eye, Weidenfeld and Nicolson, London.

GREGORY, R.L. (1972), Cognitive contours, Nature, (Lond.), 238, 51 - 52.

GUILD, J. (1931), The colorimetric properties of the spectrum, Phil. Trans., 230A, 149 - 187.

GUILLERY, R.W. (1974), Visual pathways in albinos, Sci. Amer., May, 44 - 54.

GUILLERY, R.W., CASSAGRANDE, V.A. and OBERDORFER, M.D. (1974), Congenitally abnormal vision in siamese cats, Nature, (Lond.), 252, 195 - 199.

GUILLERY, R.W. and KAAS, J.H. (1971), A study of normal and congenitally abnormal retino-geniculate projections in cat, J. Comp. Neurol., 143, 73 - 99.

HAMSHER, K. de S. (1978), Stereopsis and unilateral brain disease, Invest. Ophthal. and Visual Sci., 17, 336 - 343.

HARRIS, C.S. and GIBSON, A.R. (1968), Is orientation-specific colour adaptation in human vision due to edge detectors, after-images or 'dipoles'?, Science, 162, 1506 - 1507.

HARTLINE, H.K. (1938), The response of single optic nerve fibres of the vertebrate eye to illumination of the retina, Amer. J. Physiol., 121, 400 - 415.

HECHT, S. (1928), The relation between visual acuity and illumination, J. Gen. Physiol., 11, 255 - 281.

HECHT, S. (1932), The nature of the visual process, in reprint of The Harvey Lecture (1937 - 1938).

HECHT, S. (1944), Energy and Vision, Amer. Scientist, 32, 159 - 177.

VON HELMHOLTZ, H.L.F. (1852), Über die Theorie der zusammengesetzten Farben, Ann. Phys. Lpz., 87, 45 - 66.

VON HELMHOLTZ, H.L.F. (1911), Handbuch der physiologischen Optik, Ed. W. Nagel, A. Gullstrand and J. von Kries, 3rd Edn., Hamburg and Leipzig, Voss.

HENNING, G.B., HERTZ, B.G. and BROADBENT, D.J. (1975), Some experiments bearing on the hypothesis that the visual system analyses spatial patterns in independent bands of spatial frequency, Vision Res., 15, 887 - 897.

HENRY, G.H. (1977), Receptive field classes of cells in the striate cortex of the cat, Brain Res., 133, 1 - 28.

HENRY, G.H., BISHOP, P.O. and COOMBS, J.S. (1969), Inhibitory and subliminal excitatory receptive fields of simple units in cat

striate cortex, Vision Res., 9, 1289 - 1296.

HERING, E. (1875), Zur Lehre vom Lichtsinne. VI. Grundzüge einer theorie des Farbensinnes, SBK. Akad. Wiss Wien. Math. naturwiss. K., 70, 169 - 204.

HESS, R.F. and HOWELL, E.R. (1977), The threshold contrast sensitivity function in strabismic amblyopia: evidence for a two-type classification, Vision Res., 17, 1049 - 1055.

HOLMES, G. (1918), a. Disturbances of vision by cerebral lesions, Brit. J. Ophthal., 2, 353 - 384. b. Disturbances of visual orientation, Brit. J. Ophthal., 2, 449 - 468, 506 - 516.

HOLMES, G. (1944), The organization of the visual cortex in man, Proc. Roy. Soc., (Lond.), 132B, 348 - 361.

HOTOPF, W.H.N. (1966), The size-constancy theory of visual illusions, Brit. J. Psychol., 57, 307 - 318.

HUBEL, D.H. and WIESEL, T.N. (1960), Receptive fields of optic nerve fibres in the spider monkey, J. Physiol., (Lond.), 154, 572 - 580.

HUBEL, D.H. and WIESEL, T.N. (1962), Receptive fields, binocular interaction and functional architecture in the cat's visual cortex, J. Physiol., (Lond.), 160, 106 - 154.

HUBEL, D.H. and WIESEL, T.N. (1963), Receptive fields of cells in striate cortex of very young, visually inexperienced kittens, J. Neurophysiol., 26, 994 - 1002.

HUBEL, D.H. and WIESEL, T.N. (1963), Shape and arrangement of columns in cat's striate cortex, J. Physiol., (Lond.), 165, 559 - 568.

HUBEL, D.H. and WIESEL, T.N. (1965), Receptive fields and

functional architecture in two non-striate visual areas (18 and 19) of the cat, J. Neurophysiol., 28, 229 - 289.

HUBEL, D.H. and WIESEL, T.N. (1967), Cortical and callosal connections concerned with the vertical meridian of visual fields in the cat, J. Neurophysiol., 30, 1561 - 1573.

HUBEL, D.H. and WIESEL, T.N. (1968), Receptive fields and functional architecture of monkey striate cortex, J. Physiol., (Lond.), 195, 215 - 243.

HUBEL, D.H. and WIESEL, T.N. (1969), Anatomical demonstration of columns in the monkey striate cortex, Nature, (Lond.), 221, 747 - 750.

HUBEL, D.H. and WIESEL, T.N. (1970), Cells sensitive to binocular depth in area 18 of the macaque monkey cortex, Nature, (Lond.), 225, 41 - 42.

HUBEL, D.H. and WIESEL, T.N. (1970), The periods of susceptibility to the physiological effects of unilateral eye closure in kittens, J. Physiol., (Lond.), 206, 419 - 436.

HUBEL, D.H. and WIESEL, T.N. (1974), a. Sequence regularity and geometry of orientation columns in monkey striate cortex, J. Comp. Neurol., 158, 267 - 293. b. Uniformity of monkey striate cortex: a parallel relationship between field size, scatter and magnification factor, J. Comp. Neurol., 158, 295 - 305.

HUGHES, E.B.C. (1954), The visual fields: a study of the applications of quantitative perimetry to the anatomy and pathology of the visual pathways, Springfield, I, 11, Thomas.

HURVICH, L.M. and JAMESON, D. (1957), An opponent-process theory of colour vision, J. Physiol. Review, 64, 384 - 404.

IKEDA, H. and TREMAIN, K.E. (1979), Amblyopia occurs in retinal ganglion cells in cats reared with convergent squint without alternating fixation, Exp. Brain. Res., 35, 559 - 582.

JONES, E.G. and POWELL, T.P.S. (1970), An anatomical study of converging sensory pathways within the cerebral cortex of the monkey, Brain, 93, 793 - 820.

JULESZ, B. (1971), Foundations of cyclopean perception, The University of Chicago Press, Chicago and London.

KAAS, J.H. and GUILLERY, R.W. (1973), The transfer of abnormal visual field representations from the dorsal lateral geniculate nucleus to the visual cortex in siamese cats, Brain Res., 59, 61 - 95.

KANEKO, A. (1970), Physiological and morphological identification of horizontal, bipolar and amacrine cells in goldfish retina, J. Physiol., (Lond.), 207, 623 - 633.

KANEKO, A. (1971), Electrical connexions between horizontal cells in the dogfish retina, J. Physiol., (Lond.), 213, 95 - 105.

KANEKO, A. and YAMADA, M. (1972), S-potentials in the dark adapted retina of the carp, J. Physiol., (Lond.), 227, 261 - 273.

KANIZSA, G. (1955), Rivista di Psicologia, 49, 7.

KELLY, J.P. and VAN ESSEN, D.C. (1974), Cell structure and function in the visual cortex of the cat, J. Physiol., (Lond.), 238, 515 - 547.

KERR, L.G. and THOMAS, J.P. (1972), Effect of selective adaptation on detection of simple and compound parafoveal stimuli, Vision Res., 12, 1367 - 1379.

KINCAID, W.M., BLACKWELL, H.R. and KRISTOFFERSON, A.B. (1960), Neural formulation of the effects of target size and shape upon visual detection, J. Opt. Soc. Amer., 50, 143 - 148.

KÖNIG, A. (1894), Über den menschlichen Sehrpurpur und seine Bedeutung für das Sehen, S.B. Akad. Wiss., Berlin, 577 - 598.

KÖNIG, A. and DIETERICI, C. (1886), Die Grundempfindungen und ihre Intensitäts - Vertheilung im Spectrum, S.B. Akad. Wiss., Berlin, 805 - 829.

KOZAK, W., RODIECK, R.W. and BISHOP, P.O. (1965), Responses of single units in lateral geniculate nucleus of cat to moving visual patterns, J. Neurophysiol., 28, 19 - 47.

KUFFLER, S.W. (1952), Neurones in the retina: organization, inhibition and excitation problems, Cold Spring Harb. Sympos. Quart. Biol., 17, 281 - 292.

KUFFLER, S.W. (1953), Discharge patterns and functional organization of mammalian retina, J. Neurophysiol., 16, 37 - 68.

KULIKOWSKI, J.J. and KING-SMITH, P.E. (1973), Spatial arrangement of line, edge and grating detectors revealed by subthreshold summation, Vision Res., 13, 1455 - 1478.

LAMB, T.D. (1976), Spatial properties of horizontal cell responses in the turtle retina, J. Physiol., (1976), 263, 239 - 255.

LANDOLT, E. (1889), Tableau d'optotypes pour la determination de l'acuité visuelle, Soc. Francais d'ophthal., 157.

LE GRAND, Y. (1935), Sur la mesure de l'acuité visuelle au moyen de franges d'interférence, C.R. Acad. Sci., Paris, 200, 490 - 491.

LEIBOWITZ, H. (1952), The effect of pupil size on visual acuity for photometrically equated test fields at various levels of luminance, J. Opt. Soc. Amer., 42, 416 - 422.

LEIBOWITZ, H. (1953), Some observations and theory on the variations of visual acuity with the orientation of the test object, J. Opt. Soc. Amer., 43, 902 - 905.

LENTAU, M. and MONTAGU, A. (1971), Textbook of human genetics, Oxford.

LEVAY, S., HUBEL, D.H. and WIESEL, T.N. (1975), The pattern of ocular dominance columns in macaque visual cortex revealed by a reduced silver stain, J. Comp. Neurol., 159, 559 - 576.

LEVICK, W.R. (1967), Receptive fields and trigger features of ganglion cells in the visual streak of the rabbit retina, J. Physiol., (Lond.), 188, 285 - 307.

LEVICK, W.R., OYSTER, C.W. and TAKAKASHI, E. (1969), Rabbit lateral geniculate nucleus: sharpener of directional information, Science, 165, 712 - 714.

LOVEGROVE, W.J. and OVER, R. (1972), Colour-adaptation of spatial frequency detectors in the human visual system, Science, 176, 541 - 543.

LOVEGROVE, W.J. and OVER, R. (1973), Colour-selectivity in orientation masking and after-effect, Vision Res., 13, 895 - 902.

LOWRY, E.M. and DE PALMA, J.J. (1962), Sine-wave response of the visual system, J. Opt. Soc. Amer., 52, 328 - 335.

MACKAY, D.M. and MACKAY, V. (1974), The time course of the McCollough Effect and its physiological implications,

J. Physiol., (Lond.), 237, 38 - 39.

MAFFEI, L. and FIORENTINI, A. (1973), The visual cortex as a spatial frequency analyser, Vision Res., 13, 1255 - 1267.

MAFFEI, L., FIORENTINI, A. and BISTI, S. (1973), Neural correlate of perceptual adaptation to gratings, Science, 182, 1036 - 1038.

MARKS, W.B. (1965), Visual pigments of single goldfish cones, J. Physiol., (Lond.), 178, 14 - 32.

MARKS, W.B., DOBELLE, W.H. and MACNICHOL, E.F. (1964), Visual pigment of single primate cones, Science, 143, 1181 - 1183.

MARROCCO, R.T. (1972), Responses of monkey optic tract fibres to monochromatic lights, Vision Res., 12, 1167 - 1174.

MARROCCO, R.T. (1976), Sustained and transient cells in the monkey LGN: conduction velocities and response properties, J. Neurophysiol., 39, 340 - 353.

MAUDARBOCUS, A.Y. (1973), Response characteristics of the human visual system in the detection of spatially periodic stimuli, Ph.d. Thesis, University of London.

MAUDARBOCUS, A.Y. and RUDDOCK, K.H. (1973), a. Influence of wavelength on visual adaptation to spatially periodic stimuli, Vision Res., 13, 993 - 998. b. Non-linearity of visual signals in relation to shape-sensitive adaptation responses, Vision Res., 13, 1713 - 1737.

MAUDARBOCUS, A.Y. and RUDDOCK, K.H. (1974), Comments on "Adaptation to pairs of coloured gratings: inhibition between colour-specific spatial detectors in the human visual system?", by C.R. Sharpe, Vision Res., 14, 1485 - 1487.

MAXWELL, J.C. (1890), Collected Papers, Vol. I and II, Cambridge University Press.

MAY, J.G. (1972), Chromatic adaptation of orientation and size-specific visual processes in man, Vision Res., 12, 1509 - 1517.

McCOLLOUGH, C. (1965), Colour adaptation of edge detectors in the human visual system, Science, 149, 1115 - 1116.

MICHAEL, C.R. (1966), Receptive fields of opponent-colour units in the optic nerve of the ground squirrel, Science, 152, 1095 - 1097.

MICHAEL, C.R. (1968), Receptive fields of single optic nerve fibres in a mammal with an all-cone retina, J. Neurophysiol., 31, 249 - 282.

MICHAEL, C.R. (1978), a. Color vision mechanisms in monkey striate cortex; dual-opponent cells with concentric receptive fields, J. Neurophysiol., 41, 572 - 588. b. Color vision mechanisms in monkey striate cortex; simple cells with dual opponent-color receptive fields, J. Neurophysiol., 41, 1233 - 1249. c. Color-sensitive complex cells in monkey striate cortex, J. Neurophysiol., 41, 1250 - 1266.

MIKAELIAN, H.H. (1975), Color - selectivity and interocular transfer of color-specific tilt after-effects, Vision Res., 15, 157 - 158.

MINKOWSKI, M. (1920), Über den Verlang, die Endigung und die zentrale Repräsentation von gekreutzen und ungekreutzen Sehnerverfassern bie einigen Säugetieren und beim Menschen, Schweiz. Arch. Neurol. Psychiatr., 6, 201 - 252.

MITCHELL, D.E. and BAKER, A.G. (1973), Stereoscopic after-

effects. Evidence for disparity specific neurones in the human visual system, Vision Res., 13, 2273 - 2288.

MITCHELL, D.E. and BLAKEMORE, C. (1970), Binocular depth perception and the corpus callosum, Vision Res., 10, 49 - 54.

MITCHELL, D.E. and WARE, C. (1974), Interocular transfer of a visual after-effect in normal and stereoblind humnas, J. Physiol., (Lond.), 236, 707 - 721.

MOHLER, C.W. and WURTZ, R.H. (1976), Organization of monkey superior colliculus: intermediate layer cells discharging before eye movements, J. Neurophysiol., 39, 722 - 744.

MOHLER, C.W. and WURTZ, R.H. (1977), Role of striate cortex and superior colliculus of saccadic eye movements in monkey, J. Neurophysiol., 40, 74 - 94.

MOLLON, J.D. and POLDEN, P.G. (1979), Post-receptoral adaptation, Vision Res., 19, 435 - 440.

MOLLON, J.D., POLDEN, P.G., NEWCOMBE, F. and RATCLIFFE, G. (1980), On the presence of three cone mechanisms in a case of total achromatopsia, Mod. Prob. Ophthal., (in press).

MOTOKAWA, K., TAIRA, N. and OKUDA, J. (1962), Spectral response of single units in the primate visual cortex, Tohokn J. Exp. Med., 78, 320 - 337.

MOVSHON, J.A., CHAMBERS, B.E.I. and BLAKEMORE, C. (1972), Interocular transfer in normal humans, and those who lack stereopsis, Perception, 1, 483 - 490.

MYERS, R.E. (1962), Commissural connections between occipital lobes of the monkey, J. Comp. Neurol., 118, 1 - 16.

NAKA, K. (1977), Functional organization of catfish retina,

J. Neurophysiol., 40, 26 - 43.

NAKA, K. and NYE, P.W. (1970), Receptive field organization of the catfish retina: are at least two lateral mechanisms involved?, J. Neurophysiol., 33, 625 - 642.

NAKAYAMA, K. and ROBERTS, D.J. (1972), Line-length detectors in human visual system, Vision Res., 12, 1709 - 1713.

NAGHSHINEH, S. (1977), Adaptation effects in responses of the human visual system associated with spatially periodic light stimuli, Ph.d. Thesis, University of London.

NAGHSHINEH, S. and RUDDOCK, K.H. (1978), Properties of length-selective and non-length-selective adaptation mechanisms in human vision, Biol. Cybernetics, 31, 37 - 47.

NIKARA, T., BISHOP, P.O. and PETTIGREW, J.D. (1968), Analysis of retinal correspondence by studying receptive fields of binocular single units in cat striate cortex, Exp. Brain Res., 6, 353 - 372.

NUNN, B.J. (1978), An investigation into the spectral characteristics of metacontrast phenomena and of adaptation effects in human vision, Ph.D. Thesis, University of London.

NUNN, B.J. and RUDDOCK, K.H. (1978), Effects of adaptation to bright lights on anomalous trichromatic colour matches, Mod. Probl. Ophthal., 19, 218 - 221.

OGDEN, T.E. and MILLER, R.F. (1966), Studies of the optic nerve of the rhesus monkey: nerve fibre spectrum and physiological properties, Vision Res., 6, 485 - 506.

OIKAWA, T., OGAWA, T. and MOTOKAWA, K. (1959), Origin of the so-called cone action potential, J. Neurophysiol., 22, 102 - 111.

OONE, S. (1959), Response function of the eye, J. Appl. Phys., Japan, 28, 531.

ØSTERBERG, G. (1935), Topography of the layer of rods and cones in the human retina, Acta Ophthal., suppl. 6, 1 - 103.

PADMOS, P. and VAN NORREN, D. (1973), Increment spectral sensitivity and colour discrimination in the primate, studied by means of graded potentials from the striate cortex, Vision Res., 15, 1103 - 1113.

PANTLE, A.J. and SEKULER, R.W. (1968), Velocity-sensitive elements in human vision. Initial psychophysical evidence, Vision Res., 8, 445 - 450.

PANTLE, A.J. and SEKULER, R.W. (1969), Contrast response of human visual mechanisms sensitive to orientation and direction of motion, Vision Res., 9, 397 - 406.

PARTHE, V. (1972), Horizontal, bipolar and oligopolar cells in the teleost retina, Vision Res., 12, 395 - 406.

PASIK, T. and PASIK, P. (1965), Visual behaviour of monkeys with occipital lobe lesions, in disturbances of the occipital lobe, Proc. VIII, Int. Congr. Neurol., Vienna, 3, Wiener Med. Akad., Vienna.

PASIK, T. and PASIK, P. (1971), The visual world of monkeys deprived of striate cortex: effective stimulus parameters and the importance of the accessory optic system, Vision Res., suppl. 3, 419 - 435.

PATEL, A.S. (1965), Spatial resolution by the human and visual system; effects of mean retinal illuminance, J. Opt. Soc. Amer., 56, 689 - 694.

PERENIN, M.T. and JEANNEROD, M. (1975), Residual vision in cortically blind hemifelds, Neuropsychologia. 13, 1 - 7.

PERENIN, M.T. and JEANNEROD, M. (1978), Visual function within the hemianopic field following early cerebral hemidecortication in man. I. Spatial localization, Neuropsychologia, 16, 1 - 13.

PICKFORD, R.W. (1951), Colour vision of an albino, Nature, (Lond.), 168, 954.

PICKFORD, R.W. (1958), Colour vision of three albinos, Nature, (Lond.), 181, 361 - 362.

PICKFORD, R.W. and TAYLOR, W.O.G. (1968), Colour vision of two albinos, Brit. J. Ophthal., 52, 640 - 641.

PIRENNE, M.H. (1967), Vision and the eye, Chapman and Hall, London.

PITT, F.H.G. (1944), The nature of trichromatic and dichromatic vision, Proc. Roy. Soc., (Lond.), 132B, 101 - 117.

POGGIO, G.F. (1972), Spatial properties of neurons in striate cortex of unanesthetized macaque monkey, Invest. Ophthal., 11, 368 - 377.

POGGIO, G.F., MANSFIELD, R.J.W. and SILLITO, A.M. (1971), Functional properties of neurons in the striate cortex of the macaque monkey subserving the foveal region of the retina, in Abstracts of First Annual Meeting, Soc. for Neuroscience, Washington, D.C., p1 28.

POLYAK, S.L. (1932), The main afferent fibre system of the cerebral cortex in primates, Univ. Calif. Publ. Anat., no.2, Berkeley, California.

POLYAK, S.L. (1933), A contribution to the cerebral representation of the retina, J. Comp. Neurol., 57, 541 - 617.

POLYAK, S.L. (1941), The Retina, University of Chicago Press, Chicago.

POLYAK, S.L. (1957), The vertebrate visual system, ed. H. Klüver, University of Chicago Press, Chicago.

PÖPPELL, E., HELD, R. and FROST, D. (1973), Residual visual function after brain wounds involving the central visual pathways in man, Nature, (Lond.), 243, 295 - 296.

POTTS, A.M., HODGES, D., SHELMAN, C.B., FRITZ, K.J., LEVY, N.S. and MANGNALL, Y. (1972) a. Invest. Ophthal., 11, 980 - 988.
b. Invest. Ophthal., 11, 989 - 1002.

PUGH, E.N. Jr. and MOLLON, J.D. (1979), A theory of the Π_1 and Π_3 color mechanisms of Stiles, Vision Res., 19, 293 - 312.

REGAN, D. (1974), Electrophysiological evidence for colour channels in human pattern vision, Nature, (Lond.), 250, 437 - 439.

REGAN, D. (1975), Recent advances in electrical recording from the human brain, Nature, (Lond.), 253, 401 - 407.

RICCO, A. (1877), Ralazione fra il minimo angolo visuale e l'intensitá luminosa, Annalidi OHalmologia, 6, 373 - 479.

RIDDOCH, G. (1917), Dissociation of visual perceptions due to occipital injuries, with special reference to the appreciation of movement, Brain, 40, 15 - 57.

ROBSON, J.G. (1966), Spatial and temporal contrast sensitivity functions of the visual system, J. Opt. Soc. Amer., 56, 1141 - 1142.

RODIECK, R.W. (1973), The vertebrate retina, W.H. Freeman and Co., San Francisco.

RØNNE, H. (1914), Ueber doppel seitige Hemianopsie mit erhaltener Makula, Klin. Mbl. Augenheilk, 53, 470 - 487.

RØNNE, H. (1919), Quadrantic hemianopsia and the position of the macular fibres in the occipital visual tract, Bibl. Laeger, III, 215 - 232.

RUDDOCK, K.H. and SVAETICHIN, G. (1973), Fast and slow components of intracellularly-recorded responses from retinal units of a teleost fish (Eugewes plumien), Vision Res., 13, 1785 - 1788.

RUDDOCK, K.H., WATERFIELD, V.A. and WIGLEY, E. (1979), The response characteristics of an inhibitory binocular interaction in human vision, J. Physiol., 290, 37 - 49.

RUDDOCK, K.H. and WIGLEY, E. (1976), Inhibitory binocular interaction in human vision and a possible mechanism subserving stereoscopic fusion, Nature, (Lond.), 260, 604 - 606.

RUSHTON, W.A.H. (1956), The difference spectrum and the photosensitivity of rhodopsin in the living eye, J. Physiol., (Lond.), 134, 11 - 29.

RUSHTON, W.A.H. (1958), The cone pigments of the human fovea in colour blind and normal, in Visual problems of colour, N.P.L. Symp. No. 8, (London), H.M. Stat. Office, pp 71 - 101.

RUSHTON, W.A.H. (1963), A cone pigment in the protanope, J. Physiol., (Lond.), 168, 345 - 359.

RUSHTON, W.A.H. (1965), a. A foveal pigment in the deuteranope, J. Physiol., (Lond.), 176, 24 - 37. b. Cone pigment kinetics

in the deuteranope, J. Physiol., (Lond.), 176, 38 - 45.

RICHARDS, W. (1970), Stereopsis and stereoblindness, Exp. Brain Res., 10, 380 - 388.

RICHARDS, W. (1977), Stereopsis with and without monocular contours, Vision Res., 17, 967 - 969.

RICHARDS, W. and REGAN, D. (1973), A stereo field map with implications for disparity processing, Invet. Ophthal., 12, 904 - 909.

SACHS, M.B., NACHMIAS, J. and ROBSON, J.G. (1971), Spatial frequency channels in human vision, J. Opt. Soc. Amer., 61, 1176 - 1186.

SANDERS, M.D., WARRINGTON, E.K., MARSHALL, J. and WEISKRANTZ, L. (1974), 'Blindsight': vision in a field defect, The Lancet, April, 707 - 708.

SCHADÉ, O.H. (1956), Optical and photoelectric analogue of the eye, J. Opt. Soc. Amer., 46, 721 - 739.

SCHILLER, P.H., FINLAY, B.L. and VOLMAN, S.F. (1976), a. Quantitative studies of single-cell properties in monkey striate cortex. I. Spatiotemporal organization of receptive fields, J. Neurophysiol., 39, 1288 - 1319. b. II. Orientation specificity and ocular dominance, J. Neurophysiol., 39, 1320 - 1333. c. III. Spatial frequency, J. Neurophysiol., 39, 1334 - 1351. d. V. Multivariate statistical analyses and models, J. Neurophysiol., 39, 1362 - 1374.

SCHILLER, P.H. and KOERNER, F. (1971), Discharge characteristics of single units in superior colliculus of the alert rhesus monkey, J. Neurophysiol., 34, 920 - 936.

SCHILLER, P.H., STRYKER, M., CYANDER, M. and BERMAN, N. (1974), Response characteristics of single cells in the monkey superior colliculus following ablation or cooling of the visual cortex, J. Neurophysiol., 37, 181 - 194.

SCHLAER, S. (1937), The relation between visual acuity and illumination, Amer. J. Physiol., 21, 165 - 188.

SCHNEIDER, G.E. (1969), Two visual systems, Science, 163, 895 - 902.

SELWYN, E.W.H. (1948), The photographic and visual resolving power of lenses, Photo. J., 88B, 6 - 12.

SHATZ, C.J. and LEVAY, S. (1979), Siamese cats; altered connections of visual cortex, Science, 203, 328 - 330.

SNELLEN, H. (1862), Probebushstabenzur Bestimmung der Sehchärfe, Utrecht.

SPALDING, J.M.K. (1952), a. Wounds of the visual pathway. I. The visual radiation, J. Neurol. Neurosurg. Psychiat. 15, 99 - 109. b. II. The striate cortex, J. Neurol. Neurosurg. Psychiat. 15, 169 - 183.

SPEKREIJSE, H., WAGNER, H.G. and WOLBARSHT, M.L. (1972), Spectral and spatial coding of ganglion cell responses in goldfish retina, J. Neurophysiol., 35, 73 - 86.

SPERLING, H.G. and HARWERTH, R.S. (1971), Red-green cone interactions in the increment threshold spectral sensitivity of primates, Science, 172, 180 - 184.

SPRAGUE, J.M. (1966), Interaction of cortex and superior colliculus in mediation of visually guided behaviour in the cat, Science, 153, 1544 - 1547.

STERN, C. (1973), Principles of human genetics, Freeman.

STELL, W.K. (1967), The structure and relationships of horizontal cells and photoreceptor-bipolar synaptic complexes in goldfish retina, Amer. J. Anat., 121, 401 - 423.

STILES, W.S. (1939), The directional sensitivity of the retina and the spectral sensitivities of the rods and cones, Proc. Roy. Soc. (Lond.), 127B, 64 - 105.

STILES, W.S. (1949), Increment thresholds and the mechanisms of colour vision, Docum. Ophthal., 3, 138 - 163.

STILES, W.S. (1955), Interim report to the CIE Zurich, 1955, on the N.P.L.'s investigation of colour matching, Optica Acta, 2, 168 - 176.

STILES, W.S. (1959), Colour vision: the approach through increment threshold sensitivity, Proc. Nat. Acad. Sci., 45, 100 - 114.

STILES, W.S. (1978), Mechanisms of colour vision, Academic Press, London.

STILES, W.S. and BURCH, J.M. (1959), N.P.L. colour matching investigations; final report, Optica. Acta., 6, 1 - 26.

STILES, W.S. and CRAWFORD, B.H. (1933), The luminous efficiency of rays entering the pupil at different points, Proc. Roy. Soc., 112B, 428 - 450.

STONE, J. and DREHER, B. (1973), Projection of X- and Y-cells of the cat's lateral geniculate nucleus to areas 17 and 18 of the visual cortex, J. Neurophysiol., 36, 551 - 567.

STONE, J. and FABIAN, M. (1966), Specialized receptive fields in the cat's retina, Science, 152, 1277 - 1279.

STROMEYER, C.F. III (1972), Edge-contingent colour after-effects spatial frequency specificity, Vision Res., 12, 717 - 737.

STROMEYER, C.F. and KLEIN, S. (1975), Evidence against narrow-band spatial frequency channels in human vision: delectability of frequency modulated gratings, Vision Res., 15, 899 - 910.

SVAETICHIN, G. (1953), The cone action potential, Acta. Physiol. Scand., 29, suppl. 106, 565 - 600.

SVAETICHIN, G. (1956), Spectral response curves of single cones, Acta physiol. scand., suppl. 134, 18 - 46.

SVAETICHIN, G. and MACNICHOL, E.F.Jr., (1958), Retinal mechanisms for chromatic and achromatic vision, Ann. N.Y. Acad. Sci., 74, 385 - 404.

TALBOT, S.A. and MARSHALL, W.H. (1941), Physiological studies on neural mechanisms of visual localization and discrimination, Amer. J. Ophthal., 24, 1255 - 1263.

TEUBER, H.L., BATTERSBY, W.S. and BENDER, M.B. (1960), Visual field defects after penetrating missile wounds of the brain, Cambridge, Mass., Harvard University Press.

THOMAS, J.P. and KERR, L.G. (1971), Evidence of role of size-tuned mechanisms in increment threshold task, Vision Res., 11, 647 - 655.

THOMAS, J.P., PADILLA, G.J. and ROURKE, D.L. (1969), Spatial interactions in identification and detection of compound visual stimuli, Vision Res., 9, 283 - 292.

THOMSON, L.C. and WRIGHT, W.D. (1947), The colour sensitivity of the retina within the central fovea of man, J. Physiol., (Lond.), 105, 316 - 331.

TOLHURST, D.J. (1972), Adaptation to square-wave gratings: inhibition between spatial frequency channels in the human visual systems, J. Physiol., (Lond.) 226, 231 - 248.

TOMITA, T. (1965), Electrophysiological study of the mechanisms subserving colour coding in the fish retina, Cold Spring Harb. Symp. Quant. Biol., 30, 559 - 566.

TOMITA, T., KANEKO, A., MURAKAMI, M. and PANTLER, E.L. (1967), Spectral response curves of single cones in the carp, Vision Res., 7, 519 - 531.

TOYODA, J.I., NOSAKI, H. and TOMITA, T. (1969), Light-induced resistance changes in single photoreceptors of Necturus and Gekko, Vision Res., 9, 453 - 463.

TYLER, C.W. (1973), Stereoscopic vision: cortical limitation and disparity scaling effect, Science, 18, 276 - 278.

VAN ESSEN, D.C. and KELLY, J.P. (1973),a.Correlation of cell shape and function in the visual cortex of the cat, Nature, (Lond.) 241, 403 - 405.

VAN ESSEN, D.C. and KELLY, J.P. (1973),b.Morphological identification of simple, complex and hypercomplex cells in the visual cortex of the cat, in Intracellular staining in neurobiology, ed. KATER, S.B. and NICHOLSON, C., N.Y.: Springer : Verlag.

VAN MEETEREN, A. and VOS, J.J. (1972), Resolution and contrast sensitivity at low luminances, Vision Res., 12, 825 - 833.

VAN NES, F.L. and BOUMAN, M.A. (1967), Spatial modulation transfer in the human eye, J. Opt. Soc. Amer., 57, 401 - 406.

VAN NES, F.L., KOENDERINK, J.J., NAS, H. and BOUMAN, M.A. (1967),

Spatiotemporal modulation transfer in the human eye, J. Opt. Soc. Amer., 57, 1082 - 1088.

VON BONIN, G., GAROL, H.W. and McCULLOCH, W.S. (1942), The functional organization of the occipital lobe, Biol. Symp., 7, 165 - 192.

WAGNER, H.G., MACNICHOL, E.F.Jr. and WOLBARSHT, M.L. (1960), The response properties of single ganglion cells in the goldfish retina, J. Gen. Physiol., 43, suppl. 6, 46 - 62.

WALD, G. and BROWN, P.K. (1956), Synthesis and bleaching of rhodopsin, Nature, (Lond.), 177, 174 - 176.

WARD, R. and MORGAN, M.J. (1978), Perceptual effect of pursuit eye movements in the absence of a target, Nature, (Lond.), 274, 158 - 159.

WARE, C. and MITCHELL, D.E. (1974), On interocular transfer of various visual after-effects in normal and stereoblind observers, Vision Res., 14, 731 - 734.

WÄSSLE, H., LEVICK, W.R. and CLELAND, B.G. (1975), The distribution of the X-type of ganglion cells in the cat's retina, J. Comp. Neurol., 159, 419 - 438.

WEISKRANTZ, L. (1963), Contour discriminations in a young monkey with striate cortex ablation, Neuropsychologia, 1, 145 - 164.

WEISKRANTZ, L. (1972), Behavioural analysis of the monkey's visual nervous system, Proc. Roy. Soc., (Lond.), 182B, 427 - 455.

WEISKRANTZ, L, WARRINGTON, E.K., SANDERS, M.D. and MARSHALL, J. (1974), Visual capacity in the hemianopic field following a restricted occipital ablation, Brain, 97, 709 -728.

WERBLIN, F.S. (1970), Responses of retinal cells to moving spots: intracellular recording in Necturus Maculosus, J. Neurophysiol., 33, 342 - 350.

WERBLIN, F.S. (1973), The control of sensitivity in the retina, Sci. Amer., JAN, 71 - 79.

WERBLIN, F.S. and DOWLING, J.E. (1969), Organization of the retina of the mudpuppy, Necturus Maculosus. II. Intracellular recording, J. Neurophysiol., 32, 339 - 355.

WESTHEIMER, G. (1959), Retinal light distribution for circular apertures in Maxwellian view, J. Opt. Soc. Amer., 49, 41 - 44.

WESTHEIMER, G. (1960), Effect of binocular magnification devices on stereoscopic depth resolution, J. Opt. Soc. Amer., 46, 278 - 281.

WESTHEIMER, G. (1963), Spatial frequency and light-spread descriptions of visual acuity and hyperacuity, J. Opt. Soc. Amer., 67, 207 - 212.

WESTHEIMER, G. (1965), Spatial interactions in the human retina during scotopic vision, J. Physiol., 181, 881 - 894.

WESTHEIMER, G. (1966), The Maxwellian view, Vision Res., 6, 669 - 682.

WESTHEIMER, G. (1967), Spatial interactions in human cone vision, J. Physiol., 190, 139 - 154.

WHITE, K.D. and MANDLER, M. (1978), McCollough effects established by grid-like patterns having 'anomalous appearances', Conf. on "Sensory and Perceptual Processes", 20th Meeting, German Exp. Psychol. Soc., Marburg, W.G.

WIESEL, T.N. (1960), Receptive fields of ganglion cells in the

cat's retina, J. Physiol., (Lond.), 153, 583 - 594.

WIESEL, T.N. and HUBEL, D.H. (1966), Spatial and chromatic interactions in the lateral geniculate body of the rhesus monkey, J. Neurophysiol., 29, 1115 - 1156.

WIESEL, T.N., HUBEL, D.H. and LAM, D.M.K. (1974), Autoradiographic demonstration of ocular dominance columns in the monkey striate cortex by means of transneuronal transport. Brain Res., 79, 273 - 279.

WIGLEY, E. (1977), Monocular and binocular responses of the human visual system to spatially structured stimuli, Ph.d. Thesis, University of London.

WITKOVSKY, P. and DOWLING, J.E. (1969), Synaptic relationships in the plexiform layers of carp retina, Z. Zellforsch., 100, 60 - 82.

WRIGHT, W.D. (1929), A re-determination of the trichomatic mixture data, Med. Res. Counc. Spec. Rep., 139, 1 - 38.

WRIGHT, W.D. (1927-28), A trichromatic colorimeter with spectral primaries, Trans. Opt. Soc., 29, 225 - 242.

WRIGHT, W.D. (1936), The breakdown of a colour match with high intensities of adaptation, J. Physiol., (Lond.), 87, 23 - 33.

WRIGHT, W.D. (1946), Researches on normal and defective colour vision, Henry Kimpton, London.

WURTZ, R.H. and GOLDBERG, M.E. (1972), Activity of superior colliculus in behaving monkey, a. III. Cells discharging before eye movements, J. Neurophysiol., 35, 575 - 586. b. IV. Effects of lesions on eye movements, J. Neurophysiol., 35, 587 - 596.

WURTZ, R.H. and MOHLER, C.W. (1976), Organization of monkey

superior colliculus: enhanced visual response of superficial layer cells, J. Neurophysiol., 39, 745 - 765.

WYSZECKI, G. and STILES, W.S. (1967), Colour Science, John Wiley and Son, New York.

YATES, J.T. (1974), Chromatic information processing in the foveal projection (area striata) of unanaesthetized primate, Vision Res., 14, 163 - 173.

YOUNG, R.W. (1969), The organization of vertebrate photoreceptor cells, in The Retina; Morphology, Function and Clinical characteristics, ed. Straatsma, B.R., Hall, M.O., Allen, R.A. and Crescitelli, F., 177 - 210. Forum in Medical Sciences, No.8. Berkley: Univ. Calif. Press.

YOUNG, R.W. (1970), Visual cells, Sci. Amer., 223, 80 - 91.

YOUNG, T. (1810), a. On the theory of light and colours, Phil. Trans., 1802, 12 - 48. b. An account of some cases of the production of colours not hitherto described, Phil. Trans., 1802, 387 - 397.

ZEKI, S.M. (1969), Representation of central visual field in prestriate cortex of monkey, Brain Res., 14, 271 - 291.

ZEKI, S.M. (1970), Interhemispheric connections of prestriate cortex of monkey, Brain Res., 19, 63 - 75.

ZEKI, S.M. a. (1974), Functional organization of a visual area in the posterior bank of the superior temporal sulcus of the rhesus monkey, J. Physiol., (Lond.), 236, 549 - 573.

b. (1978), The cortical projections of foveal striate cortex in the rhesus monkey, J. Physiol., (Lond.), 277, 227 - 244. c. The third visual complex of rhesus monkey pre-striate cortex,

J. Physiol., (Lond.), 277, 245 - 272. d. Uniformity and diversity of structure and function in rhesus monkey prestriate visual cortex, J. Physiol., (Lond.), 277, 273 - 290. e. (1978), Functional specialization in the visual cortex of the rhesus monkey, Nature, (Lond.), 274, 423 - 428.

ACKNOWLEDGEMENTS

I am indebted to Dr. K.H. Ruddock for his guidance, encouragement and sense of humour throughout my research, and also for his critical reading of this manuscript.

I would like to express my thanks to all the other people who have helped me during the course of my studies by showing so much kindness and interest, especially Dr. T.H. Williams for his encouragement and assistance in the application of electronics and for the loan of a silk-screen printing press, also for the guidance and helpful discussions from Dr. G.J. Burton, Dr. B.J. Nunn and Dr. S. Naghshineh, which helped to introduce me to the techniques of psychophysical measurements.

I would like to acknowledge my observers, Mr. I.E. Halliday, Mr. D. Cameron, Mr. M. White, Mr. G. Young, Mr. C. Challis, Mr. D. Pinless and Mr. A. Cormier for showing so much patience and for giving up their valuable time, and also the Science Research Council for the award of a Research Studentship, which provided funds for this study.

My thanks go to Mrs. J. Mills, who has most successfully interpreted my handwritten script to produce such a skilfully typed layout. Thank you also for being an un-tiring proof-reader!

I would like to express my most sincere appreciation and thanks to my Parents, who have always given me so much help and encouragement in so many ways.

Finally, my deepest gratitude and appreciation goes to my fiancé, John, for his unfailing support, patience, understanding and affection, which have made possible the realization of this thesis.

I would like to dedicate my thesis to him - To John, Vicki A. Waterfield.

Neuroscience Letters, 8 (1978) 93—98

SELECTIVE LOSS OF FUNCTION ASSOCIATED WITH A CENTRAL VISUAL DEFECT

K.H. RUDDOCK and VICKI A. WATERFIELD

Biophysics Section, Department of Physics, Imperial College, London SW7 2BZ (United Kingdom)

(Received November 30th, 1977)
(Revised version received February 9th, 1978)
(Accepted February 15th, 1978)

SUMMARY

In this paper, the highly abnormal visual responses of a male subject are described and the organisation of the central visual pathways in man implied by these responses is discussed. The subject does not perceive images formed in light of wavelength $\lambda \geqslant 610$ nm, his visual acuity under such illumination being at least some 1° of visual angle. Nonetheless, he is able to construct stereo-images formed by fusion of a red and a green array of random elements [7], although he cannot perceive the elements of the red pattern. Other functions of central vision, such as binocular rivalry and contrast threshold elevation for grating stimulus patterns, are also elicited by unperceived red patterns. The results are examined in relation to the electrophysiological organisation of the central visual pathways.

We report psychophysical observations on a male subject, M.W. aged 26 years, who possesses a very unusual colour vision defect and also suffers loss of pattern recognition for long wavelength stimuli. The several abnormal features of his colour vision have previously been reported in detail [2], and his inability to resolve red objects is associated with abnormal increment threshold sensitivity for long-wavelength stimuli. Thus, his dark adapted threshold sensitivity for a foveally fixated 1° circular target of wavelength 650 nm is about 10^5 times less than that of normal vision, but increment threshold sensitivity *increases* when the target is superimposed on a maintained background field. The subject describes light stimuli of wavelength $\lambda > 610$ nm as black when they are seen in daylight, whereas red lights seen by the dark adapted eye are described as 'silvery-grey'. In red light, he can perceive only gross spatial features subtending 1° to 2° of visual angle, and his grating visual acuity, measured with 100% modulated, high illumination level sinusoidal interference fringes derived from a 632.8 nm He—Ne laser beam, was less than

0.5 cycle/°, compared with a value of about 60 cycle/° for normal subjects. His acuity for white light grating patterns is, however, normal and equivalent to 6/5 vision with either eye. In spite of M.W.'s low sensitivity to red light, measurements [2] reveal activity of the π_5 (red-sensitive) increment threshold mechanism and pupil reflex was observed for red lights which he could not detect visually. We deduce, therefore, that M.W.'s visual defect arises at least partially from malfunction of units in the central visual pathways and we have investigated other functions of central vision. These are: (i) the contrast threshold elevation effect for linear grating stimulus patterns (e.g. ref. 4). This effect, which is transferred interocularly, probably arises in the primary visual cortex [9]. (ii) Recognition of stereoscopic images constructed from two-coloured, randomly distributed elements (anaglyphs) [7]. Steroscopic fusion requires convergence of neural signals from the two eyes, and there occur cortical neurones capable of steroscopic depth discrimination [1,6]. (iii) Binocular rivalry between crossed linear gratings which arises only after signals from the two eyes converge, probably at a level of the visual system central to the mechanism responsible for the contrast threshold elevation effect [3,13].

All three functions depend upon visual resolution of spatially patterned light stimuli and in each case we employed long wavelength lights such that the patterns were not perceived by M.W. Long wavelength stimuli were obtained by filtering white light through a 630 (±5) nm narrow band interference filter (Balzer, type B40). Although it was not always possible to place the interference filter in parallel light beam, spectrophotometric measurements established that for a ±7° angle of incidence, equal to the maximum value employed in the experiments, the filter transmission curve was shifted to shorter wavelengths by only some 5 nm. The observations and results for each experiment were as follows.

(i) The *contrast threshold elevation effect* for linear gratings was measured for dichoptic presentation of the test and adaptation gratings, with a blue test grating presented to the right eye and a high contrast adaptation grating, which could be either red (630 nm) or blue, presented to the left eye. The gratings were presented dichoptically because under these conditions, the contrast threshold elevation effect for normal vision is non-colour selective [10], whereas colour selectivity has been observed in monoptic experiments [12,11]. Data (Fig. 1) are given for a single square-wave test grating, of fundamental spatial frequency, f_t, equal to 5.6 cycle/° and for a series of adaptation gratings of different fundamental spatial frequencies, f_a. Results for a female subject with normal vision (V.A.W. aged 22 years) show that for both red and blue adaptation gratings, the amplitude of the effect, Δ, is a maximum for f_a equal to f_t (5.6 cycle/°) and falls to an insignificant value for $f_a = \frac{1}{2}f_t$ and $f_a = 2f_t$ (Fig. 1), as has been reported in previous investigations [4,10]. Results for subject M.W. (Fig. 1) yield similar Δ values for both adaptation gratings, but they deviate markedly from those of the normal subject for adaptation to a uniform ($f_a = 0$) adaptation gratings. M.W. was unable to perceive any of the red adaptation gratings, all of which appeared as a uniform 'silvery-grey' area,

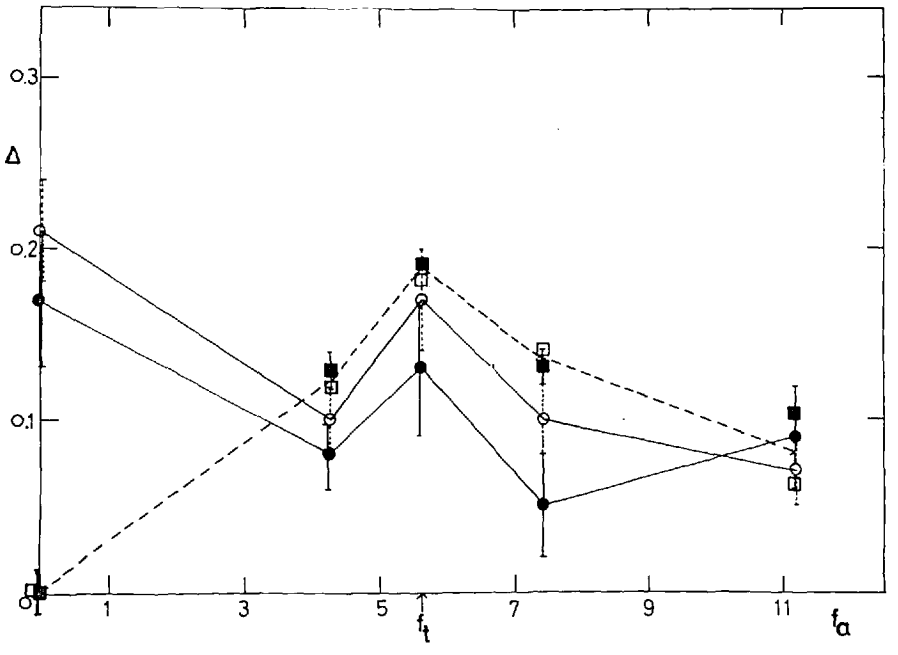

Fig. 1. Contrast threshold elevation, Δ [10,11], measured for a blue (436 ± 15 nm) test grating and both red (630 ± 5 nm) and blue (436 ± 15 nm) adaptation gratings, with the test grating presented to the right eye and the adaptation grating to the left eye. The test grating was of fundamental spatial frequency, f_t, equal to 5.6 cycle/° , and the adaptation gratings were of fundamental spatial frequency f_a. Closed symbols refer to the red and open symbols to the blue adaptation grating. Each point is the mean of four observations and error bars denote the standard error; for $f_a = 0$, the points were measured fourteen times for observer M.W. The lines through the data points serve to connect successive values of Δ. Data for subject M.W. (circles); data for subject V.A.W. (squares), the mean values of which are joined by the broken line. Similar errors were obtained for all data points and for clarity, only selected error bars are included.

but, as the results establish, these unperceived red gratings induce the same adaptation effects as do the blue adaptation gratings, which he readily perceived. The measurement for the uniform adaptation grating ($f_a = 0$) was repeated fourteen times with each adaptation colour, and despite the intrinsic difficulties of such threshold measurements, we are satisfied that M.W.'s data deviate significantly from the normal response pattern for this adaptation condition.

(ii) *Stereoscopic fusion* Julesz anaglyphs [7], printed in red and green inks, were viewed with a red (630 nm) interference filter placed before one eye and a green (530 nm) interference filter placed before the other. Experiments were conducted both under artificial fluorescent lighting and under Northern daylight (colour temp. 6500 K) and essentially similar results were obtained for both illumination conditions. M.W.'s acuity for vision through

the 630 nm filter was such that he could identify the edge region of high contrast, bar shaped patterns of width greater than 2° and could detect some variation in contrast for bars of width greater than 1°. He detected no spatial structure in the anaglyphs when viewing through the red interference filter, but the anaglyph elements, the width of which subtended some 12′ at the subject's eye, were resolved through the green (530 nm) filter. A number of anaglyphs were presented in random order and examples from the series containing different degrees of correlation between the red and green patterns (Figs. 8.1.2 A to G [7]) were interposed at intervals throughout the observations. M.W. had not previously seen the anaglyphs, but as a further percaution, the descriptive text was obscured. M.W. was able to identify, in both stereo perspectives, the anaglyphs containing graded correlations at 100 and 90%, and could partially identify that at 80%; subject K.H.R. gave very similar results but subject V.A.W. could identify completely the pattern at 80% correlation and could identify, in part, that at 70%. In general, M.W.'s ability to identify the different anaglyphs was similar to that of the reference subjects with normal vision, K.H.R. and V.A.W. Attempts, by normal subjects, to simulate M.W.'s responses by placing either neutral density filters or scattering glass before the red filter were unsuccessful, as in neither case could the anaglyphs be identified correctly for grating visual acuity of less than some 5 cycle/deg., compared with M.W.'s maximum acuity of ½ cycle/°. The results show that M.W.'s ability to fuse stereo-images is unimpaired by the functional abnormality which causes the loss of acuity for red patterns.

(iii) *Binocular rivalry* was investigated by presenting crossed vertical and horizontal, high contrast square wave gratings, one to each eye, in a stereo-viewer. The gratings, which were produced photographically on square white cards, were of fundamental spatial frequency 3 cycle/° and the side of the cards, subtended 10° at the subject's eye. The gratings were viewed under Northern daylight and the subject was requested to indicate a change in dominant appearance from vertical to horizontal bars, or vice versa, by pressing a buzzer. The sequence of changes was timed over five minute periods. M.W. could resolve the gratings under daylight illumination, and reported detection of the vertical bars for 69% of the presentation time and of the horizontal bars for 31% of the time. With the horizontal grating viewed through the 630 nm interference filter and the vertical grating viewed through the 530 nm interference filter, he detected the vertical grating for 68% of the presentation time, but for the remaining 32% of the time, he reported that this was suppressed, although no clear structure was then seen. In both these measurements, the vertical grating was seen for periods of some 8-sec duration and was suppressed for periods of some 3.5-sec duration. With the horizontal grating viewed through the green filter and the vertical grating through the red filter, M.W. detected the horizontal grating for 58% of the presentation time and no clear structure was seen for 42% of the time, corresponding to average detection periods of some 11 and 8 sec respectively. Finally, when the horizontal grating was replaced by a uniform white card, M.W. detected the vertical

grating without binocular suppression both when viewing in daylight and with the vertical grating and the uniform field viewed through the green and red filters respectively. This last observation establishes that the binocular rivalry depends upon the presentation of crossed grating structures to the two eyes. Thus, although M.W. was unable to perceive the 3 cycle/deg. grating when viewing through the red filter, this grating was capable of producing rivalry effects with a crossed, green grating seen through the other eye.

All three experiments indicate that for subject M.W., unperceived red spatial patterns contribute to responses arising in central visual mechanisms. His very unusual dichromatic colour matching characteristics and increment threshold responses [2] imply that M.W.'s abnormal responses are associated with malfunction of the primary visual pathways, although his visual response characteristics do not correspond to any previously reported. His defect, which may be one of the colour aphasias described briefly by Duke-Elder [5], appears to be non-progressive, as he has been aware of it since early childhood and his response functions have remained stable during the six years of our study. Ophthalmoscopic investigation has revealed no abnormalities in his retina or ocular media. No other members of his family are known to exhibit similar visual responses, although congenital redgreen deficiencies were found in both paternal and maternal families. Our observations show that M.W. suffers from a visual defect which severely impairs his detection of red coloured spatial patterns, but does not interfere with stereoscopic vision or binocular rivalry effects elicited by red patterned stimuli. The contrast threshold elevation effect can also be elicited by red grating patterns although there is evidence of some abnormality in responses associated with this effect (Fig. 1). The visual defect is therefore restricted to certain functions involving the detection of red light stimuli. This implies that either the neural pathways processing stereoscopic function, binocular rivalry etc. are organised in parallel with the defective pathways, or the defect arises at a stage of processing central to the mechanisms responsible for normal responses such as stereoscopic fusion. Lu and Fender [8] have demonstrated that stereoscopic fusion of Julesz anaglyphs cannot be mediated by chromatic contrast, and infer independence between the visual mechanisms responsible for colour discrimination and those responsible for stereoscopic fusion, and inference consistent with M.W.'s response characteristics. Neurophysiological evidence suggests that different attributes of the visual image, such as stereoscopic depth [6] and colour [14], may be processed in different areas of the visual cortex and psychophysical evidence such as that presented here could provide information on this question.

ACKNOWLEDGEMENTS

We wish to express our gratitude to our subject, M.W. and to Air Commodore Price, F.R.C.S., D.O.M.S., R.A.F. for bringing M.W.'s vision to our attention and for providing detailed ophthalmoscopic data for M.W.'s eyes. V.A.W. acknowledges with thanks the award of a Science Research Council studentship.

REFERENCES

1 Barlow, H.B., Blakemore, C. and Pettigrew, J.D., The neural mechanism of binocular depth discrimination, J. Physiol. (Lond.), 193 (1967) 327–342.
2 Bender, B.G. and Ruddock, K.H., The characteristics of a visual defect associated with abnormal responses to both colour and luminance, Vision Res., 14 (1974) 383–393.
3 Blake, R. and Fox, R., Adaptation to invisible gratings and the site of binocular rivalry suppression, Nature, 249 (1974) 488–490.
4 Blakemore, C. and Campbell, F.W., On the existence of neurones in the human visual system selectively sensitive to the orientation and size of retinal images, J. Physiol. (Lond.), 203 (1969) 237–260.
5 Duke-Elder, W.S., Text-book of Ophthalmology. Vol. IV. The neurology of vision. Motor and optical anomalies. Chap. 43. Henry Kimpton, London, 1949.
6 Hubel, D.H. and Wiesel, T.N., Cells sensitive to binocular depth in area 18 of macaque monkey cortex, Nature, 225 (1970) 41–42.
7 Julesz, B., Foundations of Cyclopean Perception. University Press, Chicago, 1971.
8 Lu, C. and Fender, D.H., The interaction of color and luminance in stereoscopic vision, Invest. Ophthalmol., 11 (1972) 482–490.
9 Maffei, L., Fiorentini, A. and Bisti, S., Neural correlate of perceptual adaptation to gratings, Science (N.Y.), 182 (1973) 1036–1038.
10 Maudarbocus, A.Y. and Ruddock, K.H., The influence of wavelength on visual adaptation to spatially periodic stimuli, Vision Res., 13 (1973) 993–998.
11 Maudarbocus, A.Y. and Ruddock, K.H., Comments on "Adaptation to pairs of coloured gratings: inhibition between colour specific spatial detectors in the human visual system" by C.R. Sharpe. Vision Res. 14 (1974) 1485–1487.
12 May, J.G., Chromatic adaptation of orientation and size-specific visual processes in man, Vision Res., 12 (1972) 1509–1517.
13 Ruddock, K.H. and Wigley, E., Inhibitory binocular interaction in human vision and a possible mechanism subserving stereoscopic fusion. Nature, 260 (1976) 604–606.
14 Zeki, S.M., Colour coding in rhesus monkey pre-striate cortex. Brain Res., 53 (1973) 422–427.

DISTORTIONS OF RETINAL IMAGES INHERENT IN SIGNAL TRANSMISSION BY THE VISUAL PATHWAYS

K.H. Ruddock and Vicki A. Waterfield

Depts. Physics (Biophysics) and Zoology, Imperial College, London SW7 2BZ.

INTRODUCTION

Visual pattern recognition requires both transmission from the eye to the cortical centres of signals elicited by the retinal image and association of the transmitted signals with known objects. Vision research is largely concerned with the mechanisms of signal transmission and both psychophysical and electrophysiological studies have shown that these mechanisms exhibit responses which are highly specific for different stimulus characteristics (4,5). It is difficult to analyse the 'association' stage of pattern recognition but the activity of the underlying cognitive mechanism has been inferred from the illusory appearance of certain stimulus parameters (3). It has been proposed, however, that visual illusions are the result of distortions introduced during transmission of signals along the visual pathways and some illusory effects can be computed on the basis of spatial filters which simulate known visual response characteristics (2). We present experimental data relevant to this problem which were obtained in studies on a male subject, M.W. This subject possesses a highly unusual visual defect (1) and the experiments exploit a particular aspect of this defect, namely, that he is unable to resolve red ($\lambda >$ 610 nm) patterns which subtend less than 1^{0} visual angle at the eye. His visual acuity for black and white patterns is normal, at about 1' visual angle and previous experiments (6) have established that several functions of central vision, including global stereoscopy are unaffected by the abnormality, which is revealed specifically in the perception of chromatic, particularly red, patterns.

METHODS

A number of illusory patterns were printed either in red or in red and black and were presented to M.W., together with related 'null' patterns The visual illusions printed in this form were detected by normal subjects and M.W. was able to identify all the illusions when they were printed in black and white. The sets of printed patterns are illustrated in Fig. 1, together with drawings of them made by M.W., and these latter show clearly the impairment of spatial resolution for the red components of the patterns. The illusory effects are as follows: Fig. 1Aia; the Kanizsa triangle, appears as a bright triangle with apices formed by the segments cut from the circles. The right hand side of the triangle is lost in the 'null' patterns (Fig. 1Aib,c). Fig. 1Bia, the Ehrenstein effect, gives a bright circle with circumference delimited by the inner ends of the lines. The effect is also

seen as a semi-circle in Fig. 1Bic, but is lost in Figs. 1Bib,d. Fig. 1Cia is the Poggendorf illusion, in which the two diagonal lines appear discontinuous, although they are parts of the same straight line. The null pattern of Fig. 1Cib shows that the effect is due to the parallel vertical lines. The Müller-Lyer effect is seen as a length difference in the two horizontal lines (Fig. 1Dia) which are of the same physical length, and as the displacement of the short, central vertical line (Fig. 1Eia) to the left. The effects are lost in the null patterns (Figs. 1Dib and 1Eib). The Ponzo illusion (Fig. 1Fia), in which the upper of the two horizontal lines appears longer, although they are of equal physical length, is lost in the null printing (Fig. 1Fib).

RESULTS

Forty copies of each pattern were printed and the patterns relating to each illusion were presented in random order to M.W., who was asked to state for each pattern whether or not he could detect the appropriate illusion. The results are summarized in Table 1, which gives the percentage of presentations on which the illusion was perceived.

CONCLUSIONS

The results show that the illusory patterns can be divided into two groups; those, such as the Kanizsa triangle (Fig. 1a) which are detected by M.W., even though he does not perceive all components of the illusory pattern, and those such as the Müller-Lyer illusion, which he does not detect unless all components of the pattern are perceived. We conclude that the former group of illusions cannot depend on the activity of cognitive mechanisms, as M.W. does not perceive the patterns which give rise to them, and they must therefore be the result of distortions introduced during signal transmission along the visual pathways. The second group of illusions may also be caused by signal distortions arising in transmission mechanisms central to the site of abnormal function in M.W.'s visual system, or they may be caused by cognitive activity. It can be demonstrated that visual illusions can be divided into two groups according to responses of normal subjects and that these groups correspond to those found in the experiments with M.W. (5).

REFERENCES

1. B.G. Bender and K.H. Ruddock, Vision Research, 14, 383 (1974).
2. A.P. Ginzburg, Nature, 257, 219 (1975).
3. R.L. Gregory, The Intelligent Eye, Weidenfeld and Nicolson, London (1970).
4. K.H. Ruddock, Rep. Prog. Phys., 40, 603 (1977).
5. K.H. Ruddock, in Proc. ICO-11 (Madrid) (1978).
6. K.H. Ruddock and V.A. Waterfield, Neuroscience Lett., 8, 93 (1978).

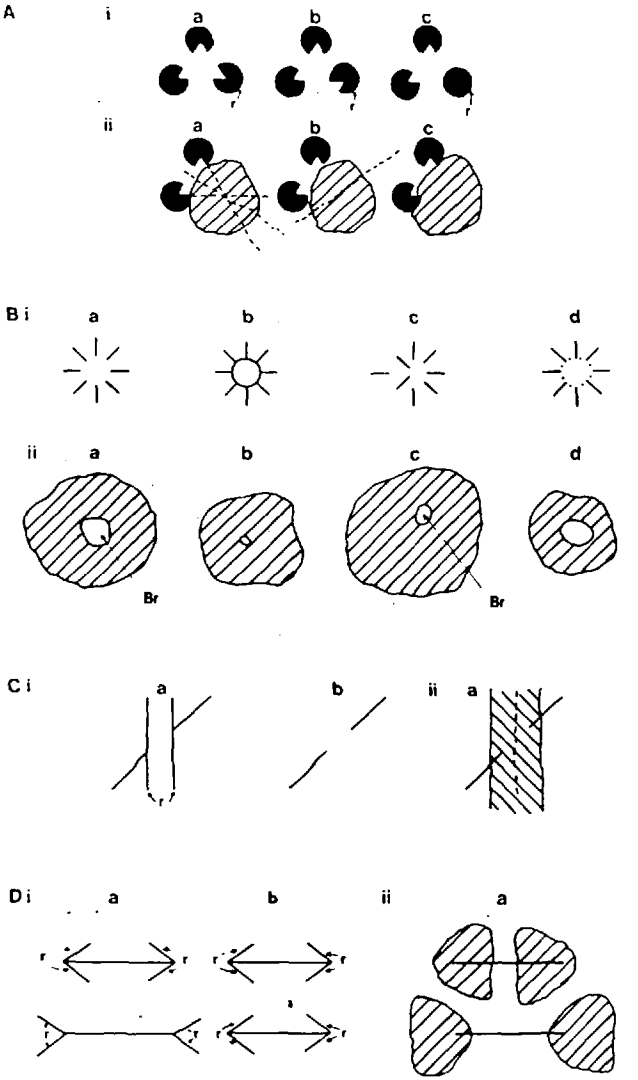

Fig. 1 Ai to Di. Illusory and 'null' patterns used in the investigation. Elements printed in red are denoted 'r', except for patterns Bi, which were printed entirely in red. Aii to Dii illustrate drawings made by M.W. of the printed patterns. The broken lines of Fig. Aii represent bright lines seen by M.W., and the central areas marked 'Br' in Biia and Biic were seen as brighter than the general background.

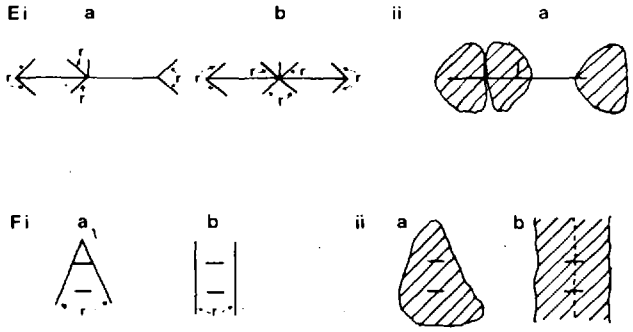

Fig. 1 Ei and Fi. As Fig. 1 A to D; Ei and Fi show illusory and 'null' patterns and Eii and Fii show drawings made by subject M.W.

	a	b	c	d
Ai	100	0	0	
Bi	100	5	100	10
Ci	100	0		
Di	5	0		
Ei	20	0		
Fi	0	0		

Table I

Percentage of presentations on which the patterns of Fig. 1 were identified as the appropriate illusion.

J. Physiol. (1979), **290**, *pp.* 37–49
With 5 text-figures
Printed in Great Britain

THE RESPONSE CHARACTERISTICS OF AN INHIBITORY BINOCULAR INTERACTION IN HUMAN VISION

BY K. H. RUDDOCK, VICKI A. WATERFIELD AND ELIZABETH WIGLEY

From the Biophysics Section, Physics Department, Imperial College, London SW7 2BZ

(*Received 28 April 1978*)

SUMMARY

1. The contrast threshold level for visual detection of a linear grating consisting of parallel light and dark bars is increased by adaptation to a high contrast grating of spatial characteristics similar to those of the test grating (e.g. Blakemore & Campbell, 1969). This so-called contrast threshold elevation effect is significantly reduced if two adaptation gratings, with appropriate different spatial characteristics, are presented one to either eye (Ruddock & Wigley, 1976). We have studied the contrast threshold elevation effect obtained with a test and an adaptation grating presented to one eye and a second adaptation grating, referred to as the conditioning grating, presented to the other.

2. Preliminary data are presented for three subjects with normal stereoscopic vision. In each case, the contrast threshold elevation effect for a pair of spatially identical test and adaptation gratings is significantly reduced by a conditioning grating of spatial frequency in the range 1–5 c/deg.

3. Reduction in the contrast elevation effect is observed whether the conditioning and adaptation gratings are of the same or of different wave-lengths and the effect of the conditioning grating increases to a steady-state level over a period of some 30 sec following onset of its presentation.

4. Measurements were made with a 5 deg diameter circular test grating presented at retinal locations up to 8 deg in the horizontal and vertical meridians from a foveal fixation point. It was found that in the horizontal meridian, the amplitude of the suppression effect associated with the conditioning grating falls as the displacement angle of the test field from the fixation point increases. For displacements in the vertical meridian, however, the amplitude of the suppression effect is virtually independent of the retinal location of the test field.

5. Under experimental conditions which yield suppression of the contrast threshold elevation effect for subjects with normal stereoscopic vision, no suppression was found for three subjects who possessed neither global nor fine stereoscopic vision. Results for a subject who possessed fine, but not global stereoscopy, did, however, show the suppression effect.

INTRODUCTION

Psychophysical studies of binocular vision in humans have been concerned largely with summation of brightness or the characteristics of binocular fusion and depth perception. Recently, however, it has been shown that a number of visual effects

0022-3751/79/3300-0616 $01.50

associated with one-dimensional, spatially periodic light stimuli (called grating stimuli) are transferred interocularly and consequently new information regarding the organization of binocular vision has been obtained. The effects which can be transferred interocularly include the elevation of threshold contrast level for detection of a test grating which is associated with pre-adaptation to a grating of similar spatial periodicity and orientation (Gilinsky, 1968; Pantle & Sekuler, 1968; Blakemore & Campbell, 1969). Electrophysiological studies of light evoked signals recorded from single neurones in the primary visual cortex of cat and primate have shown that neurones are sensitive to bar-shaped stimuli of appropriate width and orientation in the visual field (Hubel & Wiesel, 1962, 1965, 1968). It was also shown that all such neurones are to some extent controlled by appropriate stimuli presented to either eye, even though the signals received from one eye may be expressed only in inhibition of those received from the other (Henry, Bishop & Coombs, 1969). The demonstration that some psychophysical phenomena associated with bar-shaped stimuli can be transferred interocularly is, therefore, consistent with the response characteristics of neurones in the primary visual cortex.

Both psychophysical and electrophysiological investigations into binocular vision have usually employed similar light stimulus configurations for eliciting signals from both eyes. When two light stimuli of different spatial characteristics are presented, one to either eye, perception of the two stimuli alternates in time, and this is known as binocular rivalry. It has been shown that under experimental conditions which simulate binocular rivalry, the contrast threshold elevation effect remains unchanged (Blake & Fox, 1974), from which observation it was deduced that the neural centres for binocular rivalry are centrally located in relation to those responsible for the adaptation effect. We have studied the contrast threshold elevation effect by presenting, simultaneously, two different adaptation gratings, one to either eye. The original aim of the experiments was to determine a summation index for signals from the two eyes, but as has been shown, only inhibitory interactions between signals from the two eyes are found (Ruddock & Wigley, 1976).

METHODS

Equipment

One-dimensional sinusoidal spatial distributions of illumination were formed on the retina by laser interference methods (Le Grand, 1937; Byram, 1944; Arnulf & Dupuy, 1960; Campbell & Green, 1965). The interference fringes produced in this way were of high contrast and high space-average illumination level, and by using either a tunable Argon ion laser (Coherent Radiation Model 54) or a helium-neon laser (Spectra-Physics Model 120), a selection of wavelengths was available. The interference fringe patterns were produced by means of a Mach-Zehnder type interferometer (Born & Wolf, 1970), which has been described in detail by its designer (Burton, 1973). The radiometric flux levels of all light stimuli were measured with a photomultiplier system (EMI type 9698) and the equivalent photometric flux values were measured with a lumeter (Holophane type 48A). The instrument provides 30 deg diameter, circular visual fields, but in some experiments (data from which are plotted in Fig. 4), the diameter of visual fields was reduced to 5 deg by placing a circular stop in the back focal plane of the microscope objective which forms the interferometer eyepiece.

Experimental procedure

The experimental procedure follows closely that introduced by Blakemore & Campbell (1969), using the modified method of Maudarbocus & Ruddock (1973*b*). The adaptation effect associated with a high luminance grating stimulus was determined under monoptic presentation of the test and adaptation gratings. The adaptation grating was presented for two minutes, during which time the observer scanned the grating pattern so as to avoid local adaptation effects. The test grating was then presented for 3 sec, during which time the observer could adjust its space-average illumination level. The adaptation grating was then presented for a further 10 sec, followed by a further 3 sec presentation of the test grating, and the cycle was continued until the subject set the test grating to an illumination level such that it could just no longer be resolved. The illumination level corresponding to this threshold condition is denoted by I'. The experiment was repeated, but the adaptation grating was replaced by a uniform field of illumination level equal to the space-average illumination level of the adaptation grating. The illumination level required for threshold detection of the test grating, I, was again determined and the grating threshold adaptation effect arising from the grating structure was measured as

$$\Delta = \log I' - \log I. \tag{1}$$

This method of determining the grating threshold adaptation effect differs somewhat from that used by Blakemore & Campbell (1969) in which the contrast threshold level of the test grating was determined at the same mean illumination level as the adaptation grating. It has been shown, however, that the two methods of measurement yield broadly similar response characteristics (see Maudarbocus & Ruddock, 1973*b*). In the majority of the experiments to be described, a second grating (the conditioning grating) was presented contralaterally to the test and adaptation gratings. The conditioning grating was presented in a 10 sec on, 3 sec off cycle, in synchrony with the adaptation grating cycle. The space-average illumination levels of the adaptation and conditioning gratings have been defined on a logarithmic scale, the zero value of the scale corresponding to the threshold illumination level for threshold detection of the grating. The reason for choosing this scale was that adaptation gratings of different spatial frequency values and different wave-lengths, but with the same illumination level on this scale, yield the same values of Δ for a spatially matched test grating (Maudarbocus & Ruddock, 1973*b*). Except where otherwise stated, each adaptation grating was set at a space-average illumination level 4·5 log units above the threshold level for its detection. This is equivalent to a retinal illumination level of some 4 log td, although the photometric equivalent varies slightly with change of spatial frequency and/or wave-length. The combinations of non-matching adaptation and conditioning patterns produced binocular rivalry, which manifested itself as wholesale disappearance of one or other pattern. No subject reported a stereoscopic tilt effect, although each was instructed to look for it when the patterns favoured its appearance (Balkemore, 1970).

Observers

All subjects possessed normal colour vision and were not astigmatic for detection of vertically or horizontally oriented lines. E.W., aged 24 yr, female, V.W., aged 22 yr, female, R.D., aged 19 yr, male, T.L., aged 25 yr, male, and K.R., aged 36 yr, male, possessed normal stereoscopic vision. Global stereoscopy was assessed by the ability of the subject to identify stereoscopic images formed by fusion of two-colour anaglyphs (Julesz, 1971). Fine stereoscopy was measured with a pair of vertical rods, which could be varied in relative distance from the observer. Three stereo-blind subjects took part in the investigation: A.C., aged 24 yr, male, D.P., aged 21 yr, male, and D.C., aged 33 yr, male. The first two have received correction for congenital squint, and D.C. is an albino with spatial resolution for linear gratings restricted to values $\leqslant$ 4 c/deg. Subject G.Y., aged 21 yr, male, has a hemianopic visual field, with sparing for some 3 deg around the central fovea. This condition followed an accident, as a result of which the optic radiation of the left hemisphere was severed. G.Y. was unable to fuse the anaglyphs, but possessed normal foveal fine stereo-acuity as measured with the vertical rods.

RESULTS

The suppression of the contrast threshold elevation effect by the conditioning grating is illustrated in Fig. 1, which includes data for three subjects with normal stereoscopic vision. Similar results have been found for a further three normal subjects. Measurements were made for fixed test and adaptation gratings, both of spatial frequency 7 c/deg, presented to the right eye, and a conditioning grating presented to the left eye. Values of Δ were determined for a number of spatial

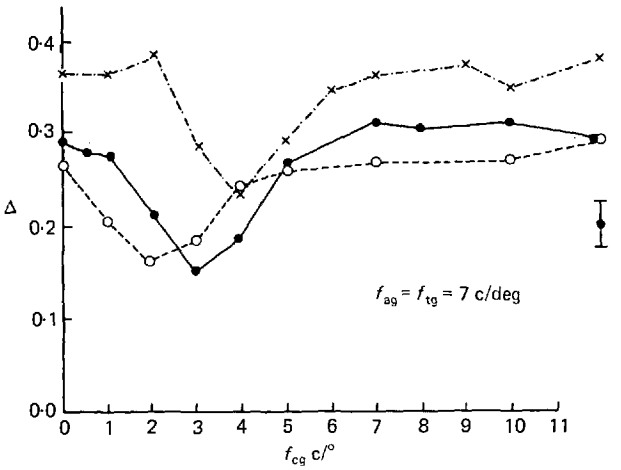

Fig. 1. Values of Δ (eqn. (1)) plotted against the spatial frequency, f_{cg}, of the conditioning grating. The test and adaptation gratings, both of spatial frequency 7 c/deg, were presented to the right eye and the conditioning grating to the left eye. All gratings were oriented in the vertical meridian and were of wave-length 632·8 nm. The adaptation grating was set at an illumination level 4·5 log units above its threshold illumination level and the conditioning grating set such that its space-average illumination level was equal to that of the adaptation grating. Data for three observers with normal stereoscopic vision, R.D. (—·—), T.L. (---) and E.W. Each point is the mean of ten observations and a typical standard deviation bar is shown to the lower right of the Figure.

frequency values, f_{cg}, of the conditioning grating. With the spatial frequency of the conditioning grating in the frequency range 1 to 5 c/deg, there is for each subject a significant fall in the value of Δ, and even at 7 c/deg the value of Δ for each subject is less than that found in the absence of the conditioning grating. A similar result is obtained for other spatial frequency values of the test and adaptation gratings (Ruddock & Wigley, 1976). The effect of the conditioning grating has been determined for a number of different experimental conditions. In Fig. 2, Δ has been plotted against log I, the space-average illumination level of the conditioning grating. Data are given for two wave-lengths of the conditioning grating, 632·8 nm (open circles) and 488 nm (crosses), the test and adaptation gratings being of wave-length 632·8 nm in each case. The variation of Δ with log I is similar for both conditioning wave-lengths, thus the suppression of the contrast threshold elevation effect by the conditioning grating is not wave-length selective. The contrast threshold elevation effect itself is similarly non-wave-length selective for dichoptic presentation of the

test and adaptation gratings (Maudarbocus & Ruddock, 1973*a*). Also plotted in Fig. 2 are values of Δ measured for different illumination levels of the adaptation grating in the absence of the conditioning grating (filled circles). The range of illumination level over which Δ varies and the slope of the Δ-log *I* curve is similar for both functions plotted in Fig. 2, except that Δ increases with increase in the illumination level, *I*, of the adaptation grating and decreases with increase in the illumination level

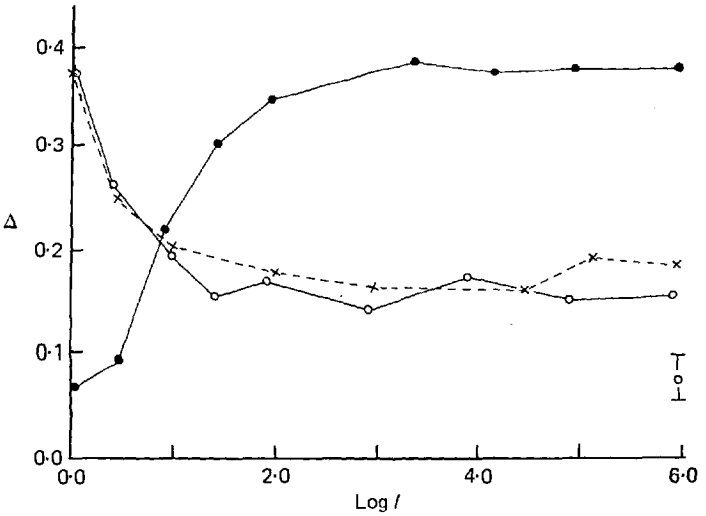

Fig. 2. Values of Δ (eqn. (1)) plotted against the logarithm of the relative illumination level, *I*. The test and adaptation gratings, both of spatial frequency 7 c/deg and wave-length 632·8 nm, were presented to the right eye and the conditioning grating, of spatial frequency 3 c/deg, was presented to the left eye. Data represented by the open circles and crosses refer to conditioning gratings of wave-lengths 632·8 and 488 nm respectively, presented at space-average illumination levels *I*. The adaptation grating was set at a space-average illumination level of 4·5 log units (log *I* equal to zero corresponding to threshold illumination level for detection of the adaptation grating). Data represented by filled circles correspond to Δ values determined without the conditioning grating, and for an adaptation grating of space-average illumination level, *I*. All points are the mean of ten determinations and a typical standard error bar is shown to the right of the Figure. Observer E.W.

of the conditioning grating. The similarity of the two different Δ–log *I* functions suggests that the same non-linear responses contribute both to the contrast threshold elevation effect and to its suppression by the conditioning grating. The Δ–log *I* function for the contrast threshold elevation effect itself is consistent with the non-linear signal transformations observed in electrophysiological responses of retinal neurones (Maudarbocus & Ruddock, 1973*b*) and if the non-linear function were indeed of retinal origin, it would necessarily operate on all visual signals transmitted to the central pathways.

The time course of the inhibitory action of the conditioning grating was determined by measuring Δ as a function of t_{cg}, the duration of presentation of the conditioning grating. The experimental data are given in Fig. 3, which also shows the build-up of Δ as a function of t_{ag}, the duration of presentation of the adaptation stimulus. Initially,

a uniform conditioning field, which has only a small suppression effect, was presented to the left eye, with the adaptation and test gratings presented to the right eye. The data points were each obtained in a single presentation cycle of the adaptation and test gratings, and the duration t_{ag} of adaptation was increased by 10 sec on each presentation, with the test grating presented for 3 sec in each case. The adaptation

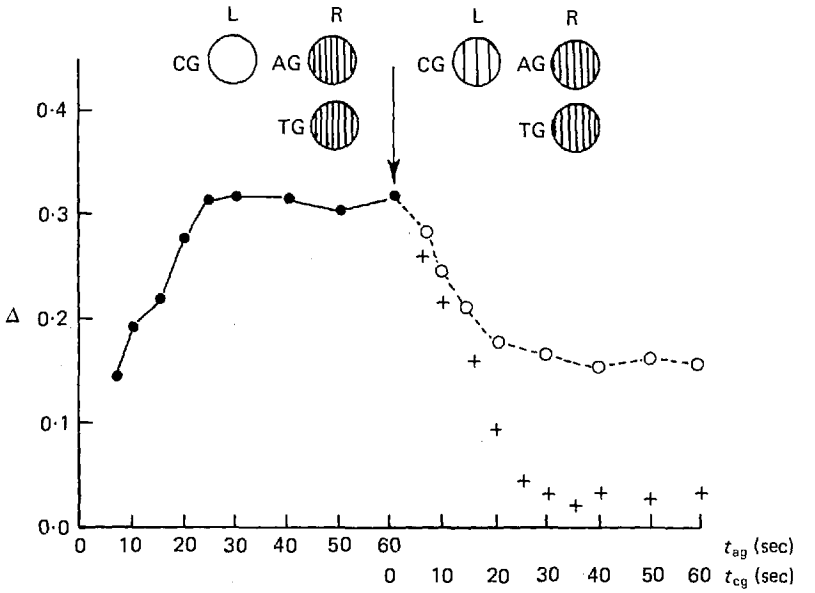

Fig. 3. Δ plotted as a function of time, t, in seconds. The build-up of the adaptation effect (filled circles) was determined with a uniform conditioning field presented to the left eye for a period t_{ag}, simultaneously with the presentation of the adaptation grating to the right eye (left inset). The fall-off of Δ (open circles) was determined by replacing the uniform conditioning field with a conditioning grating of spatial frequency 3 c/deg, Δ being determined as a function of t_{cg}, the duration of presentation of the conditioning grating (right inset). Also shown (crosses) is the time course of Δ when the adaptation grating is replaced, at time t_{cg} equal to zero, by a uniform field of illumination level equal to the space-average illumination level of the adaptation grating, and with a uniform field conditioning grating in the other eye.

The other stimulus parameters were the same as those in Fig. 1. Observer E.W.

effect, as measured by Δ, saturates for a value of t_{ag} equal to some 20 sec, as was found by Blakemore & Campbell (1969). The time course of the suppression effect was established by replacing, after one minute of adaptation, the uniform conditioning grating with one of spatial frequency 3 c/deg, and determining the value of Δ for different durations, t_{cg}, of presentation of the 3 c/deg conditioning grating. Also plotted in Fig. 3 (crosses) are points obtained by replacing the adaptation grating with a uniform field of the same mean illumination level. The time course of Δ is similar for both the 3 c/deg conditioning grating and the uniform field substitution, although in the latter case, the value of Δ falls to zero rather than to the steady value of about 0·16 observed with the 3 c/deg conditioning grating. Presentation of the conditioning grating to the left eye thus leads to a temporal sequence of changes in Δ which is similar to those observed if the adaptation grating stimulus is

replaced by a uniform field. We propose, therefore, that the suppression action of the conditioning grating is essentially an inhibitory control on the signals arising from the adaptation grating stimulus, that is, the conditioning grating effectively shuts off the

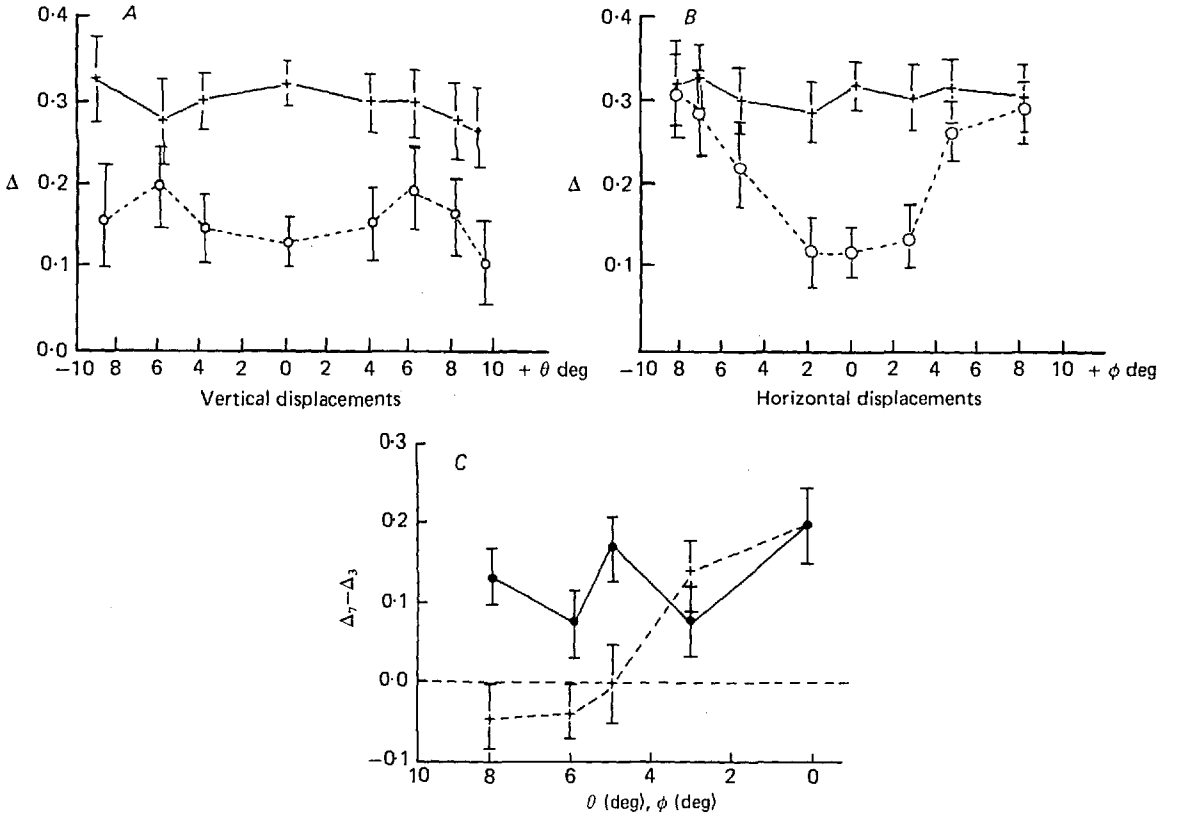

Fig. 4. Δ plotted against θ or ϕ, the angle of eccentricity from the central fovea of the circular test and adaptation grating field centres, the fields being 5 deg in diameter. The circular conditioning grating was of 30 deg diameter. *A*, values for displacement in the vertical meridian of the test and adaptation gratings. Open circles correspond to a conditioning grating stimulus of spatial frequency 3 c/deg, crosses to values obtained with a 7 c/deg conditioning grating. Stimulus of wave-length 632·8 nm. The data points are the mean of ten values and the error bars refer to the standard deviations for each point. Observer E.W. *B*, as Fig. 4*A*, but for displacement in the horizontal meridian. Observer E.W. *C*, the difference between values of Δ measured with conditioning gratings of spatial frequency 7 c/deg (Δ_7) and 3 c/deg (Δ_3), plotted against retinal location of the test and adaptation gratings. Crosses correspond to the values for displacements θ deg, along the horizontal meridian, and filled circles to values for displacement, ϕ deg, along the vertical meridian. Observer K.R.

adaptation stimulus, although the finite value of Δ obtained in the steady state ($t_{cg} > 30$ sec) shows that the inhibition is incomplete.

The data presented in Figs. 1 to 3 were measured for circular visual fields of 30 deg diameter. We were able to reduce the diameter of the test and adaptation gratings to 5 deg by placing a stop in the back focal plane of the interferometer eyepiece, and by superimposing a fixation point in the field of view of the right eye, the 5 deg test and

adaptation gratings could be located with their centres up to some 10 deg from the foveal fixation point. This arrangement enabled us to determine the contrast threshold elevation effect as a function of retinal location for test and adaptation gratings of spatial frequency 7 c/deg. Measurements were made with the gratings displaced both in the vertical and horizontal meridians, and two sets of data were obtained for each meridian, one with a conditioning grating of spatial frequency 7 c/deg (for which only a small suppression effect is observed in central vision) and the other with a conditioning grating of spatial frequency 3 c/deg (for which a large suppression effect is observed, Fig. 1). It should be noted that the diameter of the conditioning grating field remained at 30 deg, thus it covered adequately the visual field area corresponding to the different locations of the test and adaptation gratings. Values of Δ measured in this way are given in Fig. 4*A* and 4*B* which refer to observer E.W. For the vertical scan (Fig. 4*A*) the values of Δ differ for the two values of the conditioning spatial frequency for all angular locations, θ, of the test and adaptation gratings. In the case of the horizontal scan, however, the values of Δ found for the two values of f_{cg} converge for presentation at some 8 deg off axis (Fig. 4*B*), the values of Δ for f_{cg} equal to 3 c/deg increasing with increase in the angle of eccentricity, θ. These data establish that the reduction in values of Δ associated with the 3 c/deg conditioning grating is restricted to retinal locations around the vertical meridian, and effectively disappears at 8 deg displacement of test and adaptation gratings along the horizontal meridian. The suppression of the contrast threshold elevation effect by the low spatial frequency conditioning grating is, therefore, a characteristic of the retinal area surrounding the vertical meridian. Similar measurements were made for observer K.R., and the difference in the values of Δ obtained for the two values, f_{cg}, are plotted against eccentricity (Fig. 4*C*). The results are similar to those obtained for observer E.W.; that is, the difference between Δ values obtained for the 7 c/deg and 3 c/deg conditioning gratings remains essentially unchanged for displacement of the test and adaptation gratings along the vertical meridian, but decreases with increased displacement along the horizontal meridian.

The observations with non-foveal stimulus locations were particularly difficult to make and the associated errors are large. We note also that the experimental conditions are such as to underestimate variation in Δ with change in retinal location. Ideally, the test field should be of smaller diameter, thereby giving more localized estimates of Δ, and the diameter of the adaptation grating should have been greater than that of the test grating to ensure uniform adaptation over the retinal area on which the test grating field was presented. Both improvements were attempted, but neither proved feasible with the instrumental arrangement employed in these experiments. Thus, placing a smaller stop in the back focal plane of the objective did produce a smaller test field but diffraction effects at the edge of the field became intolerably large. Again, alternation between adaptation and test fields of different diameters could, in principle, have been achieved by switching stops in the back focal plane of the interferometer eyepiece In practice, it was found that the location of stops in the objective was so critical that we were unable to obtain correct alignment of the field stops with the available switching mechanisms. Despite these experimental limitations, it is clear that the suppression of the grating threshold adaptation effect behaves differently with respect to displacement of the test field in the horizontal and vertical meridians.

It has been shown previously that the suppression of the contrast threshold elevation effect by the conditioning grating is specific to dichoptic presentation of the conditioning and adaptation gratings and that the effect is restricted to near-vertical

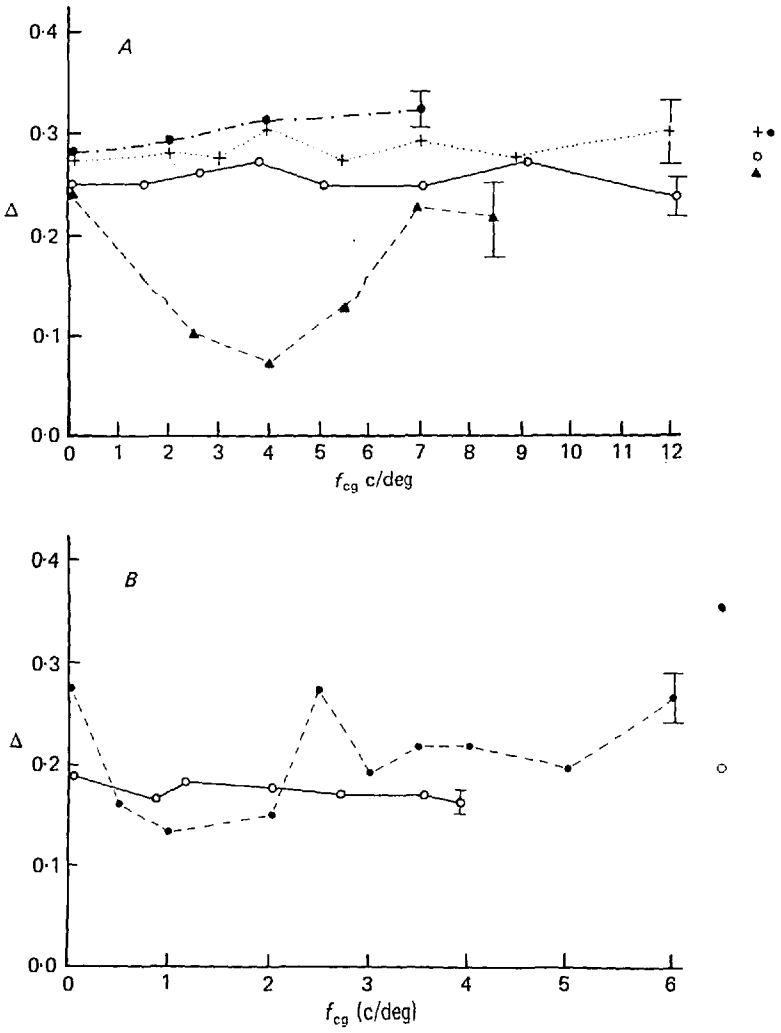

Fig. 5. Δ plotted against f_{cg}, the spatial frequency of the conditioning grating. Errors given at the right of the connected data points denote typical standard deviations for each subject. The separate data points plotted to the right of the ordinate scale denote the values of Δ obtained with *no* conditioning grating presented to the left eye. *A*, data for stereo-blind subjects D.P. (open and filled circles) and A.C. (crosses), and for the subject with fine but not global stereoscopy, G.Y. (triangles). The test and adaptation gratings, of spatial frequency 7 c/deg, were presented to the right eye, with the conditioning grating presented to the left eye, except for the filled circles, which were obtained with the test and adaptation gratings presented to the left eye and the conditioning grating to the right eye. All gratings were oriented vertically and other stimulus parameters are as for Fig. 1. Data points are the mean of five readings. *B*, data for the albino subject, D.C. (open circles), and for the normal subject, E.W. (filled circles). The spatial frequency of the test and adaptation gratings was 2 c/deg (D.C.) and 2·5 c/deg (E.W.), with other stimulus parameters as for Fig. 1. Data points are the means of four readings.

orientations of the gratings (Ruddock & Wigley, 1976). Consequently, it was suggested that the suppression effect may be associated with stereoscopic visual function. Measurements were therefore made with four subjects who possessed abnormal stereoscopic function, as described in the Methods (Observers) section. The contrast threshold elevation effect was measured for the three subjects who possess neither global nor fine stereoscopy (A.C., D.P. and D.C.), using monoptic presentation of the test and adaptation gratings. Values of Δ were obtained for vertically oriented test and adaptation gratings, of spatial frequency 7 c/deg (A.C. and D.P.) and 2 c/deg (D.C.). The values of Δ were: A.C., right eye 0·30, left eye 0·35; D.P., right eye 0·28, left eye 0·30; D.C., right eye 0·20, left eye 0·15, the mean error being on average $\pm 0{\cdot}05$. The fact that in every case the Δ values are significant establishes that both eyes are responsive to grating stimuli. The effect of presenting a conditioning grating contralaterally to the test and adaptation gratings is shown in Fig. 5. It is apparent that although the experimental conditions are such that they produce suppression of the contrast threshold elevation effect for normal vision (as in Fig 1), this is not the case for the three stereo-blind subjects. Two sets of values are given for subject D.P., with the presentation of the gratings to the right and left eyes reversed between them. Similar values of Δ were obtained for both stimulus configurations, thus showing that the subject's responses are symmetric for the two eyes. In Fig. 5, results are also given for subject G.Y., who possesses fine but not global stereoscopy. In this case, suppression of the contrast threshold elevation effect by the conditioning grating is observed, and the Δ values are similar to those found for normal vision (Fig. 1).

DISCUSSION

Our experimental results have established that certain sine-wave grating stimuli presented to one eye can suppress the adaptation effects associated with non-identical sine-wave gratings presented to the other eye. The grating threshold adaptation effect can be observed under dichoptic presentation of the test and adaptation gratings and the characteristics of the effect measured in this way are closely similar to those determined under monoptic presentation of the gratings (Blakemore & Campbell, 1969; Maudarbocus & Ruddock, 1973*b*). Thus, there are at least two classes of interaction between grating stimuli presented to the two eyes: one gives rise to the contrast threshold elevation effect for a test grating presented contralaterally to an adaptation grating, whilst the other gives rise to the suppression interaction between adaptation and conditioning gratings described in this paper. These two classes of interaction have a number of common response features, including their orientation selectivity (Ruddock & Wigley, 1976), their dependence on the space-average illumination level of the grating stimulus, and the lack of wave-length specificity (Fig. 2). The time course of Δ values following presentation of the conditioning grating is similar to that observed when the adaptation grating is obscured (Fig. 3). The action of the conditioning grating is therefore equivalent to blocking the input from the adaptation grating and for that reason, we regard its action as inhibitory on the signals arising from the contralateral adaptation grating. There are three characteristics of the inhibitory action of the conditioning grating which are markedly different from the adaptive action of an adaptation grating. First, for normal upright

head position, it is restricted to the vertical meridian (Ruddock & Wigley, 1976), whereas the grating threshold adaptation effect is observed in all meridians (Maudarbocus, 1973). Secondly, it is found only for a selected, low frequency band of spatial frequency values of the conditioning grating (Fig. 1), whereas the adaptation effect is observed for all spatial frequencies (Blakemore & Campbell, 1969). Thirdly, the inhibition effect changes significantly as the test grating location is changed along the horizontal meridian, whereas the contrast threshold elevation effect remains virtually unchanged (Fig. 4). These three responses characteristics establish that the mechanism responsible for the inhibitory action of the conditioning grating is functionally separate from that which gives rise to the contrast threshold elevation effect. Recent experiments employing dichoptic presentation of non-matching grating patterns have provided information on binocular rivalry (Abadi, 1976; Blake & Lema, 1978), but the observed response characteristics are quite different from those associated with the effect described in this paper. This is not unexpected, as binocular rivalry influences neither the contrast threshold elevation effect nor its suppression by non-matching gratings (Blake & Fox, 1974; Ruddock & Wigley, 1976). It is surprising, however, that during the experiments, no subject observed the stereoscopic tilt effect associated with dichoptic presentation of non-matching gratings (Blakemore, 1970). The experimental results show that the suppression effect is associated with fine stereoscopic visual function at the fovea (Fig. 5) and experiments with subjects possessing abnormalities of the visual pathways have established that foveal fine stereoscopy depends upon callosal projections between the two hemispheres (Blakemore, 1969; Mitchell & Blakemore, 1970). Further, the callosal fibres which connect corresponding points in the two hemispheres project, via area 18, to the boundary region between areas 17 and 18 of the monkey visual cortex, the region containing the representation of the vertical meridian in the visual field (Choudhury, Whitteridge & Wilson, 1965). That the suppression effect is restricted to stimuli located around the vertical meridian (Fig. 4) is, therefore, consistent with the involvement of callosal fibres in the effect. Subject G.Y., whose left optic radiation is severed, can make fine stereoscopic depth discriminations and displays binocular suppression of the contrast threshold elevation effect (Fig. 5*A*). Because his foveal vision is spared, for some 3 deg around the fovea, in the blind hemifield, it is uncertain which foveal projections survive and the possible influence of callosal fibres on his responses cannot, therefore, be evaluated. Electrophysiological responses of single neurones in areas 17 and 18 of cat and monkey possess spatial characteristics similar to those of the contrast threshold elevation effect (Hubel & Wiesel, 1962, 1965, 1968) and adaptation effects in these responses are similar to the psychophysical effect (Maffei, Fiorentini and Bisti, 1973). Regarding the binocular control of these neurones, disparity sensitive neurones have been observed in area 17 of cat (Barlow, Blakemore & Pettigrew, 1967) and in area 18 of monkey (Hubel & Wiesel, 1970). Hubel & Wiesel (1968) found that in the primate visual cortex, simple cells are largely excited by one eye in preference to the other and in cat, it is usually stimulation of the ipsilateral eye which yields excitatory responses (Joshua & Bishop, 1970). Henry, Bishop & Coombs (1969) subsequently showed that the contralateral eye exerts an entirely inhibitory influence on the simple cell responses. They demonstrated that there is a restricted well defined area of the contralateral receptive field for which

no inhibitory influence occurs, but that surrounding this is a relatively large receptive field area (up to 2 deg) over which inhibition is observed. The small, non-inhibitory region of the receptive field is closely defined with respect to horizontal but not to vertical displacement of the stimulus pattern and the cell characteristics were shown to be dependent on retinal location relative to the fovea. The stimulus conditions applied by Henry *et al.* (1969) in investigating the binocular control of simple cells were not the same as those used in our experiments. Their results are, however, superficially similar to ours in that they show inhibition by the contralateral eye, exercised through corresponding receptive fields, which are sharply tuned with respect to location along the horizontal meridian.

We are grateful to all our subjects who took part in the experiments and to Dr G. J. Burton for making available the interferometer. V. A. W. acknowledges with thanks the award of a research studentship by the Science Research Council.

REFERENCES

ABADI, R. V. (1976). Induction masking – a study of some inhibitory interactions during dichoptic viewing. *Vision Res.* **16**, 269–275.

ARNULF, A. & DUPUY, O. (1960). La transmission des contrastes par le système optique de l'oeil et les seuils de contrastes rétiniens. *C.r. hebd. Séanc. Acad. Sci., Paris* **250**, 2757–2759.

BARLOW, H. B., BLAKEMORE, C. & PETTIGREW, J. D. (1967). The neural mechanism of binocular depth discrimination. *J. Physiol.* **193**, 327–342.

BLAKE, R. & FOX, R. (1974). Adaptation to invisible gratings and the site of binocular rivalry suppression. *Nature, Lond.* **249**, 488–490.

BLAKE, R. & LEMA, S. A. (1978). Inhibitory effect of binocular masking suppression is independent of orientation. *Vision Res.* **18**, 541–544.

BLAKEMORE, C. (1969). Binocular depth discrimination and the nasotemporal division. *J. Physiol.* **205**, 471–497.

BLAKEMORE, C. (1970). A new kind of stereoscopic vision. *Vision Res.* **10**, 1181–1199.

BLAKEMORE, C. & CAMPBELL, F. W. (1969). On the existence of neurones in the human visual system selectively sensitive to the orientation and size of retinal images. *J. Physiol.* **203**, 237–260.

BORN, M. & WOLF, E. (1970). *Principles of Optics*, 4th edn., p. 312. Oxford: Pergamon.

BURTON, G. J. (1973). Evidence for non-linear response processes in the human visual system from measurements on the thresholds of spatial beat frequencies. *Vision Res.* **13**, 1211–1225.

BYRAM, G. M. (1944). The physical and photochemical basis of visual resolving power. Part II. Visual acuity and the photochemistry of the retina. *J. opt. Soc. Am.* **34**, 718–738.

CAMPBELL, F. W. & GREEN, D. G. (1965). Optical and retinal factors affecting visual resolution. *J. Physiol.* **181**, 576–593.

CHOUDHURY, B. P., WHITTERIDGE, D. & WILSON, M. E. (1965). The function of the callosal connections of the visual cortex. *Q. Jl. exp. Physiol.* **50**, 214–219.

GILINSKY, A. S. (1968). Orientation-specific effects of patterns of adapting light on visual acuity. *J. opt. Soc. Am.* **58**, 13–18.

HENRY, G. H., BISHOP, P. O. & COOMBS, J. S. (1969). Inhibitory and subliminal excitatory receptive fields of simple units in the cat striate cortex. *Vision Res.* **9**, 1289–1296.

HUBEL, D. H. & WIESEL, T. N. (1962). Receptive fields, binocular interaction and functional architecture of the cat's visual cortex. *J. Physiol.* **160**, 106–154.

HUBEL, D. H. & WIESEL, T. N. (1965). Receptive fields and functional architecture in two non-striate visual areas (18 and 19) of the cat. *J. Neurophysiol.* **28**, 229–289.

HUBEL, D. H. & WIESEL, T. N. (1968). Receptive fields and functional architecture of monkey striate cortex. *J. Physiol.* **195**, 215–243.

HUBEL, D. H. & WIESEL, T. N. (1970). Cells sensitive to binocular depth in area 18 of the macaque monkey cortex. *Nature, Lond.* **225**, 41–42.

JOSHUA, D. E. & BISHOP, P. O. (1970). Binocular single vision and depth discrimination. Receptive field disparities for central and peripheral vision and binocular interaction on peripheral units in cat striate cortex. *Exp. Brain Res.* **10**, 389–416.

JULESZ, B. (1971). *Foundations of Cyclopean Perception*. Chicago: University Press.

LE GRAND, Y. (1937). La formation des images rétiniennes: sur un mode de vision éleiminant les defauts optiques de l'oeil. *2e Reunion de l'Institut d'Optique, Paris.*

MAFFEI, L., FIORENTINI, A. & BISTI, S. (1973). Neural correlate of perceptual adaptation to gratings. *Science, N.Y.* **182**, 1036-1038.

MAUDARBOCUS, A. Y. (1973). Response characteristics of the human visual system in the detection of spatially periodic stimuli. PhD. thesis, University of London.

MAUDARBOCUS, A. Y. & RUDDOCK, K. H. (1973*a*). The influence of wavelength on visual adaptation to spatially periodic stimuli. *Vision Res.* **13**, 993–998.

MAUDARBOCUS, A. Y. & RUDDOCK, K. H. (1973*b*). Non-linearity of visual signals in relation to shape sensitive adaptation responses. *Vision Res.* **13**, 1713–1737.

MITCHELL, D. E. & BLAKEMORE, C. (1970). Binocular depth perception and the corpus callosum. *Vision Res.* **10**, 49–54.

PANTLE, A. & SEKULER, R. (1968). Size-detection mechanisms in human vision. *Science, N.Y.* **162**, 1146–1148.

RUDDOCK, K. H. & WIGLEY, E. (1976). Inhibitory binocular interaction in human vision and a possible mechanism subserving stereoscopic fusion. *Nature, Lond.* **260**, 604–606.

Neuroscience Letters, 15 (1979) 307–312

A COLOUR-DEPENDENT ABNORMALITY IN HUMAN VISUAL DETECTION OF STIMULUS MOTION AND SPATIAL STRUCTURE

J.L. BARBUR, K.H. RUDDOCK and VICKI A. WATERFIELD

Departments of Physics (Biophysics) and Zoology, Imperial Colllege, London SW7 2BZ (United Kingdom)

(Received April 2nd, 1979)
(Revised version received August 22nd, 1979)
(Accepted September 15th, 1979)

SUMMARY

We have studied the wavelength dependence of visual responses in a single human subject, M.W., who has an unusual visual defect. It is shown that for red stimuli, both spatial resolution for grating patterns and detection of target movement are grossly abnormal. On the basis of these and other [8] experimental data, we argue that M.W.'s response pattern implies inter-dependent central visual processing of colour, movement and spatial structure. We examine this conclusion in relation to recent anatomical and electrophysiological findings.

The human visual system provides information about a number of stimulus parameters including colour, state of motion, three dimensional spatial structure and location in the visual field. Recent electrophysiological and anatomical studies on the primate visual system [4,5,10,11] have shown that single cortical neurones possess a high degree of specificity in their responses to these different stimulus parameters and that cells located in a given visual projection area are, by and large, sensitive to a single parameter. The way in which responses arising in the different visual areas combine to produce a perceived image is little understood, and, in particular, it is not clear whether different stimulus parameters, such as motion and colour, are processed independently in the cortex. One approach to this problem is through psychophysical studies of anomalous visual responses in human subjects [7]. We have already published the results of one such study [8], which showed the selective nature of functional loss in a single subject, M.W., and in this paper we present further data on M.W.'s visual performance. The principal feature of M.W.'s vision is very low sensitivity for detection of red and orange ($\lambda > 610$ nm) targets, which he perceives only at very high illumination levels, when they appear silvery-grey, without any defined

spatial structure. His colour vision has been studied in detail [2] and analysis shows that the red-sensitive (π_5) increment threshold mechanism [9] is normal. Some central responses to spatial patterns of red light have also been described [8], although M.W. does not perceive the red patterns which elicit these responses. We have now examined M.W.'s spatial resolving power and sensitivity to movement and the results of the investigation provide evidence of coupling between the functional mechanisms responsible for motion detection, visual acuity and colour discrimination.

Visual acuity was measured in terms of the resolution limit for linear gratings, consisting of alternate, equally spaced, dark and coloured bars (inset, Fig. 1a). The gratings were produced photographically on high contrast film (Kodalith) and were placed in a Maxwellian viewing system. The subject viewed the gratings through an artificial, 2 mm pupil, and the head position

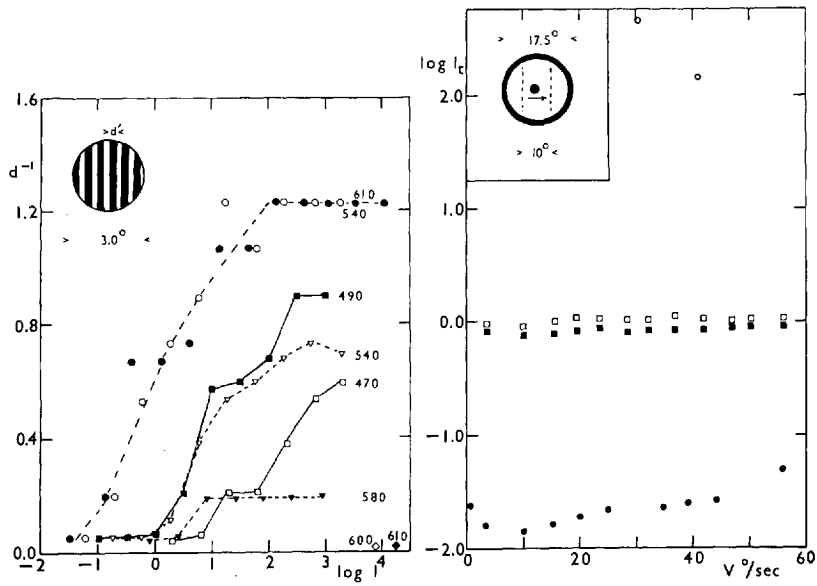

Fig. 1. (a) Grating visual acuity, expressed as d^{-1}, where d is the bar-width in min of arc of the linear square-wave test grating, plotted against the logarithm of the mean grating illumination level. Measurements were made by finding the illumination level, I, at which a grating of bar-width d, could just no longer be resolved. The modulation depth of the test grating images was >98%, and the wavelength for each set of data is denoted in nm. Data for the normal subject V.W. are given by open (540 nm) and full (610 nm) circles; all other data points refer to subject M.W. A given value of I corresponds to the same radiometric flux for the different stimulus wavelengths. (b) Log threshold illumination level, log I_t, for detection of a 3.5° diameter circular target moving at velocity v°/sec along the horizontal meridian. Squares refer to a green (540 nm) target moving against a 540 nm background field of mean illumination level 1.3 log troland; full squares, data for V.W., open squares, data for M.W. Circles refer to a 630 nm target moving against a dark background field. Full circles, data for V.W.; open circles, data for M.W. All points are the mean of four observations, with typical standard error 0.04 log trolands.

was maintained by use of a dental clamp. The illumination level of the grating was controlled with a neutral density wedge and its spectral composition by narrow-band interference filters (Balzers B40; ±5 nm half bandwidth). We measured the retinal illumination level at which a grating of given bar-width and wavelength could just no longer be resolved by the observer, and thus we determined grating visual acuity as a function of illumination level and wavelength. Data for M.W. and for a subject with normal vision, V.W., are given in Fig. 1a, in which visual acuity, expressed as the reciprocal of the grating bar-width at the resolution limit, is plotted against the mean grating illumination level. It is clear that M.W. suffers a marked loss of acuity for stimulus wavelengths $\lambda \geq 580$ nm and for $\lambda \geq 600$ nm, he is able to resolve only the coarsest gratings, with bar width of about 1° of visual angle. Thus the wavelengths for which M.W. has markedly subnormal visual acuity are the same as those for which he has low detection sensitivity and which appear 'silvery-grey' to him. Results for other wavelengths ($470 \leq \lambda \leq 540$) are more similar to those for the normal subject, V.W., and establish that M.W.'s visual system is capable of relatively high spatial resolution.

Responses to target movement were investigated in two ways. Firstly, we measured threshold illumination levels for a 3.5° diameter circular target, moving at constant velocity along the horizontal meridian. The target moved through 10° of visual angle, positioned centrally in a 17.5° diameter, 2° wide white light annulus (inset Fig. 1b). The observer maintained correct accommodation by focussing this annulus, and it also provided a guide to the position at which the moving target appeared. Both the annulus and the circular target were produced photographically, and were viewed through the 2 mm diameter pupil of a Maxwellian optical system. Threshold illumination levels obtained for M.W. and for the normal subject, V.W., are plotted as a function of target velocity in Fig. 1b. Results are given for a red (630 nm) and a green (540 nm) target, and in the latter case, the target was seen against a 540 nm, 18° diameter circular background field, located centrally with respect to the annulus. M.W.'s threshold sensitivity for the 540 nm target is similar to that of the normal subject, V.W., over the full range of velocity whereas for the 630 nm target, his detection is limited to high illumination levels and high velocity. Thus, as in the case of visual acuity, M.W.'s sensitivity to motion is markedly wavelength selective, being near-normal for green and highly abnormal for red targets. In the other experiment on motion detection, the 3.5° circular target moved along the horizontal meridian at constant velocity (15°/sec), with a vertical grating, consisting of alternate equally spaced dark and light bars as the background field (inset, Fig. 2a). The 3.5° target was white (approximate colour temperature 300 K), and the background grating was either orange (610 nm) or white (approximate colour temperature 3000 K). M.W. was unable to detect any of the 610-nm gratings, which he could not distinguish from a dark background field. The threshold illumination level for detection of the moving target was measured

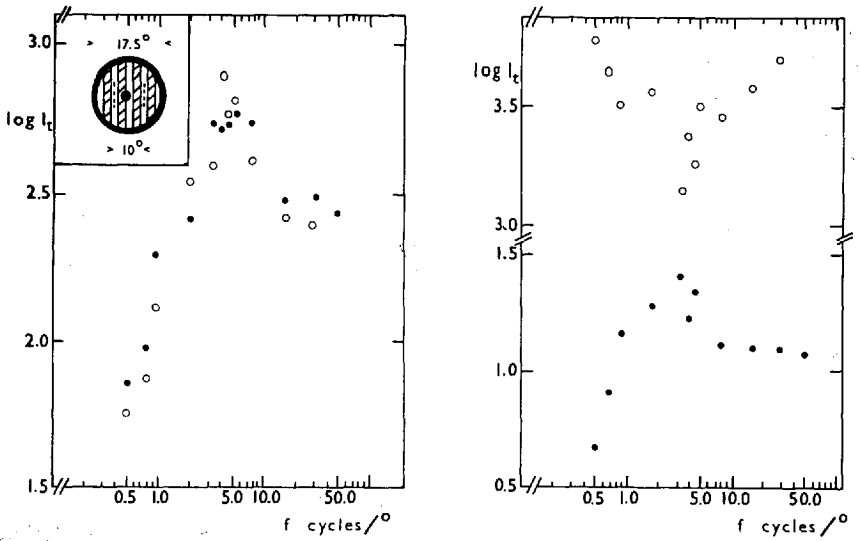

Fig. 2. Log threshold illumination level, log I_t, for detection of a 3.5° diameter circular target, moving at 15°/sec along the horizontal meridian, with a vertically oriented square-wave grating, of fundamental spatial frequency f cycles/deg., in the background field (see inset). (a) White light test and background stimuli, with a background grating of mean illumination level 3.7 log trolands. Closed circles refer to the normal subject, V.W.; open circles to M.W. (b) White light test and 610 nm background grating field, with mean grating illumination level 2.9 log trolands. Closed circles refer to the normal subject, V.W. and open circles to M.W. Each point represents the mean of four readings, with typical standard deviation 0.04. M.W.'s threshold illumination level for detection of the target moving against a dark background field was −0.7 log trolands.

for different fundamental spatial frequencies, f, (i.e. for different bar-widths) of the background grating, and the experimental values are plotted in Fig. 2a. Those for the normal subject, V.W., show the characteristic relation between threshold illumination level and bar-width [1], with a peak value for f equal to about 5 cycles/deg., and a similar result is obtained for M.W. in the white background grating condition. M.W.'s threshold for detection of the target moving across the 610 nm background gratings is significantly greater than the dark threshold level, even though he cannot detect the gratings (Fig. 2b). The effect of bar-width, however, is the inverse of that which occurs in the other cases, with *minimum* threshold illumination level for f equal to some 4 cycles/deg., thus the red gratings clearly exert an anomalous influence on M.W.'s motion detection.

The results of this investigation establish that M.W.'s visual acuity and motion detection are near normal for some target wavelengths and grossly abnormal for others ($\lambda \geq 610$ nm). Thus his anomaly is expressed in a number of different visual functions, including those described in this paper, but is limited to a restricted range of spectral stimuli. We have considered the following interpretations of these results:

(i) All central signals originating from absorption in the red-sensitive cones are abnormal, leading to general visual malfunction in response to long-wavelength stimuli. M.W. can, however, identify stereoscopic images constructed from red and green random-dot patterns [8], even though he is unable to perceive the red pattern. This implies that the normal signals associated with red patterns are transmitted to M.W.'s central visual pathways.

(ii) The retinal projection which gives rise to global stereoscopic vision is separate from all other projections, and is unaffected by M.W.'s visual anomaly. Electrophysiological studies indicate that at ganglion cell level, responses to flicker and motion are differentiated from those associated with spatial structure [3,5], but no special group associated with disparity sensitive cortical neurones have been identified.

(iii) The central mechanisms which process colour, motion and spatial structure are interdependent and consequently anomalies of the central visual pathways may affect all three functions.

As was discussed in the introduction, there appear to be multiple cortical projection maps of the visual field, and each map has a specific associated response, such as colour discrimination or movement detection [10,11]. One interpretation of such organisation is that different parameters of the retinal image are analysed independently in the cortex. Our conclusion (iii above) implies, however, that even if this is the case, some form of signal interaction must occur subsequent to the stage of visual processing represented by the spatially discrete, parametrically independent cortical maps. Such interaction could arise, for instance, in the synthesis of the final image percept.

ACKNOWLEDGEMENTS

We are very grateful to our subject M.W., for his continued interest and participation in the experimental work. V.W. acknowledges with thanks the award of an SRC research studentship.

REFERENCES

1 Barbur, J.L. and Ruddock, K.H., The effects of background structure and target size on movement detection by the foveal and parafoveal retina, 'Optica Hoy y Mañana Proc. 11th Congress of the International Commission for Optics, Sociedad Española de Optica, Madrid, 1978, pp. 125—128.
2 Bender, B.G. and Ruddock, K.H., The characteristics of a visual defect associated with abnormal responses to both colour and luminance, Vision Res., 14 (1974) 383—393.
3 Enroth-Cugell, C. and Robson, J.G., The contrast sensitivity of retinal ganglion cells of the cat, J. Physiol. (Lond.), 187 (1966) 517—552.
4 Hubel, D.H. and Wiesel, T.N., Receptive fields and functional architecture of monkey striate cortex., J. Physiol. (Lond.), 195 (1968) 215—243.
5 Hubel, D.H. and Wiesel, T.N., Cells sensitive to binocular depth in area 18 of macaque monkey cortex, Nature (Lond.), 225 (1970) 41—42.
6 Levick, W.R., Form and function of cat retinal ganglion cells, Nature (Lond.), 254 (1975) 659—662.

7 Ruddock, K.H., The organisation of human vision for pattern detection and recognition, Rep. Prog. Phys., 40 (1977) 603—663.
8 Ruddock, K.H. and Waterfield, V.A., Selective loss of function associated with a central visual defect, Neurosci. Lett., 8 (1978) 93—98.
9 Stiles, W.S., Colour vision, the approach through increment-threshold sensitivity, Proc. nat. Acad. Sci. (Wash.), 45 (1959) 100—114.
10 Zeki, S., Cortical projections of foveal striate cortex in the rhesus monkey, J. Physiol. (Lond.), 277 (1978) 227—244.
11 Zeki, S., Uniformity and diversity of structure and function in rhesus monkey prestriate visual cortex, J. Physiol. (Lond.), 277 (1978) 273—290

[*From the Proceedings of the Physiological Society*, 21–22 *September* 1979
Journal of Physiology, **298**, 20*P*]

Psychophysical determination of post-receptoral spectral functions

By K. H. Ruddock and Vicki A. Waterfield. *Departments of Physics (Biophysics) and Zoology, Imperial College, London SW7 2BZ*

Colour matching and increment threshold responses are characterized by broad-band spectral functions closely related to single-cone absorption spectra. Using binocular adaptation to high-contrast spatial patterns, we have determined narrow-band spectral functions similar to those observed in electrophysiological responses of post-receptoral neurones. The threshold illumination level, I_t, for detection of a grating is measured after adaptation to a square wave form grating and a matrix of circular spots, presented to the right and left eyes respectively. After 2 min adaptation, the square wave form test grating (present to the right eye) and the adaptation fields are alternated for 3 sec and 10 sec respectively, until a threshold setting is made. Fig. 1 shows I_t plotted against λ, the spot matrix wave length, for three

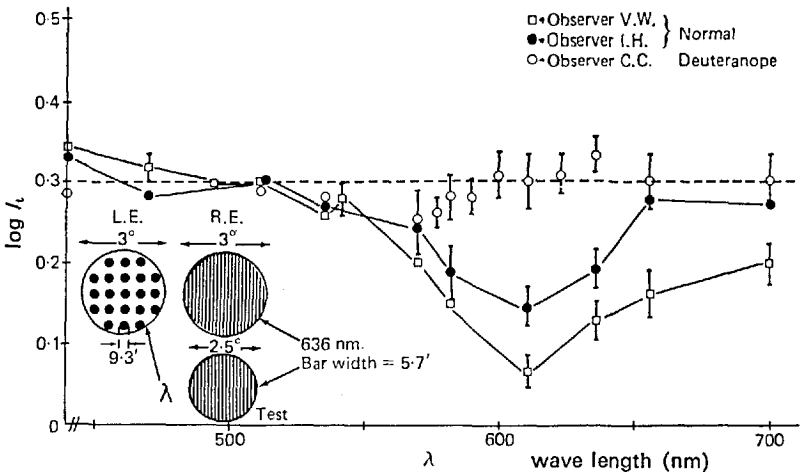

Fig. 1. Log relative threshold illumination level for detection of the test grating, log I_t, plotted against the spot matrix wave length, λ. The matrix was set at the same photometric level for each λ.

subjects with normal binocular vision, two normal trichromats (□, ●) and a deuteranopic dichromat (○). The broken line represents the value of I_t after adaptation to the grating alone and for normal trichromats, binocular adaptation produces spectral variation in I_t. The red–green opponent mechanism implied by these data is absent for the deuteranope, who lacks the green-sensitive cone mechanism (Rushton, 1965).

REFERENCE

Rushton, W. A. H. (1965). *J. Physiol.* **176**, 24–37.